Transplantation Imaging

Ghaneh Fananapazir
Ramit Lamba
Editors

Springer

Transplantation Imaging

Ghaneh Fananapazir • Ramit Lamba
Editors

Transplantation Imaging

Springer

Editors
Ghaneh Fananapazir
Department of Radiology
University of California Davis
Sacramento, CA
USA

Ramit Lamba
Department of Radiology
University of California Davis
Sacramento, CA
USA

ISBN 978-3-319-75264-8 ISBN 978-3-319-75266-2 (eBook)
https://doi.org/10.1007/978-3-319-75266-2

Library of Congress Control Number: 2018937512

Printed on acid-free paper

This Springer imprint is published by the registered company Springer International Publishing AG part of Springer Nature
The registered company address is: Gewerbestrasse 11, 6330 Cham, Switzerland

Contents

Contributors

Kristine S. Burk, M.D. Department of Radiology, Massachusetts General Hospital, Boston, MA, USA

Michael T. Corwin, M.D. University of California, Davis, Davis, CA, USA

Brandon Doskocil, M.D. Kaiser TPMG Sacramento, Sacramento, CA, USA

Ghaneh Fananapazir, M.D. Department of Radiology, University of California Davis Medical Center, Sacramento, CA, USA

Ely R. Felker, M.D. Department of Radiological Sciences, David Geffen School of Medicine at UCLA, Ronald Reagan UCLA Medical Center, Los Angeles, CA, USA

H. Henry Guo, M.D., Ph.D. Department of Radiology, Stanford University, Stanford, CA, USA

Daniel Helmy, M.D. Department of Radiology, University of California Davis Medical Center, Sacramento, CA, USA

Michael Kadoch, M.D. Department of Radiology, University of California Davis Medical Center, Sacramento, CA, USA

Alexander Y. Kim, M.D. Division of Vascular and Interventional Radiology, Medstar Georgetown University Hospital, Washington, DC, USA

Angela D. Levy, M.D. Department of Radiology, Medstar Georgetown University Hospital, Washington, DC, USA

David S. K. Lu, M.D. Department of Radiological Sciences, David Geffen School of Medicine at UCLA, Ronald Reagan UCLA Medical Center, Los Angeles, CA, USA

Akemi Miller, M.D. Division of Vascular and Interventional Radiology, Medstar Georgetown University Hospital, Washington, DC, USA

Eitan Novogrodsky, M.D. Department of Radiological Sciences, David Geffen School of Medicine at UCLA, Ronald Reagan UCLA Medical Center, Los Angeles, CA, USA

Steven S. Raman, M.D. Department of Radiological Sciences, David Geffen School of Medicine at UCLA, Ronald Reagan UCLA Medical Center, Los Angeles, CA, USA

Dushyant Sahani, M.D. Department of Radiology, Massachusetts General Hospital, Boston, MA, USA

Kumaresan Sandrasegaran, M.D. Department of Radiology and Imaging Sciences, Indiana University School of Medicine, Indianapolis, IN, USA

Lucas Sheen, M.D. Kaiser TPMG Central Valley, Modesto, CA, USA

Daniel R. Swerdlow, M.D. Department of Radiology, Medstar Georgetown University Hospital, Washington, DC, USA

Temel Tirkes, M.D. Department of Radiology and Imaging Sciences, Indiana University School of Medicine, Indianapolis, IN, USA

Christoph Troppmann, M.D. Department of Surgery, University of California Davis Medical Center, Sacramento, CA, USA

Catherine T. Vu, M.D. University of California Davis, Sacramento, CA, USA

Chapter 1
Preoperative Imaging Evaluation of Living Liver Transplant Donors

Kristine S. Burk and Dushyant Sahani

Introduction

Liver transplantation is a lifesaving treatment for patients with end-stage liver disease and is in high demand with 14,619 candidates on the waiting list as of November 2016 [1]. Unfortunately, organ availability has been unable to keep up with demands. In 2014, 6199 adult liver transplants were performed, but 14,632 candidates remained on the waiting list at the end of the year. Furthermore, over the course of that year, 1821 patients died while waiting for a liver, and 1290 others were removed from the waiting list because they became too sick to qualify for a transplant [2]. Transplantation of partial livers from both living and deceased donors has developed as a method for increasing the number of grafts available. However, these surgeries are less often performed than whole-cadaveric liver transplants. In 2014, only 220 adult living donor liver transplants (LDLT) and 63 split-cadaveric transplants were performed, in contrast to 5916 whole-cadaveric transplants [3].

Partial liver transplantations, particularly from living related donors, offer substantially increased challenges to both the surgeon and the radiologist. For these operations, imaging plays a crucial role in candidate selection and surgical planning. Contrast-enhanced CT and MRI are the standard imaging modalities utilized in the evaluation, as these provide complete assessment of the liver parenchyma, biliary system, and vascular anatomy. Imaging protocols are highly tailored and routinely utilize techniques for iron and fat quantification, volumetric analysis, and 3D reformations. In addition to understanding these imaging techniques and anatomy, diagnostic radiologists must also understand the nuances of donor and recipient selection and have a knowledge of the transplant operations themselves.

K. S. Burk, M.D. (✉) • D. Sahani, M.D.
Department of Radiology, Massachusetts General Hospital, Boston, MA, USA
e-mail: ksburk@partners.org; dsahani@partners.org

G. Fananapazir, R. Lamba (eds.), *Transplantation Imaging*,
https://doi.org/10.1007/978-3-319-75266-2_1

This chapter will review the different types of transplant operations, discuss the imaging modalities and protocols most commonly utilized in this clinical setting, and provide an in-depth discussion of the evaluation of a potential LDLT donor.

Transplant Operations

There are three types of liver transplants performed today: the whole-liver cadaveric transplant, the split-liver cadaveric transplant, and the living donor liver transplant.

Whole-Liver Cadaveric Transplant

The most common type of transplant performed in the USA is the whole-liver cadaveric transplant, in which a complete donor liver is transplanted into the recipient [4]. In this procedure, the native liver and gallbladder are removed and an entire donor liver is put in its place. Anastomoses are required at the hepatic artery, at the portal vein, at the hepatic veins to the inferior vena cava (IVC), and at the common bile duct. The advantage of this operation is the relative technical simplicity and large amount of healthy liver given to the recipient. However, this operation alone cannot meet the demands of the waiting list population. This has led to the development of other transplant operations.

Split-Liver Cadaveric Transplant

Split-liver cadaveric transplants are the least common type of transplant operation, accounting for only 1.0% of transplants performed in 2014 [2]. The most commonly utilized transection plane is just to the right of the falciform ligament, resulting in a right tri-segment graft (segments I and IV–VIII) intended for an adult recipient and a left lateral graft (segments II–III) intended for a pediatric recipient. An alternative technique intended for two adult recipients involves a transection plane just to the right of the middle hepatic vein (MHV), resulting in a right hemi-liver graft (segments V–VIII ± I) and a left hemi-liver graft (segments II–IV ± I) [5–7]. These transections can be performed in situ (in the donor prior to organ removal) or ex vivo (on a back table following organ harvesting) (Fig. 1.1) [8, 9]. Although this operation allows candidates on the waiting list to receive liver grafts sooner, there is an increased risk of postoperative complications compared to whole-cadaveric liver transplants [10–12].

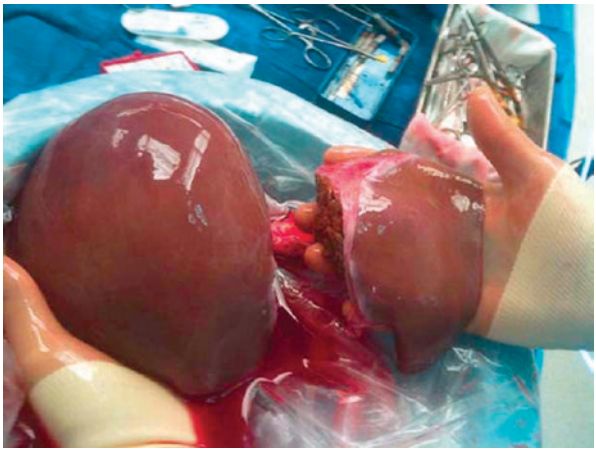

Fig. 1.1 Ex vivo split-liver cadaveric transplant—the right tri-segment graft was transplanted into an adult recipient with HCC, while the left lateral segment graft went to an infant with fulminant hepatic failure. Adapted from Burk KS, Singh AK, Vagefi PA, Sahani D, Pretransplantation imaging workup of the liver donor and recipient. *Radiology Clinics of North America* 2016; 54(2):185–197

Living Donor Liver Transplant

In a living donor liver transplant, a part of the donor's liver is removed and transplanted into the recipient (Fig. 1.2). Selection of the transplanted lobe is based on the donor's anatomy, the age of the recipient, and the predicted sizes of the residual liver and grafts. In order to ensure the liver donor does not develop hepatic failure postoperatively, no more than 70% of their liver volume can be resected. In order to ensure the liver recipient does not develop hepatic failure postoperatively (small-for-size syndrome), the liver graft to recipient body weight ratio must be greater than 0.8 [4].

For a pediatric liver graft recipient, the left lateral segmentectomy technique is most popular. In this operation, the transection plane runs just to the right of the falciform ligament, and segment IV and the MHV are left in the donor (Fig. 1.3a). There are two surgical options for adult recipients: the right lateral hepatectomy technique and the left hepatectomy technique. Historically, the right lateral hepatectomy technique has been more popular. In this operation, the transection plane runs approximately 1 cm to the right of the MHV, close to Cantlie's line connecting the IVC to the gallbladder fossa (Fig. 1.3b). More recently, there has been a rise in popularity of the left hepatectomy technique. In this operation, the MHV and segment IV are included as part of the left hepatic lobe graft; the caudate lobe may or may not also be included. Since less liver is removed from the donor in this operation compared to the right lateral hepatectomy technique, it is thought to transfer the risk of postoperative complications away from the healthy donor and onto the recipient [13].

The overall risk of postoperative complication for the partial liver donor is 40%, and the risk of postoperative death is 0.15–0.20%. Though this overall complication rate seems high, 95% of these complications are minor in severity—Clavien grade

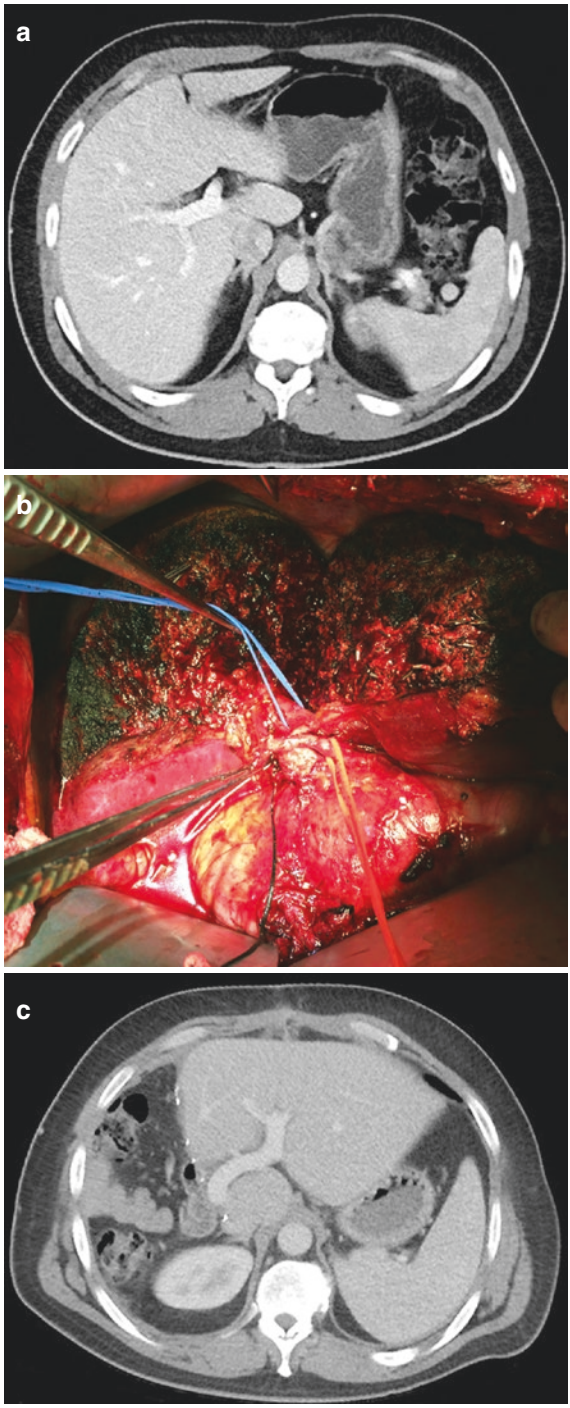

Fig. 1.2 Right lobe living donor liver transplant. (**a**) Preoperative donor image. (**b**) Intraoperative photograph after liver parenchymal division but prior to vascular division. (**c**) Postoperative donor image showing growth in the remnant left hepatic lobe. Adapted from Burk KS, Singh AK, Vagefi PA, Sahani D, Pretransplantation imaging workup of the liver donor and recipient. *Radiology Clinics of North America* 2016; 54(2):185–197

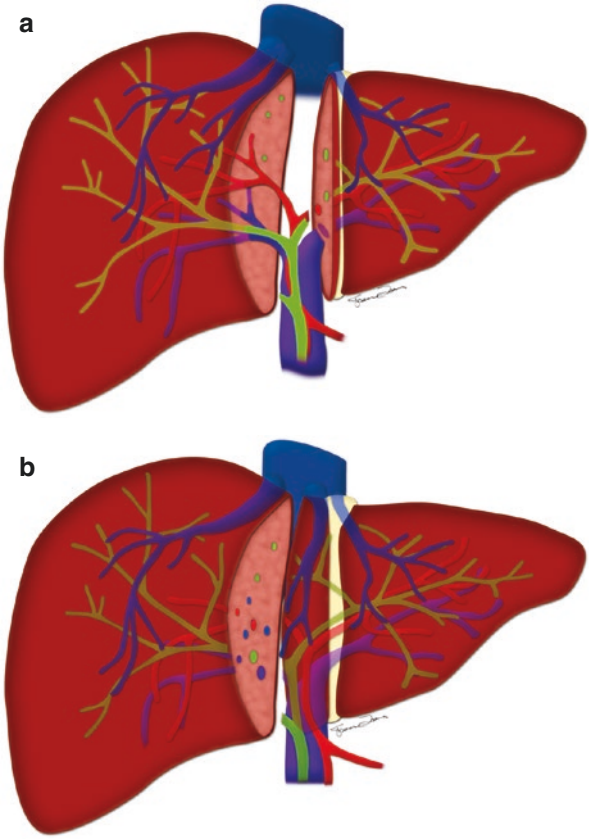

Fig. 1.3 (**a**) The left lateral segmentectomy LDLT plane runs to the left of the MHV. (**b**) The right lobe LDLT plane connects the gallbladder fossa and IVC and runs 1 cm to the right of the MHV. Adapted from Burk KS, Singh AK, Vagefi PA, Sahani D, Pretransplantation imaging workup of the liver donor and recipient. *Radiology Clinics of North America* 2016; 54(2):185–197

I or II. These require only conservative, medical management, or at most a percutaneous intervention [14, 15]. Compared to whole-liver cadaveric donation, recipients of living donor grafts also experience a higher rate of postoperative complications. However, this increased risk is felt to be offset by the ability to achieve liver transplant sooner and by the markedly healthy state of liver allografts donated [16].

Imaging Techniques

CT and MRI are the modalities most commonly used to evaluate liver donors and recipients in the preoperative setting. Indeed, with the advent of biliary contrast agents and imaging post-processing techniques, older modalities including conventional angiography, ERCP, and intraoperative cholangiography have largely been replaced. Though MRI can be used as a sole imaging modality for preoperative evaluation, CT and MRI are more commonly used *together* as their strengths are complimentary to one another [17].

CT/CTA

CT/CTA has superior spatial resolution compared to MRI and is therefore better at delineating small segmental hepatic arteries and accessory hepatic veins [18]. As a result, dual energy CT/CTA is the first examination performed on potential liver donors at our institution. In addition to describing the vascular anatomy, these examinations are used as an initial screening for hepatic parenchymal abnormalities such as steatosis, iron overload, and focal lesions, which would preclude liver donation [19]. In the past, CT cholangiography was also used to evaluate the biliary anatomy (Fig. 1.4). However, it is no longer performed as the biliary excreted iodinated contrast agent was removed from the US market a few years ago. Biliary evaluation is now performed via MRCP.

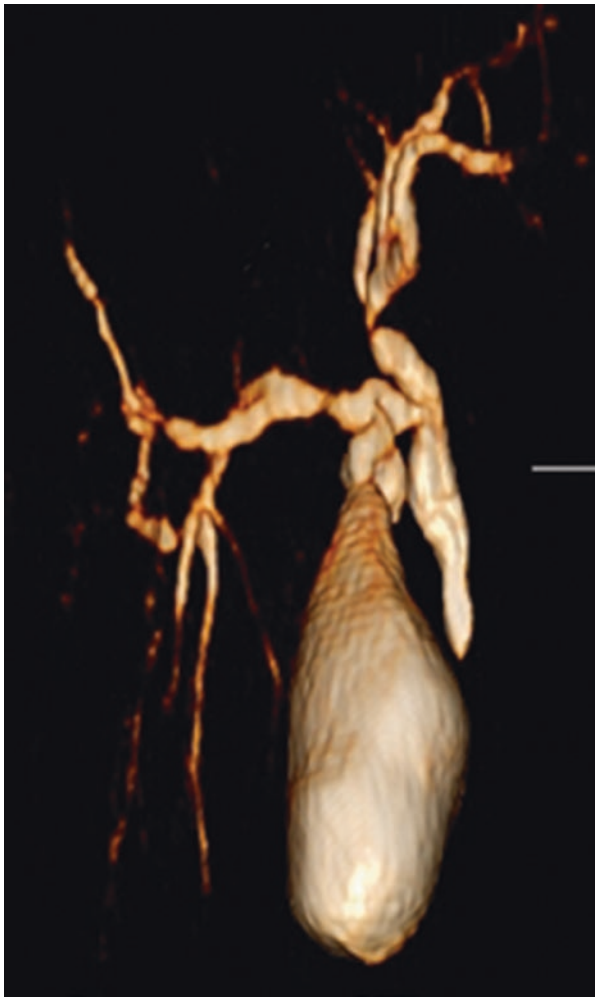

Fig. 1.4 3D reformatted image of a CT cholangiogram showing the common bile duct and intrahepatic biliary ducts

Since liver donors are often young and healthy without other medical comorbidities, reduction in radiation dose for these exams is important. Methods to reduce radiation dose routinely used at our institution include limiting the field of view to the abdomen on arterial phase images, using iterative reconstruction and weight-based kVp techniques (80 kVp if <150 bs, 100 kVp if 150–200 lbs, 120 kVp if >200 lbs) on portal/hepatic venous phase images, and using dual energy techniques (140 and 80 kVp) on only a limited number of thick slices (2–4 slices depending on liver size) for steatosis evaluation.

MRI/MRCP

MRI/MRCP with and without a hepatobiliary contrast agent—Gd-BOPTA (MultiHance) or Gd-EOB-DTPA (Eovist)—is the second examination performed at our institution for evaluation of liver donors. Fat and iron deposition is assessed with Dixon sequences. The biliary system is evaluated with traditional T2-weighted non-contrast-enhanced 3D MRCP images in the coronal plane, T2-weighted SSFSE images in the coronal and axial planes, T1-weighted post-contrast biliary-phase images in the coronal and axial planes, and/or a 20-min delayed post-contrast 3D MRCP. Additionally, focal liver lesions are characterized with traditional T2, T1 pre-contrast, and T1 post-contrast images in the arterial, portal venous, and delayed phases [20, 21]. For all the above, fast pulse sequences such as spoiled gradient echo and parallel imaging techniques are utilized to decrease image acquisition time and minimize motion artifacts.

Image Post-processing

At our institution, all CT and MRI examinations undergo post-processing to allow for evaluation of the anatomy in the ideal plane. For CT examinations, processed images submitted for use at interpretation include standard multi-planar reformations, maximal intensity projection (MIP) 3D reconstructions in the axial plane for evaluation of the hepatic arteries and hepatic veins, maximal intensity projection (MIP) 3D reconstructions in the coronal plane for evaluation of the portal venous system, and volume renderings. Liver volume rendering involves tracing the margins of the hepatic parenchyma on each axial section and summing them into a 3D model. This can either be done manually or with the aid of computer software products which calculate the volumes automatically/semiautomatically [22]. These automated techniques not only drastically decrease processing time, but also improve the reproducibility of measurements [23]. This analysis is performed on the entire liver parenchyma, as well as on individual segments/hepatic lobes. It is used to estimate the size of the liver graft and residual liver in mL and percentage of total liver volume [24]. These volume renderings and vascular MIP models can be

superimposed upon one another for a more detailed delineation of the 3D anatomy. For MRI examinations, 3D T2-weighted MRCP and T1-weighted post-contrast images in the coronal oblique plane are routinely submitted for evaluation of the biliary anatomy.

Preoperative Imaging of the LDLT Donor

Multiple features are assessed during preoperative imaging of the LDLT donor. The vascular and biliary anatomy is defined to identify variants that may change the surgical plan, and the hepatic parenchyma is assessed for steatosis, iron deposition, focal lesions which would preclude donation, and for calculation of volumes of the liver graft and remnant liver. Many potential donors have vascular (44%) and/or biliary (48%) anatomic variants which impact the surgical plan. However, with advances in microvascular surgical techniques, only 1.9% of donors are ultimately excluded for these reasons. More common reasons for liver donor exclusion are inadequate remnant liver volume seen in 21.6% of potential donors, >30% fatty infiltration seen in 10.4% of potential donors, and an anticipated small for size graft seen in 3.4% of donors [25, 26].

Hepatic Arteries

In embryologic hepatic perfusion, the left lateral segment is supplied by the left gastric artery (LGA), the paramedian segment is supplied by the common hepatic artery (CHA), and the right lateral segment is supplied by the superior mesenteric artery (SMA). After a complex pruning and fusion process, this embryologic perfusion pattern is converted into the adult hepatic arterial anatomy. In "classic" hepatic arterial anatomy (Michel type I), the celiac trunk gives off the CHA, which becomes the proper hepatic artery after the takeoff of the gastroduodenal artery (GDA), which then gives off the left, right, and middle hepatic arteries (LHA, RHA, MHA). Though this anatomy is the most common configuration, it is found in only 55% of the population [20, 27]. Nine other variant configurations have been described, in which arteries that *substitute* normal arteries are termed "aberrant" or "replaced" and arteries that persist *in addition* to normal arteries are termed "accessory." In general, replaced and accessory right hepatic arteries arise from the SMA, while replaced and accessory left hepatic arteries arise from the LGA—reminiscent of the embryologic hepatic perfusion pattern described above. These less common variants occur in 0.5–11% of the population, depending on variant type, and are described in more detail in Table 1.1 (Fig. 1.5).

Though these anatomic variations are common, only a handful are surgically relevant, and their relevance depends on the type of LDLT operation being performed [17]. For example, if there is a replaced or accessory *right* hepatic artery and the patient is undergoing a *right* LDLT, arterial ligation will require an extra step.

Table 1.1 Michel classification of hepatic artery anatomy

Type	Frequency of occurrence (%)	Description
I	55	Standard anatomy—RHA, MHA, LHA from CHA
II	10	Replaced LHA from LGA
III	11	Replaced RHA from SMA
IV	1	Replaced RHA from SMA and LHA from LGA
V	8	Accessory LHA from LGA
VI	7	Accessory RHA from SMA
VII	1	Accessory RHA from SMA and LHA from LGA
VIII	4	Replaced RHA and accessory LHA or replaced LHA and accessory RHA
IX	4.5	CHA replaced to SMA
X	0.5	CHA replaced to LGA

RHA right hepatic artery, *MHA* middle hepatic artery, *LHA* left hepatic artery, *CHA* common hepatic artery, *LGA* left gastric artery, *SMA* superior mesenteric artery

Fig. 1.5 CT 3D reformatted image showing Michel IX anatomy with the common hepatic artery replaced to the superior mesenteric artery

The same goes for replaced or accessory *left* hepatic arteries in a potential *full-left* or *left lateral segment* LDLT donor. The two hepatic arterial findings which would render someone ineligible for donation are if the extrahepatic segment of the lobar hepatic artery to be grafted is <2 mm (unable to perform surgical anastomosis) or if the *middle* hepatic artery would not remain in the donor (must be preserved to prevent postoperative hepatic failure).

Hepatic Veins

Hepatic venous variants are less common than arterial variants, seen in 16–33% of the population. However, they are more often surgically relevant since poor venous drainage can lead to postoperative hepatic insufficiency in either the donor or

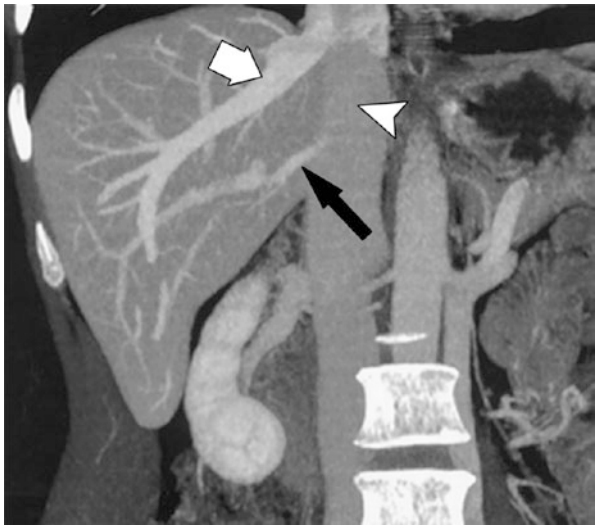

Fig. 1.6 Coronal reformatted image from a contrast-enhanced CT demonstrating an accessory RHV (*black arrow*) draining into the IVC (*white arrow*head), separate from the RHV (*white arrow*). This was separately anastomosed in the recipient. Adapted from Sahani D, Mehta A, Blake M et al., Preoperative hepatic vascular evaluation with CT and MR Angiography: Implications for Surgery, *RadioGraphics* 2004; 24:1367–1380

recipient [26]. Surgically relevant hepatic venous variants affect approximately 30% of LDLT donations [28–30].

As with hepatic arterial variants, different hepatic venous variants affect different types of LDLT operations [17]. For a *right* LDLT, three anatomic variants are relevant: the presence of an accessory vein(s) draining segments VI, VII, and V (Fig. 1.6), drainage of a right hepatic segment into the middle hepatic vein (MHV) rather than the right hepatic vein (RHV) (Fig. 1.7), or drainage of segment IV into the LHV rather than the MHV. For the first two, additional anastomoses are required of the accessory veins to preserve venous drainage of that segment. For the latter, the hepatectomy plane should be moved to the left of the MHV (the MHV will be part of the graft rather than staying with the donor) since it is not required for remnant liver drainage. A *left lateral segment* LDLT becomes slightly more complicated when there is a common trunk of the MHV and LHV; extra care must be taken to ensure the MHV is preserved in the donor for remnant liver drainage. *Full-left* LDLT may be contraindicated in patients with a small RHV and a large MHV draining a significant portion of the right hepatic lobe. Finally, early confluence of the hepatic veins deep within the liver parenchyma complicates all types of LDLT operations and may even be a contraindication to donation.

Since there is a genetic predisposition for hepatic venous variants, the presence of variants in a living related donor should prompt investigation of the recipient venous anatomy as well [28].

Portal Veins

Imaging of the portal veins involves two steps: first, defining the portal venous anatomy, and second, measuring vein diameter at the anticipated sites of anastomoses. Anastomoses between two veins of similar size decreases the risk of thrombosis

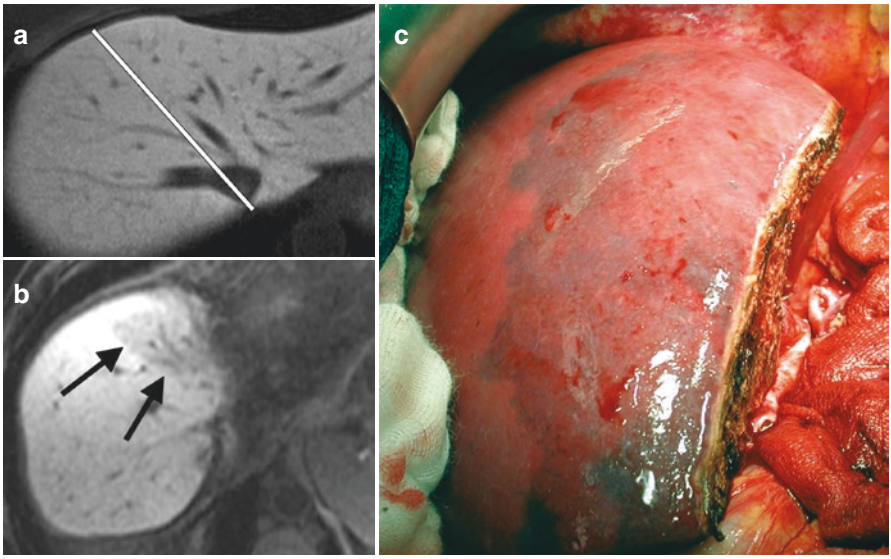

Fig. 1.7 Segment VIII drainage into the MHV. (**a**) Axial T1-weighted preoperative image of a living donor shows a tributary vein draining segment VIII into the MHV. The hemi-hepatectomy plane transects this accessory vein. (**b**) Postoperative axial T1-weighted MR image of the recipient shows atrophy of segment VIII due to inadequate drainage. (**c**) Corresponding intraoperative photograph shows congestion of segment VIII. Adapted from Catalano OA, Singh AH, Uppot RN, et al. Vascular and biliary variants in the liver: implications for liver surgery. *RadioGraphics* 2008; 28:359–378

and/or stenosis—one of the most common portal venous complications of transplantation. As a result, large differences in vein size may change the surgical plan [31].

Portal venous anatomic variants are less common and less often surgically relevant than hepatic arterial and hepatic venous variants. As with the hepatic arterial and hepatic venous variants, the relevance of portal venous variation depends on the type of surgery being performed. The general rule is that portal venous flow to the remnant liver cannot be compromised by the LDLT donation operation. For a *right* LDLT, the left portal vein (LPV) arising from the right anterior portal vein (RAPV) is a relative contraindication to donation. For a *left* LDLT, a RAPV arising from the LPV is a relative contraindication to donation. For both types of LDLT, trifurcation of the main portal vein into an LPV, right posterior portal vein (RPPV), and RAPV affects the surgical plan—in a *right* LDLT, you must anastomose the RPPV and RAPV separately in the recipient, and in a *left* LDLT, you must take care to exclude the RAPV from the graft (Fig. 1.8).

Biliary System

A detailed preoperative analysis of the donor biliary system with MRCP is critical as biliary complications are the most common cause of morbidity post transplant, occurring in up to 40% of patients [31]. A thorough preoperative understanding of

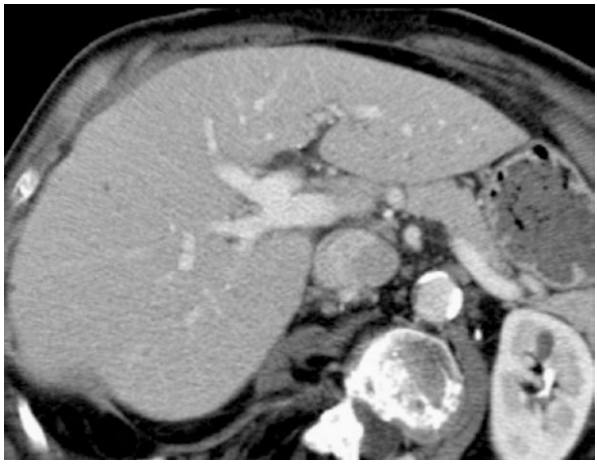

Fig. 1.8 Axial CT scan in the portal venous phase demonstrates trifurcation of the portal veins. Adapted from Burk KS, Singh AK, Vagefi PA, Sahani D, Pretransplantation imaging workup of the liver donor and recipient. *Radiology Clinics of North America* 2016; 54(2):185–197

the donor biliary anatomy decreases the rates of these complications, including bile duct stricture, and bile leak from caudate branches, the hepatic duct stump, or the parenchymal transection surface [17, 21, 32].

Biliary system anatomic variations are associated with portal venous variants, and are seen in up to 33% of the population [33]. As with the other types of anatomic variants described, different biliary variants have different surgical implications depending on the type of LDLT operation being performed [4]. If one of the right hepatic ducts (right posterior hepatic duct (RPHD) or right anterior hepatic duct (RAHD)) drains into the left hepatic duct (LHD), a *right* LDLT will require an additional anastomosis and a *left* LDLT is contraindicated. The converse is true if the LHD drains into one of the RHDs. Trifurcation of the hepatic duct into the RPHD, RAHD, and LHD increases surgical complexity for all types of LDLT operations, as does the presence of an accessory hepatic duct draining a liver segment separately (Fig. 1.9). The latter may be a contraindication to donation, depending on the patient.

Liver Parenchyma

After the vascular and biliary anatomy and considerations have been described, the final step of preoperative donor imaging is evaluation of the liver parenchyma. This involves approximate quantification of hepatic steatosis, detection and characterization of any focal lesions, and measurement of liver volumes.

Greater than 30% fatty infiltration of the liver is considered a contraindication to LDLT donation since the risk of postoperative hepatic insufficiency is markedly increased in both the donor and recipient [34]. On non-contrast-enhanced CT images, this corresponds to hepatic density more than 10 HU below that of the spleen, a hepatic density to splenic density ratio of <0.8, or absolute hepatic density < 40 HU [35–37]. The MRI finding indicative of this degree of steatosis is

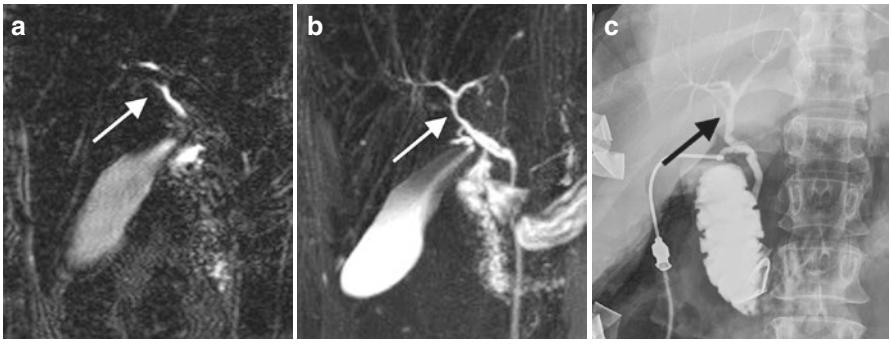

Fig. 1.9 An accessory right posterior hepatic duct (*arrow*) drains into the proximal common hepatic duct. Additionally, a segment IV duct drains into the right anterior hepatic duct. This right LDLT donation was aborted due to these anatomic variants. (**a**) Source coronal T2 image showing the accessory right posterior hepatic duct draining into the CHD. (**b**) MIP coronal T2 MRCP image shows this duct proximal to the bifurcation. (**c**) Intraoperative cholangiogram confirmed the findings. Adapted from Burk KS, Singh AK, Vagefi PA, Sahani D, Pretransplantation imaging workup of the liver donor and recipient. *Radiology Clinics of North America* 2016; 54(2):185–197

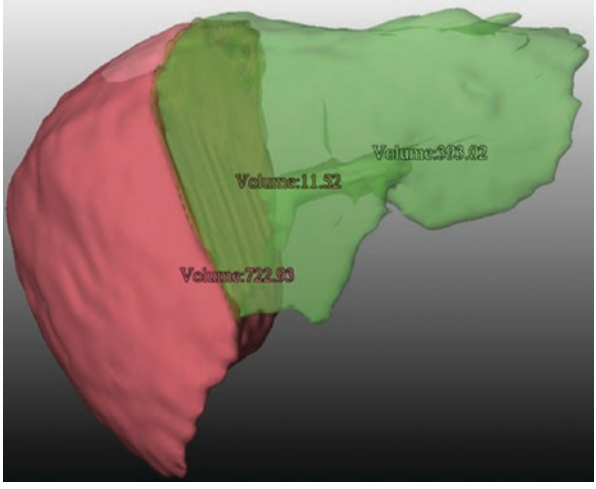

Fig. 1.10 Liver volume imaging with a virtual hepatectomy plane running through the donor liver with calculation of graft and remnant donor liver volumes

greater than or equal to 30% signal drop-out on Dixon in- and out-of-phase images normalized to the spleen (SI inphase-SI outphase/SI inphase × 100, where SI = average liver intensity/average spleen intensity) [38].

Focal liver lesions such as cysts, focal nodular hyperplasia, and hemangiomas are seen in up to 18% of donors. Qualification for liver donation depends upon lesion etiology (benign vs. malignant), size, and location [31]. Finally, the volumes of the remnant liver, liver graft, and total liver are calculated from single breath-hold images (either CT or MRI). Volume ratios are calculated to ensure that >30% of the total liver volume remains in the donor. Additionally, graft volume is compared to recipient body size to predict the risk of small-for-size syndrome in the recipient (Fig. 1.10).

Table 1.2 Pre-LDLT donor imaging report components

Structure evaluated	Components of report
Liver parenchyma	Description of fatty/iron infiltration Characterization of focal lesions
Liver volume	Total liver volume = X Left lobe volume = Y Right lobe volume = Z
Hepatic artery anatomy	Description of normal anatomy or accessory/replaced hepatic arteries The segment IV artery is a branch of X
Portal venous anatomy	Description of bifurcation/trifurcation
Hepatic venous anatomy	Description of three hepatic veins and the common trunk Description of any accessory hepatic veins
Biliary anatomy	Description of bile duct bifurcation/trifurcation Description of any accessory or anomalous ducts

Conclusions

In conclusion, preoperative imaging with CT and MRI/MRCP is critical for the LDLT donor to ensure they are eligible for donation and to make a surgical plan. Hepatic arterial, hepatic venous, portal venous, and biliary anatomic variants can all be significant, though relevance to the surgeon depends on the type of variation and the type of LDLT being performed. Since donors are typically young, healthy patients, risk reduction in imaging with short MRI protocols, efficient use of intravenous contrast, and low radiation doses for CT examinations are important. An understanding of the types and steps of the different LDLT transplant operations can help radiologists craft a meaningful report (Table 1.2).

References

1. optn.transplant.hrsa.gov Accessed 11/13/2016 at 6:36 pm.
2. Kim, WR, Lake JR, Smit, JM et al. OPTN/SRTR 2014 Annual data report: liver.
3. Vagefi PA, Ascher NL, Freise CE, et al. Use of living donor liver transplantation varies with the availability of deceased donor liver transplantation. Liver Transpl. 2012;18(2):160–5.
4. Singh A, Cronin CG, Verma HA, et al. Imaging of preoperative liver transplantation in adults: what radiologists should know. RadioGraphics. 2011;31:1017–30.
5. Humar A, Ramcharan T, Sielaff TD, et al. Split liver transplantation for two adult recipients: an initial experience. Am J Transplant. 2001;1(4):366–72.
6. Vagefi PA, Parekh J, Ascher NL, et al. Ex vivo split-liver transplantation: the true right/left split. HPB (Oxford). 2014;16(3):267–74.
7. Azoulay D, Castaing D, Adam R, et al. Split-liver transplantation for two adult recipients: feasibility and long-term outcomes. Ann Surg. 2001;233(4):565–74.
8. Vagefi PA, Parekh J, Ascher NL, et al. Outcomes with split liver transplantation in 106 recipients: the University of California, San Francisco, experience from 1993 to 2010. Arch Surg. 2011;146(9):1052–9.

9. Yersiz H, Renz JF, Farmer DG, et al. One hundred in situ split-liver transplantations: a single-center experience. Ann Surg. 2003;238(4):496–505; discussion 506–7.
10. Foster R, Zimmerman M, Trotter JF. Expanding donor options: marginal, living, and split donors. Clin Liver Dis. 2007;11(2):417–29.
11. Broering DC, Wilms C, Lenk C, et al. Technical refinements and results in full-right full-left splitting of the deceased donor liver. Ann Surg. 2005;242(6):802–812; discussion 812–3.
12. Wilms C, Walter J, Kaptein M, et al. Long-term outcome of split liver transplantation using right extended grafts in adulthood: a matched pair analysis. Ann Surg. 2006;244(6):865–872; discussion 872–3.
13. Roll GR, Parekh JR, Parker WF, et al. Left hepatectomy versus right hepatectomy for living donor liver transplantation: shifting the risk from the donor to the recipient. Liver Transpl. 2013;19(5):472–81.
14. Abecassis MM, Fisher RA, Olthoff KM, et al. A2ALL Study Group, Complications of living donor hepatic lobectomy—a comprehensive report. Am J Transplant. 2012;12(5):1208–17.
15. Clavien PA, Camargo CA, Croxford R, et al. Definition and classification of negative outcomes in solid organ transplantation: application in liver transplantation. Ann Surg. 1994;220:109–20.
16. Freise CE, Gillespie BW, Koffron AJ, et al. A2ALL Study group, Recipient morbidity after living and deceased donor liver transplantation: findings from the A2ALLRetrospective Cohort Study. Am J Transplant. 2008;8(12):2569–79.
17. Catalano OA, Singh AH, Uppot RN, et al. Vascular and biliary variants in the liver: implications for liver surgery. RadioGraphics. 2008;28:359–78.
18. Guiney MJ, Kruskal JB, Sosna J, et al. Multi–detector row CT of relevant vascular anatomy of the surgical plane in split-liver transplantation. Radiology. 2003;229(2):401–7.
19. Schroeder T, Malagó M, Debatin JF, et al. "All-in-one" imaging protocols for the evaluation of potential living liver donors: comparison of magnetic resonance imaging and multidetector computed tomography. Liver Transpl. 2005;11:776–87.
20. Hennedige T, Anil G, Madhavan K. Expectations from imaging for pre-transplant evaluation of living donor liver transplantation. World J Radiol. 2014;6(9):693–707.
21. Goldman J, Florman S, Varotti G, et al. Non-invasive preoperative evaluation of biliary anatomy in right-lobe living donors with mangafodipir trisodium-enhanced MR cholangiography. Transplant Proc. 2003;35(4):1421–2.
22. Fananapazir G, Bashir MR, Marin D, Boll DT. Computer-aided liver volumetry: performance of a fully-automated, prototype post-processing solution for whole-organ and lobar segmentation based on MDCT imaging. Abdom Imaging. 2015;40(5):1203–12.
23. Gotra A, Chartrand G, Massicotte-Tisluck K, Morin-Roy F, et al. Validation of a semi-automated liver segmentation method using CT for accurate volumetry. Acad Radiol. 2015;22(9):1088–98.
24. Kazemier G, Hesselink EJ, Lange JF, Terpstra OT. Dividing the liver for the purpose of split grafting or living related grafting: a search for the best cutting plane. Transplant Proc. 1991;23(1 pt 2):1545–6.
25. Tsang LL, Chen CL, Huang TL, et al. Preoperative imaging evaluation of potential living liver donors: reasons for exclusion from donation in adult living donor liver transplantation. Transplant Proc. 2008;40(8):2460–2.
26. Sahani D, Mehta A, Blake M, et al. Preoperative hepatic vascular evaluation with CT and MR angiography: implications for surgery. Radiographics. 2004;24:1367–80.
27. Michel NA. Blood supply and anatomy of the upper abdominal organs with a descriptive atlas. Philadelphia: Lippincott; 1955. p. 64–9.
28. Fan ST, Lo CM, Liu CL. Technical refinement in adult-to-adult living donor liver transplantation using right lobe graft. Ann Surg. 2000;231:126–31.
29. Kennedy PA. Surgical anatomy of the liver. Surg Clin North Am. 1977;57:233–44.
30. Huguet C. Technique of hepatic vascular exclusion for extensive liver resection. Am J Surg. 1992;163:602–5.

31. Sahani D, D'souza R, Kadavigere R, et al. Evaluation of living liver transplant donors: method for precise anatomic definition by using a dedicated contrast-enhanced MR imaging protocol. RadioGraphics. 2004;24:957–67.
32. Itamoto T, Emoto K, Mitsuta H, et al. Safety of donor right hepatectomy for adult-to-adult living donor liver transplantation. Transpl Int. 2006;19(3):177–83.
33. Lee VS, Morgan GR, Lin JC, et al. Liver transplant donor candidates: associations between vascular and biliary anatomic variants. Liver Transpl. 2004;10(8):1049–54.
34. Piekarski J, Goldberg HI, Royal SA, Axel L, Moss AA. Difference between liver and spleen CT numbers in the normal adult: its usefulness in predicting the presence of diffuse liver disease. Radiology. 1980;137:727–9.
35. Boll DT, Merkle EM. Diffuse liver disease: strategies for hepatic CT and MR imaging. Radiographics. 2009;29:1591–614.
36. Kodama Y, Ng CS, Wu TT, et al. Comparison of CT methods for determining the fat content of the liver. AJR Am J Roentgenol. 2007;188:1307–12.
37. Park SH, Kim PN, Kim KW, et al. Macrovesicular hepatic steatosis in living liver donors: use of CT for quantitative and qualitative assessment. Radiology. 2006;239:105–12.
38. Kreft BP, Tanimoto A, Baba Y, et al. Diagnosis of fatty liver with MR imaging. J Magn Reson Imaging. 1992;2:463–71.

Chapter 2
Preoperative Imaging Evaluation of Living Kidney Transplant Donors

Daniel Helmy, Christoph Troppmann, and Ghaneh Fananapazir

Introduction

Kidney transplantation is considered the treatment of choice for most patients with end-stage renal disease and is associated with improved mortality rates compared to maintenance on dialysis [1]. Kidney donation may occur from living or deceased donors. While the overall demand for kidney grafts has grown, the number of deceased donor kidneys available for transplantation has not increased. Fortunately, the number of living donors has increased, especially in the United States, where kidneys from living donors comprise almost half of the kidney donors [2]. Kidneys from live donors can eliminate the considerable time (i.e., up to 10 years) that transplant candidates may have to wait for a deceased donor kidney and have significantly better short-term and long-term outcomes when compared with those from deceased donors [3]. For the live kidney donor, there can be profound psychosocial gain from the donation, which can help to justify the risk associated with the procedure. Because live donors are by definition very healthy individuals with an above-average life expectancy, the medical and psychosocial assessment of live donor candidates must adhere to very strict standards in order to minimize the short-term (i.e., perioperative) risk and long-term (e.g., chronic kidney disease) risk [4]. Potential kidney donors have an extensive review of their medical history, a thorough physical examination, and undergo extensive laboratory, cardiac, and imaging evaluations. If a donor has one kidney that is slightly abnormal or functions suboptimally, this kidney is generally transplanted to leave the donor with the "healthier"

D. Helmy, M.D. • G. Fananapazir, M.D. (✉)
Department of Radiology, University of California Davis Medical Center, Sacramento, CA, USA
e-mail: fananapazir@ucdavis.edu

C. Troppmann, M.D.
Department of Surgery, University of California Davis Medical Center, Sacramento, CA, USA

G. Fananapazir, R. Lamba (eds.), *Transplantation Imaging*,
https://doi.org/10.1007/978-3-319-75266-2_2

kidney. Any significant abnormalities in one of the donor candidate's kidneys will generally preclude donation. Anatomical abnormalities that may affect the decision to proceed with donation include cortical scarring, renal cysts and masses, renal stones, duplicated collecting system, ureteropelvic junction obstruction, and major arterial and venous anomalies and variants. Preoperative imaging plays a crucial role in the evaluation for these abnormalities and variants and must depict the renal vasculature to the highest possible detail [5].

Imaging Techniques

Historically, preoperative imaging for potential living kidney donors included intravenous urography (IVU) to evaluate the urinary tract and conventional angiography to evaluate the renal vasculature [6]. However, conventional angiography is an invasive procedure that carries its own set of risks and is limited in its evaluation of the parenchyma and venous system. Additionally, the performance of IVU and conventional angiography has to be split over 2 days. The appeal for evaluating living kidney donors with computed tomography angiography (CTA) was quickly realized and replaced conventional angiography in the early- to mid-1990s since CTA allows for evaluation not only of the arteries and veins but also of the parenchyma and ureters [7]. Early studies showed that CTA had high agreement with findings at surgery and led to a 35–50% cost reduction compared to preoperative evaluation by conventional angiography and IVU [8, 9].

In most institutions, CT remains the modality of choice in the preoperative evaluation of living renal donors [10]. CT can accurately depict the arterial and venous anatomy as well as parenchymal abnormalities. Typically, multiple phases are required: noncontrast, arterial, nephrographic, and urographic. A noncontrast CT scan provides ideal viewing for renal calculi and atherosclerotic calcifications as well as providing a base for assessing for renal lesion enhancement. Arterial-phase CT provides the best information for arterially enhancing renal masses in addition to depicting both arteries and veins. Venous drainage from the kidney is rapid, and arteries and veins are better contrasted on arterial-phase images than on more delayed images. Therefore, the arterial phase is also useful in the depiction of the kidneys' venous outflow. The nephrographic phase allows for optimal visualization of hypovascular renal masses and can be used to evaluate draining veins not seen on the arterial phase [11]. Finally, a urographic phase can be obtained to evaluate the collecting system and ureters. The radiation dose of such a large number of CT phases can be quite significant. However, several newer techniques can be applied to decrease the number of phases and thus the radiation exposure. These include use of dual-energy CT scans to create virtual unenhanced images, split-bolus techniques to combine phases, and CT topogram during the urographic phase to provide urographic information. Using such techniques, it is feasible to perform a donor CT examination in a single phase; however, this can be technically challenging [12, 13].

Some institutions rely primarily on MRI for assessing the living donor. MRI has the advantage of not subjecting the often younger donor candidates to ionizing radiation. MRI in the preoperative setting has yielded promising results. With intraoperative findings as the reference standard, contrast-enhanced MRA has shown comparable results to conventional angiography in depicting renal arterial anatomy and is superior in evaluating renal venous anatomy [14]. In comparing MRA with CTA, Liefeldt et al. found that while MRA performed equally well to CTA in depicting renal venous and ureteral anatomy, CTA was superior in depicting renal arterial anatomy [15]. Bhatti et al. also found that CTA outperformed CE-MRA not only in depicting renal arteries but also the veins [16]. Other studies have found equivalent performance of MR and CT in describing renal vascular anatomy [17, 18]. Gulati et al. found that CTA and MRA were equal in describing arterial anatomy; however, CTA was superior for depicting venous anatomy, stones, and upper urinary tract variants [19].

While improvements in MR technique are promising and may indicate a future in which living renal donors may avoid ionizing radiation, presently CT remains the first-line modality for preoperative evaluation of living renal donors at most institutions because of its superiority in depicting renal vasculature and renal calculi. Additionally, MRI is more operator-dependent, time-consuming, more expensive, and less widely available. Additionally, the lengthened scanning times of MRI compared with CT are less well tolerated. In one study, 10% of patients withdrew from pre-donation screening with MRI owing to claustrophobia [20].

Preoperative Imaging of the Living Kidney Donor

Renal Parenchyma

Information about the renal parenchyma can provide absolute and relative contraindications to renal transplant, can direct a surgeon to specifically procure the left versus the right kidney, and can give prognostic clues as to the future function of a transplanted kidney.

Kidney Size

Kidney size has been correlated with future renal function in the recipient, and if there is a substantial difference in size (i.e., function) between both kidneys, the donor should be left with the larger kidney. Therefore, measurement of both kidneys is important in kidney donor candidates.

Both length and volume of kidneys have been correlated with future function and both are typically reported. However, the renal length measurement in the coronal plane is subject to greater variability since the lie of the kidney is variable. While a multiplanar reformatted image can provide the most accurate renal length, the

multi-image sagittal closely approximates this measurement and is more readily measurable [21]. Kidney volume is part of the routine report of a living kidney donor CT. Kidney volumes are also preferred to simple kidney length measurements in order to determine whether the donor candidates' global renal function is evenly distributed between both kidneys (as discussed above, this parameter may drive the decision regarding which kidney to recover for transplantation). Donor kidney volume also correlates directly with subsequent recipient glomerular filtration rate [22]. Multiple studies have demonstrated that larger kidney volume predicts better post-transplant graft outcomes [23]. Additionally, smaller kidney volume is associated with a greater risk of delayed graft function [24]. Volume measurement can usually be done in a semiautomated fashion using post-processing software and is usually not too time-consuming.

Better recipient renal function with larger kidney volume is likely related to the direct relationship between the number of nephrons, the functional unit of the kidney, and the whole kidney volume. This hypothesis is supported by studies which suggest that the volume of the renal cortex rather than the overall kidney volume may in fact more accurately predict post-transplant graft function [25, 26].

Anatomic Abnormalities

There are specific anatomic abnormalities of the kidney that are contraindications to transplant. Absolute contraindications include unilateral agenesis, medullary sponge kidney, autosomal dominant polycystic kidney disease (ADPKD), horseshoe kidney, and severe cortical atrophy (Fig. 2.1). Patients with one or two mild parenchymal scars and many of those with lesser forms of ectopia can potentially proceed with donation, although this is institution-dependent. In the case of scarring, the kidney with the scar(s) is typically chosen for donation [10].

Renal Masses and Cysts

The most commonly encountered solid renal masses of the kidney include renal cell carcinoma, angiomyolipoma, and oncocytoma. Donation of kidneys with solid renal masses is controversial but can be performed, even in cases where these

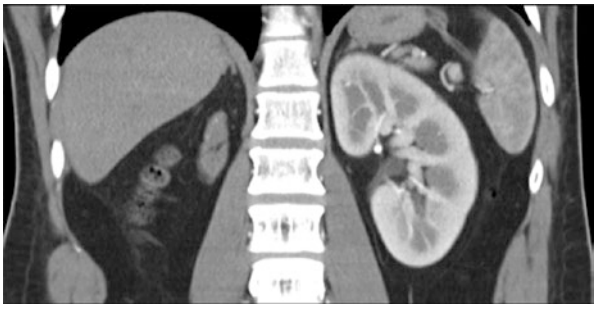

Fig. 2.1 Coronal CT image in the arterial phase demonstrates severe atrophy of the right kidney with compensatory hypertrophy of the left kidney in a potential kidney donor

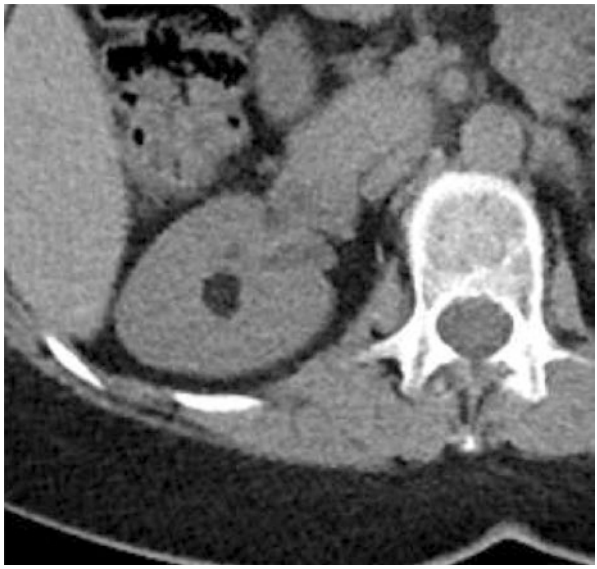

Fig. 2.2 Axial CT image without contrast demonstrates a fat-density mass in the right kidney consistent with an angiomyolipoma

represent small renal cell carcinomas [27]. While imaging can sometimes be diagnostic for classic angiomyolipomas (Fig. 2.2), lipid-poor angiomyolipomas, renal cell carcinomas, and oncocytomas can have overlapping radiologic appearances. In clear-cut cases of malignant solid enhancing masses, the potential donor would be precluded from donation and appropriate urologic follow-up obtained. However, in cases of small, often indeterminate solid masses, some institutions will procure the affected kidney, perform a back-table resection of the lesion, and obtain surgical pathological evaluation prior to implantation. If pathology shows the lesion to be benign, then surgical implantation of that kidney can proceed. However, if pathology shows a renal cell carcinoma with negative surgical margins, then the affected kidney may still be implanted, although this approach is somewhat controversial and will be institution-specific [27, 28]. What is important from a radiologist's standpoint is to correctly identify such lesions, which may be challenging when they are small. Small solid lesions can sometimes be more conspicuous on the arterial or nephrographic phases depending on their vascularity and their (peripheral versus central) location. If a donated kidney with an unresected renal cell carcinoma were to be transplanted, it could have dire consequences for the recipient, as malignant tumors can grow and disseminate rapidly in an immunocompromised patient.

Renal angiomyolipomas are the most common solid renal mass, with an overall prevalence of 0.6% in women and 0.3% in men [29]. Most angiomyolipomas are predominantly fatty tumors and are easily diagnosed; however, 4.5% of angiomyolipomas are lipid-poor and may be indistinguishable from other solid renal masses [30]. Kidneys with small angiomyolipomas can be safely donated [27]. If an angiomyolipoma in a donated kidney is large, it may be amenable to resection after the recovery ex vivo on the back table prior to implantation. If there are multiple angiomyolipomas, syndromes such as tuberous sclerosis should be ruled out as these may preclude donation.

Cysts within kidneys are common and considered normal in older patients. Simple renal cysts are thin-walled, well-marginated, fluid-attenuating (0–20 HU) lesions which do not enhance with IV contrast (<20 HU change on post-contrast phases) and are found in 30–40% of individuals receiving CT scans [31, 32]. Simple renal cysts do not in principle represent a contraindication to donation and transplant (except in cases of large or endophytic or completely intraparenchymal cysts that replace a substantial amount of functional parenchyma). The risk of malignancy of more complex renal cysts remains near 0% even if there are a few, thin septations or calcifications that are too thin to measure. These can be confidently diagnosed by CT and should be described according to the Bosniak system [33]. Bosniak IIF and more complex lesions should be further evaluated for potential malignancy before donation. If a donor candidate is ultimately diagnosed with a unilateral Bosniak IIF cyst, then donation of the affected kidney may still proceed. If that cyst is not amenable to ex vivo resection on the back table, the recipient will require regular follow-up according to prevailing medical standards. Conversely, bilateral Bosniak IIF cysts in a donor would preclude donation.

The presence of cysts at an early age or the presence of multiple cysts in older should raise the concern for ADPKD. Specifically in patients with risk factors for ADPKD, the presence of two cysts in either kidney in the 15–29-year-old population, two cysts in each kidney in the 30–59-year-old population, or four cysts in each kidney in the ≥60-year-old population is diagnostic for the disease [34]. ADPKD is a contraindication to donation. Besides the radiologic imaging assessment for ADPKD, genetic testing of donor candidates has become widely available and further enhances the donor selection process for individuals at risk for ADPKD.

Renal lesions smaller than 1 cm are subject to volume averaging and pseudoenhancement on CT. Thus, they are often too small to confidently characterize. While the follow-up for such lesions is institution-dependent, follow-up imaging with MRI can lead to a confident diagnosis 99% of the time and can sometimes alter the side of kidney donation [35].

Renal Arteries

During laparoscopic donor nephrectomy, surgeons must correctly identify and divide the donor kidney's arterial inflow vessel(s) while preserving maximal vessel length for the recipient surgeon. The decision regarding which kidney to recover may also be driven at least in part by the number, location, and length of the renal arterial vessel(s). Detailed reporting of a donor's renal arterial anatomy is thus essential for surgical planning.

Accessory Renal Arteries

Classically, a single renal artery branches from the aorta and enters the kidney through the renal hilum, where it branches into segmental arteries. This occurs in over 70% of kidneys [36]. Variants in renal arterial origin and number exist. Renal

arteries may originate from the common iliac, internal iliac, inferior mesenteric, or other intra-abdominal arteries [37]. Multiplicity in renal arteries occurs in about 20% of the general population (Fig. 2.3) [38]. The presence of multiple renal arteries renders the laparoscopic kidney recovery more complex and complication-prone. Transplantation of a kidney with multiple arteries can require a lengthier and more complex back-table preparation of the graft, leading to increased ischemic times; however, short- and long-term outcomes are not affected [38–40]. In a kidney with multiple renal arteries, the largest renal artery by diameter is referred to as the main renal artery and the others are accessory renal arteries. Most accessory renal arteries enter the hilum, but some enter the kidney in the superior or inferior pole, penetrating the renal cortex. These are referred to as polar arteries (Fig. 2.4). Superior polar arteries less than 2 mm in diameter are typically sacrificed during the transplantation process as the small parenchymal loss does not adversely affect graft function. Polar branches to the inferior pole are considered more important since they may also provide arterial supply to the proximal ureter and may, if not carefully preserved, result in ureteral necrosis. Polar arteries may be difficult to distinguish from capsular arteries, which are typically very small in size and supply the capsule of the kidney rather than the parenchyma itself (Fig. 2.5). These will not pierce the

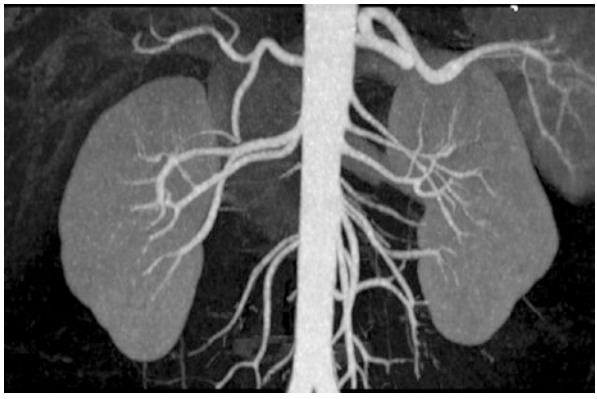

Fig. 2.3 Coronal CT MIP image in the arterial phase demonstrates multiple left renal arteries in a potential kidney donor. Additionally, the right renal artery demonstrates early branching

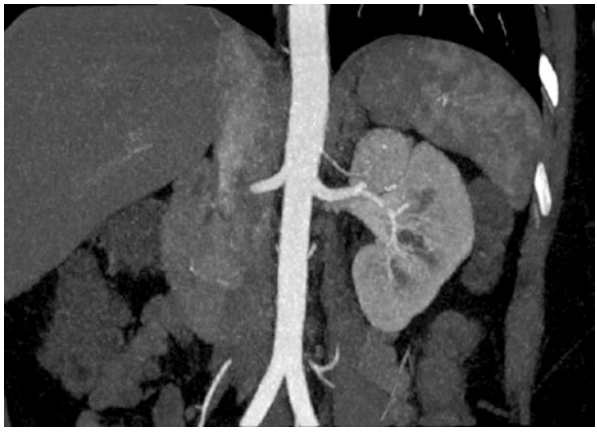

Fig. 2.4 Coronal CT MIP image in the arterial phase demonstrates a superior polar artery to the left kidney in a potential donor. This patient ultimately donated the left kidney uneventfully. The superior polar artery seen in this image was sacrificed during surgery

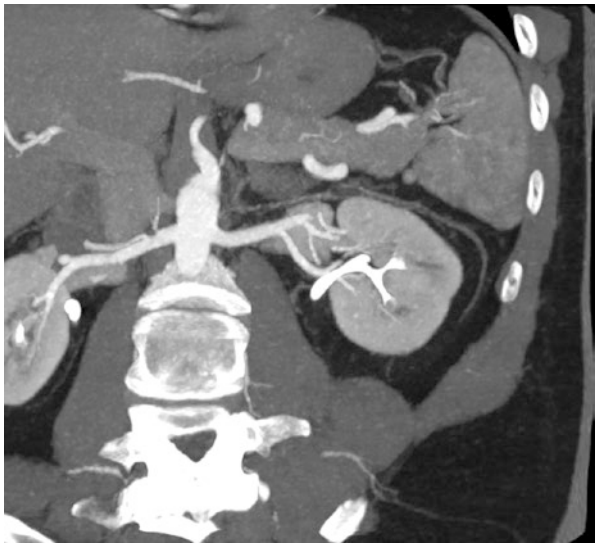

Fig. 2.5 Multiplanar reformatted MIP image during the arterial phase demonstrates a capsular artery to the left kidney of a potential kidney donor

kidney but will be seen on multiplanar reformatted images to be coursing tangential to the kidney parenchyma.

Early Branching

Although renal arteries typically branch into segmental arteries after entering the renal hilum, early branching can also occur (Fig. 2.6). Before arteries are surgically divided, they need to be secured to prevent them from bleeding. In the past era of open nephrectomy, arteries were most commonly suture-ligated, oversewn, or both, which allowed for very short remnant vascular stumps on the aorta. In the current laparoscopic era, vascular staplers, which staple the vessel off and divide it in a single step, are most commonly used for this important operative step. Due to the width of these staplers' jaws, 1–1.5 cm of arterial length is "used" to accommodate the staple lines and the area where the linear cut is made by the stapler. If an extrahilar arterial branching point would likely be covered (and thus divided) by the vascular stapler, it is referred to as early branching. Division of a renal artery at, or in the vicinity of, an early branching point will result in a graft with two renal arteries, which will typically need to be surgically reconstructed ex vivo on the back table prior to implantation. Information about early branching is thus crucial for surgical planning—with respect to the choice of the kidney to be recovered (left versus right), for donor nephrectomy operation, and for the post-recovery back-table reconstruction. In the case of the left kidney, early branching is defined as a distance from the left lateral margin of the aorta to the first branch of less than

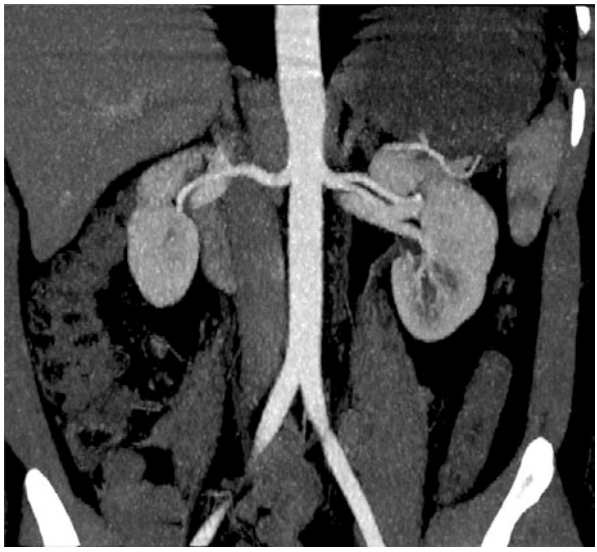

Fig. 2.6 Coronal CT MIP image in the arterial phase demonstrates early branching of the left renal artery in a potential kidney donor

1–2 cm (depending on the institution). In the case of the right renal artery, any branching behind the inferior vena cava to 1 cm from the right lateral margin of the inferior vena cava is considered early branching.

Other Considerations

Atherosclerosis of the abdominal vessels is common and of increasing relevance as the donor pool has considerably broadened over the past decade and now includes donor candidates of more advanced age and with preexisting medical conditions. Atherosclerosis may involve the origin of the renal artery. In cases with atheromatous plaque at the level of renal artery ostium, the renal artery may require shortening during the back-table preparation to remove the atheromatous area prior to implantation. A kidney with plaque extending or present higher up toward the hilum would not typically be procured for transplant.

Fibromuscular dysplasia is a non-atheromatous, noninflammatory disease process involving abnormal collagen deposition within the wall of medium-sized arteries which can lead to stenosis, aneurysm, dissection, and occlusion. The carotid and renal arteries are most commonly affected. These vessels classically demonstrate a "string of beads" appearance on CT angiography. The presence of bilateral fibromuscular dysplasia will most often preclude donation (Fig. 2.7). If this disease is unilateral, donation would be directed toward the kidney with fibromuscular dysplasia. However, patients with unilateral fibromuscular dysplasia can later develop

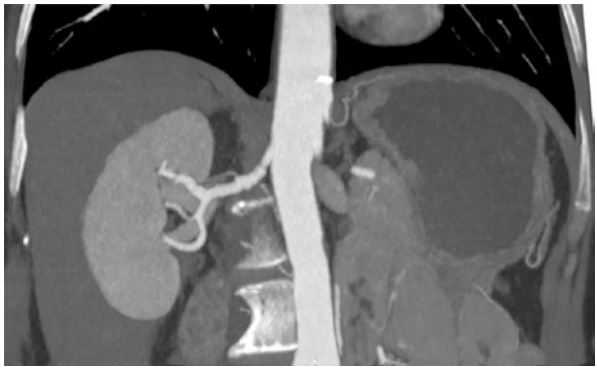

Fig. 2.7 Multiplanar reformatted MIP image during the arterial phase demonstrates a beaded appearance, classic for fibromuscular dysplasia, of the right renal artery in a potential kidney donor

bilateral disease. Therefore, if the patient is young and disease is unilateral, donation may be contraindicated; however, if the patient is older, donation may not have adverse outcomes for the donor [41].

Renal Veins

The right and left renal veins lie anterior to the renal arteries and drain directly into the inferior vena cava. The right renal vein is shorter, measuring on average 2.5 cm in length, while the left renal vein measures 7.5 cm. Because of the difference in renal vein length, the left kidney is usually the default choice for procurement if all other factors are equal. The right renal vein is more frequently duplicated than the left; 7% of patients undergoing imaging studies have multiple right renal veins, compared with 1–2% having multiple left renal veins [42, 43]. The right renal vein usually receives no tributaries over its short course. The left renal vein generally receives drainage from the left adrenal, left gonadal, and retroperitoneal veins such as the ascending lumbar and hemiazygos veins. As a general rule, venous tributaries from extrarenal organs should be reported if they are greater than 5 mm in diameter, as surgical awareness of veins of this size minimizes the risk for complications and as special techniques for surgical division may be required.

The left renal vein shows more complex variability than its right counterpart. Classically, it crosses the aorta anteriorly. However, the left renal vein may take a completely retro-aortic course, referred to as a retro-aortic left renal vein (3% prevalence) (Fig. 2.8), or may split into a double (ante- and retro-aortic) left renal vein and form a "renal collar" around the aorta, referred to as a circumaortic left renal vein (17% prevalence) [44, 45]. Raising the recovering surgeon's awareness of these important anatomical variants preoperatively is paramount in order to minimize intraoperative, potentially avoidable complications. For instance, retro-aortic left renal veins take an oblique course, as opposed to the straight transverse course of a regular ante-aortic left renal vein, from the kidney hilum toward the distal inferior

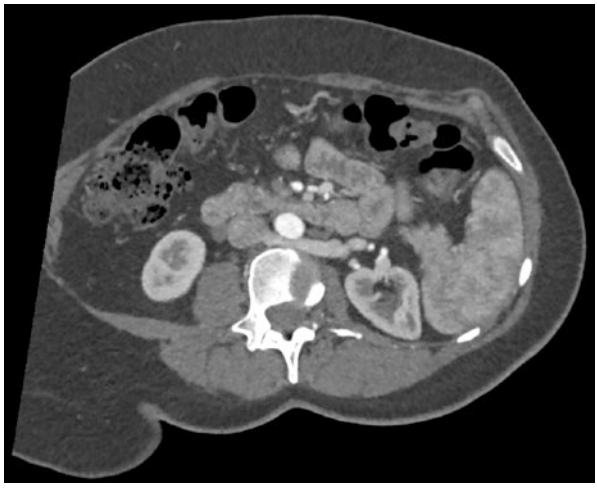

Fig. 2.8 Multiplanar reformatted CT image in the arterial phase demonstrates a retro-aortic left renal vein in a potential kidney donor

vena cava. Thus they are much more susceptible to surgical injury and bleeding if this variant is not known to be present when starting a donor nephrectomy.

Collecting System

Ureteropelvic junction obstruction should be suspected in cases of hydronephrosis and caliectasis with a transition point to a normal caliber ureter at the ureteropelvic junction. This should be distinguished from an extrarenal pelvis (in which case there is usually no caliectasis), and confirmation of obstruction can be obtained from furosemide renography. Ureteropelvic junction obstruction can be bilateral, in which case the patient may not proceed to donation; however, if it is unilateral, the affected side would be chosen for procurement [46].

Duplication of the urinary collecting system is an anatomic variation present in about 0.2% of the population (Fig. 2.9) [47]. Renal duplication can be partial or complete. In partial duplication, separate renal pelvises of the upper and lower poles drain into separate ureters, which later fuse into one ureter before emptying into the bladder. In complete duplication, ureters empty separately. The upper pole ureter inserts ectopically medial and inferior to the insertion of the lower pole ureter. The lower pole is orthotopic in its insertion into the bladder but is susceptible to urinary reflux [48].

Ureteral duplication is not a contraindication to renal transplantation; however, it is important for surgical planning. A surgeon should be made aware of a duplicated system so as to avoid separating the ureters during living donor nephrectomy. Separation of the ureters may partly disrupt blood supply, and the resultant ischemia can lead to ureteral strictures. The radiologist should also search for infundibular stenosis and papillary necrosis on pre-donation imaging studies.

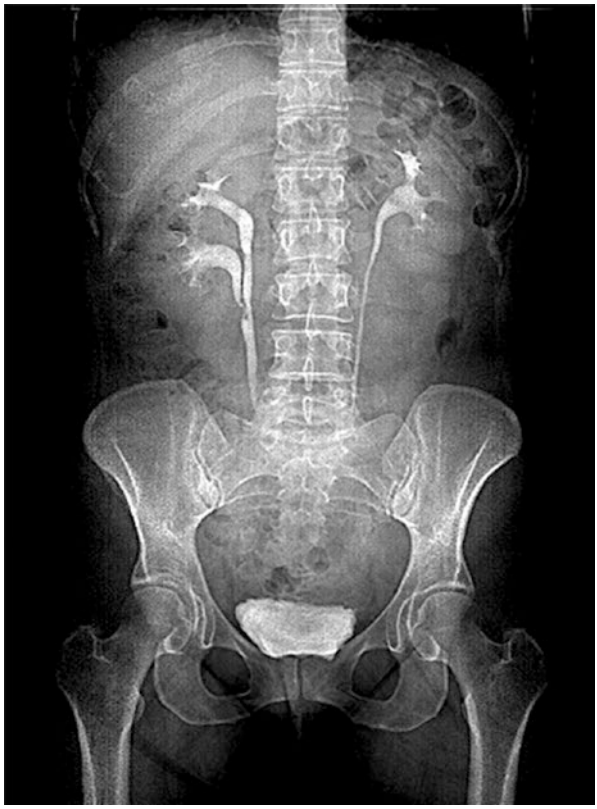

Fig. 2.9 Scout CT image during the urographic phase demonstrates a duplicated collecting system of the right kidney in a potential kidney donor

Nephrolithiasis

Renal and ureteral stones are common in asymptomatic patients. In donor candidates, the evaluation must gauge the risk for future stone disease and for the development for urolithiasis-related chronic kidney disease. For the post-transplant management of recipients of a live donor kidney, it is important to know whether the kidney contains a preexisting stone as that information might expedite the work-up in case of graft dysfunction or suspected ureteral obstruction. Therefore, documentation of the presence and size of kidney stones on CT is important. The mere presence of urinary stones is not necessarily considered a contraindication to donation [49]. Donors in whom urinary stones are found may be screened for underlying metabolic abnormalities that would predict recurrence of stones after nephrectomy. In the absence of underlying disease, donation may proceed and stones may be treated pre- or intraoperatively or will simply be followed in the recipients of those kidneys. MRI has limited sensitivity for detection of stones, and a pre-donation MRI may be coupled with an abdominal radiograph or unenhanced CT through the level of the kidneys.

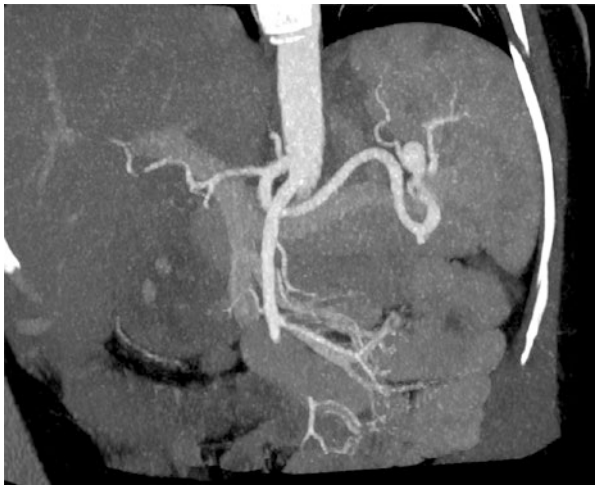

Fig. 2.10 Multiplanar reformatted MIP image during the arterial phase demonstrates an incidental splenic artery aneurysm in a potential kidney donor

Extra-Genitourinary Findings

Findings outside of the genitourinary system and its vascularity can be important in the donation decision-making process. On the pre-donation CT (or MRI), the lung bases and cardiac size can be assessed, as diseases of both these organs can be a contraindication to donation. Incidental tumors identified in the liver, spleen, pancreas, or bowel also deserve a full work-up as any malignancy will preclude donation. Finally, the overall health of the vascular system is important to note. An incidental aneurysm—such as a splenic aneurysm (Fig. 2.10)—or atherosclerotic disease will alert the transplant team to underlying vascular pathology which may also preclude donation and will allow the donor candidate to be referred for further evaluation and screening.

References

1. Ojo AO, Hanson JA, Meier-Kriesche H-U, Okechukwu CN, Wolfe RA, Leichtman AB, et al. Survival in recipients of marginal cadaveric donor kidneys compared with other recipients and wait-listed transplant candidates. J Am Soc Nephrol. 2001;12(3):589–97.
2. Karam G, Kälble T, Alcaraz A, Aki F, Budde K, Humke U, et al. Guidelines on renal transplantation. European Association of Urology. 2013;7.
3. Nemati E, Einollahi B, Pezeshki ML, Porfarziani V, Fattahi MR. Does kidney transplantation with deceased or living donor affect graft survival? Nephrourol Mon. 2014;6(4):e12182.
4. Reimer J, Rensing A, Haasen C, Philipp T, Pietruck F, Franke GH. The impact of living-related kidney transplantation on the donor's life. Transplantation. 2006;81(9):1268–73.
5. Kawamoto S, Montgomery RA, Lawler LP, Horton KM, Fishman EK. Multi–detector row CT evaluation of living renal donors prior to laparoscopic nephrectomy. Radiographics. 2004;24(2):453–66.

6. Riehle R Jr, Steckler R, Naslund E, Riggio R, Cheigh J, Stubenbord W. Selection criteria for the evaluation of living related renal donors. J Urol. 1990;144(4):845–8.
7. Rubin GD, Leipsic J, Schoepf UJ, Fleischmann D, Napel S. CT angiography after 20 years: a transformation in cardiovascular disease characterization continues to advance. Radiology. 2014;271(3):633–52.
8. Rubin GD, Alfrey EJ, Dake MD, Semba CP, Sommer FG, Kuo PC, et al. Assessment of living renal donors with spiral CT. Radiology. 1995;195(2):457–62.
9. Cochran S, Krasny R, Danovitch G, Rajfer J, Barbaric Z, Wilkinson A, et al. Helical CT angiography for examination of living renal donors. AJR Am J Roentgenol. 1997;168(6):1569–73.
10. Sebastià C, Peri L, Salvador R, Buñesch L, Revuelta I, Alcaraz A, et al. Multidetector CT of living renal donors: lessons learned from surgeons. Radiographics. 2010;30(7):1875–90.
11. Yuh BI, Cohan RH. Different phases of renal enhancement: role in detecting and characterizing renal masses during helical CT. AJR Am J Roentgenol. 1999;173(3):747–55.
12. Kawamoto S, Lawler LP, Fishman EK. Evaluation of the renal venous system on late arterial and venous phase images with MDCT angiography in potential living laparoscopic renal donors. Am J Roentgenol. 2005;184(2):539–45.
13. Kahn J, Grupp U, Rotzinger R, Kaul D, Schäfer M-L, Streitparth F. CT for evaluation of potential renal donors–how does iterative reconstruction influence image quality and dose? Eur J Radiol. 2014;83(8):1332–6.
14. Giessing M, Kroencke TJ, Taupitz M, Feldmann C, Deger S, Turk I, et al. Gadolinium-enhanced three-dimensional magnetic resonance angiography versus conventional digital subtraction angiography: which modality is superior in evaluating living kidney donors? Transplantation. 2003;76(6):1000–2.
15. Liefeldt L, Klüner C, Glander P, Giessing M, Budde K, Taupitz M, et al. Non-invasive imaging of living kidney donors: intraindividual comparison of multislice computed tomography angiography with magnetic resonance angiography. Clin Transplant. 2012;26(4):E412–E7.
16. Bhatti AA, Chugtai A, Haslam P, Talbot D, Rix DA, Soomro NA. Prospective study comparing three-dimensional computed tomography and magnetic resonance imaging for evaluating the renal vascular anatomy in potential living renal donors. BJU Int. 2005;96(7):1105–8.
17. Rankin S, Jan W, Koffman C. Noninvasive imaging of living related kidney donors: evaluation with CT angiography and gadolinium-enhanced MR angiography. Am J Roentgenol. 2001;177(2):349–55.
18. Gluecker TM, Mayr M, Schwarz J, Bilecen D, Voegele T, Steiger J, et al. Comparison of CT angiography with MR angiography in the preoperative assessment of living kidney donors. Transplantation. 2008;86(9):1249–56.
19. Gulati M, Dermendjian H, Gómez AM, Tan N, Margolis DJ, Lu DS, et al. 3.0 Tesla magnetic resonance angiography (MRA) for comprehensive renal evaluation of living renal donors: pilot study with computerized tomography angiography (CTA) comparison. Clin Imaging. 2016;40(3):370–7.
20. Blankholm AD, Pedersen BG, Stausbøl-Grøn B, Andersen G, Hørlyck A, Østrat EØ, et al. Preoperative planning of renal transplantation: a comparison of non-contrast-enhanced ultrasonography, computed tomography, and magnetic resonance angiography with observations from surgery. Acta Radiol. 2015;56(12):1527–33. https://doi.org/10.1177/0284185114562227.
21. Lisanti CJ, Oettel DJ, Reiter MJ, Schwope RB. Multiplanar reformations in the measurement of renal length on CT: is it plain which plane to use? Am J Roentgenol. 2015;205(4):797–801.
22. Herts BR, Sharma N, Lieber M, Freire M, Goldfarb DA, Poggio ED. Estimating glomerular filtration rate in kidney donors: a model constructed with renal volume measurements from donor CT scans. Radiology. 2009;252(1):109–16.
23. Poggio E, Hila S, Stephany B, Fatica R, Krishnamurthi V, Del Bosque C, et al. Donor kidney volume and outcomes following live donor kidney transplantation. Am J Transplant. 2006;6(3):616–24.

24. Jeon HG, Lee SR, Joo DJ, Oh YT, Kim MS, Kim YS, et al. Predictors of kidney volume change and delayed kidney function recovery after donor nephrectomy. J Urol. 2010;184(3):1057–63.
25. Yano M, Lin MF, Hoffman KA, Vijayan A, Pilgram TK, Narra VR. Renal measurements on CT angiograms: correlation with graft function at living donor renal transplantation. Radiology. 2012;265(1):151–7.
26. Juluru K, Rotman JA, Masi P, Spandorfer R, Ceraolo CA, Giambrone AE, et al. Semiautomated CT-based quantification of donor kidney volume applied to a predictive model of outcomes in renal transplantation. Am J Roentgenol. 2015;204(5):W566–W72.
27. Mannami M, Mannami R, Mitsuhata N, Nishi M, Tsutsumi Y, Nanba K, et al. Last resort for renal transplant recipients, 'restored kidneys' from living donors/patients. Am J Transplant. 2008;8(4):811–8.
28. Lugo-Baruqui A, Guerra G, Arocha A, Burke GW, Ciancio G. Use of kidneys with small renal tumors for transplantation. Curr Urol Rep. 2016;17(1):1–7.
29. Fittschen A, Wendlik I, Oeztuerk S, Kratzer W, Akinli AS, Haenle MM, et al. Prevalence of sporadic renal angiomyolipoma: a retrospective analysis of 61,389 in- and out-patients. Abdom Imaging. 2014;39(5):1009–13.
30. Jinzaki M, Tanimoto A, Narimatsu Y, Ohkuma K, Kurata T, Shinmoto H, et al. Angiomyolipoma: imaging findings in lesions with minimal fat. Radiology. 1997;205(2):497–502.
31. Tada S, Yamagishi J, Kobayashi H, Hata Y, Kobari T. The incidence of simple renal cyst by computed tomography. Clin Radiol. 1983;34(4):437–9.
32. Carrim Z, Murchison J. The prevalence of simple renal and hepatic cysts detected by spiral computed tomography. Clin Radiol. 2003;58(8):626–9.
33. Israel GM, Hindman N, Bosniak MA. Evaluation of cystic renal masses: comparison of CT and MR imaging by using the Bosniak classification system. Radiology. 2004;231(2):365–71.
34. Pei Y. Diagnostic approach in autosomal dominant polycystic kidney disease. Clin J Am Soc Nephrol. 2006;1(5):1108–14.
35. Fananapazir G, Lamba R, Lewis B, Corwin MT, Naderi S, Troppmann C. Utility of MRI in the characterization of indeterminate small renal lesions previously seen on screening CT scans of potential renal donor patients. Am J Roentgenol. 2015;205(2):325–30.
36. Uflacker R. Abdominal aorta and branches. Atlas of vascular anatomy: an angiographic approach. 2006;2:481.
37. hua Mao Q, Li J. An accessory renal artery originating from the testicular artery, a rare variant. Indian J Surg. 2015;77(6):549–50.
38. Cooper M, Kramer A, Nogueira JM, Phelan M. Recipient outcomes of dual and multiple renal arteries following 1000 consecutive laparoscopic donor nephrectomies at a single institution. Clin Transplant. 2013;27(2):261–6.
39. Hsu TH, Su L-M, Ratner LE, Trock BJ, Kavoussi LR. Impact of renal artery multiplicity on outcomes of renal donors and recipients in laparoscopic donor nephrectomy. Urology. 2003;61(2):323–7.
40. Troppmann C, Wiesmann K, McVicar JP, Wolfe BM, Perez RV. Increased transplantation of kidneys with multiple renal arteries in the laparoscopic live donor nephrectomy era: surgical technique and surgical and nonsurgical donor and recipient outcomes. Arch Surg (Chicago, Ill: 1960). 2001;136(8):897–907.
41. Berardinelli L, Beretta C, Giussani A. Living donor transplantation of kidneys with fibromuscular dysplasia: indications, surgical techniques and long term results in 11 cases. J Nephrol Ther. 2012;2012.
42. Kaufman JA, Waltman AC, Rivitz SM, Geller SC. Anatomical observations on the renal veins and inferior vena cava at magnetic resonance angiography. Cardiovasc Intervent Radiol. 1995;18(3):153–7.
43. Satyapal K, Kalideen J, Haffejee A, Singh B, Robbs J. Left renal vein variations. Surg Radiol Anat. 1999;21(1):77–81.

44. Beckmann CF, Abrams HL. Circumaortic venous ring: incidence and significance. Am J Roentgenol. 1979;132(4):561–5.
45. Urban BA, Ratner LE, Fishman EK. Three-dimensional volume-rendered CT angiography of the renal arteries and veins: normal anatomy, variants, and clinical applications. Radiographics. 2001;21(2):373–86.
46. Soukup B, Vaidya A, Cranston D. Living kidney donation following nephrectomy due to pelviureteric junction obstruction. BMJ Case Rep. 2015;2015:bcr2015209778.
47. Privett J, Jeans W, Roylance J. The incidence and importance of renal duplication. Clin Radiol. 1976;27(4):521–30.
48. Meyer R. Normal and abnormal development of the ureter in the human embryo—a mechanistic consideration. Anat Rec. 1946;96(4):355–71.
49. Olsburgh J, Thomas K, Wong K, Bultitude M, Glass J, Rottenberg G, et al. Incidental renal stones in potential live kidney donors: prevalence, assessment and donation, including role of ex vivo ureteroscopy. BJU Int. 2013;111(5):784–92.

Chapter 3
Lung Transplantation Imaging

Michael Kadoch and H. Henry Guo

Background

The major indications for lung transplant include chronic obstructive pulmonary disease (COPD), idiopathic pulmonary fibrosis (IPF) and other interstitial lung diseases (ILD), cystic fibrosis, alpha-1 antitrypsin deficiency, end-stage sarcoidosis, pulmonary hypertension, and lymphangioleiomyomatosis [1]. Outcomes following lung transplant remain poor, with a median survival of only 5.5 years [1]. Graft failure and infections are the most common causes of death [1].

The three main types of procedures performed are single lung transplantation (SLT), double lung transplantation (DLT), and combined heart-lung transplantation (HLT). DLT has become the more common procedure for COPD and IPF. DLT is associated with better graft survival than SLT in IPF and equivalent graft survival as SLT in COPD at 5 years [2].

Surgical techniques for lung transplantation have evolved. En bloc DLT with tracheal anastomosis is now rarely performed since it is associated with an increased rate of anastomotic dehiscence [3]. Bronchial anastomosis is performed utilizing either an end-to-end or "telescope" anastomosis, with the latter generally reserved for cases where a bronchial size discrepancy exists given that an increased incidence of stricture formation is thought to occur with that technique [3].

M. Kadoch, M.D. (✉)
Department of Radiology, University of California Davis Medical Center, Sacramento, CA, USA
e-mail: mkadoch@ucdavis.edu

H. H. Guo, M.D., Ph.D.
Department of Radiology, Stanford University, Stanford, CA, USA

G. Fananapazir, R. Lamba (eds.), *Transplantation Imaging*,
https://doi.org/10.1007/978-3-319-75266-2_3

Table 3.1 Complications encountered following lung transplantation based on the time after the transplant procedure

Time since transplantation	Complications
Immediate (within 24 h)	Size mismatch
	Torsion
	Hyperacute rejection
Early (24 h to 1 week)	Reperfusion edema
	Pleural complications (including effusions and pneumothorax)
Intermediate (1 week to 2 months)	Acute rejection
	Bronchial anastomotic dehiscence
	Infections: bacterial
Primary late (2–4 months)	Bronchial anastomotic stenosis and bronchomalacia
	Pulmonary embolism
	Infections: viral and fungal
Secondary late (beyond 4 months)	Chronic rejection (including bronchiolitis obliterans)
	Organizing pneumonia
	Post-transplant lymphoproliferative disorder
	Upper lobe fibrosis (including pleuroparenchymal fibroelastosis)
	Primary disease recurrence
	Malignancy (including lung cancer)
	Transbronchial biopsy complications

Complications

Given the substantial overlap and nonspecific nature of imaging features encountered in lung transplantation imaging, postoperative complications are best distinguished based on predictable times of onset since surgery [3–5]. Immediate (within 24 h), early (24 h to 1 week), intermediate (1 week to 2 months), primary late (2 months to 4 months), and secondary late (beyond 4 months) complications may be encountered (Table 3.1).

Immediate (Within 24 h)

The most common complications encountered in the immediate post-transplant setting include donor-recipient size mismatch and hyperacute rejection.

Some size differences between donor and recipient lungs are usually tolerated. However, if the donor lung is too large for the recipient, atelectasis and scarring secondary to retained secretions and infections may ensue [3]. Partial resections of the transplanted lungs may be performed in order to downsize larger lungs to better fit within a smaller thorax. In patients with emphysema undergoing SLT, an undersized graft may be compressed by the contralateral hyperinflated native lung with resultant restrictive pulmonary function [6] (Fig. 3.1).

Hyperacute rejection is complement-mediated and occurs immediately following transplantation [5]. Radiographic findings are those of acute-onset diffuse alveolar damage with dense opacification seen throughout the grafts [7]. Limited management options include immunosuppression, plasmapheresis, and re-transplantation [7].

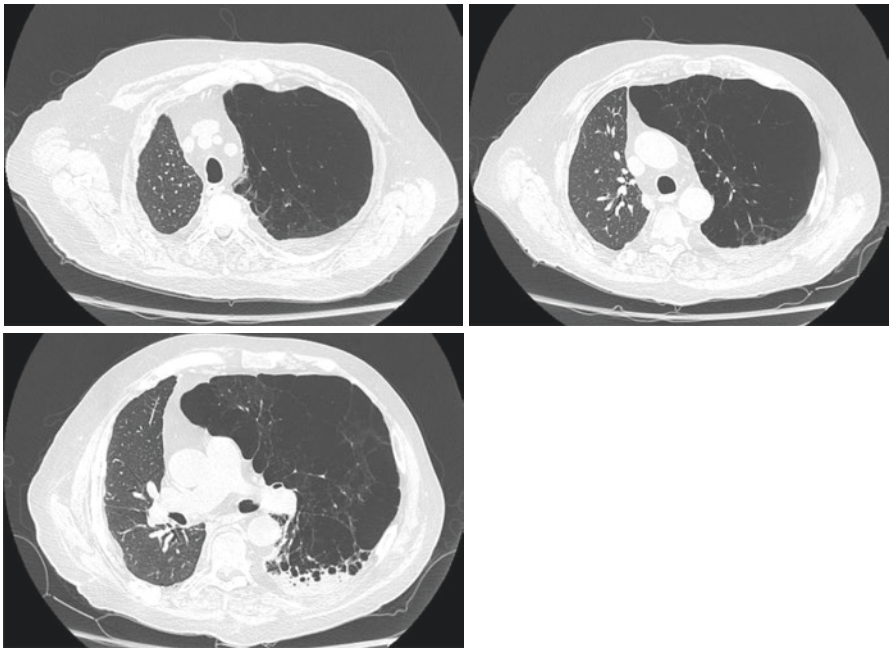

Fig. 3.1 (**a**–**c**) A 71-year-old male with severe emphysema underwent SLT. Serial axial CT images through the chest (**a**–**c**) demonstrate rightward deviation of the mediastinum with resultant compression of the transplanted right lung by the severely emphysematous and hyperinflated native left lung

Early (24 h to 1 Week)

The most common complications encountered in the early post-transplant setting include reperfusion edema and pleural complications.

Reperfusion edema appears within 72 h, peaks on postoperative day 4, and usually improves by the end of the first week [5]. It occurs in more than 95% of lung transplant patients and most often manifests as airspace disease in the middle and/or lower lung zones [8]. Persistence beyond the first week suggests acute rejection or infection [3]. Reperfusion edema is noncardiogenic and may be due to reactive oxygen species-induced oxidative damage and increased vascular permeability in the setting of ischemia-reperfusion injury within the transplanted organ. Management is largely supportive, similar to acute respiratory distress syndrome (ARDS) [8].

Pleural complications following lung transplantation include effusion, pneumothorax, empyema, hemothorax, and air leak. These are seen in approximately 22–34% of lung transplant patients [9, 10]. DLT and HLT usually result in a single communicating pleural space ("buffalo chest") [11], and fluid and gas collections are, therefore, often bilateral [12]. Pneumothorax is the most common pleural complication [10, 12] and usually resolves following chest tube placement. A new, persistent or enlarging pneumothorax should raise concern for an air leak [3]. Pleural effusions also occur in nearly all post-transplant patients but usually resolve within 2 weeks.

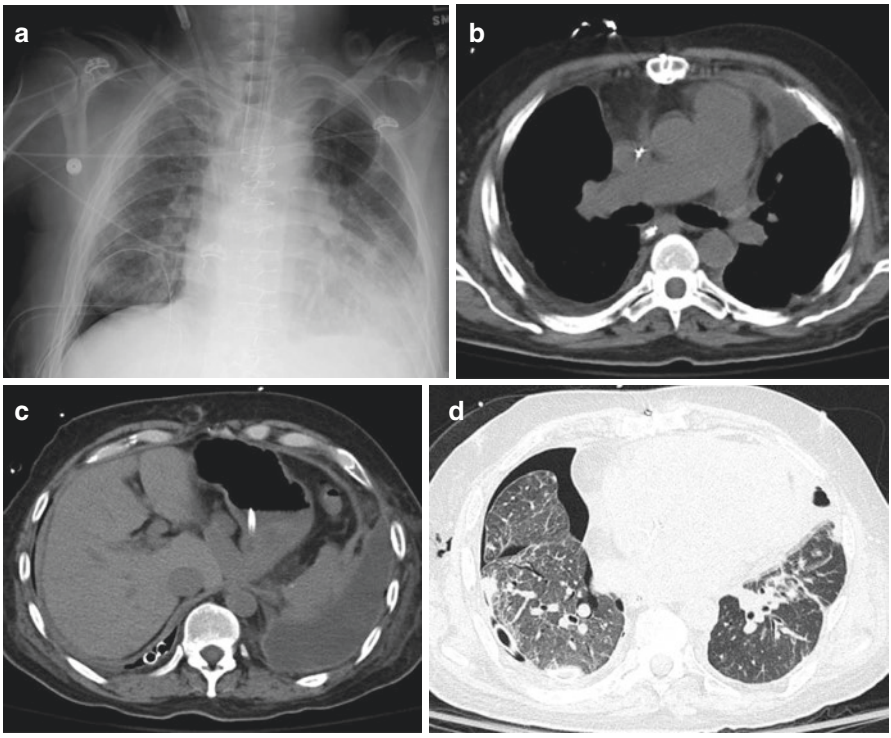

Fig. 3.2 (**a**–**d**) A 47-year-old male is status post bilateral lung transplant with pleural complications identified bilaterally as seen on chest radiography (**a**) and axial CT images (**b**–**d**). There is a multiloculated complex left-sided pleural effusion with associated pleural thickening that was found to represent an empyema and a moderate-sized right-sided pneumothorax that required chest tube placement

New, persistent, or enlarging pleural effusions should raise concern for hemothorax or empyema [3]. The development of empyema is particularly concerning in the post-transplant setting since it is the only pleural complication associated with increased mortality [10] (Fig. 3.2).

Intermediate (1 Week to 2 Months)

The most common complications encountered in the intermediate post-transplant setting include acute rejection and bronchial anastomotic dehiscence.

Acute rejection is cell-mediated [5]. It affects approximately half of lung transplant patients at least once within the first year, and recurrent episodes are considered a risk factor for chronic rejection [13]. CT features are nonspecific and may include ground-glass opacities, interlobular septal thickening, and pleural effusions, with ground-glass opacities being the most sensitive finding [4] (Fig. 3.3). Dramatic

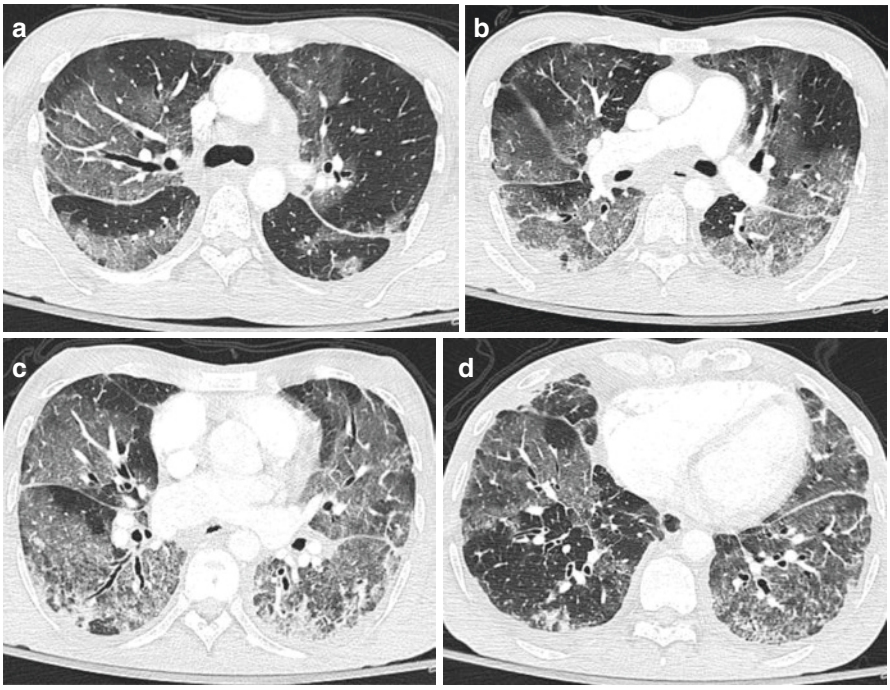

Fig. 3.3 (**a**–**d**) A 40-year-old male status post lung transplant with serial axial CT images (**a**–**d**) demonstrating extensive bilateral ground-glass opacities and trace bilateral pleural effusion in the setting of acute rejection

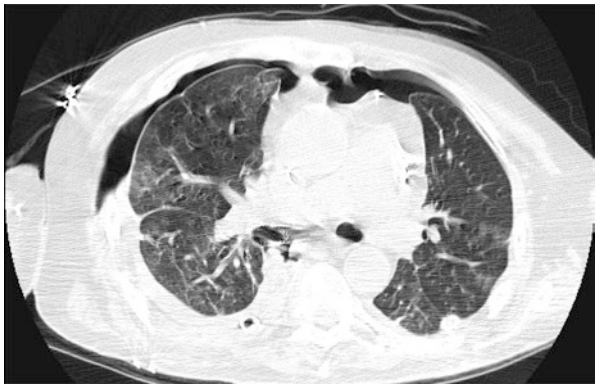

Fig. 3.4 A 67-year-old man 3 weeks after DLT, with anastomotic dehiscence of the right bronchus. A 5 mm defect involving the posterior aspect of the anastomosis communicates with the right pleural space, with hydropneumothorax. A stent has been placed over the dehiscent area

improvement within 48 h of intravenous steroid administration favors a diagnosis of acute rejection [4].

Bronchial anastomotic dehiscence occurs in approximately 2–3% of lung transplant cases and is typically seen 2–4 weeks following surgery [3]. CT may occasionally demonstrate the focal bronchial wall defect; however, extraluminal gas, a new or persistent air leak, pneumothorax, and pneumomediastinum should also raise concern for this complication [3, 14] (Fig. 3.4).

Primary Late (2 Months to 4 Months)

The most common complications encountered in the primary late post-transplant setting include bronchial anastomotic stenosis, bronchomalacia, pulmonary embolism (PE), and infections.

Bronchial anastomotic stenosis occurs in approximately 10% of lung transplant cases and is typically seen in an average of 3 months following surgery [3]. CT and virtual bronchoscopy may demonstrate areas of fixed focal narrowing and irregularity with or without associated lobar collapse [5] (Fig. 3.5). Management options include granulation tissue debridement, balloon dilatation, and/or stent placement [5]. Post-transplant bronchomalacia may be seen on expiratory CT or with dynamic CT during respiration as airway collapse or transient narrowing of the anastomosis or other airway segments [4, 15] (Fig. 3.6).

PE usually occurs within 4 months of transplantation, is identified at autopsy in 27% of lung transplant recipients, and is seen most commonly in mechanically ventilated SLT and DLT recipients [16]. PE is less commonly encountered in HLT recipients [16].

Infections are an important cause of morbidity and mortality in lung transplant patients [5]. Bacterial, fungal, viral, and mycobacterial infections all occur in this

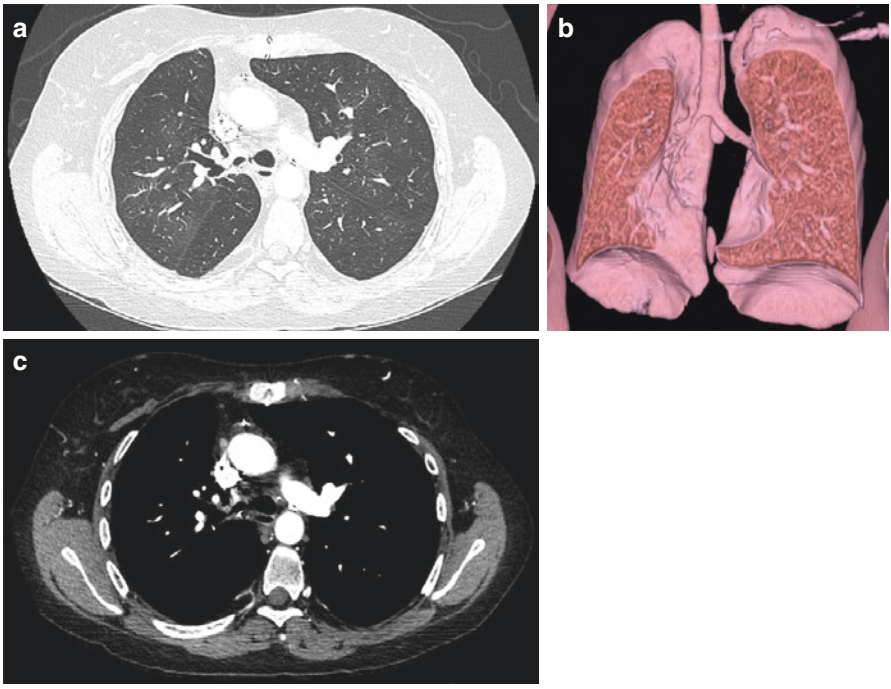

Fig. 3.5 (**a**–**c**) A 31-year-old female status post bilateral lung transplant with severe stenosis of the right mainstem bronchus near the site of surgical anastomosis as seen on axial CT (**a**, **b**) and volume-rendered (**c**) images

predisposed immunosuppressed patient population, with mycobacterial infections more common in the secondary late setting [4]. Gram-negative bacteria such as *Pseudomonas* and *Klebsiella* species as well as *Staphylococcus aureus* are common [5]. *Aspergillus fumigatus* is the most common fungal infection and can involve the airways, predisposing to ulcerative tracheobronchitis [5], and, rarely, the mediastinum [17] (Fig. 3.7). Candidal infections may also be seen as a cause of

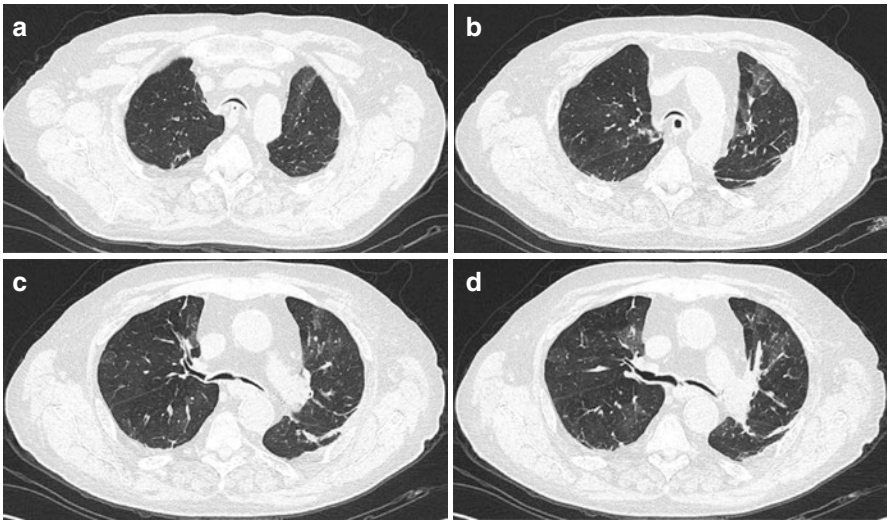

Fig. 3.6 (**a**–**d**) Serial axial expiratory CT images (**a**–**d**) performed in a 71-year-old male status post bilateral lung transplant demonstrate marked collapse of the trachea and central bronchi (greater than 50% of the luminal cross-sectional area), compatible with tracheobronchomalacia. Slight luminal irregularity is seen at the right mainstem bronchus anastomosis (**d**), which is a typical finding. There is also evidence of expiratory air trapping, which raises concern for bronchiolitis obliterans

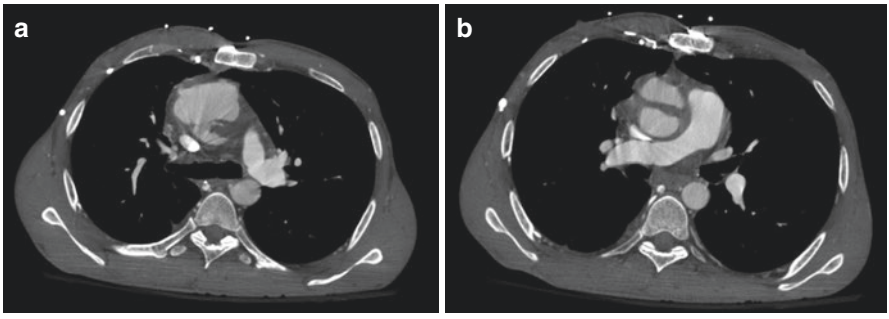

Fig. 3.7 (**a**, **b**) Serial axial contrast-enhanced CT images (**a**, **b**) in a 43-year-old male with cystic fibrosis status post bilateral lung transplant demonstrate a rare complication of *Aspergillus fumigatus* infection of the mediastinum with subsequent mycotic aneurysm formation. Slight narrowing is seen at the site of anastomosis within both central pulmonary arteries, which is a typical finding

pneumonia, mediastinitis, or esophagitis [5]. Cytomegalovirus (CMV) pneumonitis usually occurs between 1 and 6 months following transplant [18], is more common in seronegative patients receiving seropositive donor lungs [4], and is associated with the development of bronchiolitis obliterans [19]. The incidence of post-transplant CMV infection has decreased due to effective prophylactic treatment [4, 5].

Secondary Late (Beyond 4 Months)

The common complications encountered in the secondary late post-transplant setting include bronchiolitis obliterans and chronic rejection; organizing pneumonia; upper lobe fibrosis and pleuroparenchymal fibroelastosis; post-transplant lymphoproliferative disorder (PTLD); primary disease recurrence; malignancy, particularly lung cancer in the residual native lung; and complications related to transbronchial biopsies.

Chronic rejection affects at least 50% of transplant recipients at 5 years and is usually characterized by the presence of bronchiolitis obliterans [4]. CT findings include bronchiectasis, bronchial wall thickening, air trapping, mosaic attenuation, and decreased peripheral pulmonary arteries [4] (Fig. 3.8). Expiratory imaging is useful for the detection of air trapping in these patients. Gastroesophageal reflux

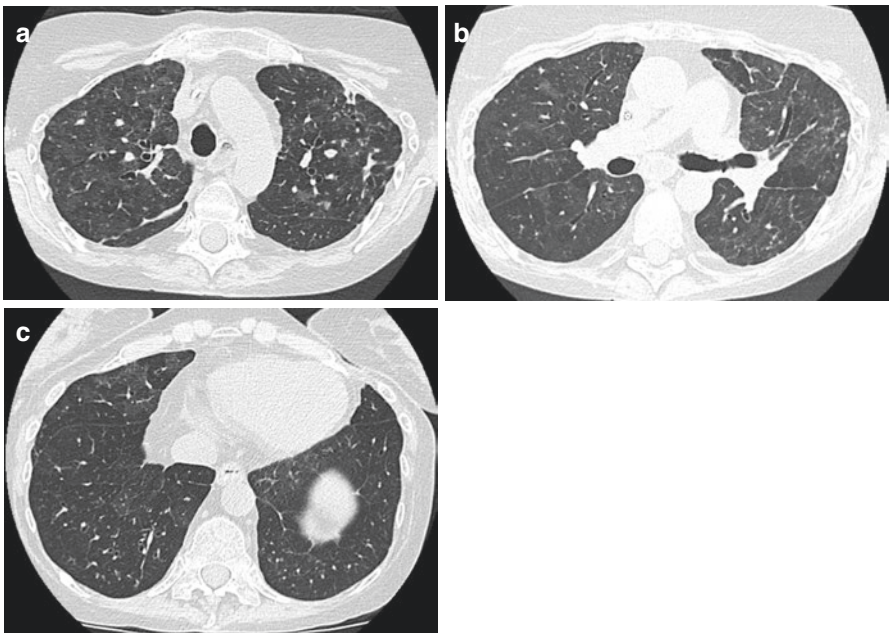

Fig. 3.8 (**a–c**) Serial axial CT images (**a–c**) were performed in a 62-year-old male patient who is status post DLT with evidence of bronchiectasis, bronchial wall thickening, and mosaic attenuation with peripheral areas of diminished pulmonary arterial vascularity, most compatible with bronchiolitis obliterans

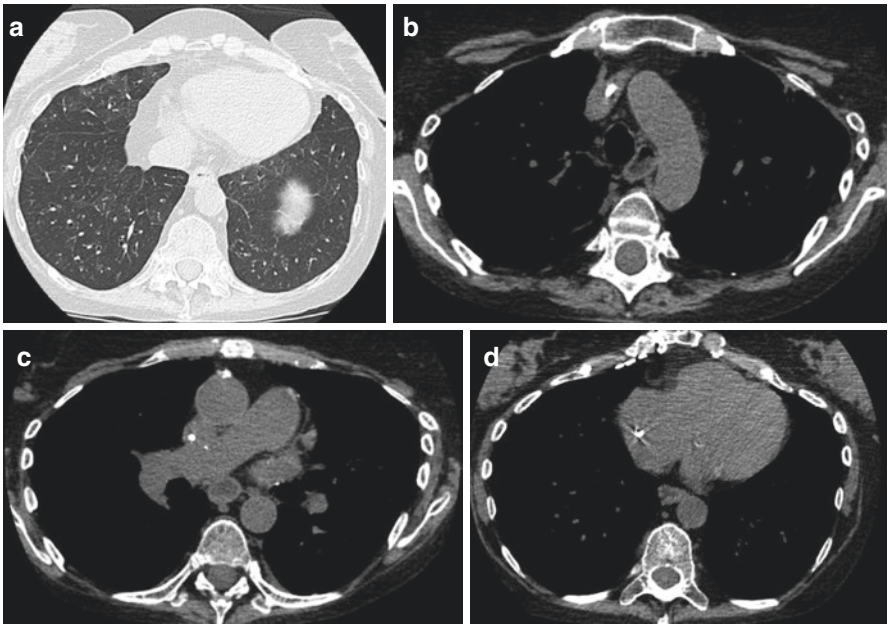

Fig. 3.9 (**a–d**) A 62-year-old male patient status post DLT with CT evidence of bronchiolitis obliterans (**a**) and GERD as manifest by a fluid-distended esophagus (**b–d**). GERD is prevalent in the lung transplant population and is a recognized modifiable risk factor for bronchiolitis obliterans

disease (GERD) is prevalent in lung transplant recipients and may represent a modifiable risk factor for bronchiolitis obliterans [20] (Fig. 3.9). Bronchiolitis obliterans causes obstructive defects that may respond to treatment with azithromycin. However, restrictive defects caused by interstitial abnormalities and fibrosis can also be seen in the setting of chronic rejection, which, in recent years, has led to increased use of the term chronic lung allograft dysfunction (CLAD) in these patients [21]. While both obstructive and restrictive CLAD phenotypes are recognized, overlap is known to occur [21] (Fig. 3.10).

Organizing pneumonia occurs in 10–28% of lung transplant patients [4]. CT findings include airspace consolidation, ground-glass opacities, perilobular opacities, and nodular or mass-like consolidation [4]. The atoll (reverse halo) sign of central ground-glass and peripheral consolidation is highly suggestive of this diagnosis (Fig. 3.11).

Gradually progressive fibrosis that predominantly involves the upper lobes with relative sparing of the basal segments is a recognized late-onset complication following lung transplantation [22] (Fig. 3.12). More recently, there has been increased recognition of pleuroparenchymal fibroelastosis as the etiology of fibrosis in at least some of these patients [23].

Other late-onset complications include PTLD, which can manifest as pulmonary nodules and/or lymphadenopathy. Primary diseases such as sarcoidosis and

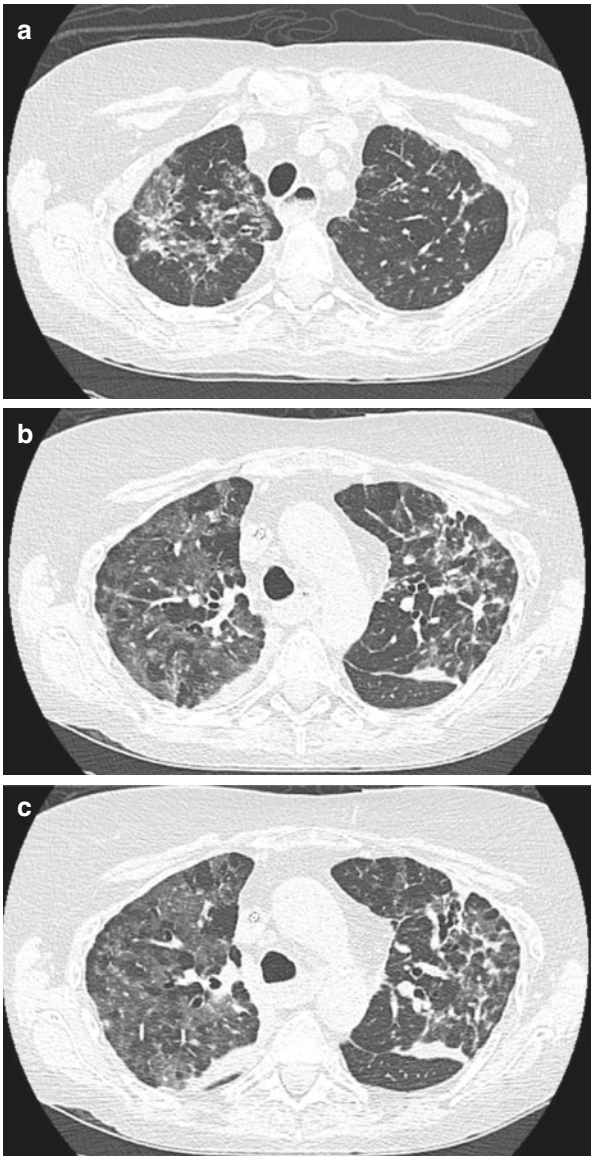

Fig. 3.10 (**a–c**) A 61-year-old female status post bilateral lung transplant. Serial axial CT images through the chest (**a–c**) demonstrate evidence of CLAD with overlapping obstructive (bronchiolitis obliterans) and restrictive (interstitial thickening and early fibrotic changes) phenotypic features within the bilateral pulmonary parenchyma

lymphangioleiomyomatosis have been reported to recur in the transplanted lungs of recipients [3]. Lung cancer may occur in the native lung of SLT recipients with reported frequencies of 1–4%, is more common in patients with underlying emphysema and pulmonary fibrosis, and is typically seen at least 1 year following transplantation [4]. Finally, transbronchial biopsies are routinely performed in lung transplant recipients, and recognition of their complications, which include solid nodules, cavities, and ground-glass opacities at the location of sampling as well as

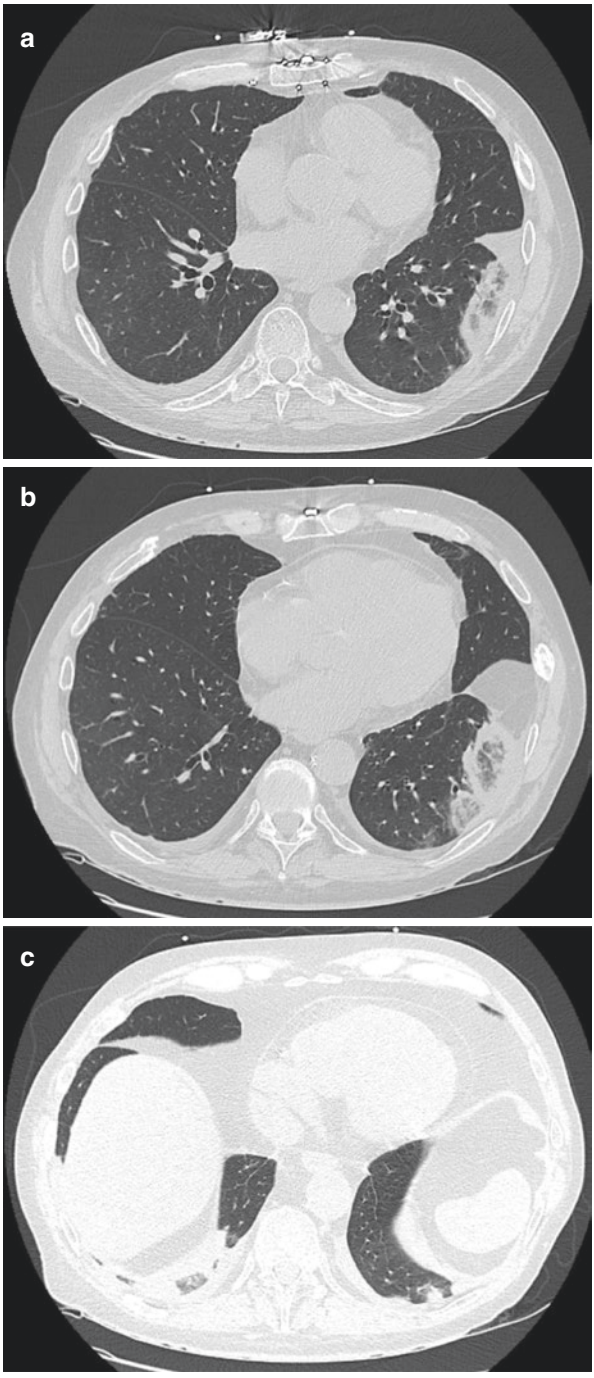

Fig. 3.11 (**a–c**) A 65-year-old male with a history of COPD status post DLT who presents with new hypoxia. Serial axial CT images through the chest demonstrate characteristic peripheral reverse halo (atoll) configuration opacities at the bases bilaterally, compatible with organizing pneumonia

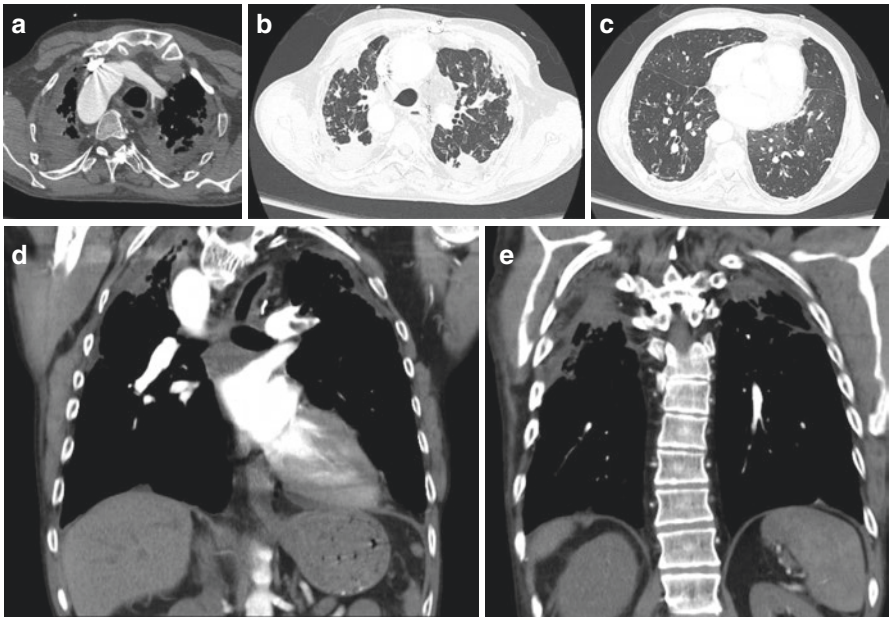

Fig. 3.12 (**a**–**e**) A 56-year-old male status post DLT with serial axial (**a**–**c**) and coronal (**d**, **e**) CT images demonstrating upper lobe predominant fibrosis and pleural thickening with sparing of the bases where additional features of bronchiolitis obliterans can be appreciated. There is increased recognition of pleuroparenchymal fibroelastosis as the etiology of this pattern of fibrosis in lung transplant patients and the imaging appearance in this case are typical of that entity

pneumothoraces [3, 4], will prevent attribution of these findings to a separate erroneous etiology.

Conclusions

Despite advancements in surgical techniques and management, outcomes following lung transplantation remain poor. Complications follow a predictable pattern based on the time after surgery, which can be helpful to keep in mind when considering the differential diagnosis as that many of the encountered CT features overlap between disease entities. Graft rejection and infections remain the most common cause of death in these patients.

References

1. Christie JD, Edwards LB, Kucheryavaya AY, Benden C, Dipchand AI, Dobbels F, et al. The Registry of the International Society for Heart and Lung Transplantation: 29th adult lung and heart-lung transplant report-2012. J Heart Lung Transplant. 2012;31(10):1073–86. https://doi.org/10.1016/j.healun.2012.08.004.

2. Schaffer JM, Singh SK, Reitz BA, Zamanian RT, Mallidi HR. Single- vs double-lung transplantation in patients with chronic obstructive pulmonary disease and idiopathic pulmonary fibrosis since the implementation of lung allocation based on medical need. JAMA. 2015;313(9):936–48. https://doi.org/10.1001/jama.2015.1175.
3. Ng YL, Paul N, Patsios D, Walsham A, Chung TB, Keshavjee S, Weisbrod G. Imaging of lung transplantation: review. AJR Am J Roentgenol. 2009;192(3 Suppl):S1–13, quiz S14–9. https://doi.org/10.2214/ajr.07.7061.
4. Krishnam MS, Suh RD, Tomasian A, Goldin JG, Lai C, Brown K, et al. Postoperative complications of lung transplantation: radiologic findings along a time continuum. Radiographics. 2007;27(4):957–74. https://doi.org/10.1148/rg.274065141.
5. Madan R, Chansakul T, Goldberg HJ. Imaging in lung transplants: checklist for the radiologist. Indian J Radiol Imaging. 2014;24(4):318–26. https://doi.org/10.4103/0971-3026.143894.
6. Ward S, Muller NL. Pulmonary complications following lung transplantation. Clin Radiol. 2000;55(5):332–9. https://doi.org/10.1053/crad.2000.0439.
7. Bittner HB, Dunitz J, Hertz M, Bolman MR 3rd, Park SJ. Hyperacute rejection in single lung transplantation—case report of successful management by means of plasmapheresis and antithymocyte globulin treatment. Transplantation. 2001;71(5):649–51.
8. Kundu S, Herman SJ, Winton TL. Reperfusion edema after lung transplantation: radiographic manifestations. Radiology. 1998;206(1):75–80. https://doi.org/10.1148/radiology.206.1.9423654.
9. Ferrer J, Roldan J, Roman A, Bravo C, Monforte V, Pallissa E, et al. Acute and chronic pleural complications in lung transplantation. J Heart Lung Transplant. 2003;22(11):1217–25.
10. Herridge MS, de Hoyos AL, Chaparro C, Winton TL, Kesten S, Maurer JR. Pleural complications in lung transplant recipients. J Thorac Cardiovasc Surg. 1995;110(1):22–6. https://doi.org/10.1016/s0022-5223(05)80005-4.
11. Grathwohl KW, Derdak S. Images in clinical medicine. Buffalo chest. N Engl J Med. 2003;349(19):1829. https://doi.org/10.1056/NEJMicm010281.
12. Erasmus JJ, McAdams HP, Tapson VF, Murray JG, Davis RD. Radiologic issues in lung transplantation for end-stage pulmonary disease. AJR Am J Roentgenol. 1997;169(1):69–78. https://doi.org/10.2214/ajr.169.1.9207503.
13. King-Biggs MB. Acute pulmonary allograft rejection. Mechanisms, diagnosis, and management. Clin Chest Med. 1997;18(2):301–10.
14. Semenkovich JW, Glazer HS, Anderson DC, Arcidi JM Jr, Cooper JD, Patterson GA. Bronchial dehiscence in lung transplantation: CT evaluation. Radiology. 1995;194(1):205–8. https://doi.org/10.1148/radiology.194.1.7997554.
15. Kshettry VR, Kroshus TJ, Hertz MI, Hunter DW, Shumway SJ, Bolman RM 3rd. Early and late airway complications after lung transplantation: incidence and management. Ann Thorac Surg. 1997;63(6):1576–83.
16. Burns KE, Iacono AT. Pulmonary embolism on postmortem examination: an under-recognized complication in lung-transplant recipients? Transplantation. 2004;77(5):692–8.
17. Shlobin OA, Dropulic LK, Orens JB, McDyer JF, Conte JV, Yang SY, Girgis R. Mediastinal mass due to Aspergillus fumigatus after lung transplantation: a case report. J Heart Lung Transplant. 2005;24(11):1991–4. https://doi.org/10.1016/j.healun.2005.02.020.
18. Collins J, Muller NL, Kazerooni EA, Paciocco G. CT findings of pneumonia after lung transplantation. AJR Am J Roentgenol. 2000;175(3):811–8. https://doi.org/10.2214/ajr.175.3.1750811.
19. Paraskeva M, Bailey M, Levvey BJ, Griffiths AP, Kotsimbos TC, Williams TP, et al. Cytomegalovirus replication within the lung allograft is associated with bronchiolitis obliterans syndrome. Am J Transplant. 2011;11(10):2190–6. https://doi.org/10.1111/j.1600-6143.2011.03663.x.
20. King BJ, Iyer H, Leidi AA, Carby MR. Gastroesophageal reflux in bronchiolitis obliterans syndrome: a new perspective. J Heart Lung Transplant. 2009;28(9):870–5. https://doi.org/10.1016/j.healun.2009.05.040.
21. Verleden GM, Raghu G, Meyer KC, Glanville AR, Corris P. A new classification system for chronic lung allograft dysfunction. J Heart Lung Transplant. 2014;33(2):127–33. https://doi.org/10.1016/j.healun.2013.10.022.

22. Konen E, Weisbrod GL, Pakhale S, Chung T, Paul NS, Hutcheon MA. Fibrosis of the upper lobes: a newly identified late-onset complication after lung transplantation? AJR Am J Roentgenol. 2003;181(6):1539–43. https://doi.org/10.2214/ajr.181.6.1811539.
23. Ofek E, Sato M, Saito T, Wagnetz U, Roberts HC, Chaparro C, et al. Restrictive allograft syndrome post lung transplantation is characterized by pleuroparenchymal fibroelastosis. Mod Pathol. 2013;26(3):350–6. https://doi.org/10.1038/modpathol.2012.171.

Chapter 4
Imaging of Liver Transplantation

Eitan Novogrodsky, Ely R. Felker, David S. K. Lu, and Steven S. Raman

Abbreviations

ALTSG	American Liver Tumor Study Group
CEUS	Contrast-enhanced ultrasound
ERCP	Endoscopic retrograde cholangiopancreatography
HAT	Hepatic artery thrombosis
HCC	Hepatocellular carcinoma
HIDA	Hepatobiliary iminodiacetic acid
INR	International normalized ratio
IVC	Inferior vena cava
LDLT	Living donor liver transplant
LFT	Liver function test
LHA	Left hepatic artery
MELD	Model for end-stage liver disease
MHV	Middle hepatic vein
MRA	Magnetic resonance angiography
MRCP	Magnetic resonance cholangiopancreatography
OLT	Orthotopic liver transplant
OPTN	Organ Procurement and Transplantation Network
PTC	Percutaneous transhepatic cholangiography
PTLD	Posttransplant lymphoproliferative disorder
RHV	Right hepatic vein
RI	Resistive index

E. Novogrodsky, M.D. • E. R. Felker, M.D. • D. S. K. Lu, M.D. • S. S. Raman, M.D. (✉)
Department of Radiological Sciences, David Geffen School of Medicine at UCLA, Ronald Reagan UCLA Medical Center, Los Angeles, CA, USA
e-mail: efelker@mednet.ucla.edu; sraman@mednet.ucla.edu

G. Fananapazir, R. Lamba (eds.), *Transplantation Imaging*,
https://doi.org/10.1007/978-3-319-75266-2_4

SFSS	Small-for-size syndrome
SMA	Superior mesenteric artery
TNM	Tumor, node, and metastasis

Surgical Techniques and Considerations

Transplant Eligibility and the Role of the Radiologist

In 2016 approximately 6500 patients underwent liver transplantation in the United States, and 16,000 patients were on waiting lists [1] with a growing organ shortage annually [2]. Since 2002, allocation of donor livers is determined based on the medical condition of the recipients, giving priority to individuals with the most urgent need for transplant using a scoring system called the model for end-stage liver disease (MELD) score [2]. Subjective measures, geographic location, and waiting times are no longer considered in assigning priority to individuals awaiting transplant [2]. MELD score is calculated using the patient's total bilirubin level, international normalized ratio (INR), and total creatinine level and predicts the 3-month mortality rate of hospitalized patients with end-stage liver disease [2, 3]. The score ranges from 6 to 40, and hospitalized patients with a score of 40 have a 3-month mortality rate of 100% [2].

In patients with hepatocellular carcinoma (HCC), the MELD score assignment also takes tumor stage into consideration, and transplant eligibility and priority are determined based on tumor size, number, and invasiveness [2]. The radiologist therefore plays a critical role in assessing the transplant eligibility of patients with HCC.

There are two systems commonly referenced for determining whether patients with HCC are likely to benefit from orthotopic liver transplant (OLT) (Table 4.1) [2, 4]. The Milan criteria stipulate that patients most likely to benefit from transplant have either a solitary tumor of ≤5 cm in diameter or ≤3 tumors each ≤3 cm in diameter (Fig. 4.1) [5]. The Milan study achieved a 4-year overall actuarial survival of 75% and a disease-free survival of 83% [5]. The less restrictive UCSF criteria

Table 4.1 Criteria to predict benefit from liver transplant in HCC patients

Criteria	Solitary lesion	Multiple lesions
Milan	≤5 cm diameter	≤3 tumors + each tumor ≤3 cm diameter
UCSF	≤6.5 cm diameter	≤3 tumors + largest tumor ≤4.5 cm diameter + total tumor diameter ≤8 cm

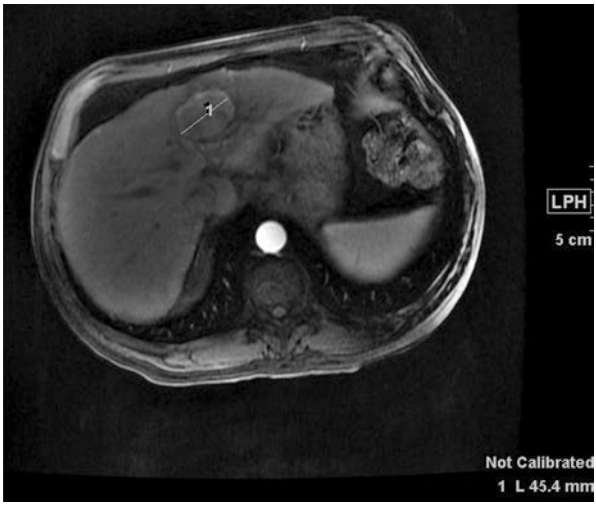

Fig. 4.1 4.5 cm LI-RADS 5 lesion, may benefit from transplant within the Milan criteria

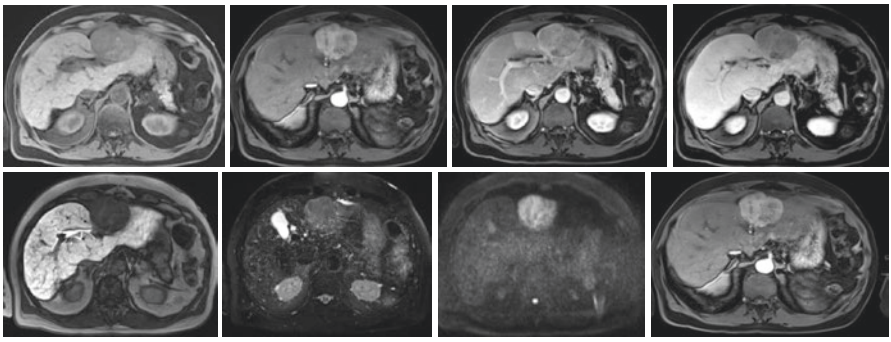

Fig. 4.2 Lesion measuring 6.6 cm, would not benefit from transplant by either the Milan or the UCSF criteria

stipulate that patients may benefit from transplant with solitary tumors up to 6.5 cm in diameter or ≤3 tumors, with the largest tumor ≤4.5 cm in diameter and total tumor diameter ≤8 cm, without gross vascular invasion (Fig. 4.2) [6]. Subsequent studies have shown that patients with total tumor volume < 115 cm^3 benefit from transplant with outcomes similar to those restricted to the Milan or UCSF criteria [2, 4].

In the United States, the American Liver Tumor Study Group (ALTSG) developed a modified tumor, node, and metastases (TNM) staging system for HCC to determine eligibility and priority for OLT (Table 4.2). Based on this system, the Organ Procurement and Transplantation Network (OPTN) has been steadily updating the criteria and schedule for applying MELD exception points for patients with HCC. Currently patients with T2 tumors (single lesion 2–5 cm or two or three lesions ≤3 cm) are the only patients eligible for exception points.

Table 4.2 American Liver Tumor Study Group modification of the TNM staging for hepatocellular cancer for the purpose of liver transplantation prioritization

T0	No tumor found
T1	One nodule, ≤1.9 cm
T2	One nodule, 2–5 cm; two or three nodules, all ≤3 cm
T3	One nodule, >5 cm; two or three nodules, at least one >3 cm
T4a	Four or more nodules of any size
T4b	T2, T3, or T4a, plus gross involvement of intrahepatic portal vein or hepatic vein, as indicated by CT, MRI, or ultrasonography
N1	Involvement of regional (porta hepatis) lymph nodes
M1	Metastatic disease including extrahepatic portal or hepatic vein involvement
Stage grouping	
Stage I	T1
Stage II	T2
Stage III	T3
Stage IVA1	T4a
Stage IVA2	T4b
Stage IVB	Any N1 or M1

Types of Liver Transplant: Cadaveric Transplant, Living Donor Liver Transplant (LDLT), and Split-Liver Grafting

Cadaveric transplant is the most common form of liver transplant. The entire liver is removed from the deceased donor and orthotopically transplanted [2].

About 10% of liver transplants are *living donor liver transplants* (*LDLT*) [2]. Living donor transplants are performed for patients with urgent need and a high likelihood of achieving a positive outcome after surgery [2]. LDLT was initially developed as a technique for pediatric liver transplants in light of the short supply of pediatric cadaveric livers [7, 8]. The most common form of LDLT, left lateral hepatectomy, was developed in this context and involves removal of segments II and III of the donor liver along with the left hepatic vein (Fig. 4.3) [2]. Left lateral lobectomy presents the smallest risk to the donor and provides a small liver for pediatric patients [7]. However, when used for an adult recipient, left lateral lobectomy increases the likelihood that the recipient will develop small-for-size syndrome (SFSS) as the liver segment may be too small to fulfill the needs of an adult [8]. A complete left lobectomy involves the complete removal of segments I–IV along with the middle hepatic vein (MHV) [2, 9]. The recipient left and middle hepatic veins are joined and anastomosed to the donor middle hepatic vein [2]. Right lobectomy, which involves transplantation of segments V–VIII, is of highest risk to the donor [2].

Split-liver grafting involves division of a cadaveric liver to facilitate two transplants. There are two forms of split-liver grafting [10, 11]. The first form involves division of the liver at the falciform ligament, similar to the division in a left lateral

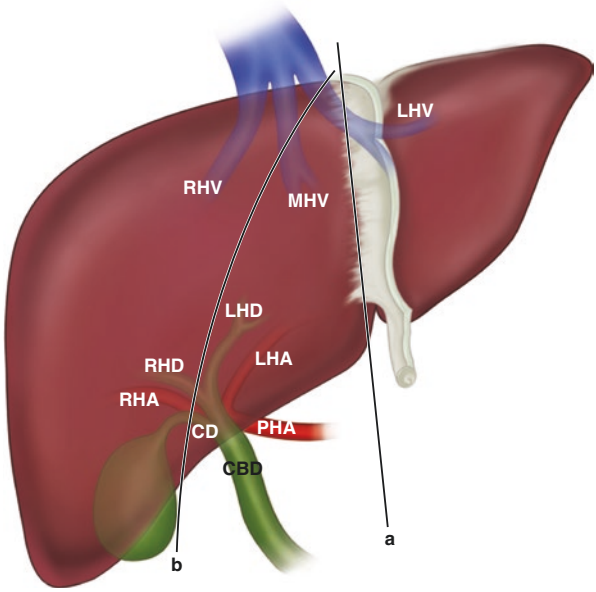

Fig. 4.3 Schematic representation of planes of dissection of donor liver): *line a* representing a segment II/III graft and *line b* representing full left lobe graft. *RHV* right hepatic vein, *MHV* middle hepatic vein, *LHV* left hepatic vein, *RHA* right hepatic artery, *RHD* right hepatic duct, *LHD* left hepatic duct, *LHA* left hepatic artery, *PHA* proper hepatic artery, *CBD* common bile duct, *CD* cystic duct. (Adapted from Broelsch CE et al., 1991)

lobectomy [2, 10]. This yields a left lateral graft (segments II and III) for a small pediatric recipient and an extended right graft (segments I and IV–VIII) for an adult recipient [2]. The second form of split-liver grafting, an extended right split, yields a right lobe graft (segments V–VIII, the common bile duct, and IVC) and a left lobe graft (segments I–IV, the main hepatic trunk, and middle hepatic vein) for two adult recipients [2]. Segment I may be included in either half of the transplant [2].

Hepatic Artery Anastomosis

For the hepatic arterial anastomosis, the donor's common hepatic artery can be anastomosed end-to-end directly to the recipient proper hepatic artery before its bifurcation or end-to-side to the recipient common hepatic artery at the origin of the gastroduodenal artery (Fig. 4.4) [12]. Alternatively, the donor common hepatic artery can be retrieved along with the celiac trunk and a small piece of surrounding aorta known as an aortic cuff [12]. The recipient's right and left hepatic arteries are cut longitudinally to facilitate the creation of a "branch patch" that is then anastomosed end-to-end to the aortic cuff from the donor [12]. If the recipient hepatic artery is not sufficient (e.g., too short or pathological) for anastomosis (Fig. 4.5a), the most common alternative technique is to interpose a graft of the internal iliac artery between the donor hepatic artery and the recipient aorta (Fig. 4.5b) [13]. The iliac is anastomosed side-to-end directly to the aorta at either the supraceliac aorta or the suprarenal aorta [13].

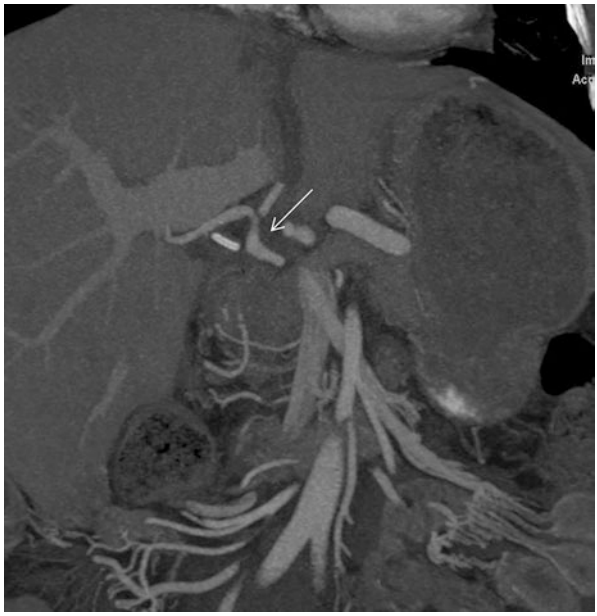

Fig. 4.4 Coronal MIP demonstrating normal hepatic artery anastomosis (*arrow*), donor common hepatic artery anastomosed end-to-end to the recipient proper hepatic artery

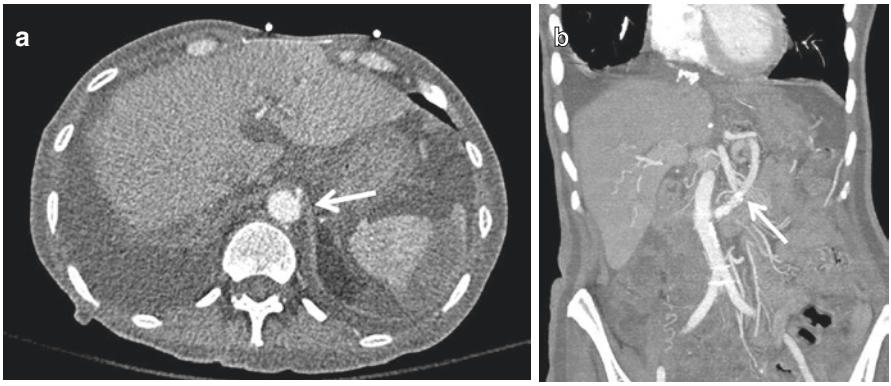

Fig. 4.5 (**a**) Celiac artery stenosis (*arrow*) in the recipient causing poor inflow. (**b**) Coronal MIPS demonstrating a jump graft fashioned from the donor iliac artery and anastomosed to the recipient infrarenal aorta (*arrow*)

Caval Anastomoses

In the standard technique for inferior vena cava (IVC) anastomosis, the recipient's IVC is removed along with the liver, and a side-to-side anastomosis of the donor IVC is performed with superior and inferior ends of remaining recipient IVC (Fig. 4.6) [12]. In the newer piggyback technique, the recipient IVC is not removed along with the liver. The recipient liver is dissected off of the right, middle, and left

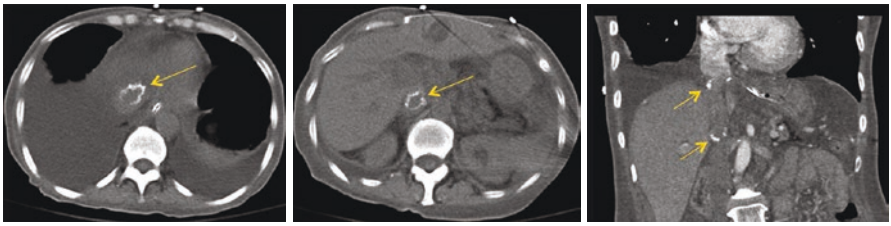

Fig. 4.6 Bicaval technique: retrohepatic IVC of the recipient is resected, and the IVCs of the recipient and donor are sutured with an end-to-end anastomosis between the superior and inferior ends (*yellow arrows*)

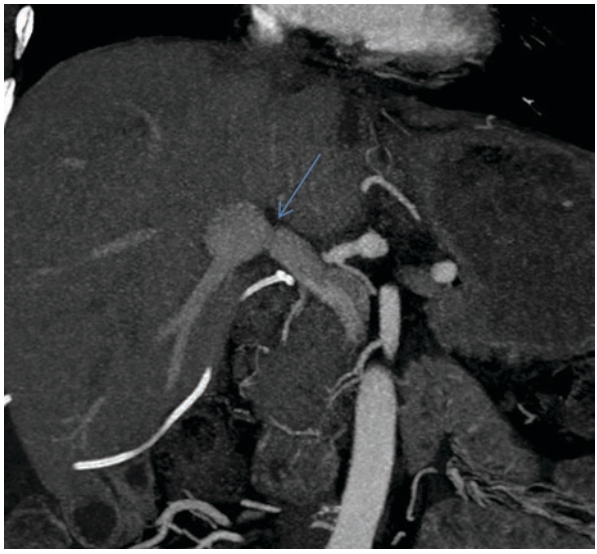

Fig. 4.7 Portal vein anastomosis (*blue arrow*) with mild "waisting" which can be a normal finding, reflecting slight discrepancy in size between donor and recipient portal veins

hepatic veins [12]. An end-to-side anastomosis is then performed between the donor's suprahepatic IVC and all three recipient hepatic veins at the common stump [12, 13].

Portal Venous Anastomosis

Donor and recipient portal veins are anastomosed end-to-end for portal venous anastomosis (Fig. 4.7) [12]. If the recipient portal vein is thrombosed, an iliac vein graft is anastomosed end-to-side to the base of the superior mesenteric vein [12]. The iliac vein conduit is pulled posterior to the antrum of the stomach and anterior to the pancreas for anastomosis with the donor portal vein [12].

Bile Duct Anastomosis

The biliary anastomosis is generally performed as a choledochocholedochostomy, an end-to-end anastomosis between donor common hepatic duct and recipient common bile duct (Fig. 4.8) [12]. Occasionally, a T-tube is placed into the bile duct, and a separate choledocotomy is created on the recipient side for external biliary drainage (Fig. 4.9) [12]. If use of the recipient bile duct is not possible, a choledochojejunostomy is performed (Fig. 4.10) [12].

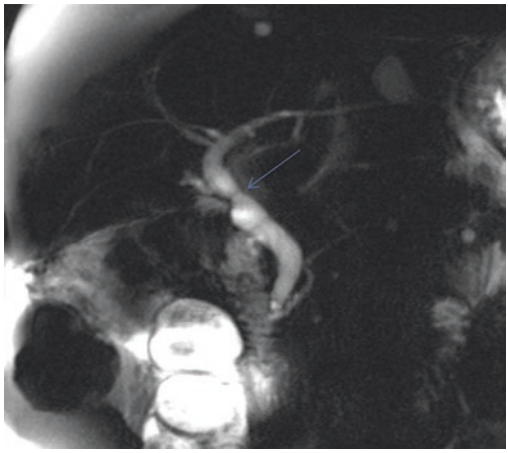

Fig. 4.8 Choledochocholedochostomy anastomosis (*blue arrow*)

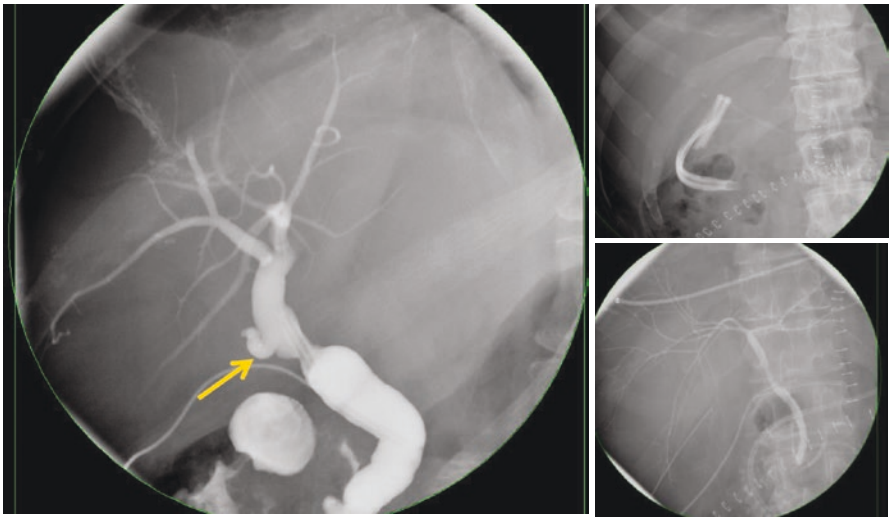

Fig. 4.9 Normal postoperative T-tube cholangiogram (**a**–**c**) showing opacification of the cystic duct stump (***a***, *yellow arrow*), a normal finding

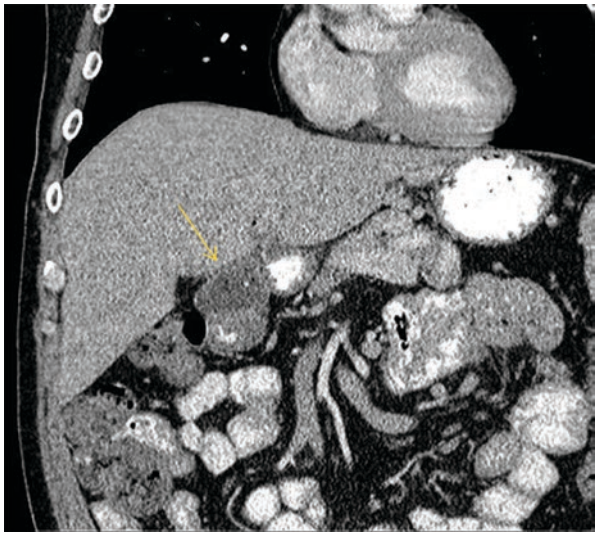

Fig. 4.10 Fluid-filled bowelloop in the porta hepatis (*yellow arrow*) consistent with a choledochojejunostomy

Preoperative Imaging

Parenchymal Imaging

The liver parenchyma of both donor and recipient should be evaluated prior to transplant with noncontrast and multiphase contrast-enhanced CT or MR imaging [2]. Imaging of the recipient liver should evaluate the size of the liver and any parenchymal abnormalities, including the size, location, and character of any lesions [2]. As discussed in the previous chapter, the donor liver is imaged to rule out excessive steatosis, iron deposition, signs of diffuse subclinical liver disease, and characterization of lesions. The donor liver volume is readily calculated to ensure adequate volume for the body mass of both the recipient and donor. Simple cysts, hemangiomas, and focal nodular hyperplasia, the three most common liver lesions, have been detected in up to 18% of evaluated living donors [14]. Their location relative to significant anatomic structures (e.g., vasculature) should be reported [2].

Vascular Imaging

Preoperative imaging of donor and recipient liver vasculature is vital for identification of vascular variants and anomalies (e.g., portal vein thrombosis) [2, 15] and may prevent operative complications [2, 15]. Variant arterial anatomy as defined by the Michel criteria is present in up to 45% of potential donors, while classical hepatic arterial anatomy (Michel type I) is present in only 55% of donors (Fig. 4.11)

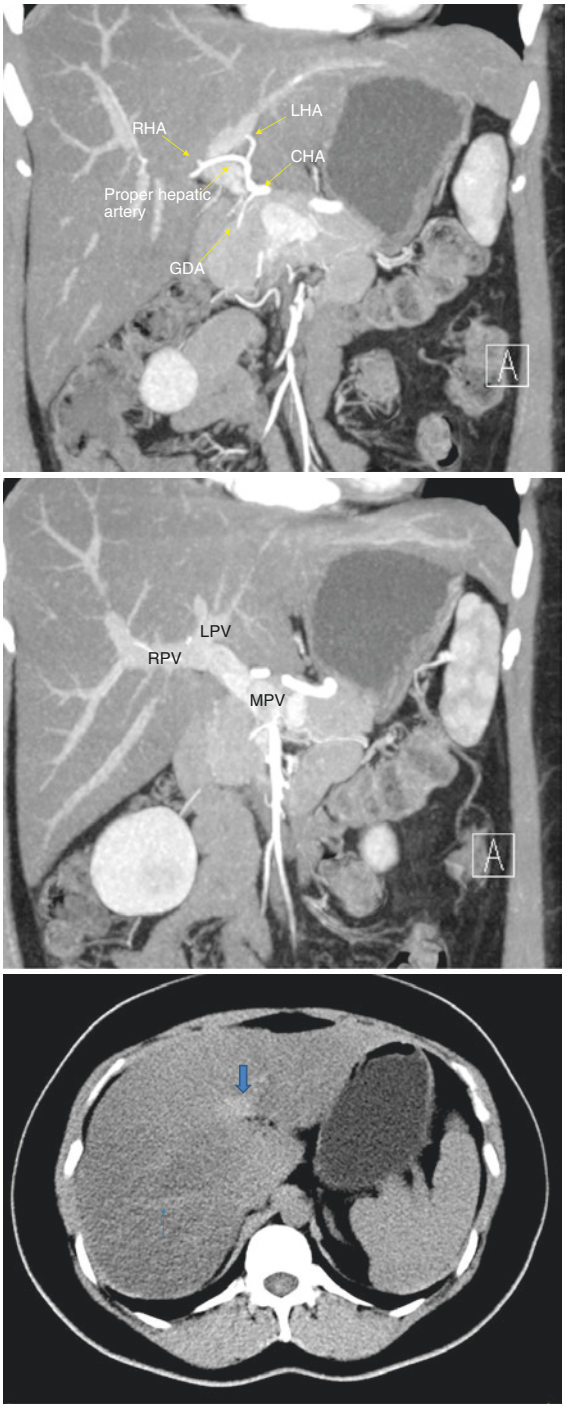

Fig. 4.11 11.1: Coronal MIP showing conventional hepatic arterial anatomy. The common hepatic artery (CHA) gives rise to the gastroduodenal (GD) artery and then becomes the proper hepatic artery. The proper hepatic artery then splits in the right hepatic artery (RHA) and left hepatic artery (LHA). 11.2: Same patient as shown in (11.1), with conventional portal venous anatomy. The main portal vein (MPV) gives rise to the right portal vein (RPV) and the left portal vein (LPV). 11.3: Same patient as shown in (11.1) showing significant steatosis, such that vessels (*small arrow*) appear hyperdense relative to the liver parenchyma. Incidentally noted focal fatty sparing in the posterior aspect segment IV, a common location for such sparing (*large arrow*)

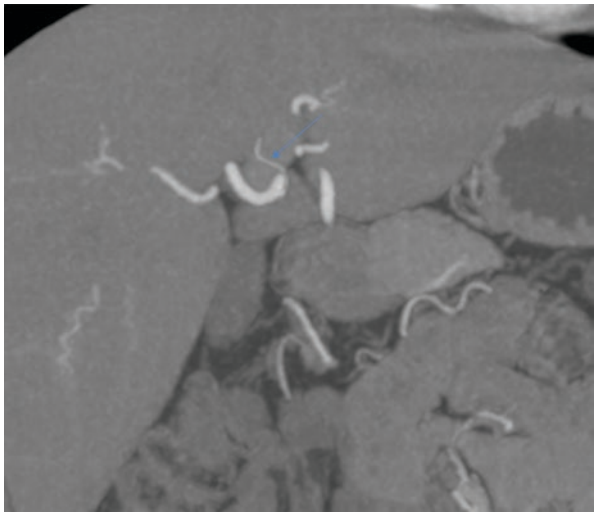

Fig. 4.12 Segment IV hepatic artery arises directly from the proper hepatic artery (*blue arrow*)

[2, 15]. Multidetector CT or MR angiography (CTA or MRA) is routinely performed during radiographic evaluation of donors [2, 14]. Several arterial variants have important implications for surgical planning. For example, the arterial supply to segment IV may arise from the right branch of the hepatic artery, the left branch, or the proper hepatic artery (Fig. 4.12) [16, 17]. For the 7–11% of patients with exclusive right hepatic arterial supply to segment IV, there is significant risk of ischemia during procurement for LDLT, as the right hepatic artery passes directly through the plane of dissection [14, 16]. Another clinically significant anatomic variant is a replaced or accessory LHA (Michel types II and V) in the recipient, which will require the surgeon to ligate the vessel during removal of the patient's native liver [15].

During LDLT, the middle hepatic vein (MHV) is retained in the donor, and radiologists should map major venous tributaries draining from right hepatic segments into the MHV and accessory veins into the IVC including measuring number, length, and diameter of these veins to help surgeons plan the number of venous anastomoses to perform during LDLT [14]. For example, if the proximal venous branches of the MHV within the resected portion of the living donor liver (segment VIII) are large (>3–4 mm diameter), they may require surgical anastomosis to the recipient IVC (rather than ligation) to ensure proper drainage of segment VIII. Failure to anastomose these branches may cause segmental hepatic venous congestion and recipient graft dysfunction [15]. Similarly, a large (>3–4 mm) accessory inferior right hepatic vein (aRHV), the most common hepatic venous variant [2, 15], must also be reimplanted to the recipient IVC [15]. The latter anastomosis can be surgically complex if the aRHV is >4 cm away from the point where the main RHV drains into the IVC [15].

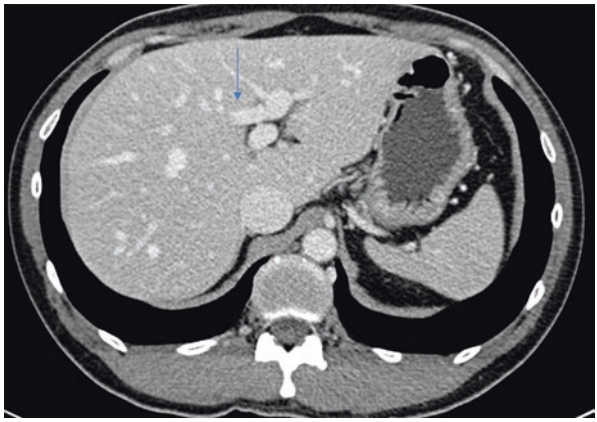

Fig. 4.13 Aberrant right anterior division portal vein, arising from the left portal vein

A surgically significant portal vein variant is trifurcation of the main portal vein into the left, right posterior, and right anterior portal venous branches. This variant requires ligation of each individual branch in the donor and a complex anastomosis in the recipient [15] (Figs. 4.11 and 4.13). The radiologist should report the length of the portal vein and the angle of bifurcation, as a short portal vein will require a graft and an acute angle of bifurcation (<45°) has been associated with occluded portal flow during liver regeneration [15].

Other clinically significant vascular abnormalities include portal vein thrombosis, celiac artery stenosis or large recipient splenorenal shunts, or splenic artery aneurysm (in donor or recipient) [15]. Diffuse portal vein thrombosis that extends into the superior mesenteric vein may preclude transplant. Celiac artery stenosis and splenic artery aneurysm can both be surgically treated at the time of transplant if identified preoperatively [15]. Also, the presence of large portosystemic shunts, such as splenorenal shunts, should be identified to determine if they need pre- or intraoperative closure.

Biliary Imaging

Donor biliary tree imaging is completed with CT cholangiography, CTA, MR cholangiopancreatography (MRCP), or MRA to facilitate "one-stop-shop" donor imaging [2]. Up to 28% of donors have biliary anatomical variants. The normal anatomy of the biliary tree is a fusion of the posterior right hepatic duct with the anterior right hepatic duct and subsequent fusion with the left hepatic duct. The most common variants include (a) fusion of the posterior right duct directly into the left hepatic duct or into the right-sided branch of the right hepatic duct and (b) "triple confluence or trifurcation" variant whereby the right anterior, right posterior, and left

hepatic ducts drain into the common hepatic duct within 1 cm of each other [14]. Both variants require two potential recipient anastomoses of the right posterior duct to preclude recipient leak or stricture [2].

Normal Postoperative Imaging Findings

The most common cause of liver failure after transplant is acute rejection [18], which requires percutaneous image-guided liver parenchymal biopsy for diagnosis [18]. Other causes include vascular complications (thrombosis, stenosis, aneurysm), biliary complications (stones, strictures, leaks), infection, and malignancy which may be diagnosed by US, CT, or MR imaging.

In diagnosing post-liver transplantation complications, it is important to recognize typically normal posttransplant changes. The first important step in imaging the posttransplant liver is to identify the four primary sites of anastomosis [18]. In the first few weeks after transplant, it may be normal to identify a right-sided pleural effusion, mild ascites, perihepatic hematoma, and periportal edema [18]. These findings should all resolve after several weeks [18].

In the immediate postoperative period, the only routine imaging that is performed is a baseline duplex US on postoperative day 1, with subsequent imaging obtained only as clinically indicated (i.e., elevated LFTs, suspicion for hepatic arterial stenosis, etc.). US should include grayscale imaging of the liver parenchyma and the biliary tree and duplex Doppler US of the hepatic vasculature [18]. The normal appearance of the transplanted liver parenchyma is homogeneous grayscale or mildly heterogeneous grayscale [18]. If no T-tube is in place, the intrahepatic and extrahepatic bile ducts should appear as they do in a normal, native liver [18]. If a T-tube is in place, the walls of the extrahepatic bile ducts may appear slightly thickened [18]. The portal vein, IVC, hepatic artery, and hepatic vein should all be assessed under Doppler US examination [18]. Each vessel has a characteristic normal waveform: the hepatic artery has a brisk systolic upstroke and continuous diastolic flow, the portal veins have continuous flow toward the liver, and the hepatic veins and vena cava have a phasic pattern, corresponding to the cardiac cycle (Fig. 4.14) [18]. Two quantities should be measured in the hepatic arteries: acceleration time—the time to peak systolic flow from the start of the upstroke (normal, <80 ms)—and the resistive index[1] (normal, 0.5–0.7) [18]. A small amount of free fluid in the perihepatic, intra-abdominal space is normal in the first week after transplant [18].

[1] (Peak systolic velocity (PSV) − peak diastolic velocity)/PSV)

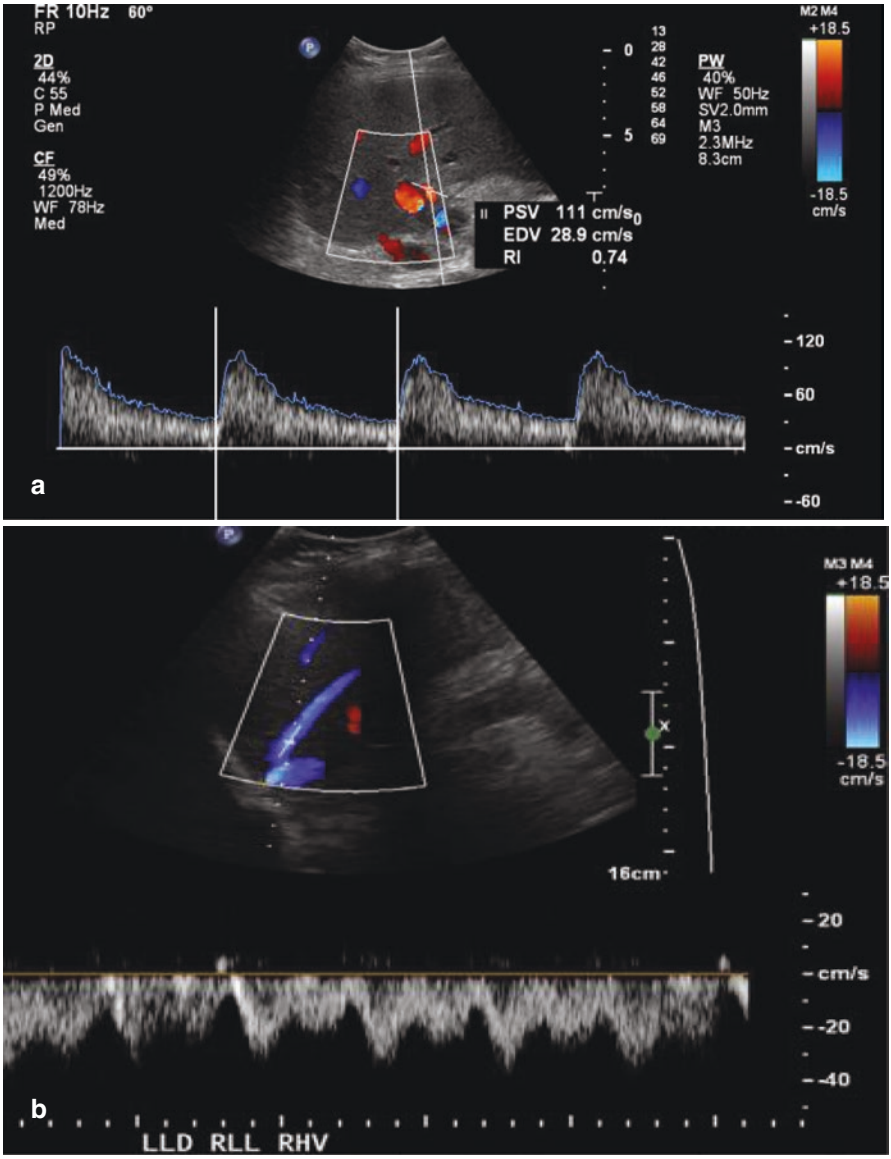

Fig. 4.14 Duplex US of hepatic artery after transplant with normal waveform (**a**), duplex US of hepatic vein after transplant with normal hepatic venous flow (**b**)

Vascular Complications

Hepatic Artery

Thrombosis

Hepatic artery thrombosis (HAT) is the most common vascular complication after liver transplant [18] occurring in 2–12% of patients and is thus a major cause of both graft loss and mortality [18, 19]. The incidence of HAT is slightly higher in children [20]. HAT may present with a variety of features that have some relation to the time of presentation. Early HAT (<4–8 weeks after transplant) typically has a morbid presentation that results in biliary complications (necrosis and stricture), acute graft failure, sepsis, abscess formation, and death [19, 21]. Late HAT can have a more clinically indolent course especially if collateral circulation develops [21]. Late HAT typically presents with elevated LFTs but can also present with cholangitis and biliary complications (stricture, leak, or abscess) [21]. As discussed below, nonanastomotic stricture of the biliary tree is almost always caused by HAT or hepatic artery stenosis, since the bile ducts are exclusively arterially perfused while hepatic parenchyma is perfused predominantly from the portal vein [18]. HAT is a severe complication that typically requires surgical management, including thrombectomy and retransplantation [18, 19, 21], while hepatic arterial stenosis may be treated by interventional radiological techniques such as angioplasty and stenting.

HAT is initially diagnosed by nonvisualization of the hepatic artery on color and spectral Doppler US with absent flow at the hepatic hilum and distal intrahepatic arterial branches [18, 20]. If an arterial waveform is imaged, the resistive index (RI) may be elevated, indicating a possible thrombosis distal to the site of Doppler US evaluation [20]. However, it should also be noted that in the immediate postoperative period (first few days) the RI is elevated in about half of transplant patients without complications [20]. If arterial flow is detected intrahepatically distal to the thrombosed hepatic artery, the Doppler waveform often corresponds to findings in hepatic artery stenosis (see below), which may be due to minimal residual flow or collateral flow. Doppler US has high sensitivity and specificity for HAT, but false negatives and positives remain: failure to visualize flow through a patent hepatic artery or imaging of collateral arteries [18, 20]. Arterial spasm and poor cardiac output preclude patent arterial Doppler US signal [18]. Use of US contrast agents can improve the sensitivity of Doppler US [20]. Imaging with CTA or MRA is usually definitive if Doppler US is inconclusive or misleading (Fig. 4.15) [18].

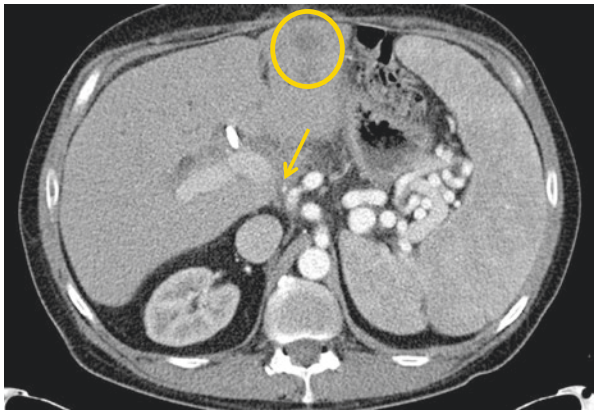

Fig. 4.15 Hepatic artery thrombosis (*arrow*) after transplant with corresponding area of infarct (*circle*)

Stenosis

Hepatic artery stenosis also occurs in 2–12% of posttransplant patients [18, 22, 23] and typically presents with graft dysfunction (e.g., elevated aminotransferases) or biliary complications secondary to ischemia, although about 20% of patients may be asymptomatic [22]. Risk factors for the development of hepatic artery stenosis include poor surgical technique, vascular trauma (e.g., from surgical clamps), graft rejection, and microvascular injury [18, 22]. If diagnosed, hepatic artery stenosis may require treatment with angioplasty or surgery [18].

Though conventional catheter angiography is considered the gold standard, CTA, and MRA are usually definitive for diagnosis of hepatic artery stenosis; however the work-up of suspected hepatic artery stenosis usually begins with duplex Doppler US due to its rapid noninvasive nature and ability to measure critical diagnostic values (resistive index, systolic acceleration time, and peak systolic velocity) [18, 24]. Hepatic artery stenosis presents with low RI (<0.5), prolonged systolic acceleration time (>0.08 s), and a focal, high-velocity flow at the strictured anastomosis in the extrahepatic artery (>200 cm/s), though the anastomosis may be difficult to visualize, [18, 24]. In the intrahepatic arteries, a tardus parvus waveform indicates a proximal upstream stenosis (Fig. 4.16) [24]. Elevated RIs (>0.8) may normally occur in the early transplant period and do not necessarily indicate arterial stenosis in isolation [18].

Technical factors such as deep arteries in obese patients or an improper insonation angle may preclude an accurate diagnosis of hepatic artery stenosis with color Doppler US. With deep arteries, it is difficult to position the ultrasound probe at the proper angle to obtain an accurate velocity measurement [18, 24]. Furthermore, not all cases of hepatic artery stenosis may have abnormal changes in RI, peak velocity, and systolic acceleration time [24].

Contrast-enhanced US (CEUS) using microbubble contrast agents may have higher sensitivity and specificity than color Doppler alone (92% and 87%, respectively) [24]. If either duplex Doppler US or CEUS suggests stenosis, CTA or MRA may be helpful for interventional or surgical planning at the site of stenosis [24].

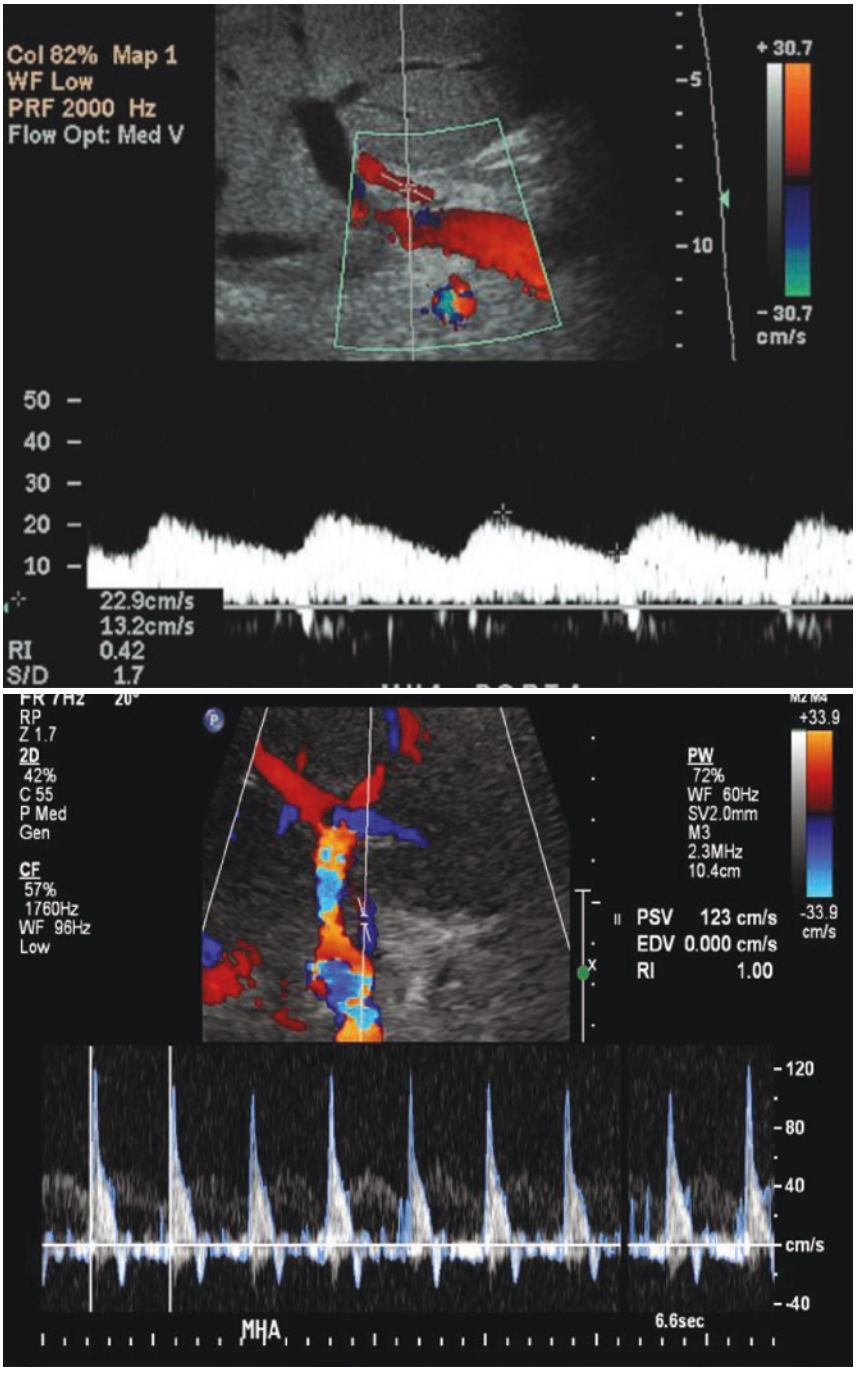

Fig. 4.16 Doppler US of hepatic artery demonstrating parvus tardus waveform with resistive index of 0.42 consistent with hepatic artery stenosis (**a**), high resistance waveform in the MHA, often seen following ischemia reperfusion injury (**b**)

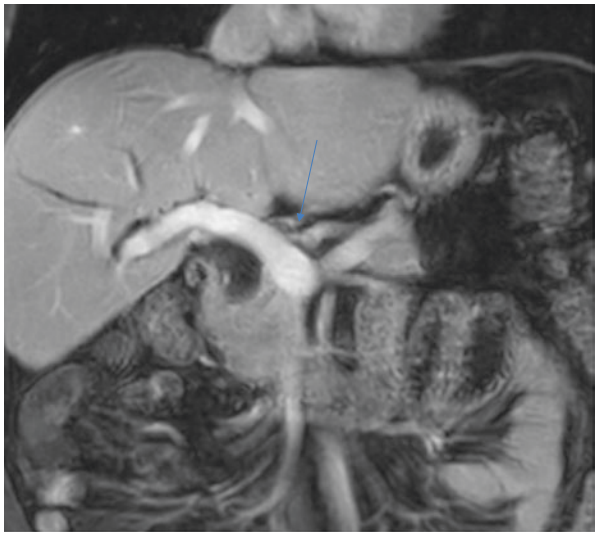

Fig. 4.17 Markedly diminutive hepatic artery ostium without visualization of the common hepatic artery distally

Although both CTA and MRA with 3D reconstruction of the hepatic artery localize the point of stenosis [18, 24], MRA acquisition is more technically complex and may have a higher false-positive rate for diagnosis of stenosis (Fig. 4.17) [18].

Pseudoaneurysm

Pseudoaneurysm is a pathological dilatation of the hepatic artery and an uncommon complication of liver transplantation (0.3–2% of transplants) that typically occurs as a consequence of surgical or interventional manipulations, but can also be a complication of local infection [18, 25, 26]. Pseudoaneurysm most commonly presents 2–3 weeks after transplant and can develop at both intra- and extrahepatic sites [25]. Intrahepatic pseudoaneurysms are more commonly due to procedures such as percutaneous biopsy or biliary interventions and are more likely to have a subclinical course [18, 25]. Extrahepatic pseudoaneurysms are often associated with local infection, angioplasty, or technical problems with the arterial anastomosis [18, 25]. Extrahepatic pseudoaneurysms are also more likely to have a rapidly progressing course. Roux-en-Y hepaticojejunostomy may be a risk factor for extrahepatic pseudoaneurysm as it creates a route for bacterial translocation from the gut that then causes local infection [25]. Other causes of sepsis, including septicemia after bowel perforation, are also risk factors [25]. Pseudoaneurysm may be clinically silent but may result in often nonspecific presentations (hemobilia, hepatic artery thrombosis, fever or graft dysfunction, falling hemoglobin) [25]. Pseudoaneurysm rupture may result in shock and hemorrhage into the peritoneum GI tract or arteriobiliary fistula [25, 26]. It is a serious, life-threatening complication that requires early treatment with coil embolization, stent placement, or resection [18, 25].

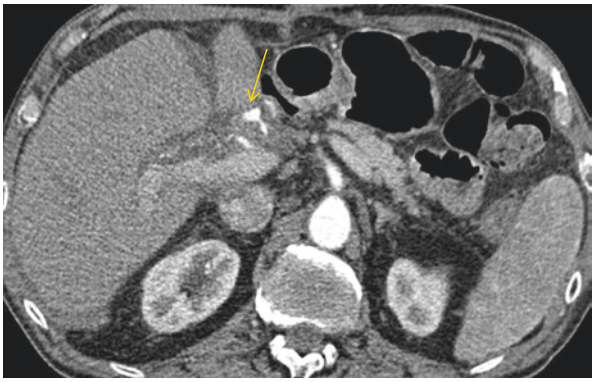

Fig. 4.18 Pseudoaneurysm of the proper hepatic artery

Doppler US is the preferred initial imaging modality for pseudoaneurysm screening. Pseudoaneurysm will demonstrate a hypoechoic, rounded region with disorganized or bidirectional flow that may resemble a yin-yang symbol [18, 25]. Intrahepatic pseudoaneurysm is more easily identified on ultrasound than extrahepatic pseudoaneurysm [25]. Contrast CT will demonstrate a low attenuation area that enhances with contrast administration (Fig. 4.18) [25]. The presence of free fluid at the site of the arterial anastomosis on any imaging modality—ultrasound or CT—is an indication for use of Doppler to rule out pseudoaneurysm, as it may indicate an area of focal infection with consequent pseudoaneurysm formation [25]. Similarly, any sign of hepatic ischemia on CT suggests the possibility of pseudoaneurysm and is an indication for Doppler or angiography [25]. The gold standard for diagnosis of pseudoaneurysm is angiography and should be completed if pseudoaneurysm is suspected (e.g., in the case of ongoing hemorrhage or graft dysfunction) even when prior imaging with other modalities has been unremarkable [25].

Portal Vein

Posttransplant portal vein complications are less common than arterial complications, occurring in only 1–13% of transplants, and tend to occur secondary to technical complications (e.g., size mismatch in donor and portal vessels or poor surgical technique) or recipient factors (e.g., hypercoagulable state, history of thrombosis) [18].

Stenosis

Portal vein stenosis tends to occur at the site of anastomosis [18]. Like arterial stenosis, portal vein stenosis is best diagnosed initially with Doppler ultrasound and the use of measurements of flow (Fig. 4.19) [18]. Portal vein stenosis is diagnosed when peak anastomotic velocity exceeds 125 cm/s or the velocity of blood flow

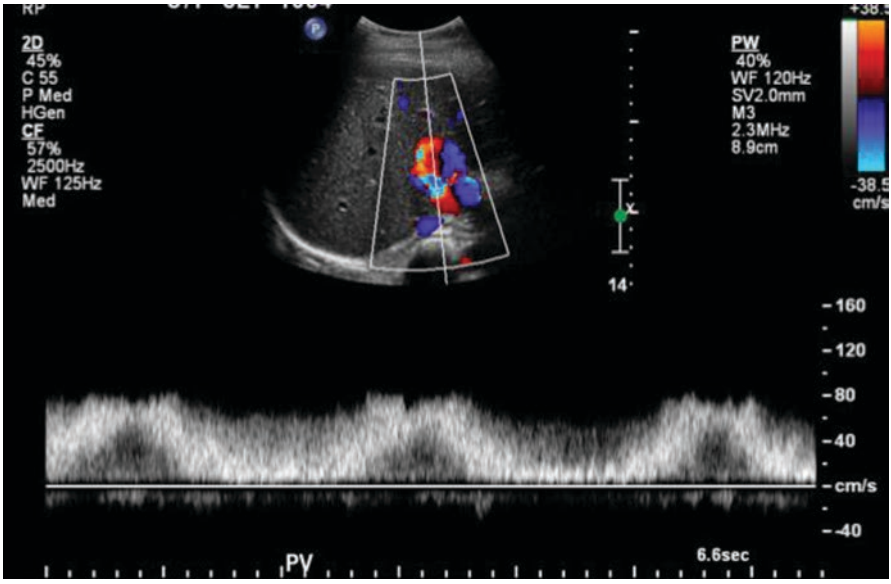

Fig. 4.19 Portal vein stenosis after liver transplant; spectral Doppler shows high-velocity, turbulent flow on postoperative day 5

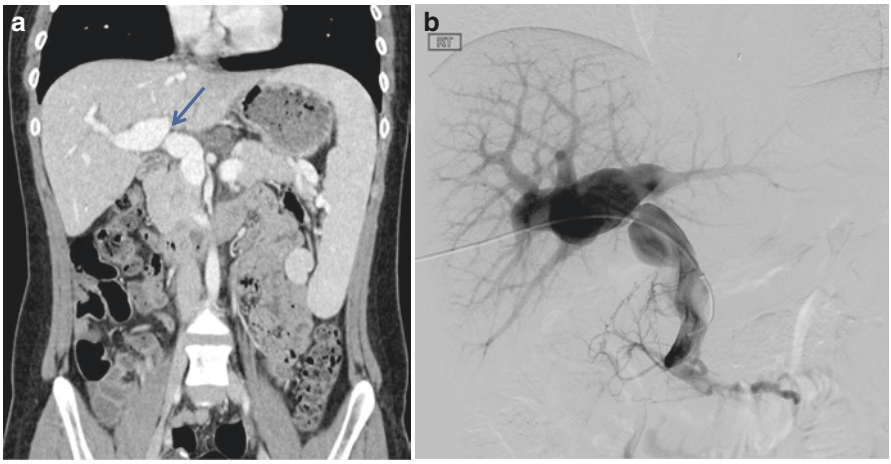

Fig. 4.20 CT demonstrating portal vein stenosis followed by angiogram performed during balloon venoplasty

increases significantly as it moves into the area of anastomosis (three times the velocity proximal to anastomosis) [18]. Mismatched size of the donor and recipient vessels can be mistaken for stenosis under ultrasound examination [18]. If this is suspected, direct percutaneous portography can confirm that there is a significant pressure gradient between the proximal and distal sides of the anastomosis (>5 mm) [18]. Other imaging modalities, including CT and MRI, can further visualize and localize a portal vein stenosis (Fig. 4.20) [18].

Thrombosis

Posttransplant portal vein thrombosis occurs in about 3% of transplants and can be diagnosed with Doppler ultrasound that demonstrates no portal flow or CT and MRI that demonstrates a filling defect in the portal vein [18]. Portal vein thrombosis occurs most commonly in the extrahepatic portal vein and is treated with any number of methods: thrombectomy, percutaneous angioplasty, stent placement, thrombolysis via SMA injection or direct percutaneous access via the transplant liver, or resection of the affected portion of the vein [18].

IVC/Hepatic Vein

Stenosis and thrombosis of the hepatic veins or IVC are rare complications after liver transplant, occurring in about 1–2% of transplants [18].

Stenosis

The IVC is most likely to become stenotic at the point of the anastomosis or secondary to compression from an external mass (e.g., liver graft, fluid, hematoma) [18]. Stenosis of the IVC is characterized by a significant increase in velocity of blood flow (three to four times normal) and distension of hepatic veins proximal to the stenosis [18]. Both CT and MR will demonstrate focal narrowing of the IVC and may also demonstrate the sequelae of obstructed venous outflow—Budd-Chiari syndrome or portal hypertension [18]. Stenosis can similarly affect the hepatic veins. Hepatic vein stenosis, however, is more common in living donor liver transplant [18]. Duplex Doppler US that demonstrates replacement of the normal triphasic hepatic vein pattern with monophasic waveforms and a venous pulsatility index of <0.45 may suggest hepatic vein stenosis [18].

Thrombosis

Thromboses of the IVC or hepatic veins are most commonly secondary to direct surgical complication or a hypercoagulable state [18]. Like other thromboses, they are identified on ultrasound by the absence of flow and on contrast-enhanced CT or MRI by intraluminal filling defect [18].

Biliary Complications

Biliary complications after liver transplant include strictures, leaks, bilomas, and stones. Biliary tract complication occurs with an incidence of 11–25% [27]. The majority (80%) of biliary complications of liver transplantation occur in the first 6 months after transplant with many even occurring within the first 3 months [28].

Stones

Biliary stones and thickened bile (sludge) after liver transplantation are uncommon, developing mainly in dilated ducts due to downstream biliary stricture (Figs. 4.21, 4.22, 4.23, and 4.24) [29]. Immunosuppressive drugs, including cyclosporine, can contribute to the formation of sludge and stones by altering the composition of bile [28]. Evaluation for choledocholithiasis after transplant is best completed via magnetic resonance cholangiopancreatography (MRCP), but may be detected with less sensitivity with US and CT (Figs. 4.22, 4.23, and 4.24). Sludge and stones will typically appear as filling defects in the dilated intra- and extrahepatic ducts proximal to the stenosis [29].

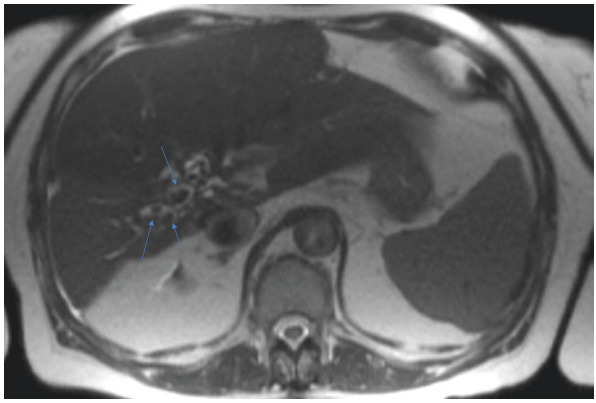

Fig. 4.21 MRI of a patient with underlying primary sclerosing cholangitis (PSC) status post-OLT that was complicated by hepatic artery thrombosis (HAT). The patient subsequently developed intrahepatic biliary stricture and numerous intrahepatic biliary stones (*arrows*)

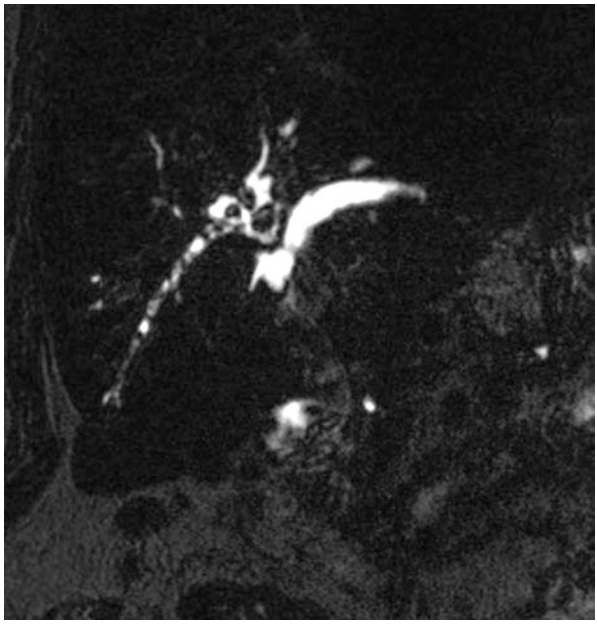

Fig. 4.22 Biliary stones

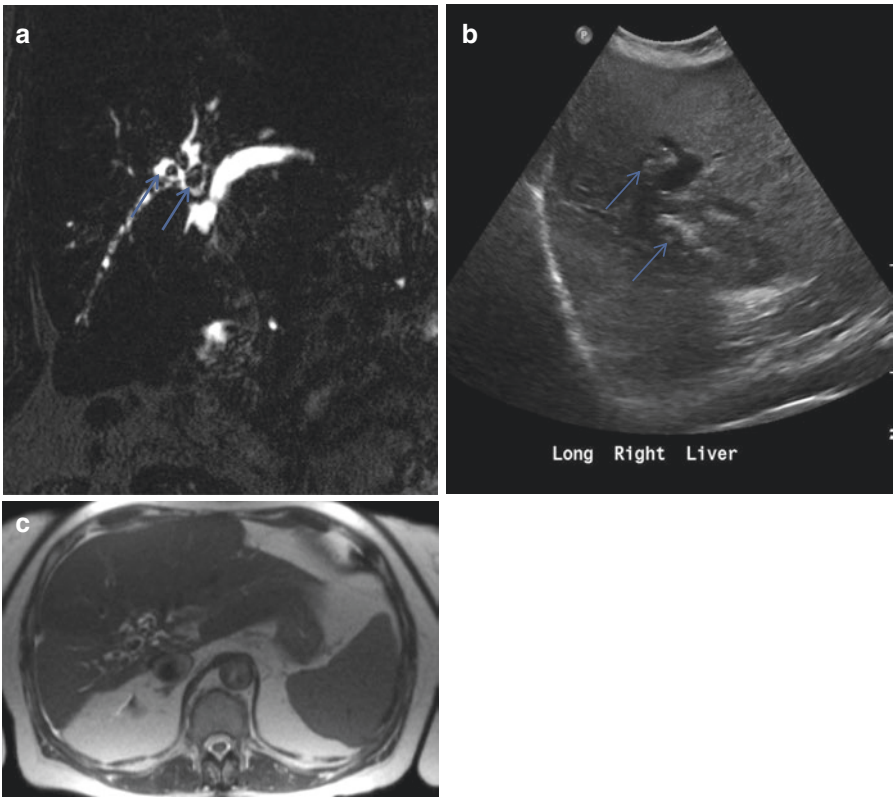

Fig. 4.23 3D MRCP (**a**), ultrasound (**b**), and MRI (**c**) showing intraductal calculi in the same patient

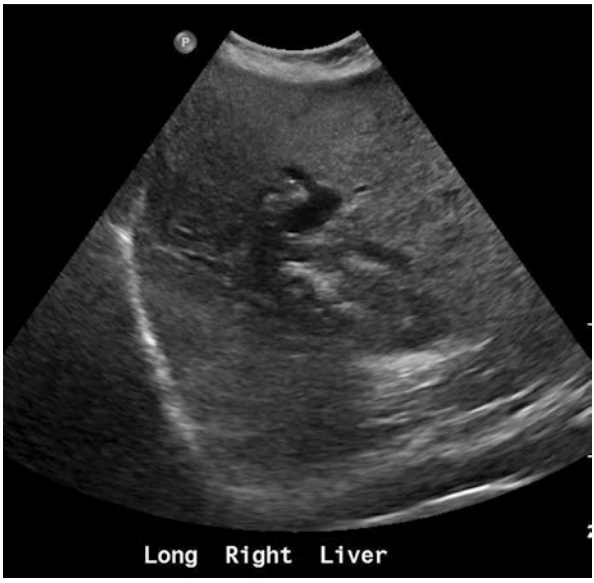

Fig. 4.24 Ultrasound demonstrating stones within the biliary tree after transplant

Stricture/Stenosis

Biliary strictures which occur in 5–15% of OLTs and in 28–32% of right lobe LDLTs, most commonly occur at the anastomosis (anastomotic stricture) or much less commonly elsewhere (nonanastomotic stricture) [27]. Stricture most often presents in asymptomatic patients with elevations in bilirubin, aminotransferases, and alkaline phosphatase. A small percentage of patients present with pruritus or abdominal pain [27].

Anastomotic strictures are most commonly unifocal and caused by tension at the anastomosis site, ischemia, or a mismatch in the size of the donor and recipient ducts. Nonanastomotic strictures are most often caused by hepatic artery thrombosis or stenosis with secondary causes including cold ischemia prior to transplantation, infection, rejection, or recurrent primary sclerosing cholangitis. All these processes result in biliary epithelial injury and ensuing ductal fibrosis [27, 29]. Nonanastomotic strictures tend to be multifocal and are more likely found in the intrahepatic bile ducts (Fig. 4.21) [29].

US is the first-line imaging technique for evaluating biliary stricture and to assess arterial patency. Although US can predict biliary stenosis with high positive predictive value in the presence of ductal dilatation, its sensitivity for biliary stenosis may vary from 38 to 71% since ducts may not dilate [27, 30].

MRCP has the highest sensitivity and specificity (>90%) for detection and characterization of biliary stricture and should be performed to comprehensively map biliary strictures (Fig. 4.25) [27, 29]. If MRCP demonstrates a flow limiting stricture, endoscopic retrograde cholangiopancreatography (ERCP) or possibly percutaneous transhepatic cholangiography (PTC) will be required for balloon dilatation and stent placement in anastomotic strictures [27, 29]. Anastomotic strictures are typically short-segment [29]. It is important to note, however, that not all cases of anasto-

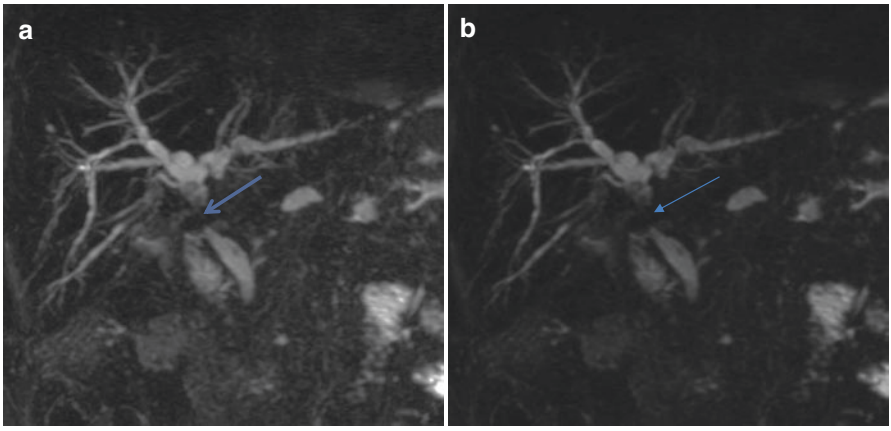

Fig. 4.25 Nonvisualization of the common bile duct in the presumed location of the anastomosis with moderate intrahepatic biliary dilatation

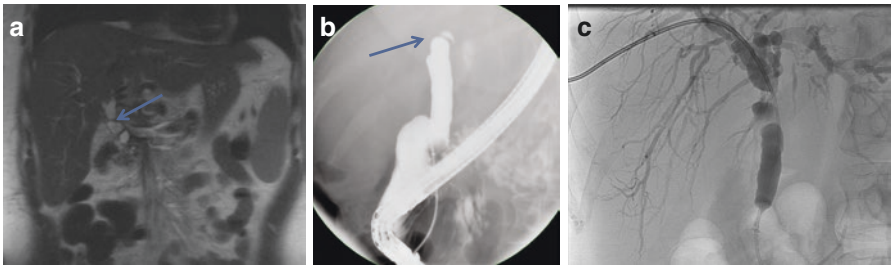

Fig. 4.26 Anastomotic strictures without intrahepatic biliary dilatation (**a**–**c**)

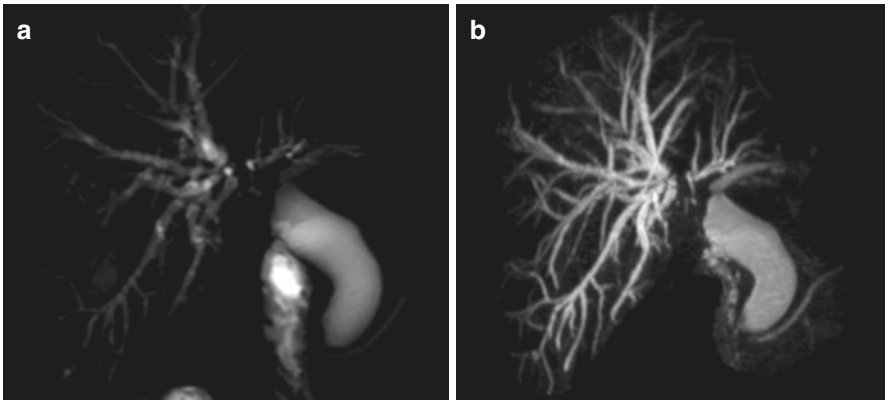

Fig. 4.27 Marked stricturing at the central right and left intrahepatic ducts (not visualized) with beaded and irregular appearance of more peripheral intrahepatic ducts

motic stricture will have proximal dilatation (Fig. 4.26). Although MRCP has high sensitivity for anastomotic stricture, there are several false positives that can be mistaken for anastomotic stricture [29]. For example, a mismatch in size of the donor and recipient ducts may appear as a stricture with proximal dilatation [29]. Additionally, susceptibility artifacts from nearby hardware can cause the appearance of stricture [29]. Nonanastomotic strictures will appear as multiple segments of narrowing and dilatation, and the finding requires subsequent imaging of the hepatic artery to assess for patency (Fig. 4.27) [29].

ERCP and PTC are complementary methods for treatment of biliary strictures by enabling balloon stricturoplasty and stent placement. If the stricture cannot be traversed, PTC enables percutaneous drainage of the biliary tree to temporize until a more permanent solution such as ductal reconstruction or choledochojejunostomy is attempted (Fig. 4.28).

Biliary leak is often discovered on imaging of asymptomatic patients. The three most common locations for biliary leak are the site of anastomosis, the site of the cystic duct remnant, and the site of a prior T-tube [29]. Direct cholangiography can diagnose bile leak by identifying areas of extravasation of contrast material

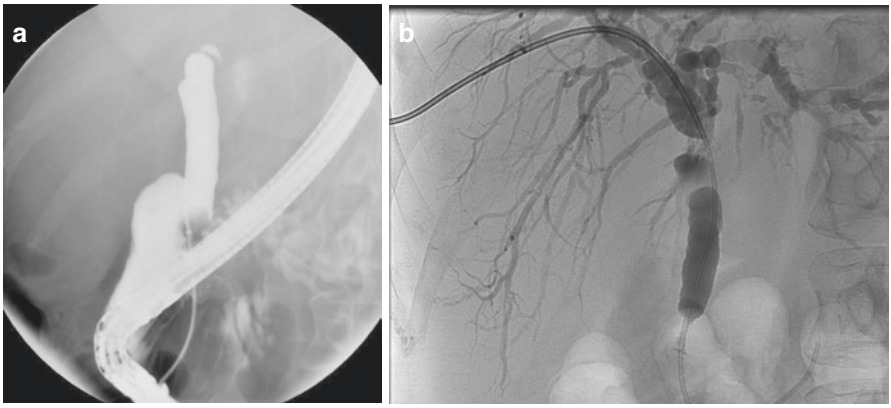

Fig. 4.28 An attempted ERCP unable to traverse a biliary stricture (**a**), placement of an internal/external biliary stent across the sites of stricture (**b**)

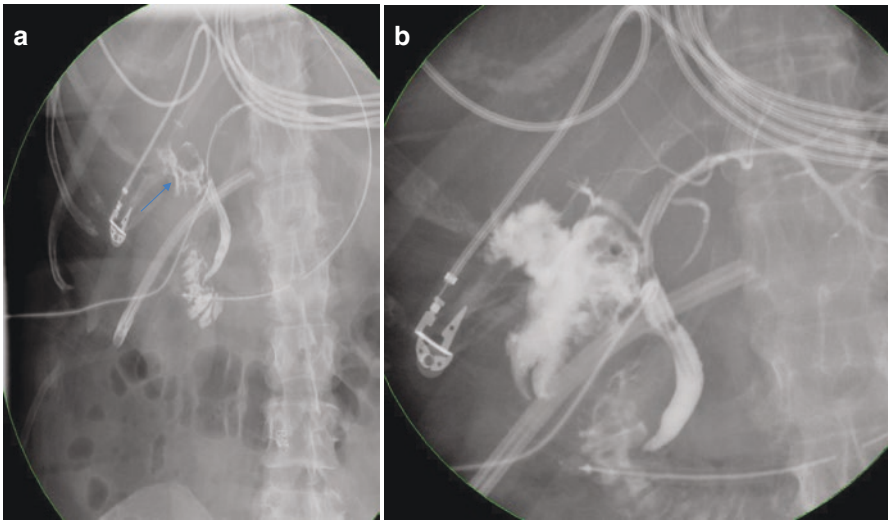

Fig. 4.29 Direct cholangiography demonstrating a large bile leak from the common bile duct at the site of entry of the T-tube. Contrast is seen extravasating from the site of T-tube entry, but there is no opacification of the right hepatic bile duct distal to the surgical clip

(Fig. 4.29) [18]. Biliary leaks are visible on ultrasound, CT, and MRI as nonspecific fluid collections requiring percutaneous sampling. The source of leaks can be localized with delayed hepatobiliary contrast-enhanced MRI or technetium HIDA nuclear medicine scans [29].

Other Complications

Infection/Abscess

Post-liver transplant-related infections occur in the first year following transplant, among patients who experience this complication, in 2/3 of cases, usually systemic from immunosuppression or much likely localized hepatic abscesses in 1–3% of patients [29, 31].

Though immunosuppression regimens after transplant increase the risk of developing unusual systemic infections, the infections of the early period following transplant (<1 month) are more likely to be common nosocomial postoperative infections, including wound infections, urinary tract infections, catheter-associated infections, and pneumonias due to common bacterial and fungal pathogens [29, 31]. *C. difficile* colitis is also common during this period [31].

From 1 to 6 months after transplant, patients are at greatest risk for developing opportunistic infections secondary to immunosuppression with opportunistic infections (*Pneumocystis carinii*, *Aspergillus*), and fungal infections (*Coccidioides*, *Cryptococcus*, *Histoplasma*) [29]. These infections have the same appearance in liver transplant patients as they have in all other patients [29]. After these first 6 months, most infections are common community-acquired infections. However, adverse situations, such as an episode of acute rejection necessitating higher immunosuppression levels, can reintroduce a risk for opportunistic infection [31]. Chronic, systemic diseases such as HIV, HBV, and HCV will also create an ongoing risk for opportunistic infection [31].

Hepatic ischemia, biliary stasis, and choledochojejunostomy all predispose patients to developing hepatic abscesses after transplant [29]. Patients who develop vascular and biliary complications after transplant are therefore at risk of developing subsequent hepatic abscesses [29]. Hepatic abscesses have a characteristic appearance in each imaging modality [29]. These findings can be seen summarized in Table 4.3 [29, 32]. If a hepatic abscess is identified, it is critical to assess the patient for any evidence of vascular or biliary complications [29].

Table 4.3 Radiographic features of hepatic abscesses

Imaging modality	Typical features
Ultrasound	Hyperechoic
Contrast-enhanced ultrasound	Honeycomb-like enhancement in all phases
CT	Low attenuation compared to parenchyma
MR T2 weighted	Hyperintense (increased intensity with increased liquidity)
MR T1 weighted	Hypointense (caveat: hemorrhage may cause hyperintensity)
Contrast-enhanced CT or MR	Arterial phase—perilesional hyperemia Portal venous/delayed phase—hypoenhancing

Hematoma

Hematoma is an early complication of liver transplant that typically occurs in the perianastomotic region during the first few postoperative weeks [18, 29]. Large hematomas may require surgical evacuation. On US, hematomas will typically be complex with mixed echotexture, and on CT they will be significantly higher attenuation (50–70 HU) than water in early stages with decreasing attenuation thereafter [18, 29]. On T1- and T2-weighted MRI, hematomas are variably hyper- and hypointense, respectively [18, 29].

Bowel Perforation

Bowel perforation is a rare but life-threatening complication after liver transplant that can occur throughout the GI tract typically from gastric or duodenal ulcers or colonic diverticulitis [33]. Risk factors for perforation include prolonged portal venous clamp time during surgery, portal venous thromboembolism, prior laparotomy, and CMV infection [33]. Patients who develop perforation after transplant are frequently immunosuppressed and on pain medications and steroids, which can cause them to have an atypical clinical presentation [33]. Perforation also places patients at elevated risk for developing intra-abdominal infection [33].

Malignancy (Recurrent HCC, PTLD, Angiosarcoma)

Malignancy is a common late complication of liver transplant that is primarily an adverse consequence of immunosuppression. Transplant patients are at increased risk for de novo malignancies of many kinds (e.g., nonmelanomatous skin cancer, lymphoma, angiosarcoma) as well as recurrent HCC. The relative risk of developing any de novo malignancy after liver transplant as compared to the general population may be as high as 4.3 and is as high as 70 for specific malignancies, such as nonmelanomatous skin cancer [34]. The development of de novo malignancies is particularly important as a cause of late death (e.g., >3 years posttransplant) in liver transplant patients, in some studies causing greater mortality than cardiovascular disease [35].

HCC patients undergoing liver transplant have an 8–18% HCC posttransplant recurrence rate [36, 37]. Recurrent HCC is typically detected in the lungs or grafted liver and may also be detected in the bone, adrenal glands, peritoneum, lymph nodes, skin, and cerebrum [28, 38]. Recurrent HCC in the first year after transplant has poorer prognosis than recurrence after 1 year posttransplant [36]. There is no accepted imaging protocol for screening transplanted HCC patients for recurrence [37]. Imaging appearance of HCC is similar to pretransplant HCC

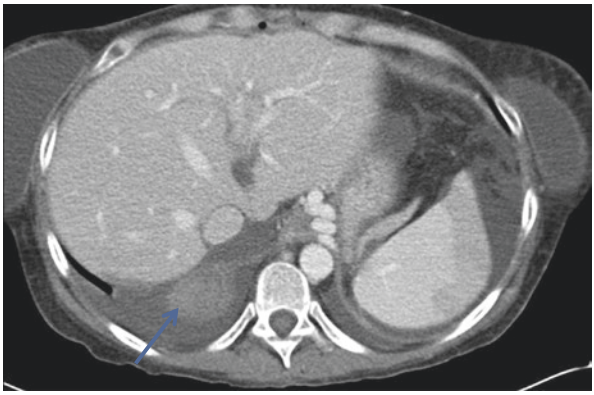

Fig. 4.30 Right adrenal gland hematoma

with up to 70% of lesions enhancing avidly after contrast with rapid washout thereafter (Fig. 4.30).

Posttransplant lymphoproliferative disorder (PTLD) is an immunosuppression-related lymphoproliferative disorder that occurs after solid-organ transplant. There is a wide range of manifestations from mononucleosis to lymphoma, from polyclonal (e.g., reactive hyperplasia) to high-grade monoclonal (e.g., non-Hodgkin lymphoma), and the disorder can be benign or life-threatening [28, 29, 39]. The majority of PTLD cases are related to Epstein-Barr virus (EBV) infection and arise from the B cells of the recipient, though the disorder can occur in the absence of EBV infection, from T cells, and from the immune system of the organ donor [39, 40]. In EBV-related cases, PTLD is thought to arise as an adverse effect of immunosuppression, as drug-induced T-cell dysfunction allows uncontrolled proliferation of infected B cells [39]. For this reason, PTLD may occur most commonly during the first year of transplant when immunosuppression levels are highest [28, 39]. The presentation of patients with PTLD is highly variable: from fever and lymphadenopathy to intestinal perforation and signs of disseminated disease [39, 40]. The World Health Organization (WHO) published a classification scheme in 2008 that categorizes PTLD into one of four basic pathological groups: (a) early lesions (e.g., mononucleosis-like); (b) polymorphic PTLD (has some malignant features); (c) monomorphic, lymphomatous PTLD; and (d) classical Hodgkin-like PTLD [39, 41]. Monomorphic, lymphomatous PTLD is further categorized by the type of lymphoma it resembles (e.g., diffuse B-cell lymphoma, Burkitt's lymphoma, etc.), and classical Hodgkin-like PTLD fulfills the criteria for a diagnosis of Hodgkin lymphoma [41].

Evaluation of patients with PTLD should include CT of the chest, abdomen, and pelvis to stage the disease as well as possible imaging of the spine, brain, and GI tract if involvement of these is suspected [40]. PTLD most commonly affects the liver and GI tract with focal or diffuse lesions within the liver and as periportal soft tissue lesions [42]. Other findings include splenomegaly, gallbladder or bowel-wall thickening, lymphadenopathy, eccentric masses, and intussusception (Fig. 4.31) [42]. Although abdominal lymphadenopathy is much less common, retroperitoneal

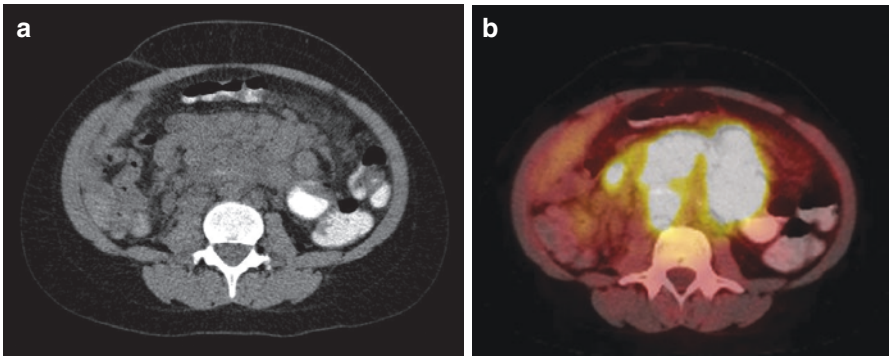

Fig. 4.31 Noncontrast CT (**a**) and fused FDG-PET CT (**b**) showing FDG-avid mesenteric and retroperitoneal lymphadenopathy in a patient with PTLD

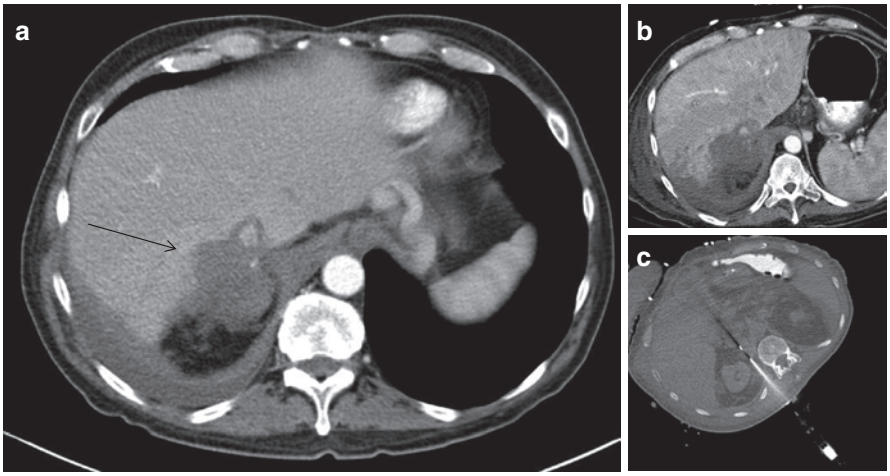

Fig. 4.32 Infiltrative mass in posterior right hepatic lobe (**a**, **b**, *arrow*) found to be an angiosarcoma on biopsy (**c**)

lymph node involvement is more common in PTLD patients [42]. Thoracic PTLD is more common after lung than liver transplant patients. In the thorax, PTLD may manifest as pulmonary nodules, thoracic masses, pulmonary consolidations, lymphadenopathy, and effusions [42]. Head and neck involvement of PTLD can include the cervical lymph nodes, the soft tissues of pharynx, and the orbit [42]. Intracranial PTLD classically appears as hemorrhage, necrosis, and peripheral enhancement in the periventricular and subcortical white matter [42].

Another posttransplant malignancy that requires radiographic evaluation is angiosarcoma. Angiosarcoma is a malignancy that arises from the endothelium of blood vessels and lymphatics [29]. Angiosarcoma is a high-grade sarcoma that appears as a peripherally enhancing infiltrative mass in either the soft tissues, breast, liver, or bone (Fig. 4.32) [29]. Other imaging options include T2-weighted MRI, which demonstrates some enhancement and PET scanning [29].

References

1. UNOS matches organs and saves lives through organ transplantation [Internet]. [cited 2016 Dec 3]. https://www.unos.org/bucketlist/.
2. Singh AK, Cronin CG, Verma HA, Boland GW, Saini S, Mueller PR, et al. Imaging of preoperative liver transplantation in adults: what radiologists should know. Radiographics [Internet]. 2011;31(4):1017–30. https://doi.org/10.1148/rg.314105197.
3. Wiesner R, Edwards E, Freeman R, Harper A, Kim R, Kamath P, et al. Model for end-stage liver disease (MELD) and allocation of donor livers. Gastroenterology [Internet]. 2003;124(1):91–6. https://doi.org/10.1053/gast.2003.50016.
4. Toso C, Trotter J, Wei A, Bigam DL, Shah S, Lancaster J, et al. Total tumor volume predicts risk of recurrence following liver transplantation in patients with hepatocellular carcinoma. Liver Transpl [Internet]. 2008;14(8):1107–15. https://doi.org/10.1002/lt.21484.
5. Mazzaferro V, Regalia E, Doci R, Andreola S, Pulvirenti A, Bozzetti F, et al. Liver transplantation for the treatment of small hepatocellular carcinomas in patients with cirrhosis. N Engl J Med [Internet]. 1996;334(11):693–700. https://doi.org/10.1056/nejm199603143341104.
6. Yao F. Liver transplantation for hepatocellular carcinoma: expansion of the tumor size limits does not adversely impact survival. Hepatology [Internet]. 2001;33(6):1394–403. https://doi.org/10.1053/jhep.2001.24563.
7. Roll GR, Parekh JR, Parker WF, Siegler M, Pomfret EA, Ascher NL, et al. Left hepatectomy versus right hepatectomy for living donor liver transplantation: shifting the risk from the donor to the recipient. Liver Transpl [Internet]. 2013;19(5):472–81. https://doi.org/10.1002/lt.23608.
8. Bathla L, Vargas LM, Langnas A. Left lobe liver transplants. Surg Clin North Am [Internet]. 2013;93(6):1325–42. https://doi.org/10.1016/j.suc.2013.09.003.
9. Broelsch CE, Whitington PF, Emond JC, Heffron TG, Thistlethwaite JR, Stevens L, et al. Liver transplantation in children from living related donors. Surgical techniques and results. Ann Surg [Internet]. 1991;214(4):428–37; discussion 437–9. https://www.ncbi.nlm.nih.gov/pubmed/1953097.
10. Liu H, Li R, Fu J, He Q, Li J. Technical skills required in split liver transplantation. Ann Transplant [Internet]. 2016;21:408–15. https://www.ncbi.nlm.nih.gov/pubmed/27363540.
11. Emre S, Umman V. Split liver transplantation: an overview. Transplant Proc [Internet]. 2011;43(3):884–7. https://doi.org/10.1016/j.transproceed.2011.02.036.
12. Fischer JE, Bland KI, Callery MP. Mastery of surgery [Internet]. Lippincott Williams & Wilkins; 2006. 2592 p. http://books.google.com/books/about/Mastery_of_Surgery.html?hl=&id=PgUFJg_-f4YC.
13. Lladó L, Figueras J. Techniques of orthotopic liver transplantation. HPB [Internet]. 2004;6(2):69–75. https://doi.org/10.1080/13651820310020756.
14. Mortelé K. Preoperative liver donor evaluation: imaging and pitfalls. Liver Transpl [Internet]. 2003;9(9):S6–14. https://doi.org/10.1053/jlts.2003.50199.
15. Sahani D, Mehta A, Blake M, Prasad S, Harris G, Saini S. Preoperative hepatic vascular evaluation with CT and MR angiography: implications for surgery. Radiographics [Internet]. 2004;24(5):1367–80. https://doi.org/10.1148/rg.245035224.
16. Favelier S, Germain T, Genson P-Y, Cercueil J-P, Denys A, Krausé D, et al. Anatomy of liver arteries for interventional radiology. Diagn Interv Imaging [Internet]. 2015;96(6):537–46. https://doi.org/10.1016/j.diii.2013.12.001.
17. Xie YZ, Liu J, Chung GH, Kong X, Li XJ, Zhang LT, et al. Visualization of the segment IV hepatic artery using 128-section MDCT angiography. Clin Radiol [Internet]. 2014;69(9):965–73. https://doi.org/10.1016/j.crad.2014.05.001.
18. Singh AK, Nachiappan AC, Verma HA, Uppot RN, Blake MA, Saini S, et al. Postoperative imaging in liver transplantation: what radiologists should know. Radiographics [Internet]. 2010;30(2):339–51. https://doi.org/10.1148/rg.302095124.
19. Bekker J, Ploem S, de Jong KP. Early hepatic artery thrombosis after liver transplantation: a systematic review of the incidence, outcome and risk factors. Am J Transplant [Internet]. 2009;9(4):746–57. https://doi.org/10.1111/j.1600-6143.2008.02541.x.

20. García-Criado A, Gilabert R, Berzigotti A, Brú C. Doppler ultrasound findings in the hepatic artery shortly after liver transplantation. AJR Am J Roentgenol [Internet]. 2009;193(1):128–35. https://doi.org/10.2214/AJR.07.3919.
21. Silva MA, Jambulingam PS, Gunson BK, Mayer D, Buckels JAC, Mirza DF, et al. Hepatic artery thrombosis following orthotopic liver transplantation: a 10-year experience from a single centre in the United Kingdom. Liver Transpl [Internet]. 2006;12(1):146–51. https://doi.org/10.1002/lt.20566.
22. da Silva RF, Raphe R, Felício HC, Rocha MF, Duca WJ, Arroyo PCJ, et al. Prevalence, treatment, and outcomes of the hepatic artery stenosis after liver transplantation. Transplant Proc [Internet]. 2008;40(3):805–7. https://doi.org/10.1016/j.transproceed.2008.02.041.
23. Settmacher U, Stange B, Haase R, Heise M, Steinmüller T, Bechstein WO, et al. Arterial complications after liver transplantation. Transpl Int [Internet]. 2000;13(5):372–8. https://doi.org/10.1111/j.1432-2277.2000.tb01012.x.
24. Zheng R-Q, Mao R, Ren J, Xu E-J, Liao M, Wang P, et al. Contrast-enhanced ultrasound for the evaluation of hepatic artery stenosis after liver transplantation: potential role in changing the clinical algorithm. Liver Transpl [Internet]. 2010;16(6):729–35. https://doi.org/10.1002/lt.22054.
25. Marshall MM, Muiesan P, Srinivasan P, Kane PA, Rela M, Heaton ND, et al. Hepatic artery pseudoaneurysms following liver transplantation: incidence, presenting features and management. Clin Radiol [Internet]. 2001;56(7):579–87. https://doi.org/10.1053/crad.2001.0650.
26. Fistouris J, Herlenius G, Bäckman L, Olausson M, Rizell M, Mjörnstedt L, et al. Pseudoaneurysm of the hepatic artery following liver transplantation. Transplant Proc [Internet]. 2006;38(8):2679–82. https://doi.org/10.1016/j.transproceed.2006.07.028.
27. Sharma S, Gurakar A, Jabbour N. Biliary strictures following liver transplantation: past, present and preventive strategies. Liver Transpl [Internet]. 2008;14(6):759–69. https://doi.org/10.1002/lt.21509.
28. Crossin JD, Muradali D, Wilson SR. US of liver transplants: normal and abnormal. Radiographics [Internet]. 2003;23(5):1093–114. https://doi.org/10.1148/rg.235035031.
29. Camacho JC, Coursey-Moreno C, Telleria JC, Aguirre DA, Torres WE, Mittal PK. Nonvascular post–liver transplantation complications: from US screening to cross-sectional and interventional imaging. Radiographics [Internet]. 2015;35(1):87–104. https://doi.org/10.1148/rg.351130023.
30. Beswick DM, Miraglia R, Caruso S, Marrone G, Gruttadauria S, Zajko AB, et al. The role of ultrasound and magnetic resonance cholangiopancreatography for the diagnosis of biliary stricture after liver transplantation. Eur J Radiol [Internet]. 2012;81(9):2089–92. https://doi.org/10.1016/j.ejrad.2011.07.008.
31. Blair JE, Kusne S. Bacterial, mycobacterial, and protozoal infections after liver transplantation—part I. Liver Transpl [Internet]. 2005;11(12):1452–9. https://doi.org/10.1002/lt.20624.
32. Ding H, Wang W-P, Huang B-J, Wei R-X, He N-A, Qi Q, et al. Imaging of focal liver lesions: low-mechanical-index real-time ultrasonography with SonoVue. J Ultrasound Med [Internet]. 2005;24(3):285–97. https://www.ncbi.nlm.nih.gov/pubmed/15723841.
33. Fang C, Yan S, Liu J, Zheng S. Gastrointestinal perforation after liver transplantation. Surg Pract [Internet]. 2016;20(1):8–12. https://doi.org/10.1111/1744-1633.12154.
34. Haagsma EB, Hagens VE, Schaapveld M, van den Berg AP, de Vries EG, Klompmaker IJ, et al. Increased cancer risk after liver transplantation: a population-based study. J Hepatol [Internet]. 2001;34(1):84–91. https://www.ncbi.nlm.nih.gov/pubmed/11211912.
35. Pruthi J. Analysis of causes of death in liver transplant recipients who survived more than 3 years. Liver Transpl [Internet]. 2001;7(9):811–5. https://doi.org/10.1053/jlts.2001.27084.
36. Roayaie S, Schwartz JD, Sung MW, Emre SH, Miller CM, Gondolesi GE, et al. Recurrence of hepatocellular carcinoma after liver transplant: patterns and prognosis. Liver Transpl [Internet]. 2004;10(4):534–40. https://doi.org/10.1002/lt.20128.

37. Roberts JP. Tumor surveillance-what can and should be done? Screening for recurrence of hepatocellular carcinoma after liver transplantation. Liver Transpl [Internet]. 2005;(11 Suppl 2):S45–6. https://doi.org/10.1002/lt.20605.
38. Escartin A, Sapisochin G, Bilbao I, Vilallonga R, Bueno J, Castells L, et al. Recurrence of hepatocellular carcinoma after liver transplantation. Transplant Proc [Internet]. 2007;39(7):2308–10. https://doi.org/10.1016/j.transproceed.2007.06.042.
39. Gottschalk S, Rooney CM, Heslop HE. Post-transplant lymphoproliferative disorders. Annu Rev Med [Internet]. 2005;56(1):29–44. https://doi.org/10.1146/annurev.med.56.082103.104727.
40. Taylor AL, Marcus R, Bradley JA. Post-transplant lymphoproliferative disorders (PTLD) after solid organ transplantation. Crit Rev Oncol Hematol [Internet]. 2005;56(1):155–67. https://doi.org/10.1016/j.critrevonc.2005.03.015.
41. Choquet S. Classification and treatment of posttransplant lymphoproliferative disorders. Lymphoma Chronic Lymphocytic Leuk [Internet]. 2016;6:13. https://doi.org/10.4137/lcll.s34946.
42. Scarsbrook AF, Warakaulle DR, Dattani M, Traill Z. Post-transplantation lymphoproliferative disorder: the spectrum of imaging appearances. Clin Radiol [Internet]. 2005;60(1):47–55. https://doi.org/10.1016/j.crad.2004.08.016.

Chapter 5
Kidney Transplantation

Ghaneh Fananapazir and Christoph Troppmann

Surgical Techniques and Considerations

Worldwide, there were almost 80,000 kidney transplants performed in 2014, comprising the majority of solid organs transplanted. Most kidney grafts are from deceased donors, but living donor kidneys still constitute a significant percentage. For recipients of kidneys from deceased and live donors, graft survival is 94% and 98% at 1 year and 73% and 84% at 5 years, respectively [1]. Recipients require close follow-up, which includes regular urinalysis, serum creatinine measurements, monitoring of the immunosuppressive therapy, ultrasounds, and biopsies. The clinical features of graft dysfunction are often nonspecific, and imaging plays an important role not only in evaluating the kidney transplant but also in guiding graft biopsies as necessary. Before undertaking an evaluation of the transplanted kidney, it is important to be familiar with the surgical-anatomical placement of the kidney transplant, the type of donor kidney, the arterial and venous anastomoses, and the ureteral attachments.

Placement

The renal graft is usually placed in an extraperitoneal location in the recipient's right iliac fossa. The left iliac fossa is sometimes preferred for pancreas-kidney transplants, for pediatric en bloc kidney transplants, if there is underlying severe

G. Fananapazir, M.D.
Department of Radiology, University of California Davis Medical Center, Sacramento, CA, USA
e-mail: fananapazir@ucdavis.edu

C. Troppmann, M.D.
Department of Surgery, University of California Davis Medical Center, Sacramento, CA, USA

G. Fananapazir, R. Lamba (eds.), *Transplantation Imaging*,
https://doi.org/10.1007/978-3-319-75266-2_5

atherosclerotic disease involving the right iliac arteries, and in cases where the recipient has already received a prior, failed graft on the right side. In very small pediatric recipients, the kidney is sometimes placed intraperitoneally. If the iliac fossae are not suitable for transplantation, orthotopic placement of the renal graft can be performed, although this is only very rarely the case.

Donors

A live donor kidney provides the best long-term graft and recipient outcomes [2]. Deceased donor kidneys comprise the majority of kidney transplants owing to a shortage of donors. For live donor kidneys, the renal artery is used for the anastomosis to the recipient arterial inflow vessel. When deceased donor grafts are transplanted, a patch of the aorta, called a Carrel patch, is often used for anastomosis. In cases where a single kidney does not have the nephron mass to support renal function in the recipient, dual adult kidney transplantation can be performed [3]. Additionally, in very small pediatric deceased donor kidneys, it is possible to recover and transplant the kidneys en bloc as a single functional graft, with the donor aorta and IVC being used for the arterial and venous anastomoses, respectively [4].

Anastomosis

The renal artery or the Carrel patch is anastomosed in the vast majority of cases end to side to the external iliac artery. However, in recipients with severe atherosclerotic disease or in pediatric recipients, the common iliac artery and even the aorta can be used for the end-to-side anastomosis. Alternatively, and depending on technical-surgical recipient constraints, an end-to-end anastomosis can be done to the internal iliac artery or the inferior epigastric artery. Venous anastomosis is typically with the iliac vein. In cases of multiple renal arteries supplying a deceased donor kidney graft, their ostia can be included on a single Carrel patch if they are in close proximity. However, if the graft is from a living donor or if the arteries are too far apart, the multiple arteries can either be anastomosed individually and separately to the recipient's artery or can be reconstructed end to side or side to side with each other to allow for a single arterial anastomosis to the recipient vessel, thus decreasing the number of anastomoses to the recipient artery.

Ureteral Implantation

Typically, the ureter is tunneled into the dome of the bladder and anastomosed to the bladder mucosa ipsilateral to the side of implantation, referred to as a ureteroneocystostomy. In cases of multiple ureters, these can either be joined ex vivo on the

backtable to form a single ureteral orifice (allowing for a single ureteroneocystostomy) or they can be anastomosed individually (creating two ureteroneocystostomies). In the latter case, they may be tunneled together or separately. Occasionally, when the length of the ureter is limited, ureters are anastomosed to the native ureter (ureteroureterostomy). In recipients with a neurogenic bladder, the ureter can be anastomosed to a previously created ileal conduit (ureteroenterostomy).

Radiological Imaging Options

Ultrasound

Ultrasound is usually the first-line imaging modality of kidney grafts owing to its availability, decreased cost relative to other imaging modalities, and overall sensitivity in being able to detect peritransplant collections and vascular complications. Additionally, ultrasound can be used to guide biopsies.

Initial assessment of the kidney graft often involves a lower frequency probe to evaluate the transplanted kidney and bladder in longitudinal and transverse dimensions. The renal length should be measured. Grayscale assessment of the graft is useful in detecting peritransplant collections, evaluating the renal parenchyma, and assessing for hydronephrosis.

Overall perfusion of the transplanted kidney can be performed using color or power Doppler imaging. B flow is a more sensitive technique to look for perfusion and is less subject to operator variability. Perfusion should be seen throughout the cortex of the kidney, and assessment of the entire kidney is necessary to look for segmental ischemia. Ultrasound is not sensitive in identifying multiple renal arteries, and therefore familiarity with the operative report is important to increase the sensitivity in depicting vasculature. Color Doppler imaging should be obtained of the entire length of the transplanted renal vein.

Spectral Doppler should be obtained at the following sites: the iliac artery prior to the transplant renal artery anastomosis; the proximal, mid, and distal renal artery; the intrarenal arteries (segmental/interlobar/arcuate vessels); the renal vein, and the draining iliac vein. Additional evaluation of areas of aliasing within the artery or vein that may point toward a stenosis should be assessed by spectral Doppler.

Ultrasound contrast has potential emerging applications in renal transplant evaluation. Contrast may allow for more uniform and quantifiable assessment of graft perfusion [5, 6]. It has additional applications in lesion characterization [7] and in assessing for transplant renal artery stenosis, vascular thrombosis, and arteriovenous fistulas [8, 9].

The stiffness of the kidney transplant can be measured using ultrasound elastography. Presumably, the greater the stiffness of the renal parenchyma, the greater the degree of fibrosis. Adequate assessment of degree of fibrosis would be useful in assessing the graft and potentially obviate the need for some biopsies. However, ultrasound elastography suffers from operator dependence and variable rates of

collaboration with tissue stiffness based on biopsy results. Additional studies are needed before ultrasound elastography may become a clinically applicable modality.

CT

CT scans are typically performed without contrast, given concerns for contrast-induced nephropathy. Such concerns may be overstated, as recent studies have suggested that the rates of acute kidney injury following iodine-based contrast administration are very low and no higher than the general population receiving contrast [10, 11], and assessment of vascular complications related to the transplanted kidney is severely limited without contrast. CT can be useful in the evaluation of renal vasculature, peritransplant collections not visualized by ultrasound, and assessing for the presence of an abscess/infected collection, renal/ureteral stones, and renal masses.

MRI

MRI is an attractive imaging option, given its lack of ionizing radiation and use of non-nephrotoxic contrast material. However, the risk of nephrogenic systemic fibrosis limits the use of gadolinium-based contrast. Nonetheless, unenhanced MRA images can still be useful in vascular assessment of the graft [12]. More recently, ferumoxytol, an off-label ultrasmall paramagnetic iron oxide agent approved for iron replacement in patients with chronic kidney disease, has shown promise in evaluating the transplanted kidney [13–15]. However, given concerns regarding severe reactions to this agent in a very small fraction of the patients, it should be used with caution [16].

Functional MRI holds promise in assessing for graft function, although such research is preliminary. MR elastography can potentially assess for fibrosis of the graft, with the possibility of negating the need for biopsy in some cases. MR elastography allows for assessment of the entire kidney parenchyma, whereas biopsy and ultrasound elastography are limited by sample volume and therefore may under- or overestimate degree of fibrosis. However, there are conflicting reports as to how to interpret such results, and further research is needed [17, 18]. Blood oxygen level dependence (BOLD) imaging can evaluate areas of oxidative stress and in a small study was able to discriminate between acute tubular necrosis and rejection [19]. Low B-value DWI and arterial spin labeling hold promise as an unenhanced measure of organ perfusion. Diffusion tensor imaging (DTI) can look at disruption of the medullary pyramids and seem to correlate with renal dysfunction [20, 21]. Finally, pulsed arterial spin labeling sequences can allow for perfusional evaluation of transplanted kidneys without the use of contrast [22].

Peritransplant Fluid Collections

Peritransplant fluid collections are a common occurrence following renal transplantation, with reported rates up to 50% [23]. These can develop at any time posttransplantation. These collections include lymphoceles, seromas, hematomas, urinomas, and abscesses. The gold standard in diagnosing the type of peritransplant collection is fluid aspiration. However, if the patient is asymptomatic and the collection is small and non-enlarging, aspiration is typically not pursued. The presence of a collection is usually first identified on ultrasound. Ultrasound has variable sensitivity in detecting both the presence and size of peritransplant collections, especially hematomas, and CT or MRI can be used to identify those that are clinically suspected but may not visualized by ultrasound [24]. A CT can also help with determining the likelihood that a fluid collection is infected (e.g., by visualizing a rim enhancement on a contrast CT) and may guide further diagnostic (e.g., needle aspiration) and therapeutic (e.g., percutaneous drain placement or providing the indication for an operative abscess drainage) guidance.

All fluid collections can exert mass effects on surrounding structures, which makes their size, location, adjacent structures, and growth important imaging factors in guiding management. Patients can present with nonspecific symptoms such as local pain, ipsilateral leg edema, abdominal swelling, and fever. Mass effect on the bladder or transplant ureter can cause urinary incontinence or obstructive uropathy, respectively. Mass effect on regional vasculature can lead to renal graft and recipient iliac vessel (especially venous) stenosis or thrombosis [25].

All fluid collections, especially those that are large, can become infected and develop into abscesses. Interval enlargement of pretransplant collections may indicate active urine leak, ongoing vascular injury, or abscess development. In the early postoperative period, fluid collections represent most often hematomas and, more rarely, urinomas. Clinically relevant lymphoceles usually do not develop until weeks to sometimes years after the transplant [26].

Therefore, accurate identification of the location of the fluid collection, its size compared with prior examinations, complexity of the fluid contents, and mass effect and an understanding of the timing of the fluid collection relative to transplantation are important in interpreting the type and significance of peritransplant collections.

Hematomas

Hematomas are likely the most common peritransplant fluid collection and have been reported in close to a third of renal transplantations, although the vast majority of these are small (<50 mL) and unlikely to be clinically significant [27]. These usually occur in the immediate postoperative period, though these can occur later as a complication of renal transplant biopsies or ruptured mycotic pseudoaneurysms.

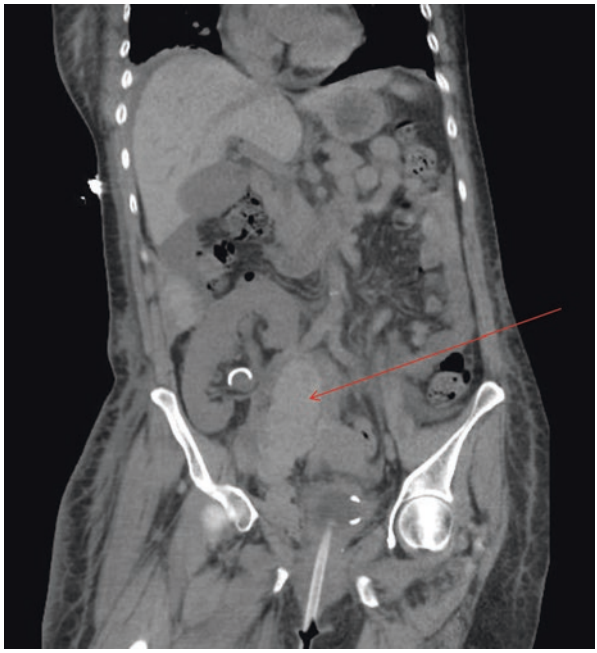

Fig. 5.1 CT abdomen and pelvis without contrast, coronal view, showing perinephric hematoma (arrow) medial to the transplanted kidney after anastomotic breakdown

Hematomas may require surgical evaluation and possibly drainage if they are large (given the concern for abscess formation as well as mass effect) or if there is concern for active bleeding (rapidly enlarging collections as well as visualized active extravasation or pseudoaneurysm). Hematomas should be described as to their location: subcutaneous, peripheral crescentic, or perihilar. Incisional site hematomas are usually self-limited, although, if large, they may require evacuation. Peripheral crescentic hematomas are the most common location for hematomas and may suggest oozing from capsular or parenchymal vessels. These too are usually self-limiting. However, a peritransplant hematoma located in the hilum may suggest the presence of an anastomotic or extrarenal pseudoaneurysm leak and may warrant additional angiographic (CT or conventional) evaluation (Fig. 5.1). Subcapsular hematomas are more prone to producing mass effect on the transplanted kidney and can produce graft dysfunction (Figs. 5.2 and 5.3).

Ultrasound has variable sensitivity in detecting posttransplant hematomas, presumably owing to their variable appearance [24]. Acute hematomas are often echogenic and can be difficult to visualize since they can be isoechoic to surrounding tissues (Fig. 5.3). As the hematoma becomes more chronic, it liquefies and becomes more hypo- to isoechoic, often with some complexity. In the setting of a negative ultrasound but clinical concern for a peritransplant hematoma, an unenhanced CT can be performed. On unenhanced CT, acute hematomas are hyperdense, while chronic hematomas become hypodense. On MRI, acute hematomas are typically hyperintense on T1- and T2-weighted images. If there is concern for active bleeding, CT angiography and conventional angiography can be performed.

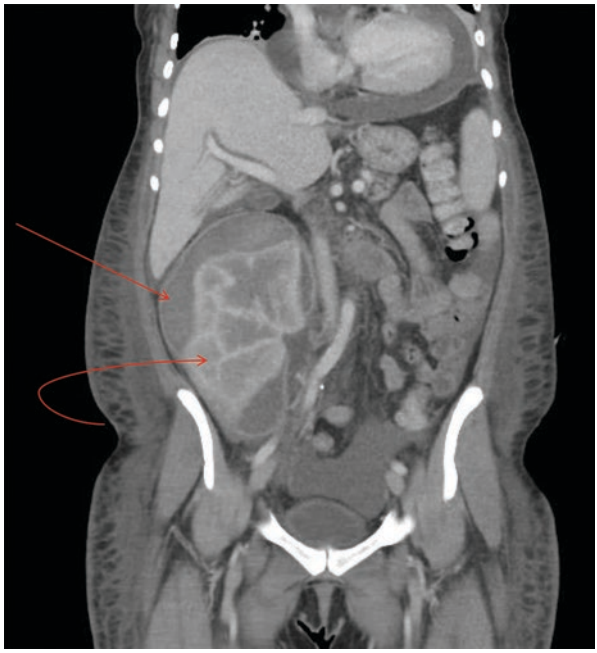

Fig. 5.2 CT abdomen/pelvis with IV contrast, coronal view, showing rim-enhancing subcapsular hematoma (straight arrow) around the renal transplant (curved arrow)

MR has a limited role, as gadolinium-based agents may not be advisable given the concern for nephrogenic systemic fibrosis. Some studies, however, have suggested a role for ferumoxytol as an off-label blood-pool agent, which increases the sensitivity to detect slower vascular leaks [14, 15].

Lymphoceles

Lymphoceles typically occur weeks to years after transplantation. These pseudocystic collections develop from disruption of the lymphatic channels as a result of the surgical dissection and mobilization of the iliac recipient vessels in preparation for the creation of the vascular anastomoses. Many nonsurgical factors have also been implicated in lymphocele development, including the use of steroids and mTOR inhibitors, diabetes, graft rejection, obesity, heparin, and diuretics [26, 28–33].

While hematomas represent the most common peritransplant collection, lymphoceles are historically the most common that require intervention, although this may have changed in the modern era [23, 34]. Most lymphoceles, however, are small and subclinical, in which case they are simply serially observed. Larger lymphoceles can impinge on the iliac/femoral veins and cause lower extremity edema or deep venous thrombosis. Lymphoceles can also lead to impaired renal function, hydronephrosis secondary to transplant ureteral compression or stretching, and pain (Fig. 5.4) [35].

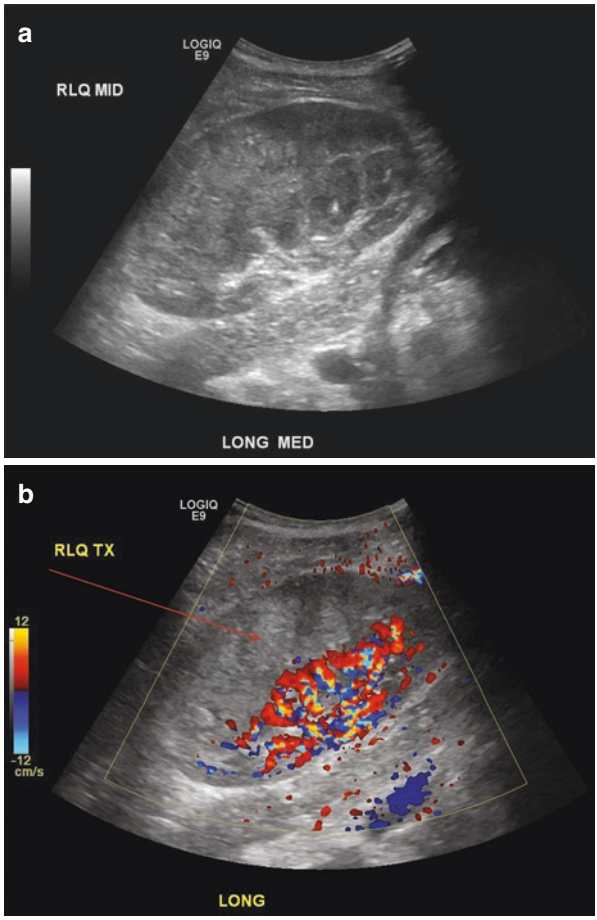

Fig. 5.3 (**a**) US grayscale showing isoechoic subcapsular hematoma. (**b**) US Doppler can be useful in assessing an isoechoic subcapsular hematoma (arrow) against the perfused transplant kidney

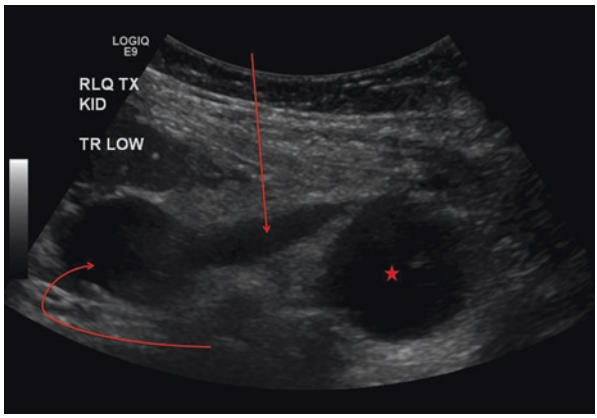

Fig. 5.4 US grayscale showing a peritransplant lymphocele (star) compressing the right ureter (straight arrow), resulting in hydronephrosis (curved arrow)

Lymphoceles typically occur medial to the transplant between the graft and the bladder (i. e., in the area of the perivascular lymphatics). Lymphoceles are anechoic collections by ultrasound but may contain thin septations. On CT, lymphoceles are typically well-circumscribed with simple fluid attenuation. By MRI, these collections are typically low intensity on T1-weighted images and high intensity on T2-weighted images.

Urinomas

Urinomas are relatively rare causes of peritransplant collections, occurring in approximately 5% of patients with renal transplants [36]. They are the result of a urine leak. The urinary extravasation can be the result of an injury to any part of the transplant ureter or the renal pelvis or of a surgical technical complication at the ureteral anastomotic site. Ureteral obstruction from ischemic ureteral strictures and stones results only extremely rarely in urinoma formation. Urinomas typically occur in the first couple of weeks after transplantation. More delayed urinomas can be seen in cases of delayed urinary obstruction (obstructing renal calculi) and as a complication of kidney graft biopsy.

Clinical presentation is nonspecific but includes decreased urine output, increased serum creatinine (in case there is associated free urine extravasation into the peritoneal cavity with reabsorption of creatinine), peritransplant pain, ipsilateral lower extremity edema, and scrotal/labial edema. Urinomas are usually located between the transplanted kidney and the bladder. On ultrasound the collection is typically anechoic without septations, in distinction to hematomas, abscesses, and some lymphoceles; however, urinomas can have variable appearances (Fig. 5.5) [37]. Urinomas can appear similar to lymphoceles, though urinomas tend to have more irregular and indistinct margins. On unenhanced CT examination, the fluid collection is of simple fluid attenuation. Diagnosis can be confirmed with CT with intravenous contrast in the

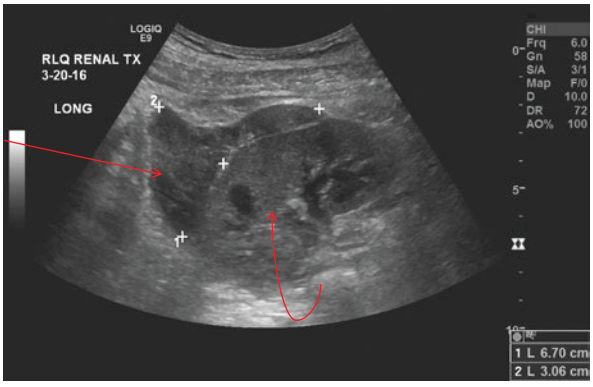

Fig. 5.5 US grayscale showing peritransplant urinoma (straight arrow) next to the transplanted kidney (curved arrow)

urographic phase depicting contrast material within the collection, which is not appreciated on the arterial or venous phases, or radionuclide imaging (with Tc99m MAG3). Invasive examinations include antegrade nephrostography or cystography which may assist with the diagnosis. A definitive diagnosis may require guided aspiration of the urinoma. The expected analysis result of a fluid creatinine far exceeding the patient's serum creatinine (while being similar to creatinine levels of urine obtained from the recipient's bladder) easily separates urinomas from other fluid collections.

Abscesses

Any peritransplant fluid collections have the potential to turn into an abscess, particularly in the setting of posttransplant immunosuppression and indwelling catheters. Abscesses may develop from within preexisting fluid collections, from blood-borne pathogens, or from acute pyelonephritis and typically occur within the early postoperative period. While some patients can present with fever and localized pain, others may have milder or subclinical symptoms [38].

Radiographically, ultrasound and CT findings can be highly variable. On ultrasound, abscesses are typically complex. The presence of air will lead to dirty shadowing by ultrasound. Inflammation can make surrounding fat appear highly echogenic. On CT, the attenuation can be more dense than simple fluid, and the presence of gas within the fluid collection can readily be seen. However, in the immediate postoperative period, the use of hemostatic agents (such as Surgicel) can mimic an abscess as the retained oxidized cellulose appears as foci of gas in the surgical bed. Therefore, familiarity with the surgical report is useful in image interpretation to see whether such agents were used. On contrast-enhanced CT, abscesses may show a rim of enhancement around the collection.

Vascular Complications

Transplant Vessel Thrombosis

The occlusion of the transplanted graft artery and vein by thrombus is a rare but devastating vascular complication, with incidence rates typically reported to be less than 1% [39, 40]. In the overwhelming majority of cases, vascular thrombosis entails graft loss. The incidence of vascular thrombosis is higher in pediatric donor kidneys, particularly in pediatric en bloc kidneys, with the incidence in this population approaching 10% [41]. However, in the case of pediatric en bloc kidneys, thrombosis can be unilateral, and patients can retain graft function with a single pediatric kidney. There are many possible etiologies for thrombosis, including vascular injury during transplantation, vascular kinking, ischemia/reperfusion injury

with a low-flow state, and rejection. The vein is more susceptible to compression-related thrombosis by adjacent peritransplant collections owing to its lower intravascular pressure. Vascular thrombosis most typically occurs within the first 2 weeks of transplantation but can also occur later, usually as a late sequela of chronic rejection or glomerulosclerosis [42]. Clinically, thrombosis presents acutely with nonspecific signs: oliguria, hematuria, renal insufficiency, and localized pain (the latter particularly in cases of acute venous thrombosis which leads to graft engorgement and oozing from the graft surface with development of a perigraft hematoma).

Transplant Renal Arterial Thrombosis

Arterial thrombosis can occur in the transplanted main renal artery or be segmental. On grayscale ultrasound, the allograft or affected portion thereof will appear hypoechoic, although this is a nonspecific finding. On color Doppler imaging, there will be a lack of flow in the parenchyma (Fig. 5.6). Optimizing the sensitivity of ultrasound is important, since other pathological processes such as severe acute tubular necrosis and rejection can lead to a low-flow, hypoperfused state. Color Doppler may show minimal flow in the ischemic areas owing to collateral vessel flow, but these will typically have low-resistance waveforms on spectral Doppler in contradistinction to the high-resistance waveforms in cases of acute tubular necrosis. The volume of ischemic parenchyma will dictate prognosis, from sub-segmental thrombus leading to minimal deterioration in graft function to main renal artery thrombosis causing complete graft loss. In cases of segmental infarction, it is important to note which segment is involved as infarction of the inferior pole may be

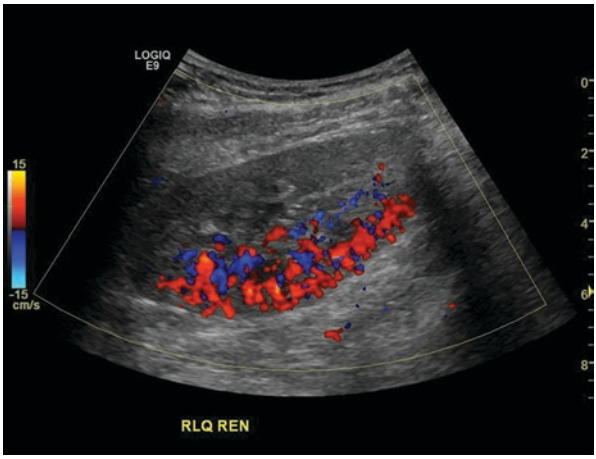

Fig. 5.6 US Doppler of renal transplant showing anterior segmental infarct and nonperfusion as a result of arterial thrombosis

associated with ureteral necrosis if the ureteral artery takes off from a thrombosed lower polar artery.

While very early identification of arterial thrombosis may occasionally lead to graft salvage, the prognosis for the affected graft or portion thereof is generally very poor. Treatment of transplant renal artery thrombosis typically involves laparotomy with thrombectomy; however, the prognosis is dismal (due to the added ischemic insult to the kidney graft), and transplant nephrectomy is a common outcome depending on how delayed the diagnosis is established. The use of endoluminal thrombolysis is not yet established, though it may have a role in select cases of early detection and low clot burden [43].

Transplant Renal Vein Thrombosis

Grayscale ultrasound may demonstrate diffuse edema and hypoechoic regions; color Doppler will demonstrate lack of venous flow with absent or severely diminished parenchymal flow. Abnormally sharp systolic arterial peaks with reversal of diastolic flow help to differentiate venous from arterial thrombosis (Fig. 5.7). Thrombosis may be complete or partial, and detection of the low echogenicity filling defect with resultant distention of the renal vein can also help to make the diagnosis.

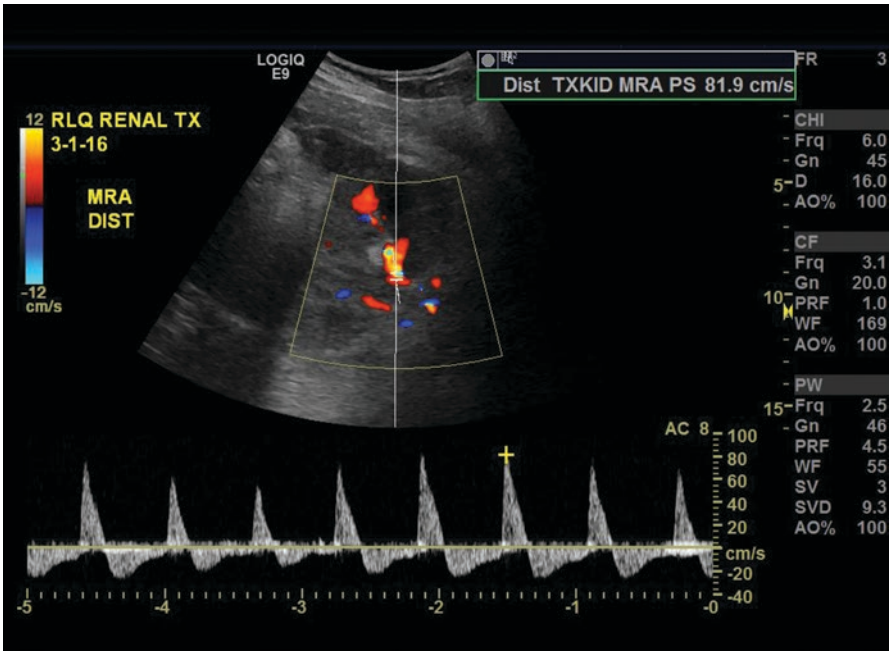

Fig. 5.7 Spectral Doppler US shows main renal artery flow reversal as a result of venous thrombosis

Treatment of transplant renal venous thrombosis, similar to that of arterial thrombosis, traditionally requires surgical laparotomy with thrombectomy and may be useful if caught early. However, venous thrombosis also portends a poor prognosis. Increased arterial pressure from venous outflow obstruction can lead to vascular rupture, leading to hemorrhagic shock. In cases of partial thrombosis, patients may be placed on anticoagulation.

Transplant Renal Artery Stenosis

Transplant renal artery stenosis is the most common vascular complication with an incidence around 5–10% [44, 45]. Most cases of transplant renal artery stenosis occur distal to the anastomosis, implicating etiologies other than surgical technique, i.e., rejection, arterial kink, de novo class II donor-specific antibodies, preservation injury, and underlying donor atherosclerotic disease [45, 46]. Transplant renal artery stenosis is rare in the immediate postoperative period (usually from kinked vessels) and typically presents around 3 months after transplantation, although stenosis can occur later. Transplant renal artery stenosis is less common in living donors and pediatric en bloc recipients [45, 47]. Clinical features include refractory hypertension, graft dysfunction, audible bruit, and edema [48]. Of note, atherosclerotic stenosis can also occur at the recipient's iliac arteries proximal to the renal arteries (e.g., due to atherosclerotic disease or due to surgical clamp injury during the transplant operation) and can affect graft function; it is referred to as transplant renal arterial pseudostenosis.

As with other vascular complications, Doppler ultrasound is the initial test of choice given its relative low cost and availability. Ultrasound usually cannot depict the stenosis on grayscale and color/power Doppler images, so the presence of a stenosis has to be inferred from sonographic flow characteristics. These include high velocity at the point of stenosis, spectral narrowing at the stenosis (from plug flow at the narrowing) and spectral broadening distal to the stenosis (indicating post-stenotic turbulence), and distal parvus tardus waveforms (decreased magnitude of flow and slowed upstroke) (Fig. 5.8). No clear consensus has emerged as to exact cutoffs for velocity, ratio, and parvus tardus waveforms [49]. However, a velocity > 300 cm/s and a ratio of velocity > 2:1 between the stenotic portion and the iliac artery would be reasonable set points. Spectral broadening should be seen as complete filling of the spectral window distal to the stenosis. Parvus tardus waveforms can be measured either in acceleration time or acceleration index. An acceleration time > 0.1 s in the intraparenchymal arteries is also suspicious for a more proximal stenosis. The point of arterial narrowing can usually be identified by judicious use of color Doppler imaging to depict the highest velocity as an area of aliasing. However, since the entire course of the renal artery may be difficult to appreciate either due to tortuosity of the vessel or obscuration by bowel gas, the identification of either spectral broadening in the distal renal artery or parvus tardus waveforms should raise the concern for a stenosis either in the nonvisualized portion of the

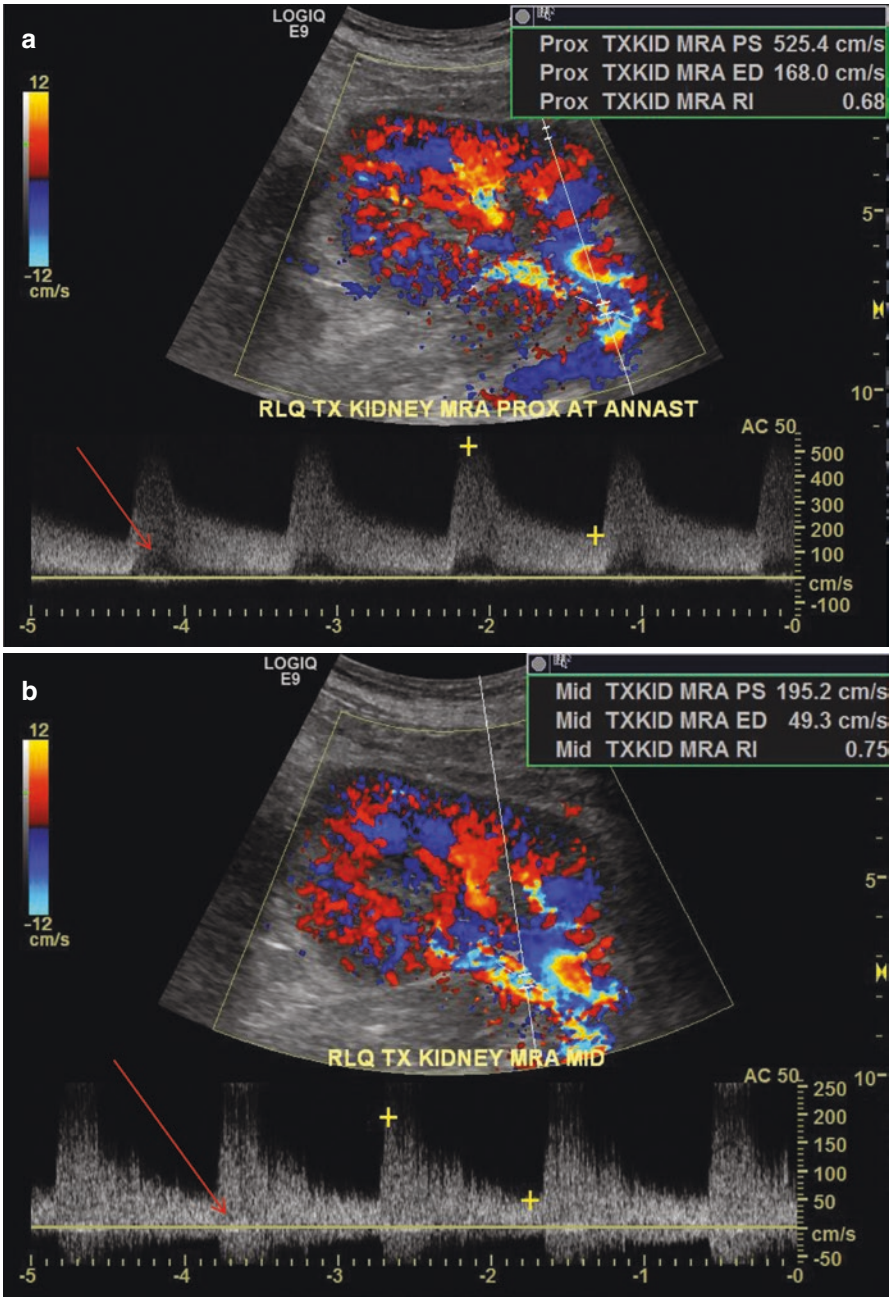

Fig. 5.8 (**a**) Spectral Doppler US shows spectral narrowing of the waveforms in the proximal main renal artery at the anastomosis, indicative of increased laminar flow through an arterial stenosis. (**b**) Spectral Doppler US shows spectral broadening of the waveforms in the mid-main renal artery, indicative of increased turbulent flow distal to the arterial stenosis

renal artery or more proximally in the iliac artery/aorta (transplant renal artery pseudostenosis). Tissue reverberation from the stenosis can be seen on color Doppler as speckled artifact which is centered around the stenotic region. While classically the intraparenchymal arterial resistive index is lower in patients with transplant renal artery stenosis, this is an unreliable finding, as fibrosis from ischemia (related to the renal artery stenosis itself) or chronic rejection can increase the resistive index [50].

While ultrasound appears to be a sensitive modality for detecting transplant renal artery stenosis, its false-positive rate of around 40% leads to a number of unnecessary conventional angiograms [45]. Given this high false-positive rate, there may be a role for additional noninvasive imaging with CTA or MRA (unenhanced or with ferumoxytol) [12–15]. Catheter angiography remains the gold standard and allows for depiction of the stenosis, pressure gradient measurements across the stenosis, and therapeutic intervention with angioplasty/stenting.

Transplant Renal Vein Stenosis

Stenosis of the transplanted renal vein is a very rare complication that may be due to intraoperative venous trauma, acute rejection, or compression from a perigraft fluid collection [51]. Given the low incidence, this diagnosis is typically suspected after exclusion of other vascular complications. The window of presentation in the literature typically occurs months after the transplant, and it most commonly presents with gradual but progressive renal insufficiency.

On Doppler ultrasound, a prestenotic to stenotic velocity gradient of 4:1 is typically required to diagnose venous stenosis. Doppler ultrasound may not be as helpful for the diagnosis of transplant renal vein stenosis, with reported cases showing only nonspecific enlargement of the graft and decreased parenchymal flow or even no abnormality [51, 52]. MR angiography, with its complete evaluation of the renal arterial and venous vascular supply, can effectively detect the venous stenosis, though non-hemodynamically significant narrowing of the vein can lead to false-positive results. Catheter-directed venography with trans-stenotic pressure gradient is the gold standard for diagnosis.

Pseudoaneurysm

A pseudoaneurysm is an acute, subacute, or chronic vascular rupture where the resultant perivascular hematoma is confined either by the vessel's adventitia or surrounding tissues. Flow enters into and exits the false aneurysm through the break in the vessel wall, referred to as its neck. This creates to and from flow of the blood within the neck which will be depicted either as alternating red and blue on color Doppler or as interchanging forward and reversed flow on spectral Doppler. As the blood circulates within the aneurysmal sac, it creates a yin-yang appearance

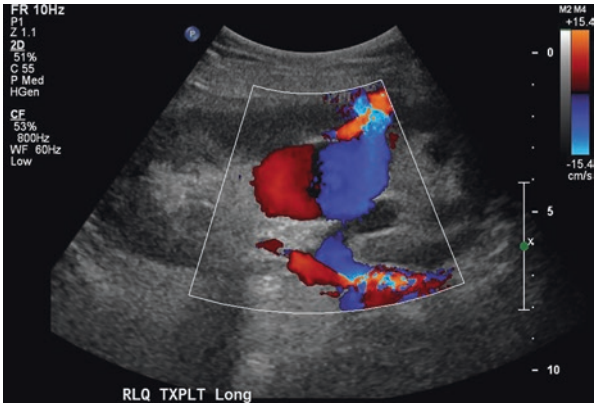

Fig. 5.9 US Doppler showing classic yin-yang appearance of pseudoaneurysm

representing the internal swirling of the blood (Fig. 5.9). The actual false aneurysm appears anechoic on grayscale, although internal mobile echoes may be seen in case of slow movement of the blood. The location of the pseudoaneurysm (intraparenchymal versus extrarenal) and the size of the pseudoaneurysm and neck are important measurements to include in a radiology report. Intraparenchymal pseudoaneurysms are usually caused by transplant biopsies, whereas extrarenal pseudoaneurysms are typically either from anastomotic breakdown or mycotic in origin. CT or MR angiography may be useful to confirm the diagnosis, demonstrating the ovoid or spherical arterial outpouching which matches the density or intensity of the arterial blood pool, and can provide a vascular map of regional vasculature for intervention.

Small asymptomatic intraparenchymal pseudoaneurysms can be managed conservatively. However, those that are growing or those >2 cm may require intervention [38]. Extrarenal pseudoaneurysms have a much poorer prognosis and commonly lead to graft loss. These can be difficult to identify by ultrasound and sometimes present with clinical and sonographic features of transplant renal artery stenosis from impingement of the pseudoaneurysm on the transplanted renal artery [53]. In these cases, CTA, MRA, or conventional angiography can be more useful in detecting extrarenal pseudoaneurysms.

Arteriovenous Fistulas

Arteriovenous fistulas typically occur following biopsy in which abnormal connections between an artery and vein are created, leading to shunting of the blood through a lower resistance pathway. The flow of the blood bypasses the arterioles and therefore creates a lower resistance pathway, leading to increased velocities at the fistula site. This rapid flow of the blood can lead to tissue vibration which can be clinically apparent as a bruit and depicted on color Doppler ultrasound (Fig. 5.10). Spectral Doppler imaging will show a high velocity lower resistance arterial

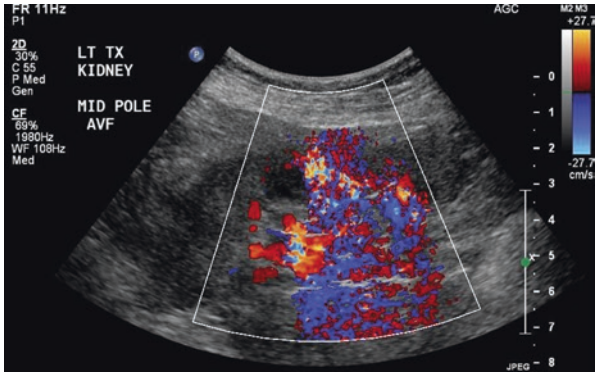

Fig. 5.10 US Doppler of renal transplant showing diffuse perivascular tissue vibration as a result of arteriovenous fistula high flow rates

waveform feeding the fistula with an arterialization of blood flow in the draining venous portion. Arteriovenous fistulas can coexist with pseudoaneurysms. Arteriovenous fistulas are a common finding post-biopsy, occurring in rates of up to 10% of patients. Patients can present with hematuria or hypovolemia due to shunting. Less frequently, high output cardiac failure, graft insufficiency, or hypertension can occur. Most arteriovenous fistulas are small and 70% resolve spontaneously within 2 years, requiring only serial ultrasound observation [54]. However, the lower resistance pathway of an arteriovenous fistula, if large, can shunt the blood away from the rest of the transplanted kidney leading to at least regional hypoperfusion and relative ischemia. The resistive index of the main renal artery is usually slightly higher than the intraparenchymal renal arteries. However, if the resistive index of the main renal artery is at least 0.05 less than the intraparenchymal resistive index of the unaffected portion of the renal parenchyma, this suggests a hemodynamically significant fistula [55].

The gold standard for diagnosis remains catheter angiography, with a characteristic finding of abnormal arterial-venous communication and early venous opacification. Identification of arteriovenous fistulas on CTA and MRA is limited given their usually small connections and the relatively early drainage of the normal renal vein.

Ureteral Complications

Patients with urinary obstruction often present with oliguria and progressive renal insufficiency. Overt pain or discomfort is uncommon owing to denervation of the graft during transplantation. Ultrasound evaluation is the test of choice and has excellent sensitivity for detecting hydroureteronephrosis. The normal transplanted kidney may demonstrate minimal calyceal and pelvic dilatation at baseline due to some combination of compensated increased urine production, loss of ureteral tone from denervation, or ureteral reflux given a full bladder. Therefore, it is important, in the setting of hydronephrosis, to perform the study with an empty bladder to exclude reflux as an etiology for hydroureteronephrosis. CT imaging has a major

role in detailing the transplant anatomy, allowing for further characterization of the hydroureteronephrosis as well as the site and etiology of obstruction, whether intrinsic (calculi, strictures) or extrinsic (fluid collections). Nuclear scintigraphy can be useful to distinguish obstructive from nonobstructive etiologies of posttransplant progressive renal insufficiency, such as acute tubular necrosis, rejection, and drug toxicity [56]. Finally, percutaneous nephrostogram is the definitive study for ureteral evaluation; however, it is an invasive procedure.

Ureteral Strictures

Ureteral strictures from ischemia are the most common cause of ureteral obstruction in the kidney graft with an incidence between 1 and 4.5% [57]. The most common location of the stricture is the distal ureterovesical junction from ischemia. However, other portions can be affected, and other etiologies include compression from peritransplant fluid collections and faulty surgical technique. The vascular supply to the ureter is usually from the lower pole branches of the renal artery. Therefore, segmental infarction of the inferior pole should raise concern for future stricture development. Patients will present with progressive renal dysfunction, which often elicits an ultrasound which will show increasing hydronephrosis. Most strictures occur within the first few months after transplantation.

Stone Disease

The incidence of stone disease within transplanted kidneys is around 1% [58]. The composition of the calculi in grafts matches that of native renal calculi; however, the rate of associated urinary tract infection is higher with calculi in grafts [59]. Most calculi in renal grafts have an underlying metabolic cause, so identification of such calculi should elicit comprehensive metabolic screening [58]. However, if an examination, such as an ultrasound or CT, demonstrates stone disease immediately after transplantation, this may be related to donor-imported stones, and a full metabolic workup may not be necessary. The clinical presentation is typically less painful when compared to nontransplant patients, owing to the denervation of the transplanted allograft. Typical presentation includes hematuria, dysuria, and worsening renal function. Dislodged stones can cause hydronephrosis, which can readily be seen by ultrasound. Careful evaluation of the obstructed ureter may allow for identification of the calculus which is usually echogenic, with posterior acoustic shadowing, and twinkle artifact on color Doppler imaging (Fig. 5.11). In some cases, the ureter cannot be adequately assessed by ultrasound, and a noncontrast CT can be helpful in these situations.

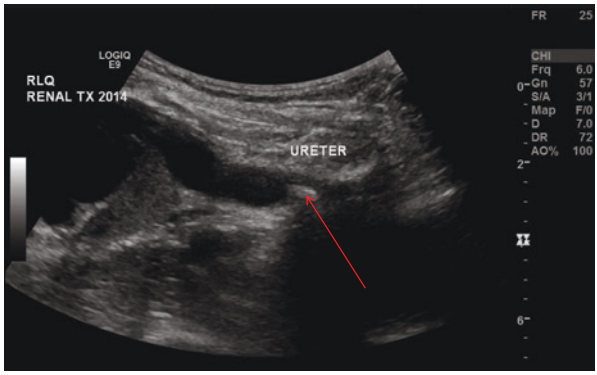

Fig. 5.11 US grayscale showing obstructive urolithiasis at the ureteropelvic junction after renal transplant

Parenchymal Causes of Renal Failure

Acute Tubular Necrosis

Acute tubular necrosis is a common cause of renal dysfunction in which decreased oxygenation leads to renal tubular damage or destruction. Overall, acute tubular necrosis occurs in 10–30% of transplant recipients [60]. It is usually an early sign of renal graft dysfunction, accounting for up to 92% of cases of delayed graft function (defined as requirement of dialysis within the first 7 days after transplantation) [61, 62]. Multiple risk factors have been identified that suggest degree and duration of ischemia with reperfusion injury to be a central cause of acute tubular necrosis. These risk factors include lengthened warm and cold ischemic time, the presence of atheromatous disease, donor age, donor hypotension, and reduced allograft blood flow [63].

Rejection

Rejection of the allograft is the second most common cause of delayed graft function [61]. The cellular subtype of acute rejection, mediated by T-lymphocytes, results in interstitial infiltration and edema, as well as cortical infiltration with mononuclear cells that characteristically affect intertubular capillaries, venules, and lymphatics a few weeks or months after transplantation (Fig. 5.12) [64]. In contrast, the B-cell or humoral form of acute rejection can present more hyperacutely with transmural arteritis and fibrinoid necrosis as a result of preformed antibodies. Risk factors for rejection include mismatched antigens, sensitization to HLA antigens, underimmunosuppression, and noncompliance with the immunosuppressive regimen.

Drug Toxicity

Calcineurin inhibitors such as tacrolimus and cyclosporine, which act to inhibit T-cell activation, carry an inherent risk of nephrotoxicity due to their afferent arteriolar vasoconstrictive effect, which can cause ischemia and fibrosis [65]. This is treated by reducing the dose of the calcineurin inhibitor. Chronic drug toxicity can lead to irreversible ischemia. The clinical presentation is similar to other etiologies of acute graft dysfunction: rising creatinine, oliguria, and nonspecific discomfort or edema.

Imaging Features of Parenchymal Causes of Renal Failure

Parenchymal causes of renal failure include acute tubular necrosis, rejection, and drug toxicity. They can all present as early or late complications of renal transplantation (although acute tubular necrosis is typically an early complication). All cause renal dysfunction, manifesting as increased serum creatinine and decreased or absent urine output. These are usually initially evaluated by ultrasound. However, the imaging findings are nonspecific and include decreased perfusion and increased intraparenchymal resistive indices (>0.8) [66]. In rejection, the graft usually appears more edematous (increased size and decreased echogenicity) when compared with acute tubular necrosis or drug toxicity (Fig. 5.12). Ultimately, however, definitive diagnosis will require biopsy and histopathologic confirmation. However, ultrasound is useful from the standpoint of excluding other processes that contribute to renal failure, including transplant vascular stenosis, vascular thromboses, and peritransplant collections. Functional MRI holds promise in distinguishing between some of these entities; however, its use is still investigational [19, 21].

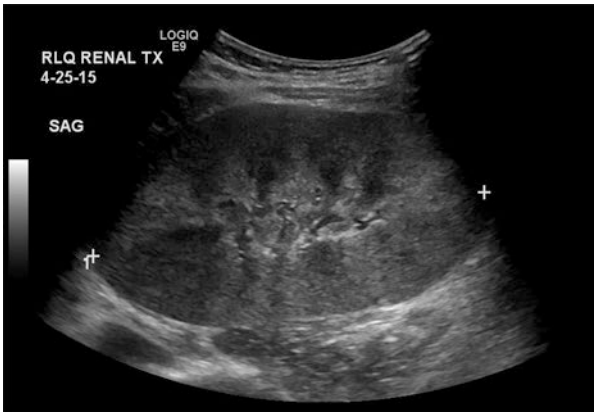

Fig. 5.12 US grayscale showing diffusely edematous parenchyma in a transplanted kidney undergoing acute rejection

References

1. Matas A, Smith J, Skeans M, Thompson B, Gustafson S, Schnitzler M, et al. OPTN/SRTR 2012 annual data report: kidney. Am J Transplant. 2014;14(S1):11–44.
2. Nemati E, Einollahi B, Pezeshki ML, Porfarziani V, Fattahi MR. Does kidney transplantation with deceased or living donor affect graft survival? Nephrourol Mon. 2014;6(4):e12182.
3. Gill J, Cho YW, Danovitch GM, Wilkinson A, Lipshutz G, Pham P-T, et al. Outcomes of dual adult kidney transplants in the United States: an analysis of the OPTN/UNOS database. Transplantation. 2008;85(1):62–8.
4. Fananapazir G, Tse G, Corwin MT, Santhanakrishnan C, Perez RV, McGahan JP, et al. Pediatric en bloc kidney transplants: clinical and immediate postoperative US factors associated with vascular thrombosis. Radiology. 2015;279(3):935–42.
5. Kay D, Mazonakis M, Geddes C, Baxter G. Ultrasonic microbubble contrast agents and the transplant kidney. Clin Radiol. 2009;64(11):1081–7.
6. Schwenger V, Hankel V, Seckinger J, Macher-Göppinger S, Morath C, Zeisbrich M, et al., editors. Contrast-enhanced ultrasonography in the early period after kidney transplantation predicts long-term allograft function. Transplant Proc. 2014;46(10):3352–7. Elsevier.
7. Harvey CJ, Alsafi A, Kuzmich S, Ngo A, Papadopoulou I, Lakhani A, et al. Role of US contrast agents in the assessment of indeterminate solid and cystic lesions in native and transplant kidneys. Radiographics. 2015;35(5):1419–30.
8. Mafeld S, Stenberg B, Elliott S. Intrarenal arteriovenous shunts in kidney transplants demonstrated by contrast-enhanced ultrasound. Clin Imaging. 2015;39(1):144–51.
9. Zeisbrich M, Kihm LP, Drüschler F, Zeier M, Schwenger V. When is contrast-enhanced sonography preferable over conventional ultrasound combined with Doppler imaging in renal transplantation? Clin Kidney J. 2015;8(5):606–14. https://doi.org/10.1093/ckj/sfv070.
10. Fananapazir G, Troppmann C, Corwin MT, Bent CK, Vu CT, Lamba R. Incidence of contrast-induced nephropathy after renal graft catheter arteriography using iodine-based contrast medium. Am J Roentgenol. 2016;206(4):783–6.
11. Fananapazir G, Troppmann C, Corwin MT, Nikpour AM, Naderi S, Lamba R. Incidences of acute kidney injury, dialysis, and graft loss following intravenous administration of low-osmolality iodinated contrast in patients with kidney transplants. Abdom Radiol. 2016;41(11):2182–6.
12. Bley T, François C, Schiebler M, Wieben O, Takei N, Brittain J, et al. Non-contrast-enhanced MRA of renal artery stenosis: validation against DSA in a porcine model. Eur Radiol. 2016;26(2):547–55.
13. Corwin MT, Fananapazir G, Chaudhari AJ. MR angiography of renal transplant vasculature with ferumoxytol:: comparison of high-resolution steady-state and first-pass acquisitions. Acad Radiol. 2016;23(3):368–73.
14. Fananapazir G, Bashir MR, Corwin MT, Lamba R, Vu CT, Troppmann C. Comparison of ferumoxytol-enhanced MRA with conventional angiography for assessment of severity of transplant renal artery stenosis. J Magn Reson Imaging. 2017;45(3):779–85.
15. Bashir MR, Jaffe TA, Brennan TV, Patel UD, Ellis MJ. Renal transplant imaging using magnetic resonance angiography with a nonnephrotoxic contrast agent. Transplantation. 2013;96(1):91–6.
16. Vasanawala SS, Nguyen KL, Hope MD, Bridges MD, Hope TA, Reeder SB, et al. Safety and technique of ferumoxytol administration for MRI. Magn Reson Med. 2016;75:2107–11.
17. Garcia SRM, Fischer T, Dürr M, Gültekin E, Braun J, Sack I, et al. Multifrequency magnetic resonance elastography for the assessment of renal allograft function. Invest Radiol. 2016;51(9):591–5.
18. Lee CU, Glockner JF, Glaser KJ, Yin M, Chen J, Kawashima A, et al. MR elastography in renal transplant patients and correlation with renal allograft biopsy: a feasibility study. Acad Radiol. 2012;19(7):834–41.

19. Han F, Xiao W, Xu Y, Wu J, Wang Q, Wang H, et al. The significance of BOLD MRI in differentiation between renal transplant rejection and acute tubular necrosis. Nephrol Dial Transplant. 2008;23(8):2666–72.
20. Hueper K, Gutberlet M, Rodt T, Gwinner W, Lehner F, Wacker F, et al. Diffusion tensor imaging and tractography for assessment of renal allograft dysfunction—initial results. Eur Radiol. 2011;21(11):2427–33.
21. Lanzman RS, Ljimani A, Pentang G, Zgoura P, Zenginli H, Kröpil P, et al. Kidney transplant: functional assessment with diffusion-tensor MR imaging at 3T. Radiology. 2013;266(1):218–25.
22. Lanzman RS, Wittsack H-J, Martirosian P, Zgoura P, Bilk P, Kröpil P, et al. Quantification of renal allograft perfusion using arterial spin labeling MRI: initial results. Eur Radiol. 2010;20(6):1485–91.
23. Silver TM, Campbell D, Wicks JD, Lorber MI, Surace P, Turcotte J. Peritransplant fluid collections. Ultrasound evaluation and clinical significance. Radiology. 1981;138(1):145–51.
24. Fananapazir G, Rao R, Corwin MT, Naderi S, Santhanakrishnan C, Troppmann C. Sonographic evaluation of clinically significant perigraft hematomas in kidney transplant recipients. Am J Roentgenol. 2015;205(4):802–6.
25. Allen R. Chapter 26: Vascular complications after kidney transplantation. In: Morris PJ, Knechtle SJ, editors. Kidney transplantation: principles and practice. 6th ed. Philadelphia: Saunders; 2008.
26. Khauli RB, Stoff JS, Lovewell T, Ghavamian R, Baker S. Post-transplant lymphoceles: a critical look into the risk factors, pathophysiology and management. J Urol. 1993;150(1):22–6.
27. Imankulov S, Doskali M, Oskenbaeva K, Ibadildina A, Baigenzhin A, Doskaliyev Z. Evaluation of kidney allograft in the early posttransplant period using ultrasonography. Exp Clin Transplant. 2015;13:62–5.
28. Zhao J, Wang K, Gao Z. The transplantation operation and its surgical complications. INTECH Open Access Publisher; 2011.
29. Ulrich F, Niedzwiecki S, Fikatas P, Nebrig M, Schmidt SC, Kohler S, et al. Symptomatic lymphoceles after kidney transplantation–multivariate analysis of risk factors and outcome after laparoscopic fenestration. Clin Transplant. 2010;24(2):273–80.
30. Tiong HY, Flechner SM, Zhou L, Wee A, Mastroianni B, Savas K, et al. A systematic approach to minimizing wound problems for de novo sirolimus-treated kidney transplant recipients. Transplantation. 2009;87(2):296–302.
31. Lundin C, Bersztel A, Wahlberg J, Wadström J. Low molecular weight heparin prophylaxis increases the incidence of lymphocele after kidney transplantation. Ups J Med Sci. 2002;107(1):9–15.
32. Szwed AJ, Maxwell DR, Kleit SA, Hamburger RJ. Angiotensin II, diuretics, and thoracic duct lymph flow in the dog. Am J Physiol—Legacy Content. 1973;224(3):705–8.
33. Troppmann C, Pierce JL, Gandhi MM, Gallay BJ, McVicar JP, Perez RV. Higher surgical wound complication rates with sirolimus immunosuppression after kidney transplantation: a matched-pair pilot study. Transplantation. 2003;76(2):426–9.
34. Pollak R, Veremis S, Maddux M, Mozes M. The natural history of and therapy for perirenal fluid collections following renal transplantation. J Urol. 1988;140(4):716–20.
35. Sansalone CV, Aseni P, Minetti E, Di Benedetto F, Rossetti O, Manoochehri F, et al. Is lymphocele in renal transplantation an avoidable complication? Am J Surg. 2000;179(3):182–5.
36. Shoskes DA, Hanbury D, Cranston D, Morris PJ. Urological complications in 1,000 consecutive renal transplant recipients. J Urol. 1995;153(1):18–21.
37. Brown ED, Chen MY, Wolfman NT, Ott DJ, Watson NE Jr. Complications of renal transplantation: evaluation with US and radionuclide imaging. Radiographics. 2000;20(3):607–22.
38. Akbar SA, Jafri SZH, Amendola MA, Madrazo BL, Salem R, Bis KG. Complications of renal transplantation. Radiographics. 2005;25(5):1335–56.
39. Keller AK, Jorgensen TM, Jespersen B. Identification of risk factors for vascular thrombosis may reduce early renal graft loss: a review of recent literature. J Transplant. 2012;2012:793461.

40. Bakir N, Sluiter W, Ploeg R, Van Son W, Tegzess A. Primary renal graft thrombosis. Nephrol Dial Transplant. 1996;11(1):140–7.
41. Fananapazir G, Tse G, Corwin MT, Santhanakrishnan C, Perez RV, McGahan JP, et al. Pediatric en bloc kidney transplants: clinical and immediate postoperative US factors associated with vascular thrombosis. Radiology. 2015:150430.
42. Lockhart ME, Wells CG, Morgan DE, Fineberg NS, Robbin ML. Reversed diastolic flow in the renal transplant: perioperative implications versus transplants older than 1 month. Am J Roentgenol. 2008;190(3):650–5.
43. Rouvière O, Berger P, Béziat C, Garnier J-L, Lefrançois N, Martin X, et al. Acute thrombosis of renal transplant artery: graft salvage by means of intra-arterial fibrinolysis. Transplantation. 2002;73(3):403–9.
44. Voiculescu A, Schmitz M, Hollenbeck M, Braasch S, Luther B, Sandmann W, et al. Management of arterial stenosis affecting kidney graft perfusion: a single-centre study in 53 patients. Am J Transplant. 2005;5(7):1731–8.
45. Willicombe M, Sandhu B, Brookes P, Gedroyc W, Hakim N, Hamady M, et al. Postanastomotic transplant renal artery stenosis: association with de novo class II donor-specific antibodies. Am J Transplant. 2014;14(1):133–43.
46. Patel NH, Jindal RM, Wilkin T, Rose S, Johnson MS, Shah H, et al. Renal arterial stenosis in renal allografts: retrospective study of predisposing factors and outcome after percutaneous transluminal angioplasty. Radiology. 2001;219(3):663–7.
47. Bent C, Fananapazir G, Tse G, Corwin MT, Vu C, Santhanakrishnan C, et al. Graft arterial stenosis in kidney en bloc grafts from very small pediatric donors: incidence, timing, and role of ultrasound in screening. Am J Transplant. 2015;15(11):2940–6.
48. Chen W, Kayler LK, Zand MS, Muttana R, Chernyak V, DeBoccardo GO. Transplant renal artery stenosis: clinical manifestations, diagnosis and therapy. Clin Kidney J. 2015;8(1):71–8. https://doi.org/10.1093/ckj/sfu132.
49. Ngo A, Markar S, De Lijster M, Duncan N, Taube D, Hamady M. A systematic review of outcomes following percutaneous transluminal angioplasty and stenting in the treatment of transplant renal artery stenosis. Cardiovasc Intervent Radiol. 2015;38(6):1573–88.
50. de Morais RH, Muglia VF, Mamere AE, Pisi TG, Saber LT, Muglia VA, et al. Duplex Doppler sonography of transplant renal artery stenosis. J Clin Ultrasound. 2003;31(3):135–41.
51. Obed A, Uihlein D, Zorger N, Farkas S, Scherer M, Krüger B, et al. Severe renal vein stenosis of a kidney transplant with beneficial clinical course after successful percutaneous stenting. Am J Transplant. 2008;8(10):2173–6.
52. Mei Q, He X, Lu W, Li Y. Renal vein stenosis after renal transplantation: treatment with stent placement. J Vasc Interv Radiol. 2010;21(5):756–8.
53. Fananapazir G, Hannsun G, Wright LA, Corwin MT, Troppmann C. Diagnosis and management of transplanted kidney extrarenal pseudoaneurysms: a series of four cases and a review of the literature. Cardiovasc Intervent Radiol. 2016;39(11):1649–53.
54. Perini S, Gordon RL, LaBerge JM, Kerlan RK, Wilson MW, Feng S, et al. Transcatheter embolization of biopsy-related vascular injury in the transplant kidney: immediate and long-term outcome. J Vasc Interv Radiol. 1998;9(6):1011–9.
55. Schwarz A, Hiss M, Gwinner W, Becker T, Haller H, Keberle M. Course and relevance of arteriovenous fistulas after renal transplant biopsies. Am J Transplant. 2008;8(4):826–31.
56. Kumar S, Ameli-Renani S, Hakim A, Jeon J, Shrivastava S, Patel U. Ureteral obstruction following renal transplantation: causes, diagnosis and management. Br J Radiol. 2014;87(1044):20140169.
57. Duty BD, Conlin MJ, Fuchs EF, Barry JM. The current role of endourologic management of renal transplantation complications. Adv Urol. 2013;2013:1.
58. Challacombe B, Dasgupta P, Tiptaft R, Glass J, Koffman G, Goldsmith D, et al. Multimodal management of urolithiasis in renal transplantation. BJU Int. 2005;96(3):385–9.
59. Hess B, Metzger RM, Ackermann D, Montandon A, Jaeger P. Infection-induced stone formation in a renal allograft. Am J Kidney Dis. 1994;24(5):868–72.

60. Mallon DH, Summers DM, Bradley JA, Pettigrew GJ. Defining delayed graft function after renal transplantation: simplest is best. Transplantation. 2013;96(10):885–9.
61. Lechevallier E, Dussol B, Luccioni A, Thirion X, Vacher-Copomat H, Jaber K, et al. Posttransplantation acute tubular necrosis: risk factors and implications for graft survival. Am J Kidney Dis. 1998;32(6):984–91.
62. Hoque MT, Mitra P, Samdani TS, Hossain G, Abedin Z, Mansur MA. Tacrolimus induced early graft dysfunction secondary to acute tubular necrosis in renal transplant recipient-a case report. BIRDEM Med J. 2012;2(1):63–5.
63. Jushinskis J, Trushkov S, Bicans J, Suhorukov V, Shevelev V, Ziedina I, et al., editors. Risk factors for the development of delayed graft function in deceased donor renal transplants. Transplant Proc. 2009;41(2):746–8. Elsevier.
64. Rifkin MD, Needleman L, Pasto ME, Kurtz AB, Foy PM, McGlynn E, et al. Evaluation of renal transplant rejection by duplex Doppler examination: value of the resistive index. Am J Roentgenol. 1987;148(4):759–62.
65. Ragab AR, Al-Mazroua MK, Al-Dakrory SA-E. Cyclosporine toxicity and toxicokinetics profiles in renal transplant recipients. J Clin Toxicol. 2013;2013.
66. Buckley AR, Cooperberg P, Reeve CE, Magil A. The distinction between acute renal transplant rejection and cyclosporine nephrotoxicity: value of duplex sonography. Am J Roentgenol. 1987;149(3):521–5.

Chapter 6
Pancreas Transplantation

Temel Tirkes and Kumaresan Sandrasegaran

Abbreviations

CT	Computerized tomography
MRI	Magnetic resonance imaging
US	Ultrasonography

Introduction

More than 30,000 pancreas transplants have been reported to the International Pancreas Transplant Registry from 1966 to 2008. Approximately 22,000 were from the USA [1, 2]. Pancreatic transplantation offers the potential for normalization of blood sugar levels in patients with diabetes mellitus. The procedure helps to stabilize or reverse many of the complications associated with diabetes, such as neuropathy, and improves quality of life.

Although pancreas transplantation has even been performed sporadically in patients with type 2 diabetes, this disease is not yet accepted to be a proven indication for pancreas transplantation [3]. Simultaneous pancreas-kidney transplantation is considered a life-saving therapy for patients with type 1 diabetes and concomitant end-stage kidney disease [4, 5]. Pancreas after kidney transplantation is performed in lower numbers. Rarely an isolated pancreatic transplant is undertaken, such as in patients with cystic fibrosis or young diabetic patients without renal disease. Complications are of allograft, bowel, infective, or vascular etiology. Major complications that require surgical intervention are infrequent and seen in about 5–10% of cases. Early allograft complications include pancreatitis, necrosis, rejection, and fistula. Clinically severe pancreatitis is found in about 10% of allografts [6].

T. Tirkes, M.D. (✉) · K. Sandrasegaran, M.D.
Department of Radiology and Imaging Sciences, Indiana University School of Medicine, Indianapolis, IN, USA
e-mail: atirkes@iupui.edu; ksandras@iupui.edu

G. Fananapazir, R. Lamba (eds.), *Transplantation Imaging*,
https://doi.org/10.1007/978-3-319-75266-2_6

Anatomic Considerations

Pancreas transplantation is usually performed using the whole organ with a concomitant duodenal patch. Transplantation of a segmental pancreas or the gland with only a small duodenal fragment is of historical interest and no longer used. The following surgical options are available for pancreas transplant [7]:

- Arterial anastomosis
  - Vascular reconstruction with donor iliac Y graft (splenic artery—internal iliac artery, superior mesenteric artery—external iliac artery)
  - Aortic patch of the celiac trunk and superior mesenteric artery
- Portal venous anastomosis
  - Systemic—venous (vena cava)
  - Portal—venous (branch of mesenteric vein)
- Exocrine drainage
  - Enteric (small bowel or duodenum)
  - Bladder

The different techniques can be mixed with one exclusion: bladder drainage cannot be performed with portal venous drainage owing to technical factors. Placement of the pancreas graft can be head-down or head-up. The pancreas graft can be placed intraperitoneally or retroperitoneally behind the right colon [8].

Surgical Techniques

Systemic Enteric Drainage

This is the most frequently used technique worldwide (85% enteric drainage, 79% systemic venous) [1]. Enteric exocrine drainage is performed using a staple technique, in which the donor duodenum is anastomosed side to side to native jejunum, 30–40 cm distal to the ligament of Treitz [9]. The portal vein of the pancreatic allograft is anastomosed to the recipient right external iliac vein. The donor common iliac artery is anastomosed to the recipient right external iliac artery (Fig. 6.1). The use of direct anastomosis is currently prevalent over Roux-en-Y loop [8]. Duodeno-duodenostomy is a further option when the pancreas is placed in the right retrocolic space [8]. This technique allows endoscopic surveillance but entails challenging repair of the recipient's duodenum in the case of allograft pancreatectomy.

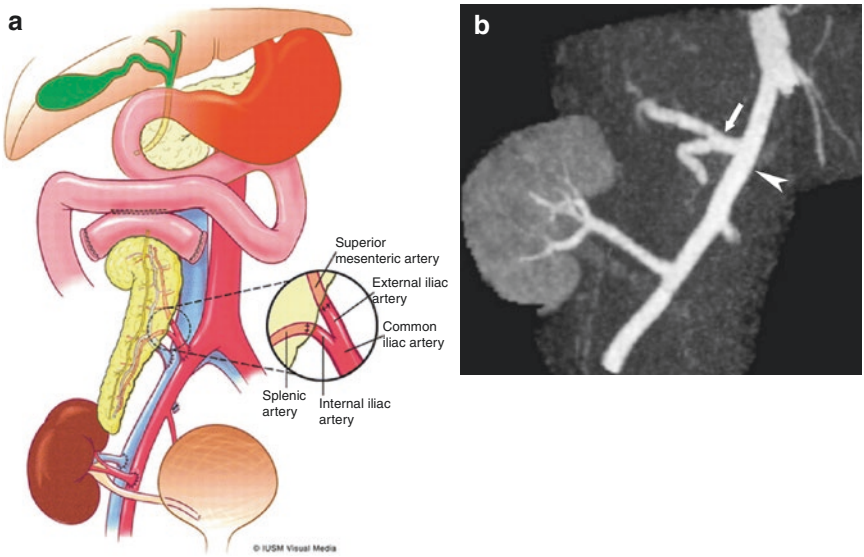

Fig. 6.1 (**a**) This illustration shows the systemic enteric drainage pancreatic transplant. The donor Y graft is anastomosed to the recipient right common iliac artery. The donor portal vein is anastomosed to the recipient common iliac vein. Enteric anastomosis for exocrine pancreatic drainage is between the donor duodenum and recipient jejunum. Renal artery and vein from the donor kidney are anastomosed to the recipient external iliac artery and vein, respectively. Inset shows construction of the Y graft (using donor vessels) by end-to-end attachment of the splenic to the internal iliac artery and the superior mesenteric to the external iliac artery. (**b**) This coronal reconstructed image of MR angiography is from a patient who is status post renal and pancreas transplantation. Arrowhead is pointing to the right common iliac artery and the arrow points to the trunk of the Y graft

Systemic Bladder Drainage

Bladder drainage helped make pancreas transplantation a routine and frequent procedure [10]. Until recently, bladder drainage was associated with a significantly lower technical failure rate according to the International Pancreas Transplant Registry data. The drainage of the exocrine secretion into the bladder allows the possibility of monitoring the graft function by measuring the amount (not concentration) of amylase secretion in the urine in 24 h. However, owing to new immunosuppressive protocols and a reduction in rejection episodes, even for these procedures enteric drainage is favored today.

Portal Enteric Drainage

Portal venous drainage has become popular since the mid-1990s when the technique was described by Gaber et al. [11]. As these methods place the pancreas graft in a mid-abdominal position, arterial anastomosis may be difficult. The physiological secretion of the insulin with a first pass through the liver (in contrast to a permanent hyperinsulinemia of the systemic venous drainage) is assumed to be beneficial. However, there is no proof of a beneficial metabolic effect of the portal venous drainage compared with systemic venous drainage.

Imaging Modalities

The radiologist must be aware of the postoperative anatomy and expected CT or US findings to avoid misinterpreting these for postoperative complications. Increasingly MRI is used to diagnose pancreatic and vascular complications, although CT remains the imaging procedure of choice for assessing infective and bowel-related complications.

Ultrasound

Gray-scale and Doppler ultrasound (US) examination of renal and pancreatic transplant are routinely performed at least once in the first three postoperative days (Fig. 6.2). The pancreatic allograft may not be visualized on the initial US scan, since the allograft may be obscured by bowel. The transplant should have a homogeneous echotexture, unless there is severe pancreatitis. The echogenicity of the pancreas transplant is higher than that of the cortex of the adjacent renal transplant but is lower than that of the native pancreas. This may be due to fatty change in the native organ and the presence of edema in transplants for the first few postoperative days. Filling of the urinary bladder may help ultrasonic visualization of the allograft (Fig. 6.3). Velocities and resistive indices of pancreatic vessels are routinely measured. Allograft (portal) vein velocities range from 10 to 60 cm/s.

Elevated arterial velocities at the anastomotic site immediately after surgery do not necessarily indicate hemodynamically significant vessel stenosis and often improve on follow-up studies. Such velocities may be due to anastomotic edema or kinking. In the few patients who had anastomotic stenosis that required angioplasty, the velocity of the donor Y graft at the anastomotic site was faster than 400 cm/s initially or remained faster than 300 cm/s on follow-up studies. Resistive indices of intra-pancreatic arteries are typically higher than those in renal transplants and may even be as high as 0.90. The reason for this is not clear but may be related to the almost universal presence of subclinical pancreatitis. Studies on bladder drainage

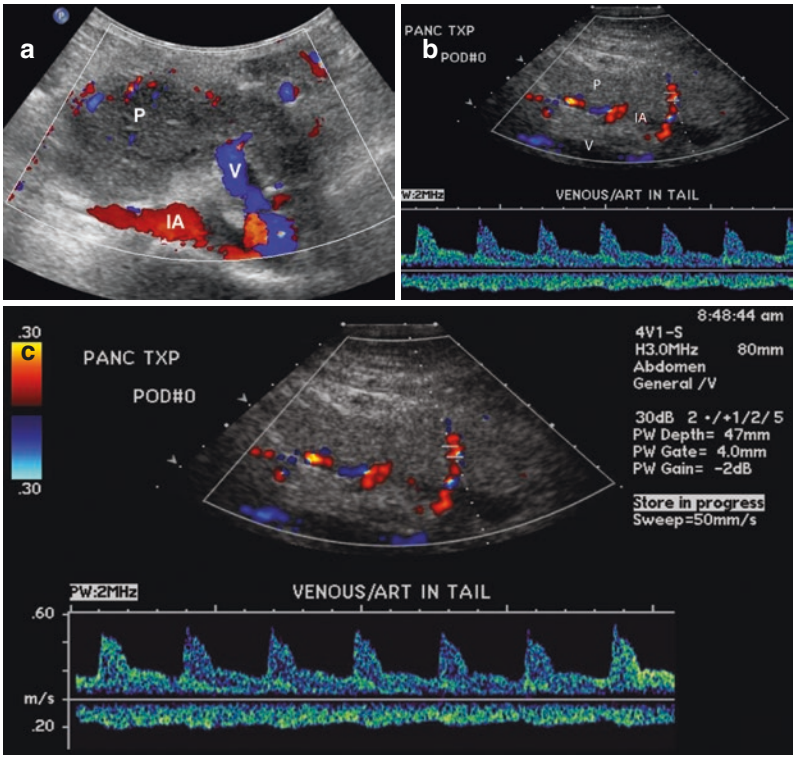

Fig. 6.2 (**a**) Doppler image of the pancreas transplant (P), iliac artery (IA), and transplant vein (V). (**b**) Doppler interrogation of the pancreatic tail demonstrating mixed arterial and venous flow. Patency of the transplant vessels is usually evaluated by ultrasound in the immediate postoperative period

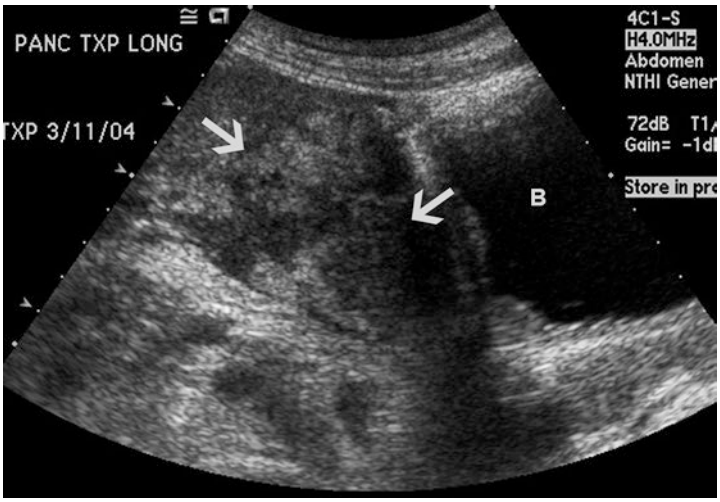

Fig. 6.3 Sagittal ultrasound image of the pelvis showing inhomogeneous echotexture of the pancreas transplant (arrows) due to acute pancreatitis. Distended bladder (B) may help visualization of the transplant

allografts have shown that resistive indices are not specific in determining the presence of acute rejection [12, 13]. Resistive indices also vary through the gland and are generally higher in the tail than in the head.

Computed Tomography

Computed tomographic (CT) examinations are usually requested for unexplained postoperative fever, abdominal tenderness, or pain. Many of the immediate postoperative examinations are performed with oral but without intravenous contrast, especially in cases of simultaneous renal transplantation. If vascular disease or transplant necrosis is suspected, Doppler sonography or gadolinium-enhanced MRI examination is typically performed. In some centers, intravenous contrast-enhanced CT with low iodinated contrast dose may be used more often for assessing postoperative complications.

Many findings are commonly seen after transplantation without adverse outcome on follow-up. The pancreatic transplant often enhances to a lesser degree than the adjacent renal transplant (Fig. 6.4). It is not uncommon to see fluid collections around the transplant in the first posttransplant month adjacent to the allograft (Fig. 6.5). Partial or complete occlusion of the donor superior mesenteric artery or vein, distal to its pancreatic branches, is seen in nearly all contrast-enhanced postoperative CT examinations (Fig. 6.6). This alarming finding does not correlate with subsequent transplant viability and may be expected since the donor artery does not supply the small bowel. The donor duodenum often does not fill with oral contrast.

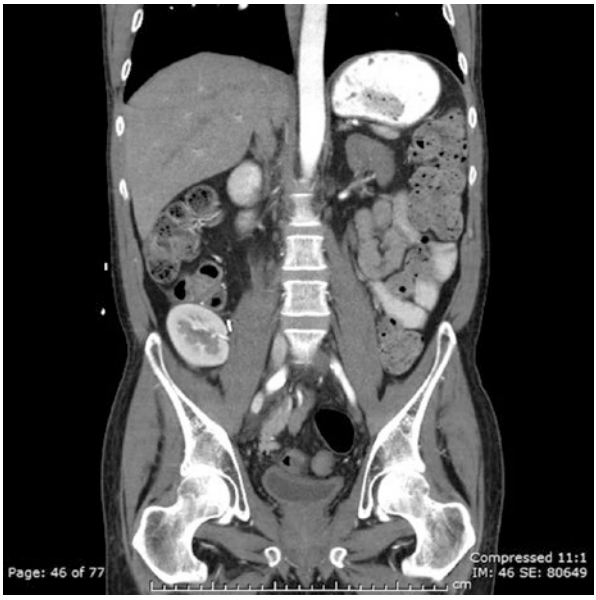

Fig. 6.4 Axial post-contrast CT of the pelvis showing the transplant kidney (black arrow) in the left iliac fossa and transplant pancreas in the midline (white arrow). It is normal for the pancreas to enhance less than the kidney. Pancreatic vasculature is patent (arrowhead)

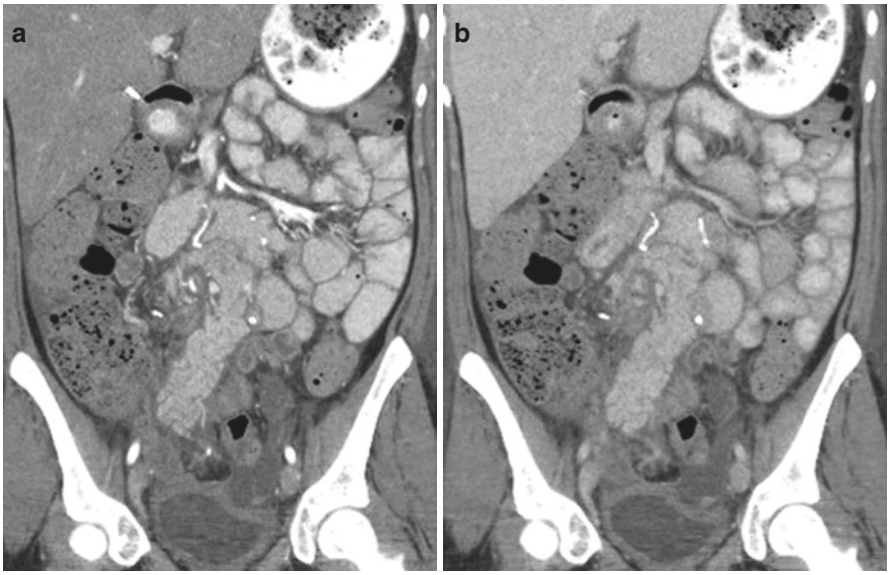

Fig. 6.5 Coronal reformatted contrast-enhanced CT of the pancreas transplant. There is small amount of fluid surrounding the pancreas (arrows)

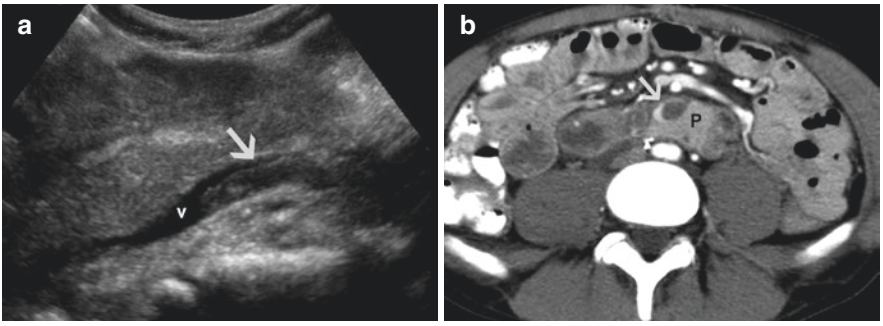

Fig. 6.6 (**a**) Gray-scale ultrasound of the pancreas transplant shows a non-occlusive thrombus (arrow) within the transplant vein (v). (**b**) Axial contrast-enhanced CT of the transplant pancreas shows a non-occlusive thrombus within the graft vein

It may be thick-walled and simulate a peripancreatic abscess (Fig. 6.7). Dilation of the main pancreatic duct is often seen and does not correlate with subsequent pancreatitis or rejection. The dome of the urinary bladder is frequently thick-walled for up to 4 weeks and should not be confused for cystitis (Fig. 6.8). This appearance may be due to irritation of the dome by fluid-rich pancreatic enzymes.

Magnetic Resonance Imaging (MRI)

MRI has been shown to be very valuable and accurate for evaluation of pancreatic transplant complications [14]. However, MRI is usually not the primary imaging modality for evaluating the complications of pancreas allograft but instead reserved for the cases

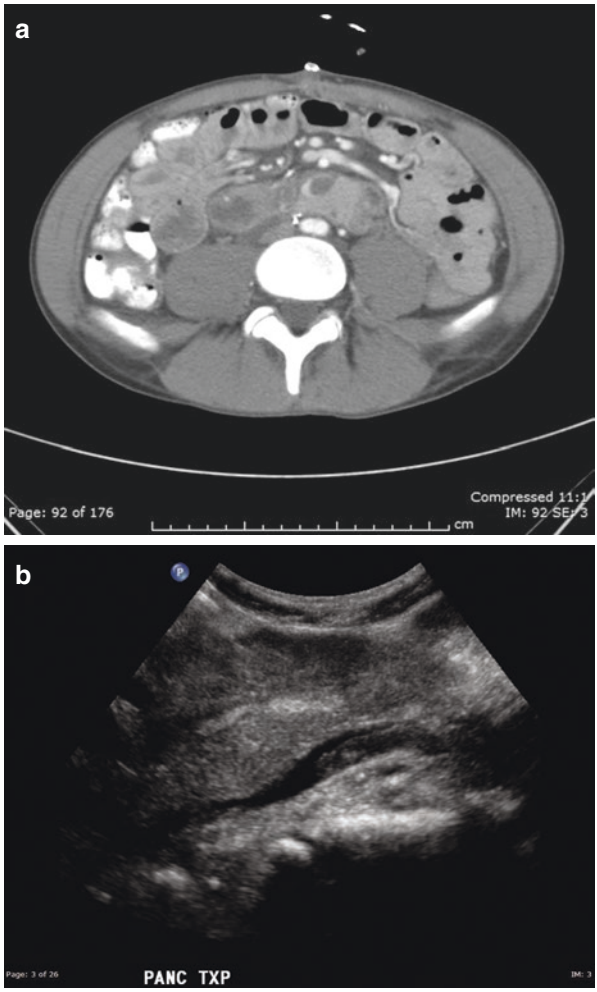

Fig. 6.7 (**a**) Axial CT image without IV contrast shows transplant kidney (K) and donor duodenum (arrows). Enteric contrast was given prior to this examination but did not fill in the duodenum. This appearance of the donor duodenum can mimic an abscess. (**b**) Coronal reformatted contrast-enhanced CT of the pancreas transplant (P). If the donor duodenum does not fill with enteric contrast, it can mimic a pretransplant collection

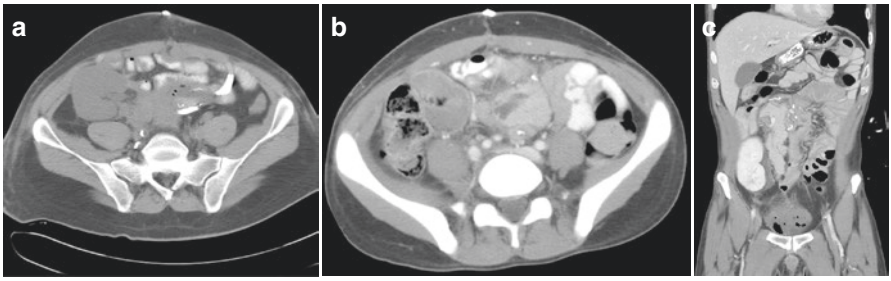

Fig. 6.8 Coronal contrast-enhanced CT image shows transplant kidney (K) and pancreas (P). Urinary bladder (B) shows wall thickening and perivesicular fat stranding (arrows) which can be seen following pancreas transplants

that could not be adequately evaluated by US or CT. MRI can be helpful to identify a fluid collection and distinguish it from a hematoma by detecting T1 hyperintensity. MRCP of the transplant pancreas can be performed to identify the anatomy of the pancreatic duct and status of the anastomosis. MRCP with IV secretin can be helpful to demonstrate exocrine function related to complications of pancreas allograft. Heverhagen et al. found that 10 min after IV secretin infusion, fluid excretion should be greater than 100 mL [15]. However, more studies are needed to evaluate value of secretin during MRCP for allograft evaluation. MRA was found to be a reliable imaging technique to identify vascular complications such as occlusion, stenosis, and infarction [16].

Vascular Complications

Vascular complications include thrombosis, pseudoaneurysm, and arterial extravasation.

Graft Thrombosis

Thrombosis of the graft portal vein or splenic vein are still the most frequent serious surgical complications, with an incidence of up to 10% [1, 17]. Clinical symptoms of pancreas graft thrombosis include sudden onset of otherwise unexplained hyperglycemia. Diagnosis of pancreas graft thrombosis may be established by imaging studies such as Doppler ultrasound, CT angiography, conventional angiography, or magnetic resonance imaging. Absent or reversed arterial diastolic low with Doppler US evaluation of pancreas transplants in the postoperative period is strongly associated with subsequent transplant failure, particularly in the setting of concurrent splenic vein thrombus [18]. With rare exceptions it results in the need for relaparotomy and transplant pancreatectomy [17]. Thus, graft thrombosis is the most frequent cause of early graft loss following pancreas transplantation. Early ultrasonic

findings include lack of venous flow in the allograft. Arterial flow may be preserved in early graft venous thrombosis (Fig. 6.9). The glandular echogenicity becomes heterogeneous. If unrecognized, graft venous thrombosis may lead to complete glandular necrosis (Fig. 6.10). Arterial thrombosis occurs less frequently and may be due to surgical technique or kinking of the Y graft. If recognized early, repositioning of the allograft, arterial stenting, or thrombectomy may help preserve the transplant.

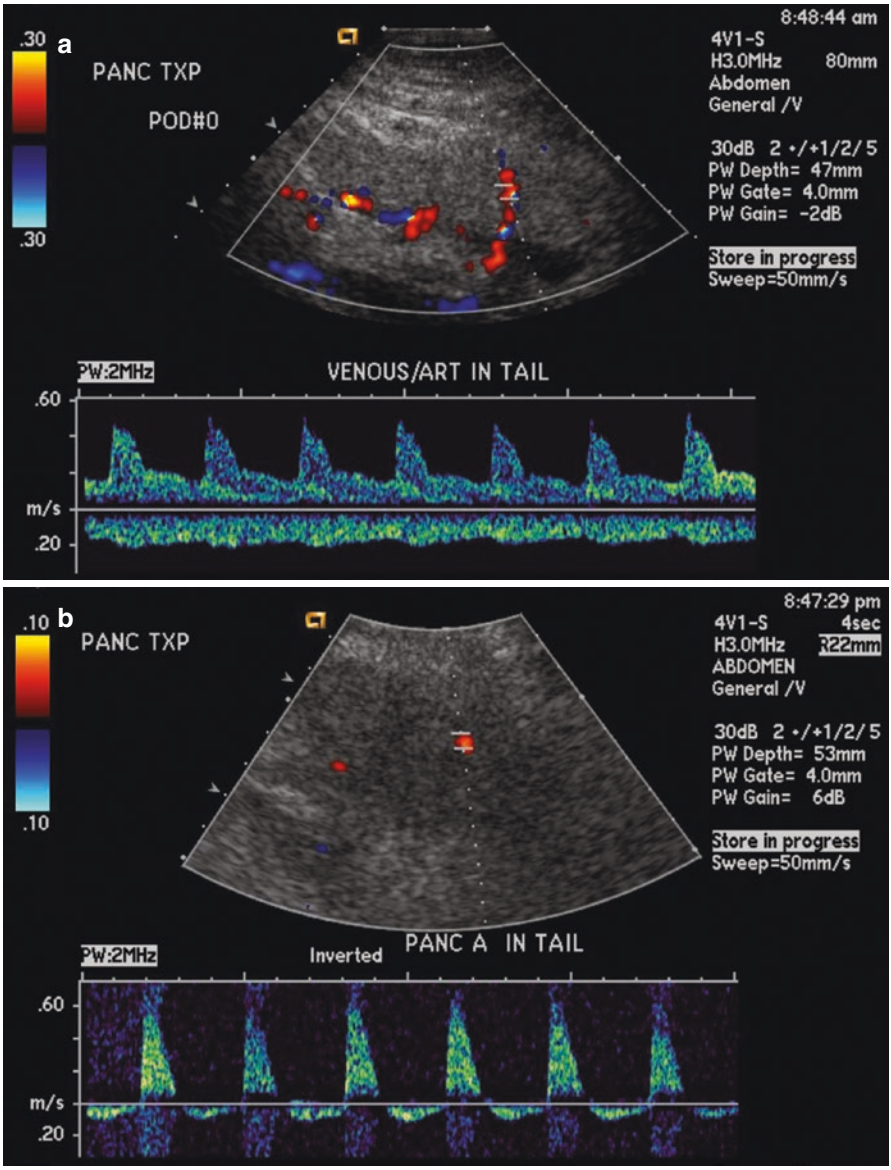

Fig. 6.9 Doppler ultrasound of the pancreas transplant (P) shows lack of venous flow (arrow) in the presence of arterial supply

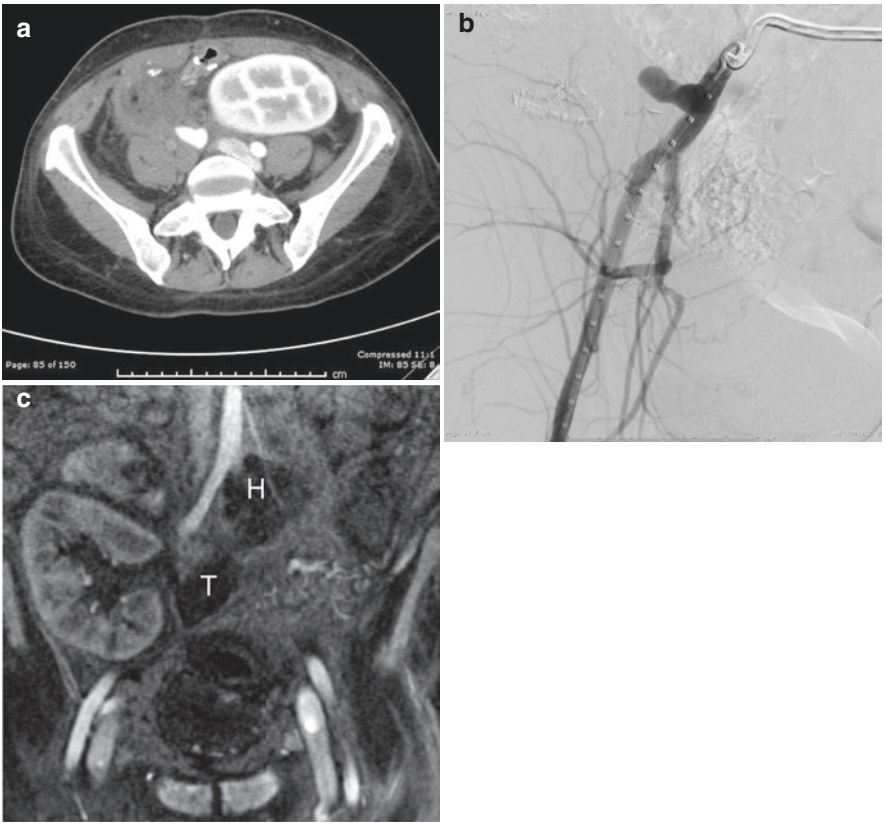

Fig. 6.10 (**a**) Axial contrast-enhanced CT of the kidney transplant in the left iliac fossa. There is complete occlusion of the transplant artery (black arrow) causing non-enhancing heterogeneous transplant pancreas (P). If undetected early, this results in transplant necrosis. (**b**) Conventional arteriogram of the iliac artery shows complete occlusion of the Y graft (arrow). (**c**) Coronal MR angiography image of the pelvis during arterial phase shows no enhancement within the head (H) and tail (T) of the pancreas transplant

Stenosis and Pseudoaneurysm

Anastomotic stenosis and pseudoaneurysm are infrequent complications of transplantation. Most pseudoaneurysms originate from the site of the vascular anastomosis. CT or MR arteriography may show vascular stenosis. Pseudoaneurysm is a rare complication of pancreatic transplantations and may be related to surgical technique, infection (mycotic aneurysm), severe pancreatitis (Fig. 6.11), or allograft biopsy.

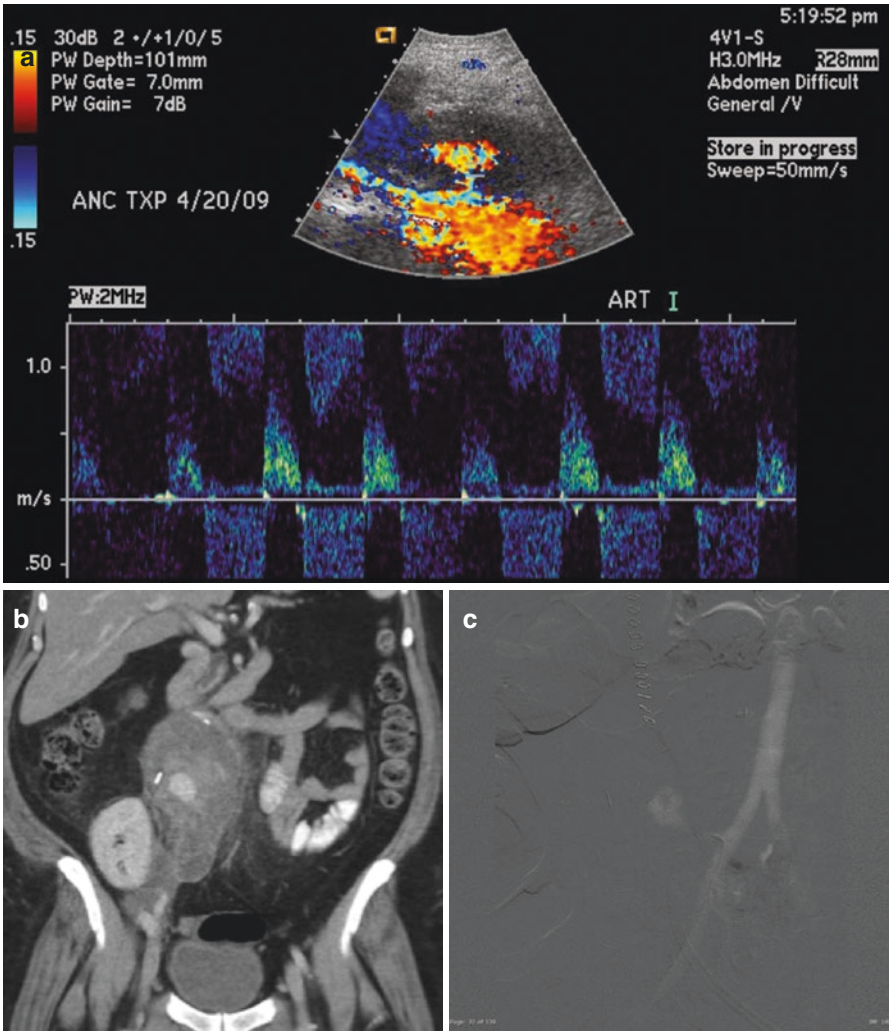

Fig. 6.11 (**a**) Doppler ultrasound image of the transplant artery shows a pseudoaneurysm (arrow). There is to-and-fro flow within the neck of the pseudoaneurysm. (**b**) Coronal reformat of the contrast-enhanced CT shows the pseudoaneurysm of the transplant pancreas artery (arrow). (**c**) This is an image from CO2 angiography. This is a pseudoaneurysm (arrow) arising from the Y graft of the pancreas transplant

Parenchymal Complications

These complications include pancreatitis, allograft necrosis, pancreatic abscess, acute graft rejection, acute graft-versus-host disease, and posttransplant lymphoproliferative disorder.

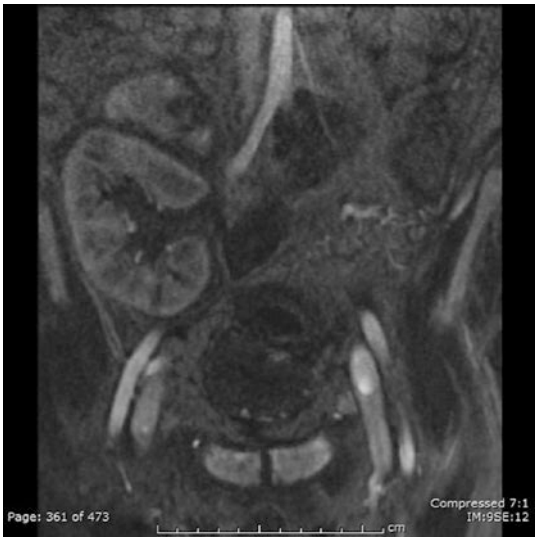

Fig. 6.12 Axial contrast-enhanced CT of the pelvis shows poor enhancement of the pancreas transplant (P). There is peripancreatic loculated fluid collection (arrow) being managed by a percutaneous drainage tube (long arrow)

Graft Pancreatitis and Related Complications

Like native pancreatitis, graft pancreatitis can be mild or severe with necrosis. Peripancreatic fluid collections can be infected and develop into an abscess or a pseudocyst (Fig. 6.12). Unless there is necrosis, conservative therapy including percutaneous drainage of collections is sufficient. The decision for re-laparotomy depends on the clinical appearance (signs of peritonitis) and laboratory results (C-reactive protein, leucocytes, amylase, lipase). A pancreatic abscess may also occur secondary to anastomotic leaks and following acute rejection (Fig. 6.13).

Acute Graft Rejection

Acute rejection is much less common in pancreatic transplantation that in renal transplantation. The diagnosis is made clinically and by surgical biopsy (Fig. 6.14). Percutaneous biopsy is possible but may be difficult because of the location of the transplant behind loops of bowel.

Posttransplant Lymphoproliferative Disease (PTLD)

PTLD is a rare long-term complication of transplantation. The predominant radiologic finding of PTLD in pancreatic transplant recipients is diffuse allograft enlargement, an appearance that may be indistinguishable from that of acute pancreatitis or transplant rejection [19]. This topic will be discussed in another chapter.

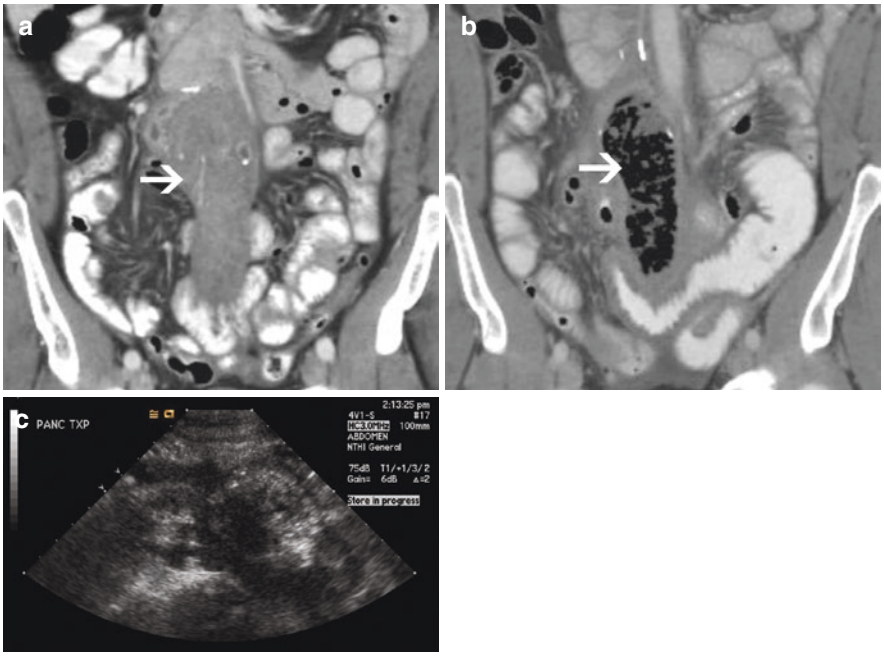

Fig. 6.13 (**a**) Coronal CT image of the pancreas (arrow) showing diffuse edema of the graft parenchyma secondary to acute rejection. (**b**) Subsequent contrast-enhanced CT study in the same patient with acute rejection shows complete necrosis of the pancreas transplant. The necrotic cavity was filled with air (arrow)

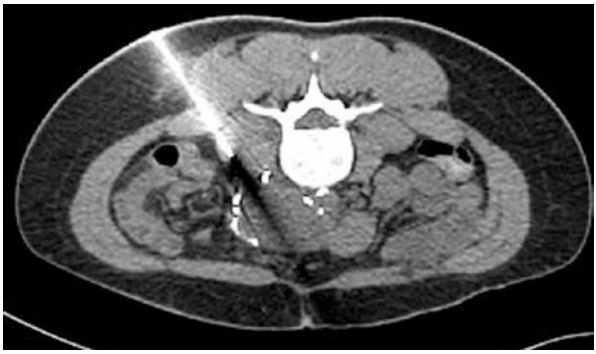

Fig. 6.14 This is a CT image during a percutaneous biopsy of the transplant pancreas (P) in a patient being evaluated for with graft rejection

Bowel Complications

Bowel-related complications include bowel obstruction, anastomotic leak, bowel fistula, and posttreatment infections, such as due to *Clostridium difficile.*

Small Bowel Obstruction

There are several causes of postoperative small bowel obstruction including adhesions, internal and external hernia, anastomotic stenosis, obturation by bezoar, and intussusception. Adhesions are the most common etiology of bowel obstruction. Intraperitoneal placement of the pancreas allograft creates the potential for internal hernia and bowel strangulation (Fig. 6.15). The mesenteric defect after this transplantation is defined by the aorta and iliac artery posteriorly, the small-bowel mesentery superiorly, the pancreas and enteric anastomosis anteriorly, and the pancreatic vascular anastomoses inferiorly. Jejunum adjacent to the anastomosis with donor duodenum may become trapped posteriorly in relation to the pancreas transplant. In cases of adhesive obstruction, unlike with an internal hernia, distended loops may not be seen posteriorly in relation to the donor duodenum [20]. It is important to make a timely diagnosis of an internal hernia, which is a closed-loop obstruction. The rate of strangulation is much higher than with an adhesion-related small bowel obstruction [21]. Conventional CT or CT enteroclysis can be used to diagnose the site, cause, and degree of small bowel obstruction and complications such as strangulation.

Anastomotic Leak

Anastomotic leaks occur rarely but remain a clinically significant entity, as they are a risk factor for intra-abdominal infection. The impact on graft and patient survival is minimal if leaks are recognized early and managed properly. As clinical appearance and therapeutic options are different, it is important to distinguish leaks in enteric and bladder-drained grafts. Recipients of enteric drained grafts develop early peritonitis and sepsis due to spillage of enteric contents. Abdominal CT can be obtained with oral contrast to confirm the diagnosis. Generalized peritonitis is less common and requires surgical intervention. Treatment consists of re-laparotomy with anastomotic revision or even transplant pancreatectomy.

Peri-transplant Collections

Abscess may complicate an anastomotic leak and is usually treated by antibiotics and percutaneous drainage. Like native pancreatitis, graft pancreatitis can range from mild to severe with necrosis. Peripancreatic fluid collections can be infected

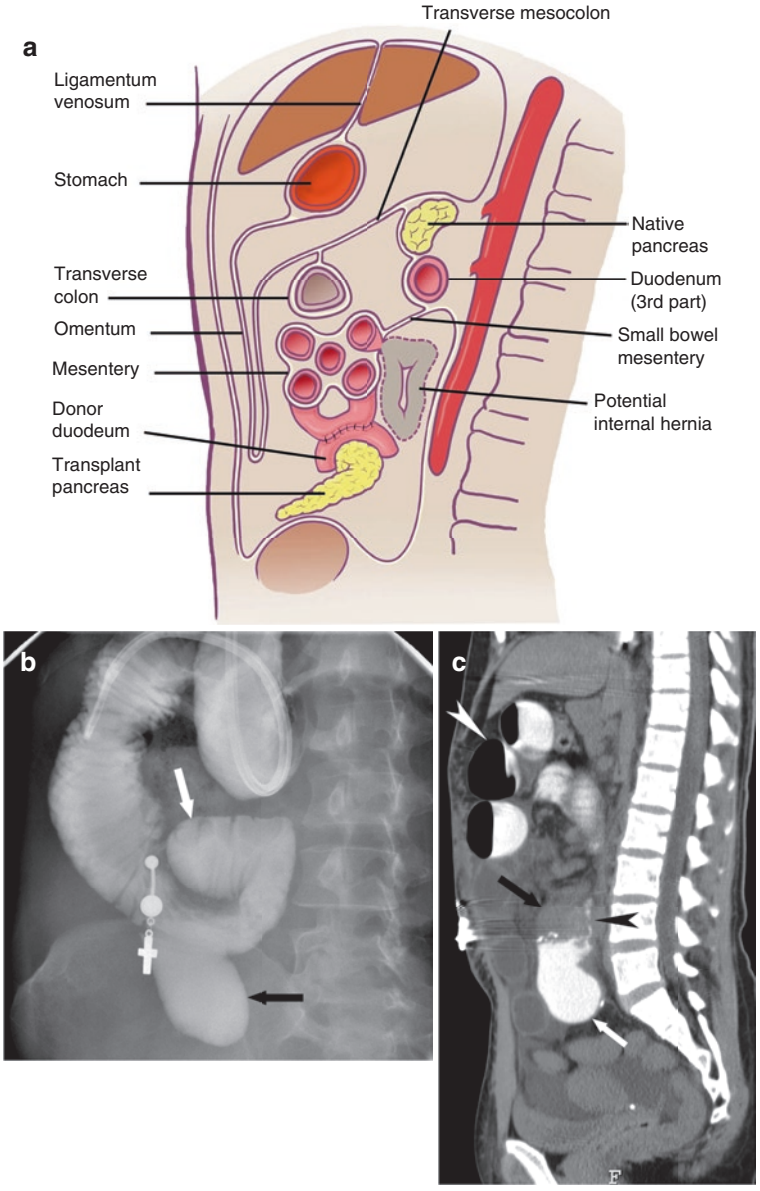

Fig. 6.15 (**a**) Sagittal illustration shows internal hernia following pancreas transplantation. Intraperitoneal placement of the transplant creates potential for internal hernia between donor duodenum/pancreatic allograft and posterior peritoneum. Hernia occurs through mesenteric defect used to attach donor duodenum to recipient jejunum. Used with permission from the Office of Visual Media, Indiana University. (**b**) This coronal fluoroscopic image from enteroclysis shows an internal hernia as a complication of pancreas transplant. Both the donor duodenum (black arrow) and loop of jejunum (white arrow) herniated through the mesenteric defect. (**c**) Sagittal CT image shows an internal following pancreas transplantation. Enteric contrast is filling the herniated jejunal loop (white arrow) through the neck of hernia (black arrowhead). Enteric contrast did not fill into the donor duodenum (black arrow). There is dilatation of the proximal small bowel loops (white arrowhead)

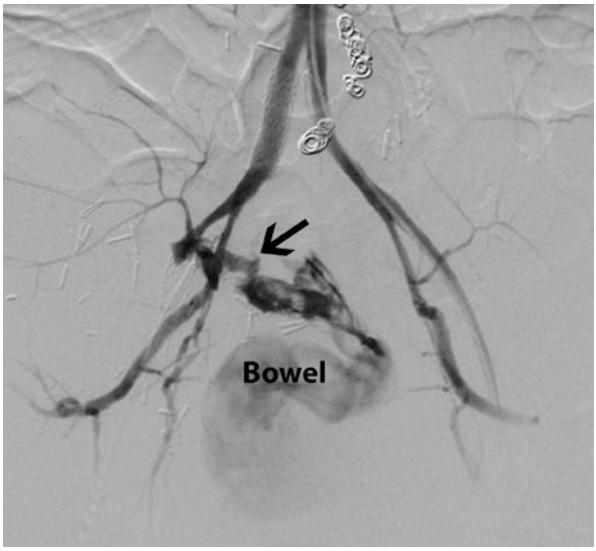

Fig. 6.16 Coronal conventional angiography image shows a fistula (arrow) between the graft artery and the bowel loop in the pelvis

and develop into an abscess or a pseudocyst. Postoperative hemorrhage is a potential complication that can be diagnosed by US, CT, or MRI. Fistula between the arterial graft and donor duodenum (Fig. 6.16) has been reported to be a source of major gastrointestinal bleeding that can be successfully treated with coil embolization [22].

References

1. Gruessner AC, Sutherland DE, Gruessner RW. Pancreas transplantation in the United States: a review. Curr Opin Organ Transplant. 2010;15(1):93–101. https://doi.org/10.1097/MOT.0b013e32833552d2.
2. Sutherland DE, Gruessner RW, Gruessner AC. Pancreas transplantation for treatment of diabetes mellitus. World J Surg. 2001;25(4):487–96. https://doi.org/10.1007/s002680020342.
3. Wullstein C, Woeste G, Zapletal C, Dette K, Bechstein WO. Simultaneous pancreas-kidney transplantation in patients with antiphospholipid syndrome. Transplantation. 2003;75(4):562–3. https://doi.org/10.1097/01.TP.0000046531.72372.48.
4. Smets YF, Westendorp RG, van der Pijl JW, de Charro FT, Ringers J, de Fijter JW, Lemkes HH. Effect of simultaneous pancreas-kidney transplantation on mortality of patients with type-1 diabetes mellitus and end-stage renal failure. Lancet. 1999;353(9168):1915–9. https://doi.org/10.1016/S0140-6736(98)07513-8.
5. Tyden G, Tollemar J, Bolinder J. Combined pancreas and kidney transplantation improves survival in patients with end-stage diabetic nephropathy. Clin Transplant. 2000;14(5):505–8.
6. Fernandez-Cruz L, Sabater L, Gilabert R, Ricart MJ, Saenz A, Astudillo E. Native and graft pancreatitis following combined pancreas-renal transplantation. Br J Surg. 1993;80(11):1429–32.
7. Guido W, Wolf OB. Handbook of renal and pancreatic transplantation. In: MacPhee IAM, Fronek J, editors. Chichester, West Sussex: Wiley-Blackwell; 2012. p. 194.

8. Boggi U, Amorese G, Marchetti P. Surgical techniques for pancreas transplantation. Curr Opin Organ Transplant. 2010;15(1):102–11. https://doi.org/10.1097/MOT.0b013e32833553de.
9. Freund MC, Steurer W, Gassner EM, Unsinn KM, Rieger M, Koenigsrainer A, Margreiter R, Jaschke WR. Spectrum of imaging findings after pancreas transplantation with enteric exocrine drainage: part 1, posttransplantation anatomy. AJR Am J Roentgenol. 2004;182(4):911–7. https://doi.org/10.2214/ajr.182.4.1820911.
10. Sollinger HW, Odorico JS, Knechtle SJ, D'Alessandro AM, Kalayoglu M, Pirsch JD. Experience with 500 simultaneous pancreas-kidney transplants. Ann Surg. 1998;228(3):284–96.
11. Gaber AO, Shokouh-Amiri H, Grewal HP, Britt LG. A technique for portal pancreatic transplantation with enteric drainage. Surg Gynecol Obstet. 1993;177(4):417–9.
12. Aideyan OA, Foshager MC, Benedetti E, Troppmann C, Gruessner RW. Correlation of the arterial resistive index in pancreas transplants of patients with transplant rejection. AJR Am J Roentgenol. 1997;168(6):1445–7. https://doi.org/10.2214/ajr.168.6.9168705.
13. Nelson NL, Largen PS, Stratta RJ, Taylor RJ, Grune MT, Hapke MR, Radio SJ. Pancreas allograft rejection: correlation of transduodenal core biopsy with Doppler resistive index. Radiology. 1996;200(1):91–4. https://doi.org/10.1148/radiology.200.1.8657950.
14. Liu Y, Akisik F, Tirkes T, Tann M, Sandrasegaran K, Jennings SG, Lin C, Kakarala B, Fridell JA, Powelson JA, Liang C. Value of magnetic resonance imaging in evaluating the pancreatic allograft transplant complications. Abdom Imaging. 2015;40(7):2384–90. https://doi.org/10.1007/s00261-015-0408-x.
15. Heverhagen JT, Wagner HJ, Ebel H, Levine AL, Klose KJ, Hellinger A. Pancreatic transplants: noninvasive evaluation with secretin-augmented MR pancreatography and MR perfusion measurements—preliminary results. Radiology. 2004;233(1):273–80. https://doi.org/10.1148/radiol.2331031188.
16. Hagspiel KD, Nandalur K, Pruett TL, Leung DA, Angle JF, Spinosa DJ, Matsumoto AH, Ahmed H, Sanfey HA, Sawyer RG, Burkholder B, Brayman KL. Evaluation of vascular complications of pancreas transplantation with high-spatial-resolution contrast-enhanced MR angiography. Radiology. 2007;242(2):590–9. https://doi.org/10.1148/radiol.2422041261.
17. Troppmann C. Complications after pancreas transplantation. Curr Opin Organ Transplant. 2010;15(1):112–8. https://doi.org/10.1097/MOT.0b013e3283355349.
18. Morgan TA, Smith-Bindman R, Harbell J, Kornak J, Stock PG, Feldstein VA. US findings in patients at risk for pancreas transplant failure. Radiology. 2016;280(1):281–9. https://doi.org/10.1148/radiol.2015150437.
19. Meador TL, Krebs TL, Cheong JJ, Daly B, Keay S, Bartlett S. Imaging features of posttransplantation lymphoproliferative disorder in pancreas transplant recipients. AJR Am J Roentgenol. 2000;174(1):121–4. https://doi.org/10.2214/ajr.174.1.1740121.
20. Lall CG, Sandrasegaran K, Maglinte DT, Fridell JA. Bowel complications seen on CT after pancreas transplantation with enteric drainage. AJR Am J Roentgenol. 2006;187(5):1288–95. https://doi.org/10.2214/AJR.05.1087.
21. Sandrasegaran K, Maglinte DD. Imaging of small bowel-related complications following major abdominal surgery. Eur J Radiol. 2005;53(3):374–86. https://doi.org/10.1016/j.ejrad.2004.12.017.
22. Lopez NM, Jeon H, Ranjan D, Johnston TD. Atypical etiology of massive gastrointestinal bleeding: arterio-enteric fistula following enteric drained pancreas transplant. Am Surg. 2004;70(6):529–32.

Chapter 7
Imaging of Intestinal Transplantation

Angela D. Levy and Daniel R. Swerdlow

Introduction

The intestine is the least common organ transplanted and is performed by a small number of transplant centers worldwide. The Organ Procurement and Transplantation Network reports 2658 intestinal transplants were performed in the United States from 1990 through 2015 in comparison to 368,750 kidney and 136,086 liver transplants in the same time period [1]. In 2015, 141 intestinal transplants were performed in the United States, 56 of these were isolated intestinal transplants and 85 were multivisceral transplants [1]. While recent data shows the number of intestinal transplants has decreased over the last decade because of improvements in the medical and surgical treatment of intestinal failure, it remains an option for patients who fail other therapies or have a high likelihood of failure [2]. In this chapter, we discuss the indications for intestinal transplant, surgical anatomy, and radiology of intestinal transplantation. Two components of the radiologic evaluation of intestinal transplantation are described in this chapter: preoperative radiologic assessment of intestinal transplant candidates and the radiologic evaluation of postoperative complications.

Indications

Intestinal failure is the inability of the small bowel to meet the nutritional, fluid, and electrolyte requirements of the body such that parenteral nutrition is required to sustain life [3]. Short bowel syndrome is the most common cause of intestinal failure, and infants are the age group most commonly affected by short bowel

A. D. Levy, M.D. (✉) · D. R. Swerdlow, M.D.
Department of Radiology, Medstar Georgetown University Hospital, Washington, DC, USA
e-mail: angela.d.levy@gunet.georgetown.edu

G. Fananapazir, R. Lamba (eds.), *Transplantation Imaging*,
https://doi.org/10.1007/978-3-319-75266-2_7

syndrome. In infants and children, short bowel syndrome may result from necrotizing enterocolitis, volvulus, intestinal atresia, and gastroschisis. In adults, short bowel syndrome occurs from loss of small bowel from mesenteric infarction, volvulus, extensive small bowel resection for Crohn disease, trauma, tumors of the small bowel mesentery such as desmoids, or resections for enterocutaneous fistulas that complicate small bowel injury or surgery. Intestinal failure may also be caused by radiation enteritis, congenital disorders of the mucosa, and neuromuscular disorders such as Hirschsprung disease and neuropathic or myopathic pseudoobstruction.

Parenteral nutrition is the principal treatment for intestinal failure. Complications of parenteral nutrition are the most common indications for intestinal transplantation. The complications of parenteral nutrition that are accepted indications for intestinal transplantation are thrombosis of two or more central veins, parenteral nutrition-induced liver failure, two or more episodes of central venous catheter-related sepsis per year requiring hospitalization (and/or single episode of central venous catheter-related fungemia, septic shock, or acute respiratory distress syndrome), and frequent episodes of severe dehydration despite adequate hydration with parenteral nutrition [4]. Intestinal transplantation may also be indicated in patients who have a high risk of mortality on parenteral nutritional therapy due to their underlying cause of intestinal failure [4, 5].

New and emerging indications for intestinal transplantation include slow-growing tumors located in the small bowel mesentery or involving the celiac or superior mesenteric artery, ultrashort segment short bowel syndrome (less than 10 cm in infants and less than 20 cm in adults), and chronic portal and mesenteric venous thrombosis or occlusion [6].

Surgical Anatomy

Intestinal transplantation may be performed by transplanting the small intestine alone, small intestine and liver, or in any combination of multivisceral transplant that may include the liver, stomach, pancreas, colon, spleen, and/or kidney. The selection of organs transplanted depends upon the patient's age, underlying disease, and anatomy.

The term *isolated intestinal transplant* refers to the jejunum and ileum with or without the colon [7]. This type of graft may be used when the indication for transplantation is related to central venous access or central venous catheter sepsis [8]. The arterial vascular anatomy for an isolated intestinal transplant is an anastomosis of the donor superior mesenteric artery or aorta (or aortic patch) to the recipient superior mesenteric artery or aorta. If the aorta is used as arterial inflow, a jump graft may be necessary. The infrarenal aorta is the usual site for anastomosis (Fig. 7.1). Venous outflow may be constructed by anastomosing the donor superior mesenteric vein to the recipient portal vein, superior mesenteric vein, splenic vein, or inferior vena cava. A venous jump graft may be utilized to create the anastomosis. Proximal intestinal continuity is achieved by anastomosing the

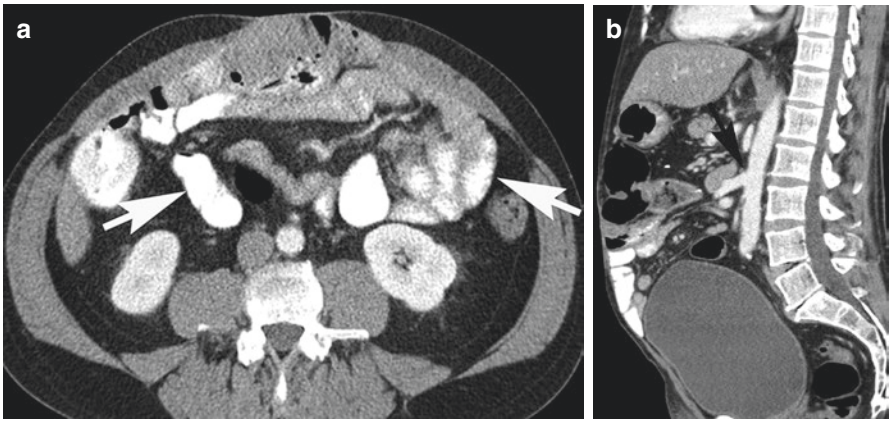

Fig. 7.1 Normal isolated intestinal transplant in a 48-year-old man who developed short bowel syndrome from multiple small bowel resections for Crohn disease. (**a**) Intravenous and oral contrast-enhanced CT scan shows the transplanted small bowel is normal in caliber with normal wall thickness and fold thickness (arrows). (**b**) Arterial inflow is from an infrarenal aortic to aortic anastomosis (arrow). The donor SMV to recipient SMV anastomosis is not shown

donor jejunum to the recipient duodenum or proximal jejunum proximally. The distal anastomosis may be the donor ileum to the recipient colon or the donor colon to the recipient colon. A loop or chimney ileostomy is created to provide access for ileoscopy. The ileostomy may be reversed at a later time dependent upon the patient's clinical course.

An en bloc combined liver and intestinal transplant (with or without the pancreas) is used for those patients with liver disease. The arterial inflow for a combined liver and intestinal transplant is from the aorta by an anastomosis with a donor aorta, aortic patch, or jump graft that gives rise to the celiac and superior mesenteric arteries. The venous anastomosis is through the classic inferior vena caval anastomosis of a liver transplant. Other organs may be included in an en bloc transplant depending upon the patients underlying disease. En bloc multivisceral transplants may be performed with leaving the native pancreas, duodenum, and spleen in place to avoid the morbidity associated with removing these organs (Fig. 7.2) [9]. The intestinal continuity is achieved in a similar manner to the isolated intestinal transplant.

Radiology of Intestinal Transplants

Radiological examinations provide important anatomic and functional information for the assessment and management of patients with intestinal failure and intestinal transplants. At our institution, fluoroscopy, cross-sectional imaging, and scintigraphy are used in the assessment of candidates prior to intestinal transplantation. In the postoperative period, CT is the imaging modality of choice for the assessment

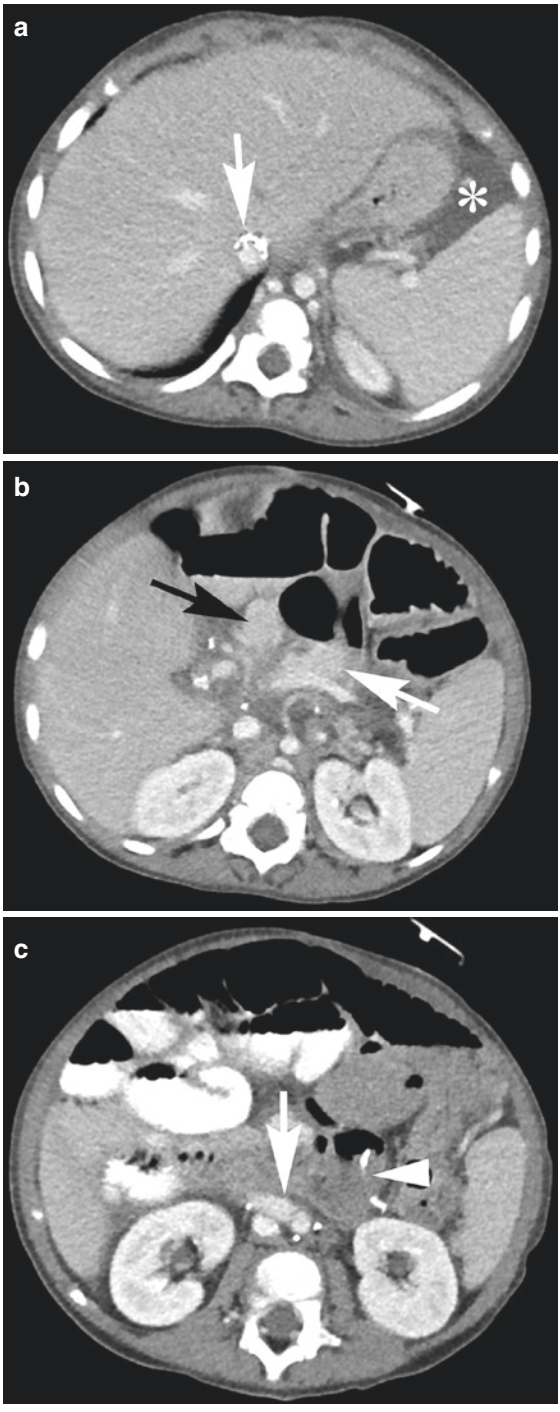

Fig. 7.2 Intravenous contrast-enhanced CT images of an en bloc liver, pancreas, and intestinal transplant in a child with short bowel syndrome show the IVC anastomosis as the venous outflow (arrow in **a**) and aorta-to-aorta anastomosis as the arterial inflow (arrow in **c**). The native pancreas is in normal anatomic position (white arrow in **b**). The donor pancreas is located anterior to the native pancreas (black arrow in **b**). Other findings include the proximal intestinal anastomosis (arrowhead in **c**) and a small amount of fluid in the left upper quadrant (asterisk in **a**)

of most complications. Ultrasound may be used for the evaluation of specific vascular structures, and fluoroscopy may be indicated to evaluate the intestinal anastomotic sites and motility.

Radiological Assessment of Intestinal Transplantation Candidates

Candidates for intestinal transplantation require imaging to evaluate their anatomy and the presence of pathological processes. The majority of patients have had previous extensive small bowel resection such that the length and anatomy of the remaining small bowel and colon are not known. Because central venous access and central venous catheter complications are indications for intestinal transplantation, assessment of vascular patency is an important component of the imaging evaluation. Comorbid conditions, enteric fistulas, and associated solid organ disease in the abdomen are also commonly present in these patients [10, 11]. Consequently, detailed anatomic evaluation of the gastrointestinal tract and cross-sectional imaging of the body that includes an assessment of vascular patency are obtained in the assessment of patients that are undergoing consideration for intestinal transplantation.

A variety and combination of imaging and fluoroscopic exams may be performed to define the anatomy required by the surgical team. CT or MRI imaging of the chest, abdomen, and pelvis and fluoroscopic evaluation of the intestine are routinely performed. Select patients undergo scintigraphic gastric emptying studies when gastric motility and preservation is a clinical concern. CT scan performed with intravenous contrast material has many advantages over MRI including speed, availability, and ability to easily cover the anatomy of the chest, abdomen, and pelvis. Anatomic coverage with MRI is more difficult than CT, and image degradation by motion may be a problem during long MR examinations, particularly in the pediatric population who often require sedation.

Fluoroscopic exams of the upper and lower gastrointestinal tract may be utilized to determine upper and lower gastrointestinal tract anatomy and motility. In addition, fluoroscopy is used to evaluate enterocutaneous fistula, defining their anatomic extent and connections. In general, fluoroscopic evaluation of the gastrointestinal tract is very helpful to answer specific questions with regard to intestinal anatomy and motility.

Ultrasound has the advantage of lack of ionizing radiation, which is of particular concern in the pediatric and young adult population. However, the breadth of anatomy required for evaluation cannot be covered easily, and its ability to image the lungs and abdomen for comorbid disease is limited. Ultrasound is used in some of these patients to evaluate specific vascular questions. Anatomic coverage and the various advantages and disadvantages of each modality for pre-intestinal transplant assessment are summarized in Table 7.1.

Table 7.1 Comparison of imaging modalities for small intestinal transplant candidates

	Anatomy delineated	Advantages	Disadvantages
CT	• Bowel • Solid organs • Vasculature	• Speed • Wide anatomic coverage • Readily available	• Radiation • Intravenous contrast may be contraindicated in some patients
MRI	• Solid organs • Vasculature • Bowel	• No ionizing radiation	• Cost • Difficult to obtain anatomic coverage efficiently • Motion sensitive • Bowel evaluation is limited
Ultrasound	• Solid organs • Vasculature	• No ionizing radiation • Readily available	• Operator dependent • Limited assessment of central veins and mesenteric vessels
Fluoroscopy	• Bowel	• Motility and transit time evaluation	• Radiation • Consider timing if obtaining concomitant CT scan

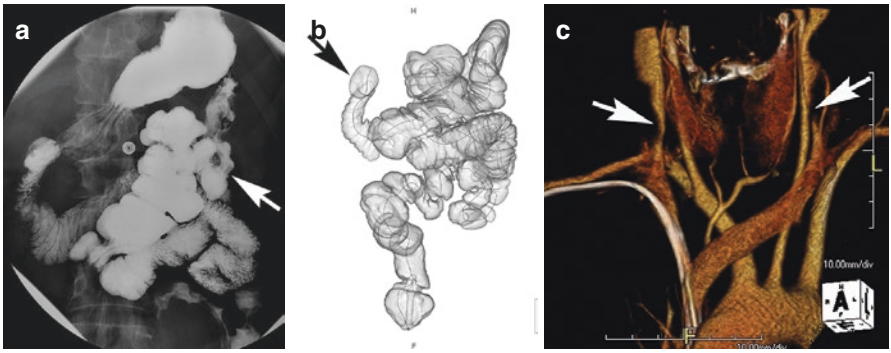

Fig. 7.3 Pre-intestinal transplant evaluation in a 54-year-old man with short bowel syndrome. (**a**) Spot radiograph from a single-contrast upper gastrointestinal series shows a very short segment of the proximal jejunum is anastomosed to the colon (arrow). (**b**) Three-dimensional reconstruction of the colon from a CT scan performed with rectal CO_2 insufflation shows a jejunal to transverse colon anastomosis (arrow). Because of the short jejunum, CO_2 insufflation during the CT exam progressed retrograde to expand the first portion of the duodenum (arrow). (**c**) Three-dimensional vascular reconstruction of the aortic arch and neck blood vessels shows bilateral internal jugular vein stenosis (arrows)

At our institution, the majority of intestinal transplant candidates are imaged with intravenous contrast-enhanced CT scans of the chest, abdomen, and pelvis, followed by fluoroscopic evaluation of the gastrointestinal tract and enterocutaneous fistulas. Our CT protocol is a scan of the chest, abdomen, and pelvis during the arterial and venous phases of contrast enhancement. We have added rectal CO_2 to the pre-intestinal transplant protocol in order to obtain three-dimensional images that show the length measurements of the colon (Figs. 7.3 and 7.4) [12].

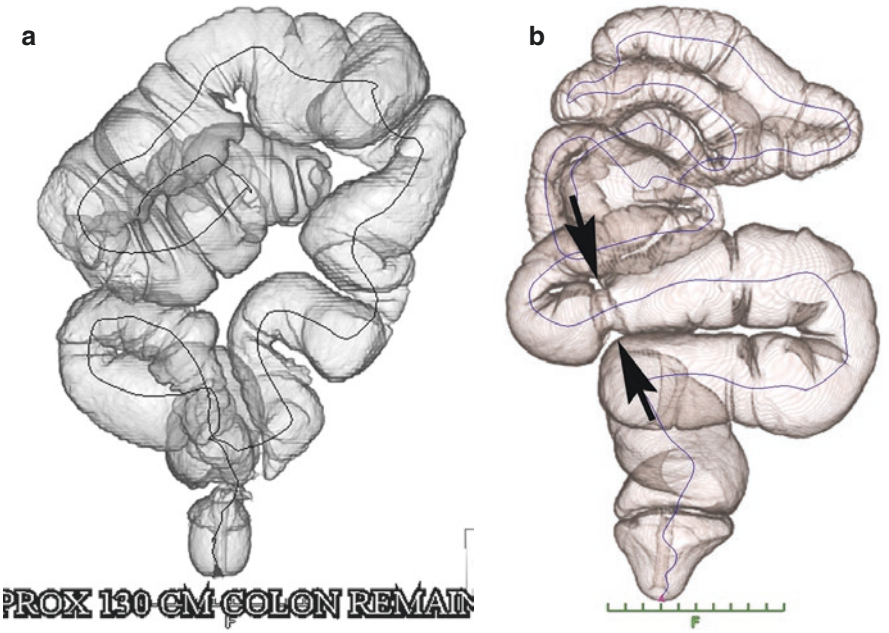

Fig. 7.4 Three-dimensional reconstructions of the colon in two different patients. Colonic reconstructions obtained from a pre-transplant evaluation CT scan with rectal CO_2 insufflation. (**a**) Three-dimensional reconstruction shows a normal complement of the colon that is approximately 130 cm in length. (**b**) Three-dimensional reconstruction of the colon in a different patient shows focal narrowing at the ileocolic anastomosis (arrows), which is at the level of the sigmoid colon

Patients also routinely undergo fluoroscopic evaluation of the gastrointestinal tract with an upper gastrointestinal series. Fistulagrams may be performed if enterocutaneous fistulas are present, and anatomic assessments of the fistula are necessary for surgical decision-making. Although barium or a water-soluble contrast material may be used for fluoroscopy, we prefer water-soluble contrast material for most patients since their anatomy is unknown and water-soluble contrast material clears more easily and rapidly from the bowel. The contrast material is administered orally or through a gastrostomy tube. A series of spot radiographs, fluoroscopic video capture, and overhead radiographs are obtained to adequately display upper gastrointestinal tract anatomy (Figs. 7.3 and 7.5). Water-soluble contrast material is also used for enterocutaneous fistula evaluation. We use a thin catheter (such as a 5 or 7 French pediatric feeding tube) appropriate to the size of the fistula. After cannulating the fistula, we slowly inject contrast to opacify the track (Fig. 7.6). An additional limited CT may be performed after the fistulagram as needed to further delineate which segment of bowel is involved. For patients with loop ileostomies in place, a Foley catheter appropriate to the size of the ostomy opening may be used to cannulate the ostomy to inject either the proximal or distal aspects to define the anatomy as clinically warranted. CO_2 insufflation of the colon with a pressure-limited

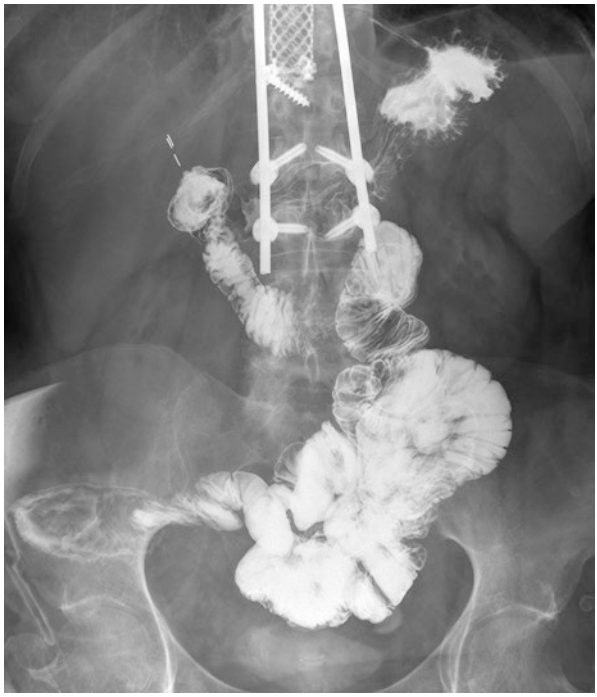

Fig. 7.5 Supine radiograph from an upper gastrointestinal series performed prior to intestinal transplant shows shortened length of small bowel of normal caliber extending to a right lower quadrant ostomy

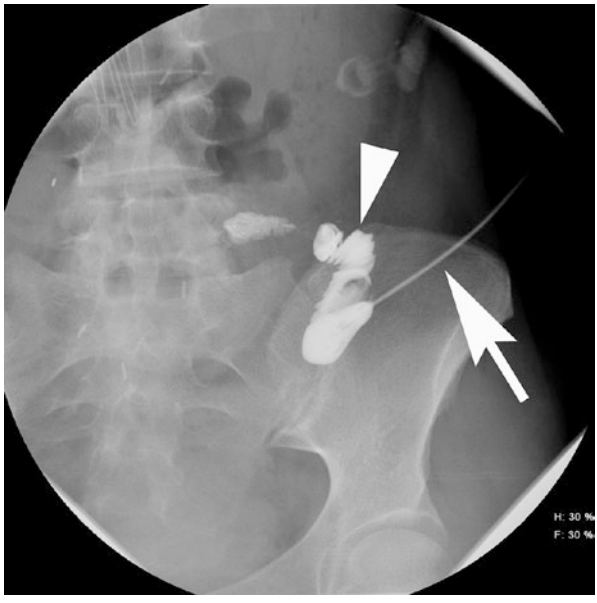

Fig. 7.6 Spot radiograph from a fluoroscopic fistulagram shows a small-caliber feeding tube (arrow) cannulating an enterocutaneous fistula in the left lower quadrant. The fistula and feeding tube extend directly into a small bowel loop (arrowhead) in the left lower quadrant. Small amount of contrast in the left upper abdomen is retained in the bowel from a previous exam

pump during CT with three-dimensional post-processed images of the colon has replaced fluoroscopic enemas of the colon to display colonic anatomy in adult patients at our institution. Water-soluble enemas are still performed in pediatric patients with unknown colonic anatomy.

MRI may be performed if there is a contraindication to CT or iodinated contrast material or if there are specific clinical questions that are better addressed by MRI. Similarly, venous ultrasound may be obtained to aid in the evaluation of central venous access sites and to evaluate for venous thrombosis or occlusion.

During CT interpretation, specific attention should be paid to sites of venous access to determine if central veins are patent, thrombosed, or occluded (Fig. 7.3). Variant arterial and venous vascular anatomy should be described. Three-dimensional data sets from CT and MRI can be used to create anatomic models of blood vessels and select portions of the gastrointestinal tract (Figs. 7.3 and 7.4). Liver volumes are routinely calculated for pediatric transplant candidates and for select adult candidates when clinically necessary. In these cases, the size of the donor liver and entire graft is an important consideration because the size of the abdominal compartment is small.

Radiologic Evaluation of Postoperative Complications

Postoperative imaging of intestinal transplant is performed to evaluate for complications. Though multiple imaging modalities are used to assess the variety of postoperative complications and complications related to immunosuppression, CT is the most frequently used technique because of its ability to rapidly scan the body and provide exquisite anatomic detail. Postoperative scans may be obtained with or without intravenous contrast material. Positive oral contrast material is desirable in order to define the anatomy of the intestinal graft and to assess the integrity of the intestinal anastomoses. The most common postoperative complications are rejection and infection. Other surgical complications common to intestinal surgeries such as anastomotic leak, obstruction, perforation, abscess, motility disorders, and fistula formation may also occur. Vascular complications, posttransplantation lymphoproliferative disorder, and pancreatic and biliary complications are less common.

Normal CT Findings of Intestinal Transplants

The normal transplanted small intestine usually has normal wall thickness (less than 3 mm) and normal fold patterns (Fig. 7.1) [13]. Not infrequently, thick small bowel wall (greater than 3 mm) may be seen in a normal transplant (Fig. 7.7) [14]. In our patient population, small bowel wall thickening was shown to be a nonspecific finding. It cannot be used to discriminate between intestinal transplant patients with normal small bowel, rejection, infection, or ischemia when compared to the findings of endoscopic biopsy [15]. Luminal dilatation (greater than 4 mm) may also be seen normally [14]. The loops of small bowel may be clustered together centrally within the abdomen, and there may be increased attenuation of the small bowel mesentery. In an en bloc combined liver and intestinal transplant, the liver and intestine are in normal anatomic position. In an en bloc multivisceral transplant

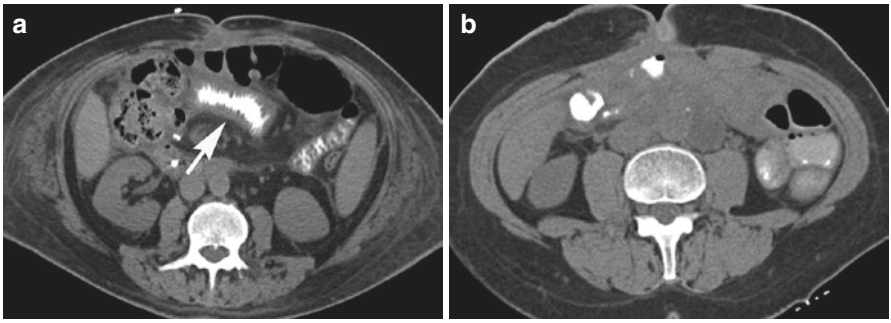

Fig. 7.7 Normal intestinal transplant in two different patients. (**a**) Noncontrast CT scan shows wall thickening and fold thickening of the transplanted small bowel. Biopsy specimens were normal with no findings of rejection or infection. (**b**) Noncontrast CT scan in a different patient shows poor definition of the transplanted small bowel wall because there is increased attenuation of the small bowel mesentery. Biopsy specimens showed no abnormality in the transplanted intestine

with the native pancreas and spleen remaining in place, the donor organs are placed anterior to the native organs such that both native organs and transplanted organs are visualized (Fig. 7.2).

Rejection and Other Immunologic Complications

Initial experiences with intestinal transplant were limited by high rates of rejection. Improvements in immunotherapy have led to improved graft and patient survival [16]. However, rejection remains the leading cause of graft failure in intestinal transplants. Other immunologic complications have also been recognized in these patients. These include graft-versus-host disease, inflammatory bowel disease-like posttransplant disorder, autoimmune disorders such as autoimmune hepatitis, and food allergies [17]. Imaging plays a minor role in the diagnosis of rejection and other immune disorders. Rejection is diagnosed by mucosal biopsy, most commonly by endoscopy through the ileostomy. Patients undergo routine surveillance biopsy to monitor for the occurrence of rejection.

CT may be performed in some patients with clinical findings of rejection in order to exclude other complications such as abscess or pneumonia or in severe cases to evaluate for ischemia or infarction that may complicate severe rejection. The CT findings of rejection are not specific and overlap with the normal appearance of an intestinal transplant as well as infection and ischemia [14, 15, 18]. The bowel wall may appear normal, thickened, or have a target pattern of enhancement (Fig. 7.8). Bowel dilatation may occur but can also be seen in some normal transplants as well as those with obstruction or motility disorders. Mesenteric edema may also be present in severe rejection.

Graft-versus-host disease (GVHD) is seen more commonly in intestinal transplants compared to solid organ transplants. The incidence has been reported as high as 9% in intestinal transplant recipients, with children, multivisceral graft

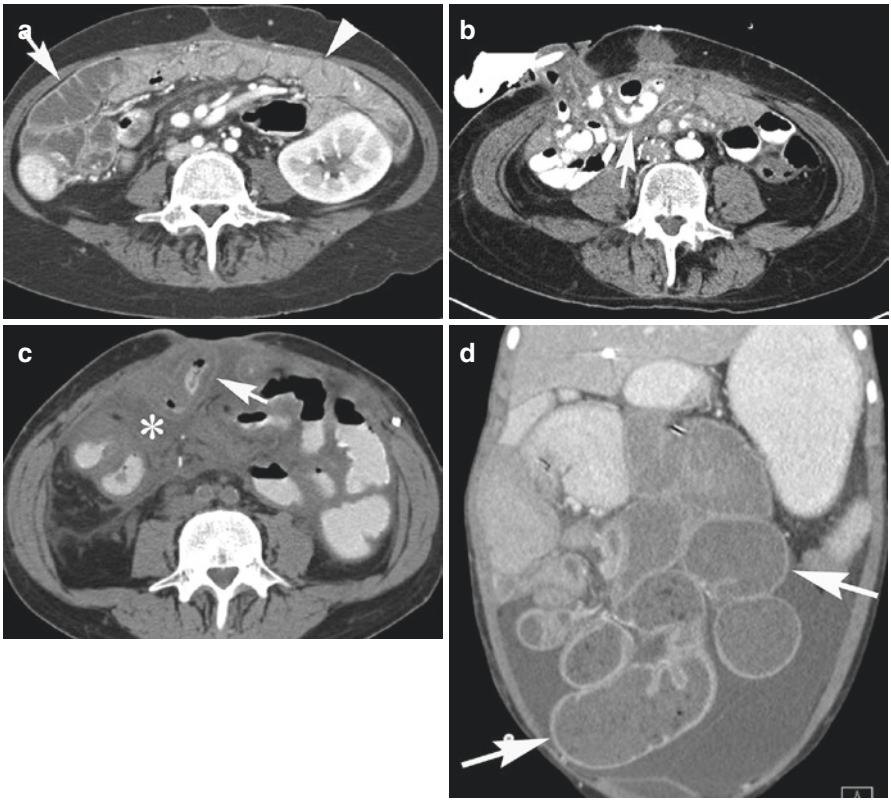

Fig. 7.8 Spectrum of CT findings in intestinal transplant rejection. (**a**) Intravenous contrast-enhanced CT in a patient who underwent intestinal and kidney transplant shows normal appearing collapsed loops of small bowel in the left abdomen (arrowhead) and fluid-filled loops in the right abdomen (arrow). There are no findings of small bowel wall thickening. Biopsy specimens were positive for rejection. The transplanted kidney is in the left lower quadrant. (**b**) Intravenous contrast-enhanced CT in a patient with biopsy findings of rejection shows mild small bowel wall thickening (arrow) and no small bowel dilatation. (**c**) Noncontrast CT scan in a patient with biopsy findings of rejection shows marked small bowel wall thickening and dilatation. There is a marked low-attenuation submucosal edema such that the muscularis propria is mildly hyperattenuating on this noncontrast exam. (**d**) Intravenous contrast-enhanced CT in a child with a small bowel transplant and biopsy-proven rejection shows small bowel dilatation (arrows), fecalization of the intraluminal contents, and ascites

recipients, and those patients who have had splenectomy at highest risk for development of GVHD [19]. GVHD may affect the skin, bone marrow, liver, and native gastrointestinal tract. In acute GVHD, the mucosa of the gastrointestinal tract becomes denuded and replaced by highly vascularized granulation tissue. The CT findings of acute GVHD include mucosal hyperenhancement, submucosal edema, wall thickening, luminal dilatation, and engorgement of the vasa recta [20]. Chronically, the bowel may appear normal with no abnormalities or be narrow in caliber.

Infection

Sepsis is the leading cause of death in intestinal transplant recipients [21]. Central venous catheters are the major source of systemic infection and sepsis. Postoperative bacterial pneumonia, intra-abdominal abscesses, and wound infections are also common [22]. In patients with signs and symptoms of infection, CT scans of the chest, abdomen, and pelvis are used to simultaneously evaluate the lungs for findings of pneumonia and the abdomen and pelvis for potential sources of intra-abdominal infection. In the abdomen and pelvis, postoperative fluid and fluid collections are commonly seen in the early postoperative period. The findings of gas bubbles and an enhancing wall are signs that a fluid collection is an abscess. Often, these findings are absent, and percutaneous sampling may be required to determine if a collection is the source of infection (Fig. 7.9). Peritonitis may occur from anastomotic leaks with extensive intra-abdominal abscess. The findings of peritonitis include peritoneal thickening with irregular or nodular enhancement. Serosal enhancement and thickening of the bowel wall, loculated ascites, or fluid collections may also be present.

Infections isolated to the intestinal graft are diagnosed by mucosal biopsy. These include cytomegalovirus, adenovirus, and Epstein-Barr virus infections. The CT findings of isolated intestinal infections are not specific and overlap with the findings of rejection and normal [15]. The findings include normal thickness of the bowel wall, bowel wall thickening, and abnormal enhancement of the bowel wall producing the target pattern.

Vascular and Other Surgical Complications

Vascular complications are less common in combined liver and intestinal and multivisceral transplants because less dissection is required and the anastomoses are larger caliber with lower incidence of thrombosis and stenosis. The most serious

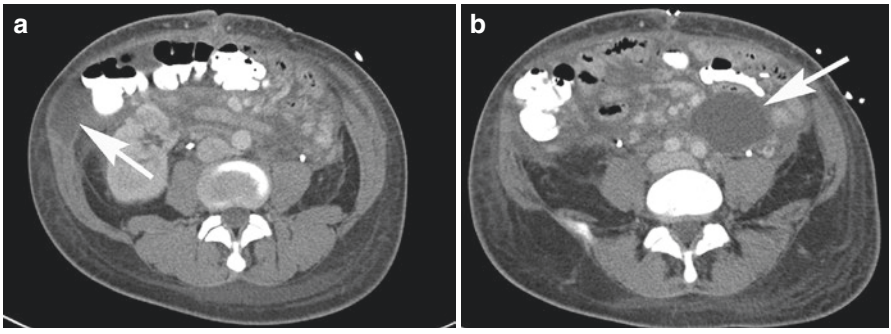

Fig. 7.9 Postoperative abscesses in a man who developed fevers during the postoperative period after an en bloc small bowel, colon, and pancreas transplant performed short bowel syndrome after surgery for a desmoid tumor of the small bowel mesentery. Intravenous contrast-enhanced CT scans show loculated fluid collection in the right anterior abdominal wall (arrow in **a**) and posterior to the intestinal graft in the left abdomen (arrow in **b**). The transplanted bowel is normal in caliber and wall thickness. Edema is present in the small bowel mesentery and subcutaneous fat

of all vascular complications following intestinal transplant is venous thrombosis. Ultrasound or contrast-enhanced CT or MRI may be used to evaluate the portal venous and mesenteric venous vasculature when there is clinical suspicion for venous thrombosis. Grayscale and color Doppler ultrasound may show intraluminal hypoechoic or mixed echotexture thrombus with diminished intrahepatic blood flow. In subacute and chronic thrombosis, collateral vessels reconstituting the portal vein may be seen. On CT, intraluminal thrombus will be seen. Arterial thrombosis, occlusion, or stenosis (Fig. 7.10) may also occur. CT is useful to assess the graft when there is venous or arterial compromise to evaluate for findings of ischemia and/or infarction such as increased thickness of the bowel wall, hypoattenuating wall edema, diminished enhancement, bowel dilatation, and pneumatosis. Hemorrhage and hematomas may be seen. These may be due to anticoagulation or complications of the anastomosis. Pseudoaneurysms are uncommon.

Complications occurring in other abdominal and intestinal surgeries may also be seen following intestinal transplantation. Anastomotic leaks, bowel obstruction, perforation, and fistula formation may occur. CT is the imaging modality of choice when these complications are suspected. Positive oral contrast should be administered for the assessment of postoperative complications, especially when an anastomotic leak or perforation is of clinical concern. Not only will extraluminal contrast establish the diagnosis of bowel leak or perforation but also aids in the delineation of the small bowel, which may be difficult to define in the early postoperative period when there is mesenteric edema and/or ascites or postoperative intra-abdominal fluid present.

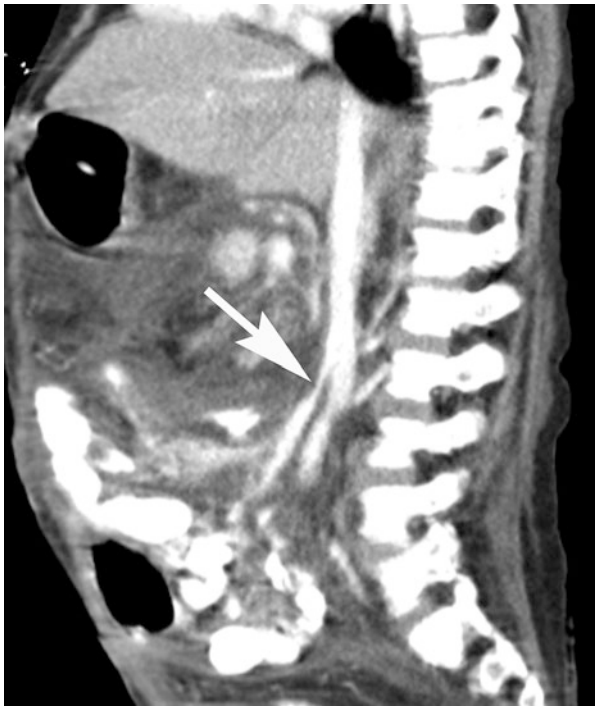

Fig. 7.10 Intravenous contrast-enhanced CT shows a stenosis of the origin of the aortic jump graft (arrow) anastomosis to the aorta. There were no findings of graft ischemia

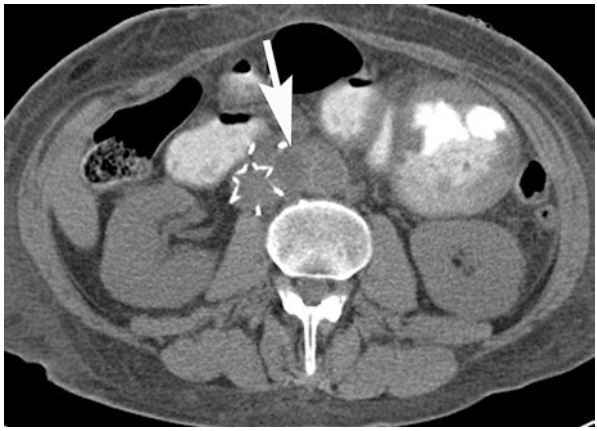

Fig. 7.11 Noncontrast CT scan shows enlarged, low-attenuation, and poorly defined lymph nodes in the aortocaval space (arrow) in a man who developed posttransplantation lymphoproliferative disorder following isolated intestinal transplantation for short bowel syndrome after abdominal trauma. An IVC filter is present

Posttransplantation Lymphoproliferative Disorder

Posttransplantation lymphoproliferative disorder (PTLD) is the most common malignancy occurring in intestinal transplant recipients. It is a serious complication that is seen in much higher incidences in intestinal transplant recipients compared to kidney and liver transplant recipients. The high incidence is likely related to the large amount of lymphoid tissue present in the intestine and the greater amount of immunosuppression required in these patients. The reported incidence is approximately 13% [23]. Children are at higher risk than adults. The development of PTLD is associated with Epstein-Barr virus in 95% of the cases [23, 24]. PTLD may arise at any site in the body and may be multifocal. Consequently, the CT findings that should raise suspicion for PTLD are enlarged lymph nodes (Fig. 7.11), which may be present anywhere in the body; focal masses in the lungs, liver, or spleen; or unexplained wall thickening of the transplanted intestine [14, 25].

Other Complications

Pancreaticobiliary complications are more common than previously reported, occurring in up to 17% of patients with either a liver-intestinal graft or multivisceral graft [26]. Many of these complications are similar to those seen in isolated liver transplants. They include ampullary stenosis, bile duct cast syndrome, bile duct stones, bile leaks, cholangitis, pancreatitis, and biliary or pancreatic duct fistula.

Conclusions

Intestinal transplantation is uncommonly performed. Radiology is important in the preoperative assessment of intestinal transplant candidates as well as the postoperative assessment of complications. Knowledge of the indications for intestinal

transplant is important in the preoperative radiologic assessment, and knowledge of surgical anatomy and postoperative complications is important in the postoperative evaluation of patients with suspected complications.

References

1. U.S. Department of Health and Human Services. Organ Procurement and Transplantation Network National Data [Web Page]. 2016. https://optn.transplant.hrsa.gov/data/view-data-reports/national-data/.
2. Smith JM, Skeans MA, Horslen SP, Edwards EB, Harper AM, Snyder JJ, et al. OPTN/SRTR 2013 Annual Data Report: intestine. Am J Transplant. 2015;15(Suppl 2):1–16.
3. Kappus M, Diamond S, Hurt RT, Martindale R. Intestinal failure: new definition and clinical implications. Curr Gastroenterol Rep. 2016;18(9):48.
4. Desai CS, Gruessner AC, Khan KM, Fishbein TM, Jie T, Rodriguez Rilo HL, et al. Isolated intestinal transplants vs. liver-intestinal transplants in adult patients in the United States: 22 yr of OPTN data. Clin Transplant. 2012;26(4):622–8.
5. Fishbein TM, Matsumoto CS. Intestinal replacement therapy: timing and indications for referral of patients to an intestinal rehabilitation and transplant program. Gastroenterology. 2006;130(2 Suppl 1):S147–51.
6. Sudan D, Rege A. Update on surgical therapies for intestinal failure. Curr Opin Organ Transplant. 2014;19(3):267–75.
7. Matsumoto CS, Kaufman SS, Fishbein TM. Inclusion of the colon in intestinal transplantation. Curr Opin Organ Transplant. 2011;16(3):312–5.
8. Desai CS, Khan KM, Girlanda R, Fishbein TM. Intestinal transplantation: a review. Indian J Gastroenterol. 2012;31(5):217–22.
9. Matsumoto CS, Fishbein TM. Modified multivisceral transplantation with splenopancreatic preservation. Transplantation. 2007;83(2):234–6.
10. Robinson JI, Spencer RW. Intestinal transplantation: the evaluation process. Prog Transplant. 2005;15(1):45–53.
11. Tzakis AG, Todo S, Starzl TE. Intestinal transplantation. Annu Rev Med. 1994;45:79–91.
12. Swerdlow DR, Trotter A, Girlanda R, Matsumoto C, Fenelly E. Computed tomography (CT) colonography with CT arteriography and venography for the workup of intestinal transplant candidates. Clin Transplant. 2013;27(1):126–31.
13. Bach DB, Levin MF, Vellet AD, Downey DB, Munk PL, Grant DR, et al. CT findings in patients with small-bowel transplants. AJR Am J Roentgenol. 1992;159(2):311–5.
14. Sandrasegaran K, Lall C, Ramaswamy R, Redelman R, Hoff S, Rajesh A, et al. Intestinal and multivisceral transplantation. Abdom Imaging. 2011;36(4):382–9.
15. Bazylewicz M, Chan CK, Allison SJ, Levy AD, editors. Small bowel transplantation: MDCT features of small bowel wall thickening with pathologic correlation. Radiologic Society of North America 99th Scientific Assembly and Annual Meeting, Chicago, 6 Dec 2013.
16. Fishbein TM, Florman S, Gondolesi G, Schiano T, LeLeiko N, Tschernia A, et al. Intestinal transplantation before and after the introduction of sirolimus. Transplantation. 2002;73(10):1538–42.
17. Quiros-Tejeira RE. Immunological complications beyond rejection after intestinal transplantation. Curr Opin Organ Transplant. 2012;17(3):268–72.
18. Unsinn KM, Koenigsrainer A, Rieger M, Czermak BV, Ellemunter H, Margreiter R, et al. Spectrum of imaging findings after intestinal, liver-intestinal, or multivisceral transplantation: part 2, posttransplantation complications. AJR Am J Roentgenol. 2004;183(5):1285–91.
19. Wu G, Selvaggi G, Nishida S, Moon J, Island E, Ruiz P, et al. Graft-versus-host disease after intestinal and multivisceral transplantation. Transplantation. 2011;91(2):219–24.

20. Schmit M, Bethge W, Beck R, Faul C, Claussen CD, Horger M. CT of gastrointestinal complications associated with hematopoietic stem cell transplantation. AJR Am J Roentgenol. 2008;190(3):712–9.
21. Andersen DA, Horslen S. An analysis of the long-term complications of intestine transplant recipients. Prog Transplant. 2004;14(4):277–82.
22. Oltean M, Herlenius G, Gabel M, Friman V, Olausson M. Infectious complications after multivisceral transplantation in adults. Transplant Proc. 2006;38(8):2683–5.
23. Abu-Elmagd KM, Mazariegos G, Costa G, Soltys K, Bond G, Sindhi R, et al. Lymphoproliferative disorders and de novo malignancies in intestinal and multivisceral recipients: improved outcomes with new outlooks. Transplantation. 2009;88(7):926–34.
24. Nassif S, Kaufman S, Vahdat S, Yazigi N, Kallakury B, Island E, et al. Clinicopathologic features of post-transplant lymphoproliferative disorders arising after pediatric small bowel transplant. Pediatr Transplant. 2013;17(8):765–73.
25. Pecchi A, De Santis M, Torricelli P, Romagnoli R, di Francesco F, Cautero N, et al. Radiologic imaging of the transplanted bowel. Abdom Imaging. 2005;30(5):548–63.
26. Borhani AA, Dasyam AK, Papachristou G, Furlan A, Almusa O, Abu-Elmagd K, et al. Radiologic features of pancreatic and biliary complications following composite visceral transplantation. Abdom Imaging. 2015;40(6):1961–70.

Chapter 8
Liver Transplant Interventions

Akemi Miller and Alexander Y. Kim

Introduction

Initial efforts at human liver transplantation in the early 1960s were marred by extremely poor postoperative survival, with the earliest organ recipients surviving for 0–23 days postoperatively [1]. Following improvements in surgical technique, the focus shifted from postoperative patient survival to survival of the graft, and efforts were concentrated on optimizing antirejection regimens [2]. In the current era, patients undergoing liver transplantation have survival rates of 82%, 70%, and 65% at 1, 5, and 10 years, respectively [3]. Despite significant improvements in survival following liver transplantation, posttransplant complications are not uncommon, and image-guided interventional strategies have emerged as a reasonable alternative to open or laparoscopic reoperation in the management of many of these complications.

Postoperative complications following liver transplantation can be divided into three broad categories: arterial, venous, and nonvascular.

Arterial Complications

Hepatic Artery Thrombosis

Hepatic artery thrombosis (HAT) is the most common arterial complication following liver transplantation, historically affecting 2–12% of liver transplant recipients [4–7]. More recent studies suggest a drop in incidence to 3–5% [8]. HAT is a

A. Miller, M.D. · A. Y. Kim, M.D. (✉)
Division of Vascular and Interventional Radiology, Medstar Georgetown University Hospital, Washington, DC, USA
e-mail: alexander.y.kim@gunet.georgetown.edu

G. Fananapazir, R. Lamba (eds.), *Transplantation Imaging*,
https://doi.org/10.1007/978-3-319-75266-2_8

leading cause of graft loss, accounting for up to 53% of cases of liver graft failure and carrying a mortality rate of greater than 80% when untreated [9, 10]. Even with intervention, this complication is fatal in approximately 1/3 of affected recipients [11, 12]. Apart from inherent risks related to surgical technique (e.g., kinking at sites of anastomosis), risk factors for the development of HAT include donor age > 60 years, back-table arterial reconstruction, use of an arterial conduit, cytomegalovirus infection, donor death secondary to cerebrovascular accident, increased cold ischemia time, rejection, ABO blood group incompatibility, and primary sclerosing cholangitis [12–15]. HAT is subdivided into early and late forms, with early HAT typically defined as occurring within 30 days of transplantation. The distinction is an important one as the clinical presentation, urgency of intervention, and impact on graft outcome are different.

The incidence of early HAT in adults ranges from 2.6 to 9% [16]. Early HAT typically occurs prior to the development of any meaningful collateral arterial vasculature, although collateral vessels have been documented angiographically as early as 2 weeks following transplantation [11]. Collateral vessels are largely derived from the phrenic vessels and typically develop 2–4 months following transplantation [16, 17], which may explain the less severe clinical course of late HAT. Early loss of arterial flow to the graft can result in acute fulminant hepatic failure, as well as necrosis of the arterial-dependent biliary ducts and uncontrollable sepsis in the immunocompromised patient [18].

The incidence of late HAT ranges from 1 to 25% [19]. Late HAT typically presents with biliary tract complications with or without fever [4] with a median time to presentation of 6 months [19].

The standard treatment of HAT is liver retransplantation; however, a shortage of available donor organs as well as the associated high mortality with retransplantation has led to a pursuit of alternate treatment options, including surgical thrombectomy (with or without anastomotic revision) and endovascular intervention in the form of intra-arterial thrombolysis (IAT), percutaneous transluminal angioplasty (PTA), and PTA with stent placement [8]. In a study by Duffy et al. [13] evaluating outcomes of vascular complications in 4200 liver transplant recipients, 65% of patients with HAT underwent surgical exploration and thrombectomy with or without anastomotic revision, 17% required retransplantation, and 3% underwent catheter-directed thrombolysis. Despite attempts at revascularization, up to 75% of liver transplant recipients who develop HAT will ultimately require retransplantation [13].

Murata et al. [18] reviewed outcomes of 120 consecutive adult patients who underwent living donor liver transplant. A total of nine patients (7.5%) developed HAT and underwent endovascular treatment with an overall reported technical success rate of 78% (7/9 patients). Intra-arterial thrombolysis (IAT) alone was successful in one patient, six patients were treated with both IAT and percutaneous transluminal angioplasty (PTA), and two patients underwent IAT with PTA and stenting. The two patients failing endovascular management were observed and did not require further intervention. Complications included hepatic arterial rupture ($n = 1$) and arterioportal shunt formation ($n = 1$).

A review by Singhal et al. [20] examined 69 cases of endovascular treatment of HAT collected from 16 separate published studies. Thrombolysis was found to be successful in 68% of cases (47/69). Among the patients successfully treated with thrombolysis, 62% ($n = 29$) required further intervention in the form of PTA alone ($n = 4$), stent placement alone ($n = 20$), and PTA with stent placement ($n = 5$). The most common reported complication was hemorrhage ($n = 18$; 38%), with three cases proving fatal.

Failed endovascular intervention may also complicate subsequent surgical intervention (either in the form or revascularization/anastomotic revision or retransplant) in the early period due to possible catheter-related intimal injury to the artery [18] or at a later period due to the presence of stents at desired anastomotic sites [21].

Sheiner et al. [22] found that graft salvage outcomes were different among patients with HAT who were asymptomatic at time of presentation versus those who were symptomatic (elevated liver function tests, bile leak, sepsis): asymptomatic patients had a graft salvage rate of 81.8% vs. only 40% among those patients with symptomatic HAT. This difference in outcomes led the authors to conclude that attempts at emergent revascularization be reserved for patients with asymptomatic HAT, while those with symptomatic HAT should undergo retransplantation.

Hepatic Artery Stenosis

Unlike HAT, hepatic artery stenosis (HAS) has a more insidious presentation with more gradual graft dysfunction (Fig. 8.1) [23, 24]. The incidence of HAS ranges from 5 to 15% [25] and typically presents within 3 months of transplant. Risk factors for HAS are similar to those of HAT, with the added risk factor of intraoperative clamp injury [26]. An untreated stenosis can progress to HAT in more than half of the patients, and many stenoses are therefore diagnosed concurrently with HAT [13, 23, 27]. Historically, these lesions were treated surgically with resection of the stenotic segment and reanastomosis with or without the use of an aortic conduit graft, interposition vein/artery graft, or vein patch angioplasty [23]. Endovascular treatment with PTA with or without stent placement has since replaced surgical intervention as the treatment of choice for HAS, except in cases of early (≤7 days posttransplant) thrombosis or stenosis where surgical revascularization remains the standard of care [25]. PTA is successful in 85–100% of patients with HAS and has a 1-year reported patency rate ranging from 50 to 90% [13, 27–32].

In a series of 870 patients who underwent liver transplantation, a total of 30 patients (3.4%) developed critical HAS, defined as >50% luminal narrowing, and were treated with endovascular intervention [25]. Patients were not candidates for endovascular intervention within the first 21 days following transplant due to risk of arterial anastomotic rupture and hemorrhage; these patients were therefore managed with systemic anticoagulation and/or antiplatelet agents until 21 days postoperatively and underwent PTA at that time. PTA was successfully completed in 27/30 patients (90%), with 23 patients undergoing PTA with stent placement and 4

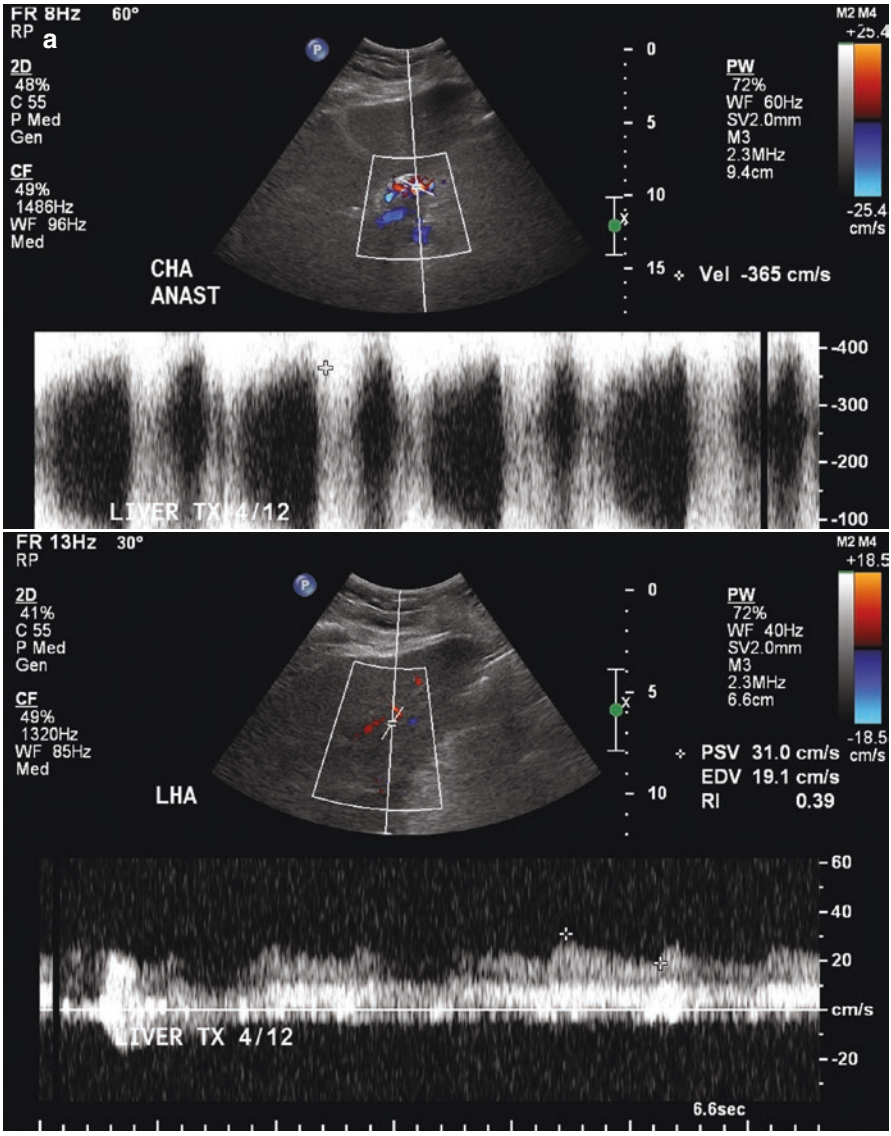

Fig. 8.1 Hepatic arterial stenosis: (**a**) Color doppler images of the transplant arterial vasculature demonstrating findings consistent with high-grade anastomotic stenosis. (**b**) Reconstructed CTA confirming the sonographic findings. (**c**) Pretreatment DSA of the high-grade stenosis. (**d**) Balloon angioplasty of the stenotic segment. (**e**) Post-angioplasty DSA demonstrating improved stenosis

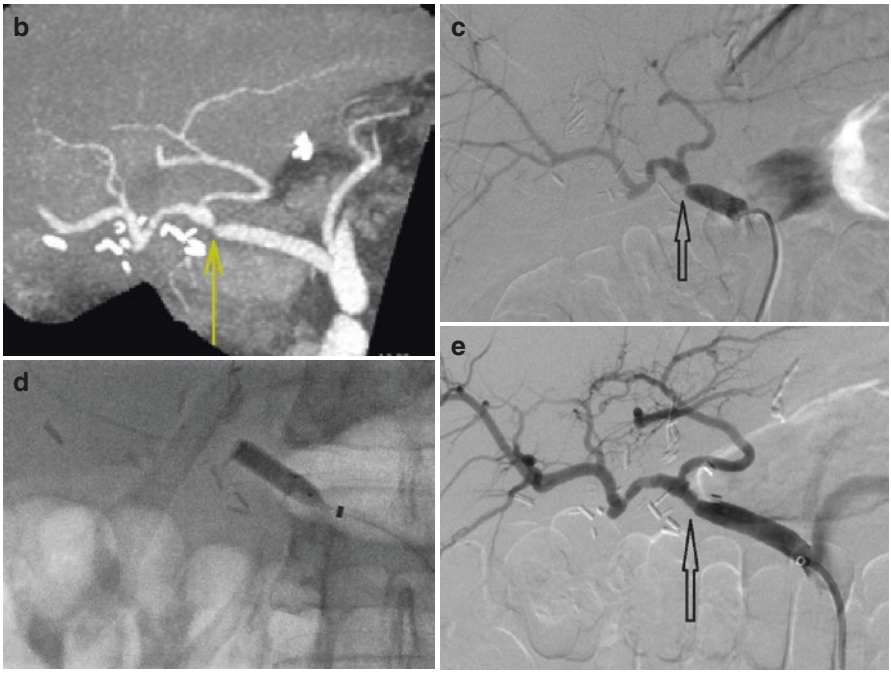

Fig. 8.1 (continued)

undergoing PTA alone. Failed intervention was secondary to an inaccessible hepatic artery in two patients and arterial dissection in one patient. A total of ten patients developed restenosis (33%)—four were restented, three were transplanted due to ischemic cholangitis, and three did not require further intervention. Eight patients were retransplanted following PTA, largely owing to symptomatic ischemic cholangitis (7/8 patients). At 1, 3, and 5 years, overall patency rates were 68%, 62.8%, and 62.8%, respectively.

A meta-analysis comparing treatment outcomes in patients with HAS undergoing either stent placement or PTA alone found similar procedural success rates (98% vs. 89%) and rates of arterial patency at ≥6 months (68% vs. 76%) [31]. There were no significant differences in complication rate or requirement for re-intervention or retransplantation.

Hepatic Artery Pseudoaneurysm

Hepatic artery pseudoaneurysms (HAP) are rare, occurring in 1–2% of liver transplant recipients (Fig. 8.2) [33]. HAP can be subclassified as extrahepatic and intrahepatic pseudoaneurysms. Historically, extrahepatic pseudoaneurysms were thought to be more spontaneous in nature, while iatrogenic pseudoaneurysms were localized to the intrahepatic hepatic arteries [33, 34].

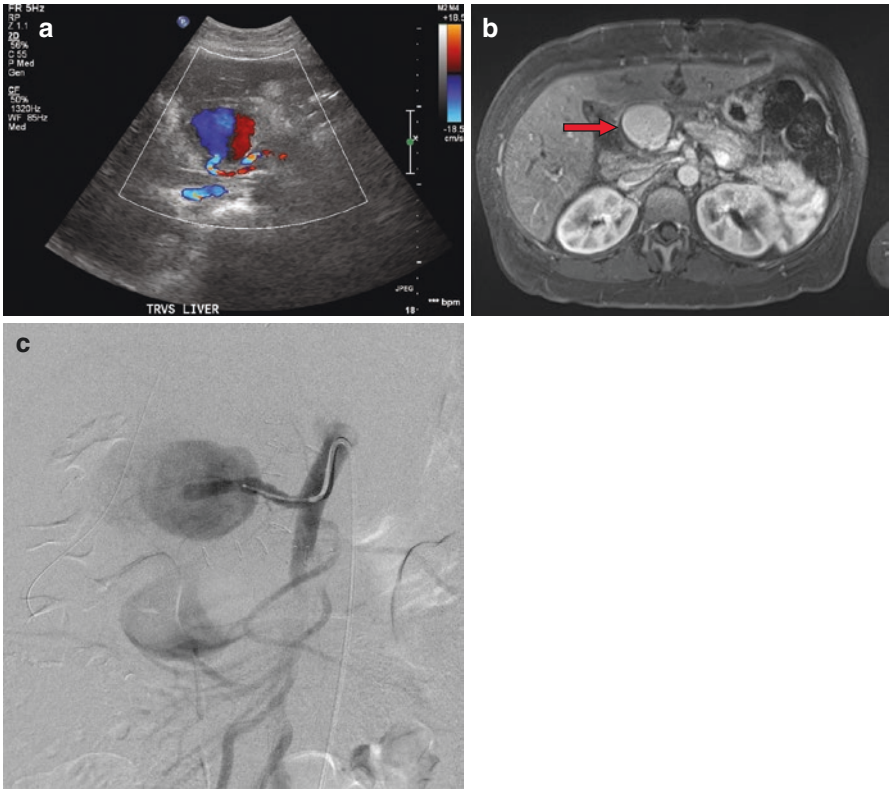

Fig. 8.2 Extrahepatic hepatic artery pseudoaneurysm: (**a**) Sonographic images demonstrating a "yin-yang" sign consistent with a pseudoaneurysm. (**b**) Post-contrast MRI shows the presence of an extrahepatic pseudoaneurysm. (**c**) DSA confirms the presence of the pseudoaneurysm

Extrahepatic pseudoaneurysms typically arise within 30–60 days posttransplant and are generally infectious (mycotic infection, postoperative infectious arteritis) or technical (dissection) in etiology [33, 35–37]. They have been reported to occur more frequently in patients with biliary-enteric anastomoses [33, 34]. Ruptured extrahepatic pseudoaneurysms typically present with hemodynamic instability (50–67%) or gastrointestinal bleeding and hemobilia (22–25%) [33, 38, 39]. Other nonspecific signs may include anemia, elevated liver function tests, and infection/sepsis.

Intrahepatic pseudoaneurysms are often iatrogenic in nature and arise either during or shortly after an interventional procedure (e.g., PTAs, percutaneous transhepatic cholangiography, biopsy) within the intrahepatic hepatic arteries [5, 6, 40]. With the advent of minimally invasive management of both HAT and HAS, an increasing number of extrahepatic pseudoaneurysms may now be classified as iatrogenic in etiology [41].

The standard treatment of HAP is surgical resection with arterial reconstruction, particularly in cases of mycotic infection where interventional efforts may provide a nidus for continued infection [42]. HAPs may be asymptomatic or can rupture into

the GI tract, peritoneum, or biliary system. In cases of active hemorrhage, emergent occlusion of the hepatic artery may be necessary. For non-mycotic extrahepatic HAPs, coil embolization and stent-graft placement are potential endovascular treatment options [5, 6, 33, 40]. In cases of extremely tortuous arterial vasculature, direct percutaneous access may be necessary for embolization and thrombin injection [37].

In a retrospective study by Saad et al. [41], a total of 20 pseudoaneurysms were identified out of 1857 liver transplants (1.1%). Of these 20, 9 were spontaneous pseudoaneurysms (extrahepatic), while the remaining 11 were iatrogenic (intrahepatic; 4 secondary to angioplasty and 7 after biliary intervention). Endovascular management was attempted in 12 patients with a technical success rate of 83% (10/12). In one patient, attempted selective embolization of the HAP resulted in thrombosis of the entire hepatic artery. Unfortunately, despite the relatively high technical success rate, the overall 1-, 3-, and 6-month graft survival rates were 70%, 40%, and 35%, respectively.

Pseudoaneurysms typically present within the first 60 days after transplant, prior to the development of significant arterial collateral vessels, when preserved arterial flow to the graft is critical [34, 36, 39, 43–45]. Incidentally discovered HAPs must be treated due to the high risk of rupture and resultant life-threatening bleeding [35]. During active hemorrhage, occlusion of the hepatic artery, either with surgical ligation or via endovascular intervention, may be necessary, with resultant graft loss [33, 35]. Independent of intervention, HAP confers a high rate of retransplantation (33–45%) and mortality (33–78%) [33, 35, 38, 39, 45–47]. Although surgical resection/revision remains the mainstay for definitive management of HAP, there may be a role for endovascular management in stabilizing or temporizing unstable patients either as a bridge to retransplantation or to allow them to undergo definitive treatment in a more elective setting [41].

Splenic Artery Steal Syndrome

In patients with longstanding liver disease and portal hypertension, splanchnic blood flow can preferentially shunt to regions of lower resistance, namely, the splenic vascular bed, with subsequent development of splenomegaly and enlargement of the splenic artery. When the degree of blood flow shunted away from the high-resistance liver parenchyma becomes clinically significant, this is termed "splenic artery steal syndrome (SASS)" and may result in hepatic failure and/or biliary injury. The diversion of blood flow away from the hepatic vascular bed can persist even after liver transplantation and may even be further augmented by graft injury, rejection, or hepatitis [48]. Proposed treatment options include splenectomy, splenic artery ligation/embolization, or the use of an interposition graft between the common hepatic artery and aorta to drive blood flow back toward the liver [49].

In a series of 350 patients who underwent orthotopic liver transplantation, Uflacker et al. [48] reported a total of 11 patients with liver ischemia secondary to SASS (3.2%). All 11 patients were treated with splenic artery coil embolization, and all demonstrated improvement in both LFTs and clinical parameters within 24 h.

One patient went on to develop hepatic artery thrombosis 24 h after embolization and required surgical intervention with an interposition graft following unsuccessful hepatic artery recanalization.

A larger retrospective series by Nüssler et al. [50] included 1250 consecutive patients who underwent orthotopic liver transplantation and reported a total of 69 cases (5.9%) of SASS via the splenic or gastroduodenal artery. Twenty-five patients were classified as having SASS prior to undergoing liver transplantation, while the remaining 44 patients were diagnosed after transplant. Of the 69 total patients with SASS, 18 were treated with splenectomy, 29 with coil embolization of the splenic or gastroduodenal arteries, and 9 with splenic artery banding.

The highest complication rates were observed in patients diagnosed with SASS after liver transplantation who were subsequently treated with coil embolization. Half of these patients developed local or systemic septic complications, 8 required secondary splenectomy, 7 required retransplantation, and 5 of the 29 patients who underwent coil embolization died (four from graft failure and one from sepsis and multiorgan failure). This high complication rate was attributed to distal placement of embolization coils in the first 15 patients with resultant splenic infarction and abscess. No complications were reported after more proximal placement of embolization coils.

Of the patients treated with splenectomy ($n = 18$), two patients died from biliary complications despite retransplantation. No complications were reported in the remaining 16 patients. Patients treated with splenic artery banding demonstrated normalization of graft perfusion without any reported associated complications.

Thirteen patients had mild symptoms of SASS and were untreated; however, three of these patients subsequently required retransplantation for biliary ischemia.

Technical Management of Arterial Complications

Hepatic Angiography

Initial angiograms are usually performed through a standard trans-femoral approach, although a trans-brachial or trans-radial approach can also be used. A 5-Fr catheter such as a C-2 Glidecath (Terumo, Tokyo, Japan) is used to select the celiac axis. Initial digital subtraction angiograms (DSA) are performed. Further DSA images may be obtained in various obliquities depending on patient anatomy. A cone-beam computed tomography (CBCT) may be of benefit to better identify sites of potential pathology.

Arterial Thrombolysis

If HAT is identified during initial angiography, mechanical and/or pharmacologic thrombolysis can be performed. Depending on the size of the occluded vessel, a 2.4- or 2.8-Fr microcatheter or a 4- or 5-Fr catheter can be advanced over a 0.018″

or 0.035″ guidewire, respectively, into the thrombus. Angiograms performed from this point may allow for evaluation of the extent of the thrombus.

Mechanical thrombolysis can be performed using various techniques including balloon maceration or suction thrombectomy. Pharmacologic thrombolysis is often performed in concert with mechanical thrombolysis. A multi-sidehole infusion catheter is positioned in the thrombus with infusion of a thrombolytic agent such as recombinant tissue plasminogen activator (r-tPA, Alteplase; Genentech, San Francisco, CA) over 12–48 h. Alteplase is infused at a rate of 0.5–1.0 μg/h often in conjunction with a basal rate (250–500 U) of heparin delivered through the sheath. Patients are often admitted to a monitored unit for serial neurologic evaluation. Serial lab values including fibrinogen, PTT and PT/INR, and hemoglobin are also assessed in regular intervals.

Arterial Angioplasty

A long vascular sheath such as a Flexor Ansel Guiding Sheath (Cook Medical, Bloomington, IN) is introduced over a 0.035″ or 0.038″ wire and seated at the celiac artery origin to provide additional support for tracking of an angioplasty balloon. The sheath is sized to accommodate the angioplasty balloon, usually 6- to 8-Fr in size. Initial angiograms can be used to determine the appropriate size of the balloon for angioplasty. Intravenous heparin (3000–5000 U bolus or 50–80 U/kg) should be delivered prior to crossing the HAS/HAT. HAS can be crossed with a 0.035″ hydrophilic guidewire such as a Glidewire (Terumo, Tokyo, Japan) or a 0.010–0.018″ microwire. An over-the-wire or monorail balloon system can be used for angioplasty once the HAS is crossed. Often, serial upsizing of the balloon is performed to reduce potential risks of arterial perforation. If suboptimal results are seen following balloon angioplasty, a scoring or cutting balloon may be utilized followed by a high-pressure balloon. These balloons should be used with caution as they may confer a higher rupture rate.

Arterial Stenting

For inadequate results following angioplasty, or complications such as vessel rupture, a stent may be placed. Given the relative rigidity of stents, a guide catheter should be utilized for delivery. If possible, the guide catheter should be advanced into the common hepatic artery to provide additional support during stent delivery and placement. Bare metal or covered stents can be utilized for persistent HAS; covered stents should be used for pseudoaneurysm or rupture. Self-expanding stents may be utilized for HAS but many prefer to use balloon-mounted stents for more accurate positioning. If a self-expanding stent is used, the stent should be upsized

10–20% above the size of the treatment vessel. Although practice varies, patients are routinely maintained on antiplatelet agents post-stent placement, especially for a covered stent.

Splenic Artery Embolization

Splenic artery embolization is performed after a standard angiogram to delineate the splenic and hepatic arteries. The splenic artery is subselected with a 3–5 Fr catheter. After sizing the vessel, embolization can be performed in the proximal splenic artery. Fibered coils are most often utilized for this purpose; however, vascular plugs can also be used. Care should be taken to perform embolization in the proximal splenic artery as distal embolization can lead to increased complications such as splenic infarction and infection.

Venous Complications

Portal Vein Thrombosis

The incidence of posttransplant portal vein thrombosis (PVT) ranges from 3 to 10.6% and occurs more frequently in pediatric population as well as in recipients with pre-existing portal hypertension, hypoplastic portal veins, donor-recipient vessel size mismatch, graft edema, significant portosystemic collaterals, prior treatment for portal hypertension (e.g., TIPS), intimal injury at time of surgery, and technical problems with the anastomosis (e.g., kinking/twisting, stenosis) [13, 51–55]. The presence of pre-transplant PVT has also historically been associated with a higher incidence of posttransplant PVT and patients with intrahepatic extension of PVT were previously ineligible for transplant [56]. The data supporting the exclusion of these patients is inconsistent, however, with one published report citing no significantly increased risk of posttransplant portal vein rethrombosis relative to controls [57] and others reporting a highly variable incidence of posttransplant rethrombosis ranging from as low as 5% to as high as 40% in some series [56, 58, 59]. Sharma et al. [60] demonstrated that patients with pre-existing extensive PVT ($n = 78$) had a significantly higher rate of non-thrombosis-related graft failure (9.0% vs. 1.3%) and retransplantation (17.9% vs. 7.7%) when compared with controls ($n = 78$). More recently, the decision to offer liver transplant to this patient population has been left to the discretion of the transplant surgical team [61].

PVT typically presents within the first month following liver transplantation (“early”), but may present later (“late”). PVT manifests clinically with symptoms of portal hypertension (e.g., ascites, splenomegaly, variceal bleeding) and with elevation of liver enzymes [21, 62]. Early PVT has been associated with a 100% rate of

graft loss [62]. Endovascular treatment options include catheter-directed thrombolysis (via percutaneous or transcatheter approach) followed by angioplasty with or without stent placement and TIPS creation [8, 62].

Limited data is available on long-term patency rates following interventional treatment of PVT; however, data is available on long-term patency rates for angioplasty with or without stent placement for portal vein stenosis and will be discussed in the following section.

For patients who are not candidates for endovascular intervention, surgical thrombectomy, anastomotic revision, or retransplantation may be necessary [5, 6, 40, 63].

Portal Vein Stenosis

Portal vein stenosis (PVS) affects approximately 5% of liver transplants and almost always occurs at the site of anastomosis [41, 62]. The majority present more than 6 months after liver transplant and manifest clinically with symptoms of portal hypertension (including ascites, splenomegaly) and may progress to PVT without treatment [8, 21, 42]. PVS is more common with split grafts, especially pediatric split grafts where the incidence has been reported to be as high as 27% [62, 64–66], and is attributed to the relative size mismatch between the recipient portal vein and the graft portal vein. Prior splenectomy has also been associated with a fivefold higher rate of PVS [65].

PVS is treated with balloon angioplasty with technical success rates ranging from 36 to 71% at 2–3 years [62, 67]. In cases of concomitant portal vein thrombus, thrombolysis may be performed for 12–48 h prior to angioplasty. If angioplasty is unsuccessful (pressure gradient >5 mmHg across the stenosis), or if there is recoil stenosis or residual stenosis greater than 30%, then a stent may be placed [8] with long-term patency rates reported to be nearly 100% at 3–5 years [62, 68] (Fig. 8.3).

Hepatic Venous Outflow Stenosis and Thrombosis

Venous outflow stenosis or occlusion involves the hepatic veins (HV) or inferior vena cava (IVC) at rates of 4–5% and 1%, respectively [69, 70]. It is more commonly seen in livers that are transplanted in piggyback fashion [71]. Patients with Suprahepatic IVC stenosis may present with ascites, pleural effusion, and/or Budd-Chiari-type symptoms, while stenoses involving the infrahepatic IVC manifest with lower extremity edema. Outflow stenosis or obstruction of the hepatic veins, on the other hand, results in vascular engorgement and passive congestion of the transplant liver. Early complications are usually related to technical issues during

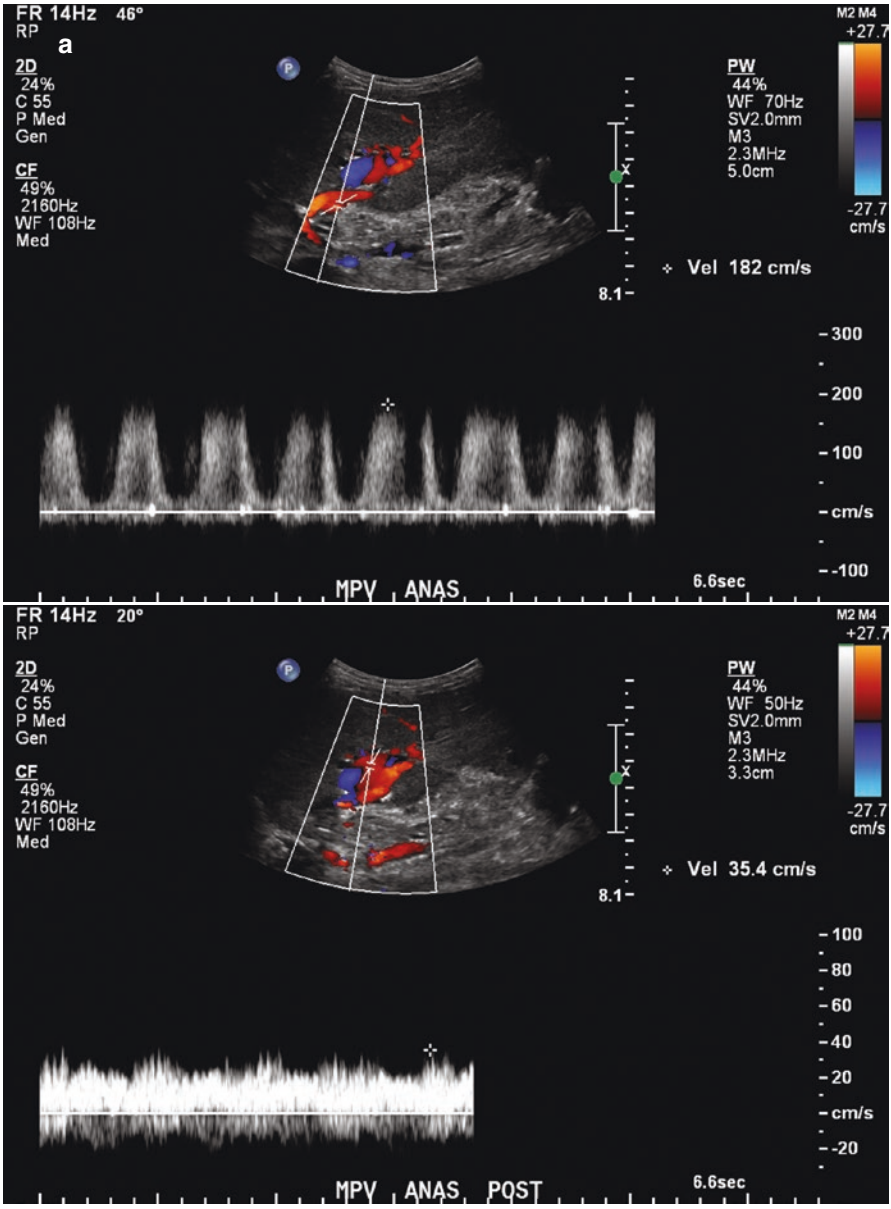

Fig. 8.3 Portal vein stenosis: (**a**) ultrasound demonstrates elevated velocities at the portal vein anastomosis. (**b**) Digital subtraction venography (DSV) of the left portal vein demonstrates stenosis of the main portal vein at the anastomosis (arrow). (**c**) Balloon angioplasty of the portal vein stenosis. (**d**) Post-venoplasty DSV demonstrates marked improvement of the stenosis

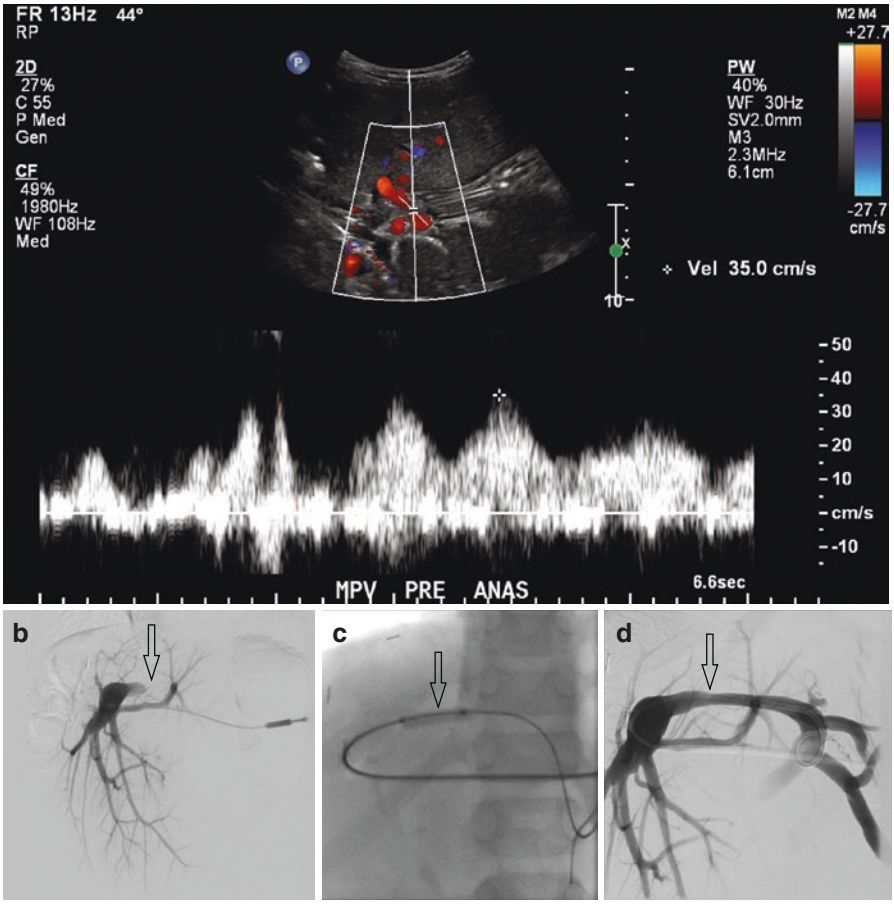

Fig. 8.3 (continued)

transplantation, while late complications are more often attributed to intimal hyperplasia and/or fibrosis at the anastomosis [72] (Fig. 8.4).

The treatment of venous outflow stenosis or thrombosis is similar to PVT/PVS and includes thrombolysis (12–48 h prior to angioplasty, if applicable) and balloon angioplasty with or without stent placement depending on the degree of residual stenosis following balloon dilation [8]. Technical success is defined as a decrease in the trans-anastomotic gradient to less than 3–5 mmHg [72, 73] for both the IVC and HV. The reported patency rate following HV angioplasty is 60% at 1 year, with an increase to nearly 100% with assisted angioplasty [74]. For IVC stenosis/occlusion, patency rates are only 40% at 1 year with angioplasty alone, with an increase to 91% following stent placement [72, 73, 75]. Due to the inferior patency rates with

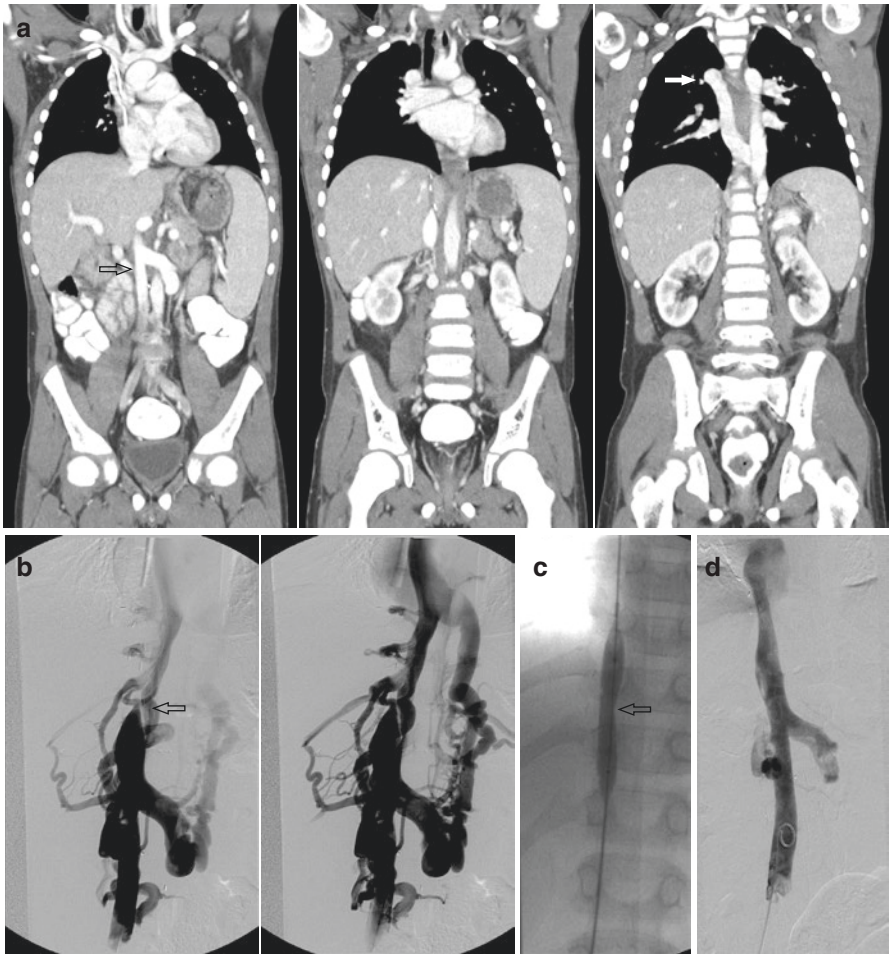

Fig. 8.4 IVC stenosis: (**a**) CT venogram demonstrates a high-grade stenosis of the intrahepatic IVC. (**b**) Conventional venacavagram demonstrates complete occlusion of the IVC and development of extensive collateral veins. (**c**) Venoplasty of the stenotic segment. (**d**) Post-venoplasty image demonstrates no residual stenosis or collateral venous flow

angioplasty alone, primary stenting is recommended for treatment of both HV and IVC stenosis/occlusion [8].

Portal Vein Thrombolysis/Venoplasty

Direct portal vein access is obtained with an 18 or 21 gauge needle under direct sonographic guidance. A trans-splenic route may be used if portal access cannot be obtained due to thrombus. A 0.035″ guidewire is advanced (through a transition set if a 21 gauge needle is used). A 6–8 Fr sheath is advanced over the guidewire. For thrombolysis, a multi-sidehole infusion catheter can be placed to perform a prolonged thrombolysis as previously described. For portal vein stenosis, an angled 5-Fr catheter is advanced through the sheath and, along with a hydrophilic wire, is traversed through the stenotic lesion. The 5 Fr catheter can be exchanged for a pigtail catheter to perform a direct portal venogram and to measure the portal venous pressure gradient. After appropriate sizing of the vessel, a prolonged balloon venoplasty is performed. Intravenous bolus of heparin may be delivered prior to venoplasty. For stenosis that is resistant to balloon venoplasty, an intraluminal stent can be placed as described in the arterial intervention section.

Transjugular Intrahepatic Portal-Systemic Shunt (TIPS) Placement

A TIPS shunt may be created to augment portal venous flow prior to thrombolysis. After obtaining jugular access, a 9 Fr sheath is advanced into the SVC. An angled 5 Fr catheter is used to select the right hepatic vein. Over a stiff wire, a TIPS access needle such as the Colapinto needle (Cook Medical, Bloomington, IN) is advanced. The needle is advanced anteriorly in attempt to select a branch of the portal vein. A partially contrast-filled syringe is attached to the back of the needle, and the needle is retracted while negative syringe pressure is applied. Once blood is aspirated, contrast is injected to confirm positioning of the needle within the portal vein. A wire is advanced through the needle into the portal venous system, and the needle is exchanged for a marking pigtail catheter. Here, direct portal venous pressures are obtained and the portal-systemic pressure gradient is calculated. Simultaneous venograms are performed through the sheath (positioned in the hepatic vein) and the pigtail catheter to measure for the appropriate stent length. The liver tract is balloon dilated—we prefer with an 8 mm diameter balloon—followed by stent deployment. A partially covered stent (Viatorr, Gore Medical, Flagstaff, AZ) is preferred due to superior patency rates over bare metal stents. The transjugular route through the TIPS can then be used to position the multi-sidehole catheter in the portal vein thrombus for thrombolysis.

Nonvascular Complications

Biliary Stricture (Anastomotic and Non-anastomotic)

The overall incidence of biliary stricture following liver transplantation is approximately 13%, as reported by a recent large meta-analysis including 14,000 patients [76]. Symptoms of biliary stricture include jaundice, abdominal pain, cholangitis, and increased liver function tests; some patients, however, may be asymptomatic [8]. Magnetic resonance cholangio-pancreatography (MRCP) can aid in the diagnosis of biliary stricture, as well as delineate the affected areas within the biliary system. Owing to the reliance of the biliary system on hepatic arterial blood supply, patients with known or suspected biliary stricture(s) should be further evaluated for arterial complications with either Doppler ultrasound or CT angiography.

The majority (75%) of biliary strictures occur at the anastomosis and may be attributed to surgical error or technique (e.g., anastomotic breakdown, local tissue ischemia, fibrosis) [77–79]. Patients with early postoperative bile leak have also been shown to be at increased risk for developing anastomotic stricture [80]. Non-anastomotic strictures occur in the setting of graft arterial compromise (hepatic artery thrombosis/stenosis) or other ischemic cholangiopathy (e.g., prolonged cold ischemia time) [81] and are often hilar in location, although they may be present intrahepatically in a diffuse manner.

Endoscopic retrograde cholangio-pancreatography (ERCP) is often attempted initially with cholangioplasty and stent placement [8]. Although treatment success rates can be as high as 90%, multiple treatment sessions are generally needed [77, 78, 82]. For patients with endoscopically inaccessible biliary systems, e.g., those with biliary-enteric anastomoses, percutaneous intervention with transhepatic biliary drain placement and cholangioplasty may be performed. Similar to ERCP intervention, sequential dilatation with or without concomitant catheter drainage is necessary for achieving the best clinical outcome. Patency rates have been reported to be close to 90% at 5 years following transplantation [83, 84] in patients amenable to percutaneous intervention. For the small subset of patients who cannot be managed endoscopically or via percutaneous methods, surgical revision of the anastomosis may be necessary.

Regarding patients with non-anastomotic strictures, treatment success is dependent on the number, location, and severity of strictures [81], with extrahepatic strictures being more likely to respond to therapy. Patients who fail treatment or who develop secondary biliary cirrhosis, recurrent cholangitis, or progressive cholestasis may require retransplantation.

Biliary Leak

Bile leaks have been reported in up to 25% of patients undergoing liver transplantation and can be classified as either early (within 4 weeks of transplant) or late (more than 4 weeks after transplant) [80, 85–87]. They generally occur at the anastomosis and may be secondary to T-tube removal, ischemia, or downstream obstruction (including sphincter of Oddi dysfunction) [88] or can occur at the cystic duct stump or along the cut edge of the graft in living donor liver transplant [89]. Patients with bile leak typically present with abdominal pain, fever, and signs of peritonitis, although these symptoms may be masked by corticosteroid administration.

Biliary leaks, including non-anastomotic leaks and communicating bilomas, may be successfully treated with diversion, either via ERCP with sphincterotomy and stent placement or with percutaneous transhepatic cholangiography and stent placement in patients not amenable to ERCP due to anatomic considerations. These interventions have been reported to be successful in 85–100% of cases [90].

Non-communicating bilomas may be treated with antibiotics with or without accompanying percutaneous drainage [76, 77]. Finally, biliary leaks occurring secondary to ischemia are more difficult to treat as the underlying cause may not be amenable to endoscopic or percutaneous intervention; in these cases, surgical intervention may be necessary for definitive management [80].

Percutaneous Transhepatic Cholangiogram (PTC) and Cholangioplasty

Pre-procedural antibiotics should be administered to reduce the risk of cholangitis. PTC can be performed through the left or the right lobe of the liver. Direct access to the biliary tree can be obtained with a 21 gauge needle under sonographic guidance. If the bile duct is not visible, the needle can be advanced under fluoroscopic guidance especially if accessing the right liver lobe. For a right liver lobe access, the

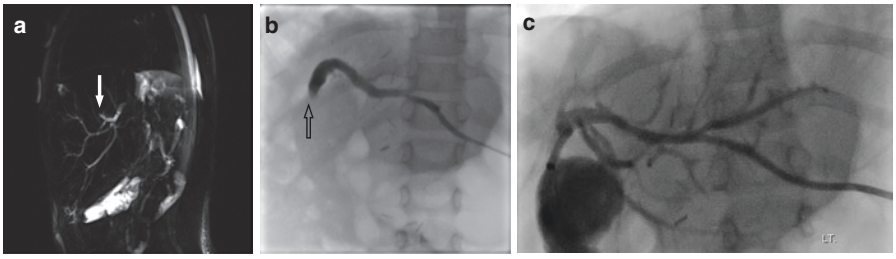

Fig. 8.5 Bile duct stricture: (**a**) MRCP demonstrating bile duct stricture with more proximal dilatation of the intrahepatic bile duct. (**b**) This finding was confirmed on PTC. (**c**) Biliary drain placed for decompression and dilation of stricture with contrast flowing through the bile duct into the duodenum

access site should be below the tenth intercostal space and anterior to the mid-axillary line to reduce the risk of pneumothorax. The needle is then slowly retracted with contrast administration under fluoroscopic guidance to demonstrate filling of the biliary tree. Once the needle tip is confirmed to be within the biliary tree, a 0.018″ wire is advanced into the biliary system. A transition set is then advanced over the wire. We prefer to perform a complete cholangiogram through the outer catheter of the transition set to assess areas of stricture or leak. A combination of an angled catheter and hydrophilic wire can be used to cross areas of stricture or leak. For lesions which are difficult to traverse, an external drain may be placed for decompression with a reattempt at crossing the lesion in 1–2 weeks. Once the stricture is crossed, an internal/external biliary drain is placed (Fig. 8.5).

For bile leaks, repeat cholangiograms may be performed every 6–12 weeks to assess for sealing of the leak. For biliary stenosis, serial cholangioplasties may be performed every 4–6 weeks. With each cholangioplasty, the drain may be exchanged for a larger diameter catheter. This may be a prolonged process, and patients should expect to have a drain in place for weeks to months. Once there is evidence of resolution of the stricture, the internal/external biliary drain is exchanged for an external biliary drain. The patient is then reevaluated in 1–2 weeks to ensure resolution of the stricture at which point the drain may be removed.

References

1. Starzl TE, Iwatsuki S, Van Thiel DH, Carlton Gartner J, Zitelli B, Malatack J, et al. Evolution of liver transplantation. Hepatology. 1982;2:614–36.
2. Starzl TE, Klintmalm GB, Porter K, Iwatsuki S, Schroeter G. Liver transplantation with use of cyclosporin a and prednisone. N Engl J Med. 1981;305:266–9.
3. Agopian VG, Petrowsky H, Kaldas FM, Zarrinpar A, Farmer DG, Yersiz H, et al. The evolution of liver transplantation during 3 decades: analysis of 5347 consecutive liver transplants at a single center. Ann Surg. 2013;258:409–21.
4. Pareja E, Cortes M, Navarro R, Sanjuan F, López R, Mir J. Vascular complications after orthotopic liver transplantation: hepatic artery thrombosis. Transplant Proc. 2010;42(8):2970–2.
5. Bhargava P, Vaidya S, Dick AAS, Dighe M. Imaging of orthotopic liver transplantation: self-assessment module. Am J Roentgenol. 2011;196(3 Suppl):S35–8.
6. Singh AK, Nachiappan AC, Verma HA, Uppot RN, Blake MA, Saini S, et al. Postoperative imaging in liver transplantation: what radiologists should know. Radiographics. 2010;30:339.
7. Crossin JD, Muradali D, Wilson SR. US of liver transplants: normal and abnormal. Radiographics. 2003;23:1093.
8. Ingraham CR, Montenovo M. Interventional and surgical techniques in solid organ transplantation. Radiol Clin North Am. 2016;54(2):267–80.
9. Tzakis AG. The dearterialized liver graft. Semin Liver Dis. 1985;5(4):375–6.
10. Langnas AN, Marujo W, Stratta RJ, Wood RP, Li SJ, Shaw BW. Hepatic allograft rescue following arterial thrombosis. Role of urgent revascularization. Transplantation. 1991;51(1):86–90.
11. Wozney P, Zajko AB, Bron KM, Point S, Starzl TE. Vascular complications after liver transplantation: a 5-year experience. AJR Am J Roentgenol. 1986;147(4):657–63.
12. Bekker J, Ploem S, De Jong KP. Early hepatic artery thrombosis after liver transplantation: a systematic review of the incidence, outcome and risk factors. Am J Transplant. 2009;9(4):746–57.

13. Duffy JP, Hong JC, Farmer DG, Ghobrial RM, Yersiz H, Hiatt JR, et al. Vascular complications of orthotopic liver transplantation: experience in more than 4,200 patients. J Am Coll Surg. 2009;208(5):896–903.
14. López-Andújar R, Moya A, Montalvá E, Berenguer M, De Juan M, San Juan F, et al. Lessons learned from anatomic variants of the hepatic artery in 1,081 transplanted livers. Liver Transpl. 2007;13(10):1401–4.
15. Oh CK, Pelletier SJ, Sawyer RG, Dacus AR, McCullough CS, Pruett TL, et al. Uni- and multivariate analysis of risk factors for early and late hepatic artery thrombosis after liver transplantation. Transplantation. 2001;71(6):767–72.
16. Stange BJ, Glanemann M, Nuessler NC, Settmacher U, Steinmüller T, Neuhaus P. Hepatic artery thrombosis after adult liver transplantation. Liver Transpl. 2003;9(6):612–20.
17. Heffron TG, Pillen T, Welch D, Smallwood GA, Redd D, Romero R. Hepatic artery thrombosis in pediatric liver transplantation. Transplant Proc. 2003;35(4):1447–8.
18. Murata Y, Mizuno S, Kato H, Tanemura A, Kuriyama N, Azumi Y, et al. Technical feasibility and clinical outcomes of interventional endovascular treatment for hepatic artery thrombosis after living-donor liver transplantation. Transplant Proc. 2016;48:1142–8.
19. Gunsar F, Rolando N, Pastacaldi S, Patch D, Raimondo ML, Davidson B, et al. Late hepatic artery thrombosis after orthotopic liver transplantation. Liver Transpl. 2003;9(6):605–11.
20. Singhal A, Stokes K, Sebastian A, Wright HI, Kohli V. Endovascular treatment of hepatic artery thrombosis following liver transplantation. Transpl Int. 2010;23:245–56.
21. Amesur NB, Zajko AB. Interventional radiology in liver transplantation. Liver Transpl. 2006;12:330–51.
22. Sheiner PA, Varma CV, Guarrera JV, Cooper J, Garatti M, Emre S, et al. Selective revascularization of hepatic artery thromboses after liver transplantation improves patient and graft survival. Transplantation. 1997;64(9):1295–9.
23. Abbasoglu O, Levy MF, Vodapally MS, Goldstein RM, Husberg BS, Gonwa TA, et al. Hepatic artery stenosis after liver transplantation—incidence, presentation, treatment, and long term outcome. Transplantation. 1997;63:250–5.
24. Gordon S, Carmody A. Arterial complications after liver transplantation. Transplant. Liver. Philadelphia: Elsevier; 2005. p. 953–61.
25. Rajakunnu M, Awad S, Ciacio O, Pittau G, Adam R, Cunha A, et al. Intention-to-treat analysis of percutaneous endovascular treatment of hepatic artery stenosis after orthotopic liver transplantation. Liver Transpl. 2016;22:923–33.
26. Frongillo F, Lirosi MC, Nure E, Inchingolo R, Bianco G, Silvestrini N, et al. Diagnosis and management of hepatic artery complications after liver transplantation. Transplant Proc. 2015;47(7):2150–5.
27. Saad WEA, Davies MG, Sahler L, Lee DE, Patel NC, Kitanosono T, et al. Hepatic artery stenosis in liver transplant recipients: primary treatment with percutaneous transluminal angioplasty. J Vasc Interv Radiol. 2005;16(6):795–805.
28. Laštovičková J, Peregrin J. Percutaneous transluminal angioplasty of hepatic artery stenosis in patients after orthotopic liver transplantation: mid-term results. Cardiovasc Intervent Radiol. 2011;34(6):1165–71.
29. Maruzzelli L, Miraglia R, Caruso S, Milazzo M, Mamone G, Gruttadauria S, et al. Percutaneous endovascular treatment of hepatic artery stenosis in adult and pediatric patients after liver transplantation. Cardiovasc Intervent Radiol. 2010;33(6):1111–9.
30. Sommacale D, Aoyagi T, Dondero F, Sibert A, Bruno O, Fteriche S, et al. Repeat endovascular treatment of recurring hepatic artery stenoses in orthotopic liver transplantation. Transpl Int. 2013;26(6):608–15.
31. Rostambeigi N, Hunter D, Duval S, Chinnakotla S, Golzarian J. Stent placement versus angioplasty for hepatic artery stenosis after liver transplant: a meta-analysis of case series. Eur Radiol. 2013;23(5):1323–34.

32. Huang M, Shan H, Jiang Z, Li Z, Zhu K, Guan S, et al. The use of coronary stent in hepatic artery stenosis after orthotopic liver transplantation. Eur J Radiol. 2006;60(3):425–30.
33. Marshall MM, Muiesan P, Srinivasan P, Kane PA, Rela M, Heaton ND, et al. Hepatic artery pseudoaneurysms following liver transplantation: incidence, presenting features and management. Clin Radiol. 2001;56(7):579–87.
34. Saad WEA. Management of nonocclusive hepatic artery complications after liver transplantation. Tech Vasc Interv Radiol. 2007;10(3):221–32.
35. Álamo JM, Gómez MA, Tamayo MJ, Socas M, Valera Z, Robles JA, et al. Mycotic pseudoaneurysms after liver transplantation. Transplant Proc. 2005;37(3):1512–4.
36. Bonham C, Kapur S, Geller D, Fung J, Pinna A. Excision and immediate revascularization for hepatic artery pseudoaneurysm following liver transplantation. Transplant Proc. 1999; 31:443.
37. Patel JV, Weston MJ, Kessel DO, Prasad R, Toogood GJ, Robertson I. Hepatic artery pseudoaneurysm after liver transplantation: treatment with percutaneous thrombin injection. Transplantation. 2003;75(10):1755–7.
38. Fistouris J, Herlenius G, Bäckman L, Olausson M, Rizell M, Mjörnstedt L, et al. Pseudoaneurysm of the hepatic artery following liver transplantation. Transplant Proc. 2006;38(8):2679–82.
39. Leelaudomlipi S, Bramhall SR, Gunson BK, Candinas D, Buckels JAC, McMaster P, et al. Hepatic-artery aneurysm in adult liver transplantation. Transpl Int. 2003;16(4):257–61.
40. Caiado AHM, Blasbalg R, Marcelino ASZ, da Cunha Pinho M, Chammas MC, da Costa Leite C, et al. Complications of liver transplantation: multimodality imaging approach. Radiographics. 2007;27:1401.
41. Saad WEA. Liver transplant-related vascular disease. In: Dake M, Geshwind J-F, editors. Abrams angiography: interventional radiology. 3rd ed. Philadelphia: Lippincott Williams & Wilkins; 2012.
42. Baheti AD, Sanyal R, Heller MT, Bhargava P. Surgical techniques and imaging complications of liver transplant. Radiol Clin North Am. 2016;54(2):199–215.
43. Finley DS, Hinojosa MW, Paya M, Imagawa DK. Hepatic artery pseudoaneurysm: a report of seven cases and a review of the literature. Surg Today. 2005;35(7):543–7.
44. Lowell JA, Coopersmith CM, Shenoy S, Howard TK. Unusual presentations of nonmycotic hepatic artery pseudoaneurysms after liver transplantation. Liver Transpl Surg. 1999;5(3):200–3.
45. Stange B, Settmacher U, Glanemann M, Nuessler N, Bechstein W, Neuhaus P. Aneurysms of the hepatic artery after liver transplantation. Transplant Proc. 2000;32:533–4.
46. Houssin D, Ortega D, Richardson A, Ozier Y, Stephan H, Soffer M, et al. Mycotic aneurysm of the hepatic artery complicating human liver transplantation. Transplantation. 1988;46: 469–72.
47. Jones VS, Chennapragada MS, Lord DJE, Stormon M, Shun A. Post-liver transplant mycotic aneurysm of the hepatic artery. J Pediatr Surg. 2008;43(3):555–8.
48. Uflacker R, Selby JB, Chavin K, Rogers J, Baliga P. Transcatheter splenic artery occlusion for treatment of splenic artery steal syndrome after orthotopic liver transplantation. Cardiovasc Intervent Radiol. 2002;25(4):300–6.
49. De Carlis L, Sansalone C, Rondinara G, Belli L, Rimoldi P, Romani F, et al. Splenic artery steal syndrome after orthotopic liver transplantation: diagnosis and treatment. Transplant Proc. 1993;25:2594–6.
50. Nüssler NC, Settmacher U, Haase R, Stange B, Heise M, Neuhaus P. Diagnosis and treatment of arterial steal syndromes in liver transplant recipients. Liver Transpl. 2003;9(6):596–602.
51. Yerdel MA, Gunson B, Mirza D, Karayalçin K, Olliff S, Buckels J, et al. Portal vein thrombosis in adults undergoing liver transplantation: risk factors, screening, management, and outcome. Transplantation. 2000;69(9):1873–81.
52. Jia Y-P, Lu Q, Gong S, Ma B-Y, Wen X-R, Peng Y-L, et al. Postoperative complications in patients with portal vein thrombosis after liver transplantation: evaluation with Doppler ultrasonography. World J Gastroenterol. 2007;13(34):4636–40.

53. Ueda M, Egawa H, Ogawa K, Uryuhara K, Fujimoto Y, Kasahara M, et al. Portal vein complications in the long-term course after pediatric living donor liver transplantation. Transplant Proc. 2005;37(2):1138–40.
54. Woo DH, LaBerge JM, Gordon RL, Wilson MW, Kerlan RK. Management of portal venous complications after liver transplantation. Tech Vasc Interv Radiol. 2007;10(3):233–9.
55. Lladó L, Fabregat J, Castellote J, Ramos E, Torras J, Jorba R, et al. Management of portal vein thrombosis in liver transplantation: influence on morbidity and mortality. Clin Transplant. 2007;21(6):716–21.
56. Manzanet G, Sanjuán F, Orbis P, López R, Moya A, Juan M, et al. Liver transplantation in patients with portal vein thrombosis. Liver Transpl. 2001;7(2):125–31.
57. Enestvedt BK, Enestvedt CK, Diggs B, Orloff SL. Hypercoagulability in liver transplant recipients: does portal vein thrombosis predict postoperative thrombotic complications? Open Journal of Organ Transplant and Surgery. 2011;1:1–7.
58. Tao Y-F, Teng F, Wang Z-X, Guo W-Y, Shi X-M, Wang G-H, et al. Liver transplant recipients with portal vein thrombosis: a single center retrospective study. Hepatobiliary Pancreat Dis Int. 2009;8(1):34–9.
59. Gimeno FA, Calvo J, Loinaz C, Meneu JC, Pérez B, Gomez R, et al. Comparative analysis of the results of orthotopic liver transplantation in patients with and without portal vein thrombosis. Transplant Proc. 2005;37(9):3899–903.
60. Sharma R, Kashyap R, Jain A, Safadjou S, Graham M, Dwivedi AK, et al. Surgical complications following liver transplantation in patients with portal vein thrombosis—a single-center perspective. J Gastrointest Surg. 2010;14(3):520–7.
61. Feltracco P, Barbieri S, Cillo U, Zanus G, Senzolo M, Ori C. Perioperative thrombotic complications in liver transplantation. World J Gastroenterol. 2015;21(26):8004–13.
62. Saad WEA. Portal interventions in liver transplant recipients. Semin Intervent Radiol. 2012;29(2):99–104.
63. Quiroga S, Sebastià MC, Margarit C, Castells L, Boyé R, Alvarez-Castells A. Complications of orthotopic liver transplantation: spectrum of findings with helical CT. Radiographics. 2001;21:1085.
64. Lerut J, Tzakis AG, Bron K, Gordon RD, Iwatsuki S, Esquivel CO, et al. Complications of venous reconstruction in human orthotopic liver transplantation. Ann Surg. 1987;205(4):404–14.
65. Settmacher U, Nuessler N, Glanemann M, Haase R, Heise M, Bechstein W, et al. Venous complications after orthotopic liver transplantation. Clin Transplant. 2000;14:235–41.
66. Buell JF, Funaki B, Cronin DC, Yoshida A, Perlman MK, Lorenz J, et al. Long-term venous complications after full-size and segmental pediatric liver transplantation. Ann Surg. 2002;236(5):658–66.
67. Funaki B, Rosenblum JD, Leef JA, Zaleski GX, Farrell T, Lorenz J, et al. Percutaneous treatment of portal venous stenosis in children and adolescents with segmental hepatic transplants: long-term results. Radiology. 2000;215(1):147–51.
68. Ko GY, Sung KB, Yoon HK, Lee SG. Early posttransplantation portal vein stenosis following living donor liver transplantation: percutaneous transhepatic primary stent placement. Liver Transpl. 2007;13(4):530–6.
69. Brouwers MA, de Jong KP, Peeters PM, Bijleveld CM, Klompmaker IJ, Slooff MJ. Inferior vena cava obstruction after orthotopic liver transplantation. Clin Transplant. 1994;8(1):19–22.
70. Cheng YF, Chen CL, Huang TL, Chen TY, Chen YS, Wang CC, et al. Angioplasty treatment of hepatic vein stenosis in pediatric liver transplants: long-term results. Transpl Int. 2005;18(5):556–61.
71. Navarro F, Le Moine MC, Fabre JM, Belghiti J, Cherqui D, Adam R, et al. Specific vascular complications of orthotopic liver transplantation with preservation of the retrohepatic vena cava: review of 1361 cases. Transplantation. 1999;68(5):646–50.
72. Darcy MD. Management of venous outflow complications after liver transplantation. Tech Vasc Interv Radiol. 2007;10(3):240–5.

73. Wang SL, Sze DY, Busque S, Razavi MK, Kee ST, Frisoli JK, et al. Treatment of hepatic venous outflow obstruction after piggyback liver transplantation. Radiology. 2005;236(1):352–9.
74. Kubo T, Shibata T, Itoh K, Maetani Y, Isoda H, Hiraoka M, et al. Outcome of percutaneous transhepatic venoplasty for hepatic venous outflow obstruction after living donor liver transplantation. Radiology. 2006;239(1):285–90.
75. Weeks SM, Gerber DA, Jaques PF, Sandhu J, Johnson MW, Fair JH, et al. Primary Gianturco stent placement for inferior vena cava abnormalities following liver transplantation. J Vasc Interv Radiol. 2000;11(2 Pt 1):177–87.
76. Akamatsu N, Sugawara Y, Hashimoto D. Biliary reconstruction, its complications and management of biliary complications after adult liver transplantation: a systematic review of the incidence, risk factors and outcome. Transpl Int. 2011;24(4):379–92.
77. Atwal T, Pastrana M, Sandhu B. Post-liver transplant biliary complications. J Clin Exp Hepatol. 2012;2(1):81–5.
78. Kothary N, Patel AA, Shlansky-Goldberg RD. Interventional radiology: management of biliary complications of liver transplantation. Semin Intervent Radiol. 2004;21(4):297–308.
79. Verdonk RC, Buis CI, Porte RJ, van der Jagt EJ, Limburg AJ, van den Berg AP, et al. Anastomotic biliary strictures after liver transplantation: causes and consequences. Liver Transpl. 2006;12(5):726–35.
80. Londoño MC, Balderramo D, Cárdenas A. Management of biliary complications after orthotopic liver transplantation: the role of endoscopy. World J Gastroenterol. 2008;14(4):493–7.
81. Kochhar G, Parungao JM, Hanouneh IA, Parsi MA. Biliary complications following liver transplantation. World J Gastroenterol. 2013;19(19):2841–6.
82. Rerknimitr R, Sherman S, Fogel EL, Kalayci C, Lumeng L, Chalasani N, et al. Biliary tract complications after orthotopic liver transplantation with choledochocholedochostomy anastomosis: endoscopic findings and results of therapy. Gastrointest Endosc. 2002;55(2):224–31.
83. Sung RS, Campbell DA, Rudich SM, Punch JD, Shieck VL, Armstrong JM, et al. Long-term follow-up of percutaneous transhepatic balloon cholangioplasty in the management of biliary strictures after liver transplantation. Transplantation. 2004;77(1):110–5.
84. Roumilhac D, Poyet G, Sergent G, Declerck N, Karoui M, Mathurin P, et al. Long-term results of percutaneous management for anastomotic biliary stricture after orthotopic liver transplantation. Liver Transpl. 2003;9(4):394–400.
85. Thuluvath PJ, Pfau PR, Kimmey MB, Ginsberg GG. Biliary complications after liver transplantation: the role of endoscopy. Endoscopy. 2005;37(9):857–63.
86. Stratta RJ, Wood RP, Langnas AN, Hollins RR, Bruder KJ, Donovan JP, et al. Diagnosis and treatment of biliary tract complications after orthotopic liver transplantation. Surgery. 1989;106(4):675–83; discussion 683–4.
87. Greif F, Bronsther OL, Van Thiel DH, Casavilla A, Iwatsuki S, Tzakis A, et al. The incidence, timing, and management of biliary tract complications after orthotopic liver transplantation. Ann Surg. 1994;219(1):40–5.
88. Scanga AE, Kowdley KV. Management of biliary complications following orthotopic liver transplantation. Curr Gastroenterol Rep. 2007;9(1):31–8.
89. Macías-Gómez C, Dumonceau J-M. Endoscopic management of biliary complications after liver transplantation: an evidence-based review. World J Gastrointest Endosc. 2015;7(6):606–16.
90. Morelli J, Mulcahy HE, Willner IR, Cunningham JT, Draganov P. Long-term outcomes for patients with post-liver transplant anastomotic biliary strictures treated by endoscopic stent placement. Gastrointest Endosc. 2003;58(3):374–9.

Chapter 9
Renal Transplant Interventions

Catherine T. Vu, Brandon Doskocil, and Lucas Sheen

Introduction

Percutaneous interventional diagnostic and therapeutic techniques are commonly employed when post-renal transplantation complications develop. Postoperative complications are less than 10%, but when they do occur, they can have a significant impact on morbidity and mortality. In addition to routine surveillance biopsies, patients with graft dysfunction typically undergo percutaneous biopsy as a diagnostic tool. Advances in interventional radiology techniques to treat vascular and urologic issues have obviated the need for surgical revision. Vascular complications include arterial and venous stenosis, arterial and venous thrombosis, arteriovenous fistula, and pseudoaneurysm. Nonvascular complications consist of urologic issues such as ureteral obstruction, including ureteral strictures and stones, pyeloureteritis cystica, and perigraft fluid collections, including urinoma, hematoma, seroma, abscess, or lymphocele.

Renal Transplant Biopsy

Most cases of acute rejection and episodes of graft dysfunction occur in the first 2 months after transplantation. Serum creatinine levels and urine protein can be used to screen for changes in renal function. The serum creatinine level is also valuable as a prognostic

C. T. Vu, M.D. (✉)
University of California Davis, Sacramento, CA, USA
e-mail: catvu@ucdavis.edu

B. Doskocil, M.D.
Kaiser TPMG Sacramento, Sacramento, CA, USA
e-mail: Brandon.J.Doskocil@kp.org

L. Sheen, M.D.
Kaiser TPMG Central Valley, Modesto, CA, USA
e-mail: Lucas.Sheen@kp.org

G. Fananapazir, R. Lamba (eds.), *Transplantation Imaging*,
https://doi.org/10.1007/978-3-319-75266-2_9

marker of subsequent graft function after transplantation [1]. When graft dysfunction or acute rejection is suspected, transplant biopsies are performed. Some centers routinely perform surveillance biopsies in the first 3 months after transplant, while others perform biopsies only if rejection is suspected or if there is evidence of graft dysfunction.

Renal transplant biopsies are often technically easier to perform than native kidney biopsy. The patient can be placed supine. The allograft is often easily seen in the pelvis with ultrasound, even with high frequency transducers. The allograft is fixed in the pelvis and does not suffer the same respiratory motion as native kidneys. Although the allograft is denervated, pain experienced with the procedure is associated with the overlying soft tissues and the surrounding fibrous capsule of the transplant, which can be anesthetized with lidocaine. In 1999 the Banff 97 guidelines and criteria for pathologic evaluation of renal transplant biopsy specimens were published. These guidelines were designed as part of a continuing effort to optimize and standardize interpretation of biopsy specimens from renal allografts. For Banff 97, an adequate specimen is defined as a biopsy with ten or more glomeruli and at least two arteries. A minimal sample is seven glomeruli and one artery. In addition, it is recommended that at least two separate cores containing cortex be obtained or that there be two separate areas of cortex in the same core [2].

To obtain an adequate specimen, the biopsy should come from the outer renal cortex. The cortical tangential technique has been described for obtaining adequate cores from renal allografts [3]. The cortical tangential approach is a technique in which the needle path parallels the outer capsule of the kidney as much as possible (Fig. 9.1). Initial ultrasound evaluation of the transplant is performed, and an approach is identified where the needle will course approximately one-third to one-half the distance from the outer capsule to the sinus fat. A 4 MHz transducer can be used for this purpose, and often the transplant is superficial enough that a high frequency (9 MHz) linear transducer is used. Higher frequency transducers can deliver more detail and better visualization of the needle. To avoid vessel injury, the needle path should be directed away from the renal hilum. Any area of the kidney can be targeted for biopsy as long as the cortex is sampled. The best approach is often dictated by the orientation of the kidney. Ideally, the needle would not pass through the renal capsule at the distal aspect of the throw. However, this will generally not cause a complication unless bowel, vascular structures, or other organs are in the path of the needle. Once an approach is identified, the skin and underlying soft tissues up to the allograft are anesthetized with lidocaine under real-time ultrasound guidance. Core biopsies should be obtained with at least an 18 gauge needle, and the core sample should be 2–3 cm in length. The biopsy needle should be advanced into the cortex under real-time ultrasound guidance. Prior to biopsy, a measurement of the needle throw is recommended using ultrasound calipers once the needle is positioned. The sample is obtained and placed in formalin for electron and light microscopy. For immunofluorescence, the sample is unfixed and prepared for frozen sections. If the sample appears adequate, some centers will stop with one sample and submit to pathology for evaluation. Some centers will have a pathologist or pathology technologist at bedside to evaluate the adequacy of the specimen to determine if additional samples are required. Using the cortical tangential technique, the success rate for adequate or minimal sample according to Banff 97 assessment cri-

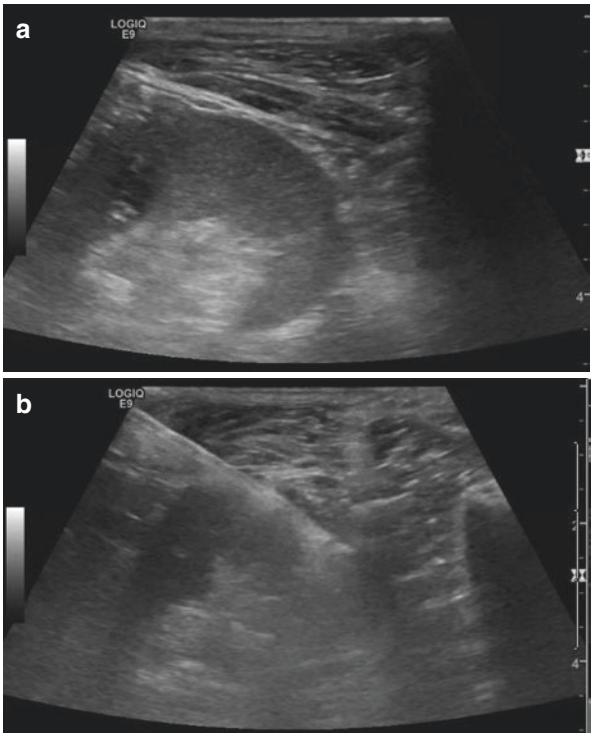

Fig. 9.1 (**a**) Initial ultrasound evaluation of a right lower quadrant transplant kidney with a short axis view of the allograft. A cortical tangential approach is planned that traverses the outer one-third to one-half of the cortex. (**b**) An 18 gauge BioPince (Argon Medical) needle is advanced under real-time ultrasound guidance into the outer cortex and a sample is obtained

teria is up to 95% when the specimen is evaluated by gross inspection. This is in comparison to prior studies that used Banff 97 which lacked uniform ultrasound-guided techniques, where the success rates ranged between 55 and 85% [3].

Renal Transplant Biopsy Complications

Complications rates are low with renal transplant biopsy. Hemorrhagic complication requiring transfusion is less than 1%. Minor self-limiting complications are less than 2% [3].

While laboratory and imaging studies are available for evaluation of allograft dysfunction, the core needle biopsy remains the gold standard of management. Despite the overall safety and low complication rates associated with biopsy, vascular complications occur and appear to be related to several technical factors including biopsy needle size, biopsy location, and total number of biopsy samples [4]. Thrombocytopenia and hypertension are also reported to be risk factors.

Arteriovenous fistula (AVF) and intrarenal pseudoaneurysms are the two most common vascular injuries related to transplant biopsy with rates of occurrence reported to be between 1 and 18% [5]. An AVF develops when an adjacent artery and vein are traumatized simultaneously. Pseudoaneurysms develop when only the arterial wall is injured. They may coexist in up to 30% of cases [6].

Many AVFs are clinically silent and those that are not seen on diagnostic imaging will often remain undetected with no clinical significance. Up to 70% will spontaneously resolve within 1–2 years; however, up to 30% will persist or become symptomatic [7]. These patients can present with ongoing hematuria, an audible bruit, transplant dysfunction, hypertension, or high cardiac output failure stemming from marked intrarenal arterial to venous steal phenomenon.

Intrarenal pseudoaneurysms generally are small and do not present with clinical symptoms. Like AVFs, they may also spontaneously resolve. An enlarging pseudoaneurysm may rupture and should be treated. Both AVFs and pseudoaneurysms are detectable on ultrasound (Fig. 9.2). Transcatheter angiography is the gold standard for AVF evaluation as it allows for assessment of the hemodynamic significance of the lesion [6]. A typical appearance is that of a dilated high flow early draining vein (Fig. 9.3). The drawbacks of angiography relate to the inherent risks of arterial access, though minimized through improved techniques.

The treatment of choice for symptomatic arteriovenous fistulas and enlarging pseudoaneurysms is transcatheter embolization. Small and/or asymptomatic lesions do not usually require intervention. Diagnostic angiography is first performed to visualize the AVF or pseudoaneurysm, using an ipsilateral or contralateral approach. The ipsilateral approach is more commonly used as it is technically simpler when the surgical anastomosis is end to side to the external iliac artery. The contralateral approach is necessary when the anastomosis is to the internal iliac artery. Under direct ultrasound guidance, the ipsilateral common femoral artery is accessed, and a long vascular sheath is placed, 6 French by 25 cm length. The anterior-posterior (AP) projection is not typically adequate to identify the renal artery anastomosis in profile. A steep anterior oblique projection is usually required. Once the anastomosis of the transplant renal artery is identified, the transplant renal artery is selected using an angled 5 French catheter, and selective renal angiogram is performed. Coaxial microcatheter technique is used to select the incident vessel and emboliza-

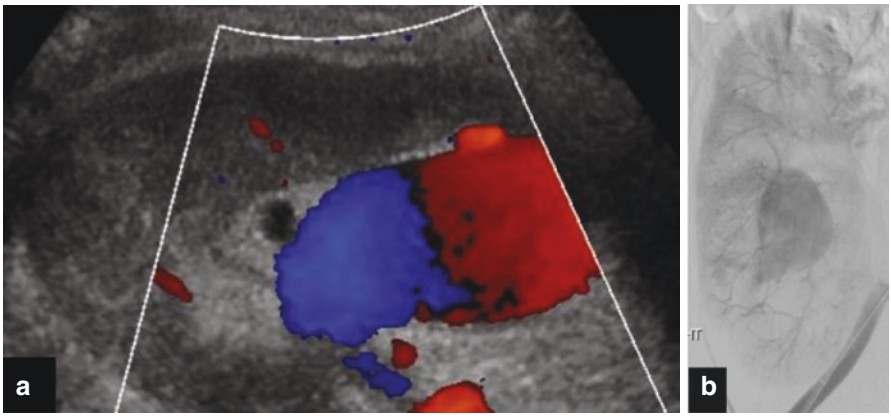

Fig. 9.2 (**a**) Color Doppler ultrasound demonstrating classic to-and-fro appearance of a large intrarenal pseudoaneurysm. (**b**) Corresponding pseudoaneurysm on spot image from an external iliac digital subtraction angiogram

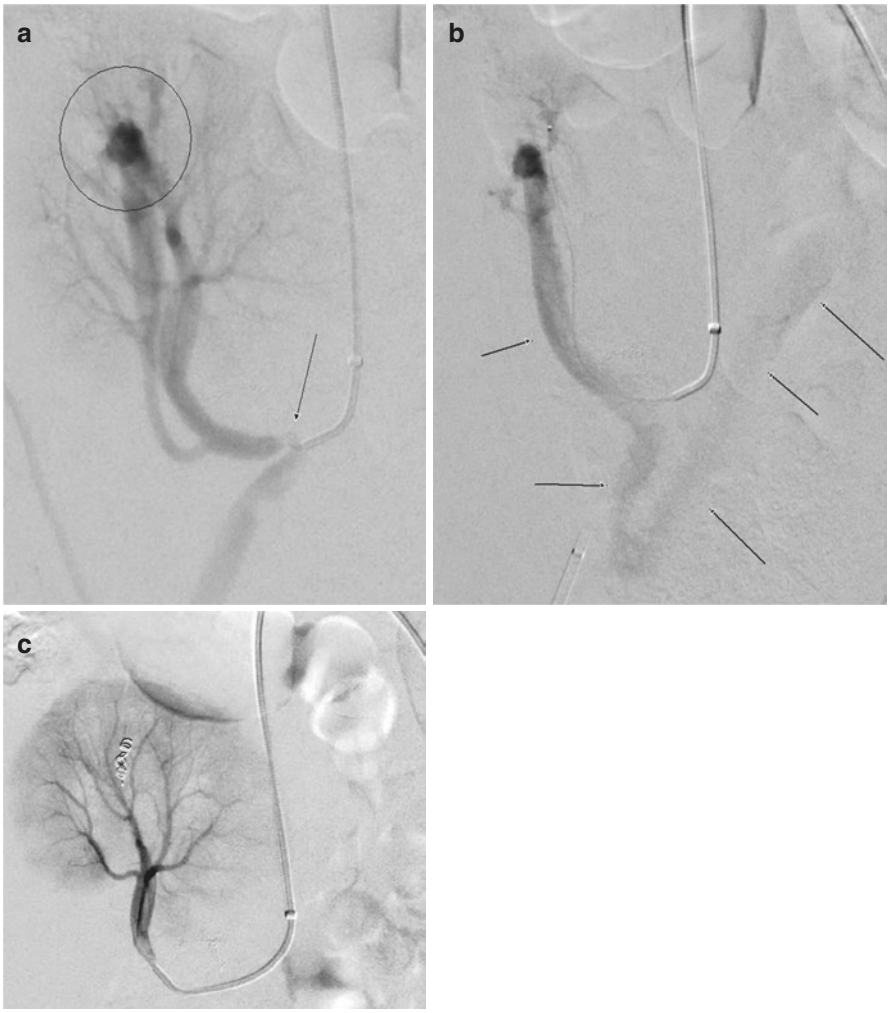

Fig. 9.3 (**a**) Transplant main renal arteriogram demonstrates an arteriovenous fistula in the midpole (circle). Incidentally, there is stenosis of the proximal transplant renal artery (arrow). This was later treated with angioplasty. (**b**) Superselective midpole arteriogram using coaxial microcatheter confirms the AVF. Early draining vein coursing toward the iliac vein is visualized (arrows). (**c**) Transplant renal arteriogram after coil embolization of the AVF demonstrates resolution

tion is performed using coils or microplugs. This is to minimize the effect of embolization on normal renal tissue. The usage of coils or microplugs allows for more precise targeting over particle embolization which can cause tissue ischemia or reflux into non-targeted vessels. The renal allograft has an end-arterial supply. This allows proximal occlusion to be adequate to exclude the AVF or pseudoaneurysm from the circulation (Fig. 9.3) [8]. In cases where an AVF has significant flow, it may be necessary to place an occlusive balloon temporarily within the draining vein

to prevent distal embolization of the coil pack into the systemic circulation. Technical success rate (defined as the ability to occlude the AV communication) of 71–100% is reported alongside alleviation of symptoms (hematuria, hypertension) in 57–88% of cases [9]. Clinical success rates are more widely varied in the literature and span 25–100% due to a portion of patients experiencing persistent or worsening renal failure. This may be due to intrinsic allograft disease or post-embolization infarction [4]. Pseudoaneurysms with narrow "necks" can be treated by packing multiple coils into the aneurysmal sac itself, thus allowing distal flow to be preserved within the renal artery. Surgical management remains an option when embolization treatment fails, consisting of partial or complete nephrectomy.

Vascular Interventions

Transplant Renal Artery Stenosis (TRAS)

Transplant renal artery stenosis (TRAS) is a well-known complication after transplant surgery and accounts for 75% of posttransplant vascular complications [10]. It occurs when the artery supplying the kidney becomes narrow and impedes blood flow to the allograft. This can occur anytime, though most frequently in the first 6 months after transplant. Early TRAS is defined as occurrence within 2 months after transplant. Arterial stenosis may be located anywhere along the transplant renal artery, pre-anastomotic stenosis at the recipient's external iliac artery or internal iliac artery, stenosis at the suture site, or stenosis of any segment of the donor renal artery.

Treatments for TRAS include conservative management, angioplasty, stenting, or surgical revascularization. Conservative medical management is best reserved for patients without significant decline of renal function, absence of hemodynamically significant stenosis on imaging, and hypertension that responds adequately to antihypertensive medications [11]. Revascularization procedures are indicated in uncontrolled hypertension, worsening renal function, and hemodynamically significant TRAS. In the author's institution TRAS is defined as greater than 50% luminal narrowing and/or greater than 10 mmHg pressure gradient across the stenosis.

First-line management begins with percutaneous transluminal angioplasty (PTA) which can be performed with or without stent placement [12]. Angioplasty alone does not preclude surgery.

Restenosis reportedly occurs in 5–30% of patients over 6–8 months which can be treated with repeat angioplasty [13]. Stenting is useful for cases of stenosis refractory to angioplasty, either when there is greater than 30% residual stenosis after angioplasty or persistent systolic pressure gradient greater than 10 mmHg. Stenting can also be used for flow limiting dissection. Potential procedural complications include renal artery dissection, thromboembolism, and restenosis of the stent. During post procedural management, patients can be prescribed antiplatelet agents for a short duration (aspirin, clopidogrel) after angioplasty and longer if they

undergo stenting to prevent restenosis or thrombosis, based on operator preference and follow-up. Hematoma, pseudoaneurysm, and other vascular injury may also occur at the access site as with any arterial procedure.

Angiography provides definitive diagnosis of TRAS and allows for simultaneous therapy with angioplasty and/or stenting. Knowledge of the type of anastomosis aids in determining the optimal arterial access site. When the anastomosis is to the external iliac artery, both ipsilateral and contralateral approaches are options depending on the anastomosis angle, though the ipsilateral approach is preferred by many operators due to the shorter distance from the access site to allograft [14]. With anastomosis to the internal iliac artery, a contralateral approach is preferred. Upper extremity access is rarely used, but can offer an advantage in cases of severe ectasia, kinking, or tortuosity. The selected site is prepared in a sterile fashion and the overlying skin and subcutaneous tissues are anesthetized with lidocaine. Under ultrasound guidance, arterial access is obtained and a vascular sheath (5 French or 6 French) placed. Selection of a catheter to access the donor renal artery is variable and frequently operator or anatomy dependent. For instance, a C2 catheter works well from a contralateral approach. In patients with pronounced hypertension, angiography of the aorta and iliac arteries is recommended to evaluate for stenosis secondary to atherosclerosis or other vascular injury that can diminish flow and cause allograft hypoperfusion. This form of inflow pre-anastomotic stenosis can closely mimic TRAS clinically.

Manipulation of catheter and wire near the arterial anastomosis should be done cautiously and kept to a minimum to reduce possible vascular injury, especially after recent transplant. Contrast injection rate depends on catheter tip location as well as guidance by fluoroscopy hand injection. Common iliac artery injections occur at 7–15 mL/s for a total of 12–30 mL. Internal iliac artery injections are performed at 5 mL/s for a total of 10 mL [14]. Often injection from these locations precludes a need to directly inject the donor renal artery. Multiple obliquities may be useful, and often lateral projections are helpful to fully image the arterial course. Cone-beam CT is employed by some operators to reduce the number of digital subtraction angiograms (DSA).

After stenosis identification, measurement, and characterization on angiography are completed, the lesion is carefully crossed using a floppy tipped 0.014–0.035 inch guidewire and appropriately shaped catheter. Pressure measurements across the stenosis provide additional objective data for treatment response. A balloon catheter is selected that has a diameter of equal to or 1 mm greater than the normal size of that segment of renal artery to perform angioplasty. Heparin is often administered prior to angioplasty with doses ranging from 3000 to 5000 units. Completion angiography is performed to determine if there is satisfactory angiographic result. When deciding to pursue stent deployment, the shortest possible stent that can cover the lesion with 1–2 mm on each side is selected and matched to equal the diameter of the normal width of the donor renal artery. Balloon expandable stents are preferred for their higher radial strength and accuracy of placement compared to self-expanding stents (Fig. 9.4).

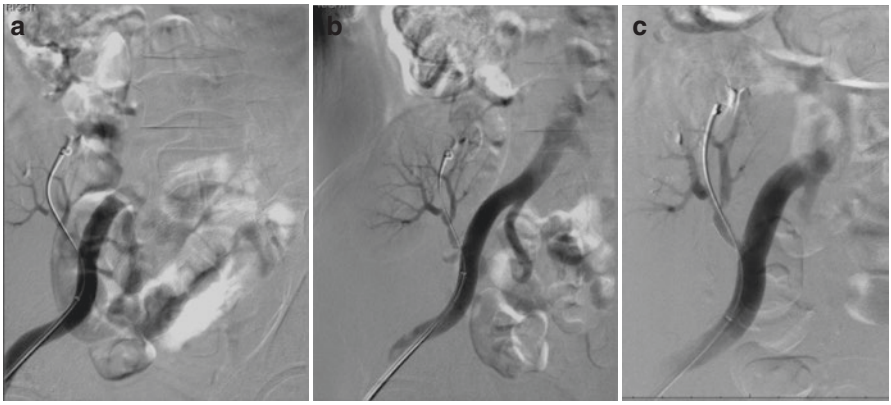

Fig. 9.4 (**a**) Right external iliac artery angiogram demonstrates severe stenosis just distal to the arterial anastomosis at the proximal transplant renal artery (arrow). (**b**) A 5 × 17 mm balloon expandable stent was positioned across the stenosis. Contrast injection performed to confirm proper stent coverage of the stenosis. Guidewire is maintained across the stenosis. (**c**) Post-stenting right external iliac angiography demonstrates significant improvement of the previously visualized stenosis. No hemodynamically significant residual stenosis. Guidewire position was maintained throughout and only removed after this confirmation of satisfactory angiographic result

Stenting is gaining more attention as a primary intervention. Retrospective studies have shown patency was significantly higher after primary stenting versus PTA, with more recent studies demonstrating drug eluting stents (DES) to be feasible and safe [15]. Outcomes of bare metal stents (BMS) versus drug eluting stents have been investigated, showing immediate and long-term reduction in serum creatinine and systolic blood pressure [16, 17]. Hanna et al. found the absolute rate of re-intervention was higher in BMS than DES, but the trend was not statistically significant [17]. The cost of BMS is half the cost of DES and should therefore be considered.

The stent is positioned across the lesion and slowly inflated to avoid dissection or stent migration. Importance is placed on obtaining images in proper obliquities to place the arterial stenosis in profile. Maintaining guidewire position across the lesion is essential throughout the entire process, both before and after treatment. Only after satisfactory angiographic result should the guidewire be removed.

Iliac Artery Stenosis

Iliac artery stenosis is a rare complication following renal transplantation which can occur both proximal and distal to the anastomotic site (Fig. 9.5). Pre-existing atherosclerotic aortoiliac disease is a common cause of stenosis in this location. Common iliac artery stenosis causes pre-anastomotic inflow limitation which can mimic TRAS clinically producing both hypertension and renal dysfunction. Doppler

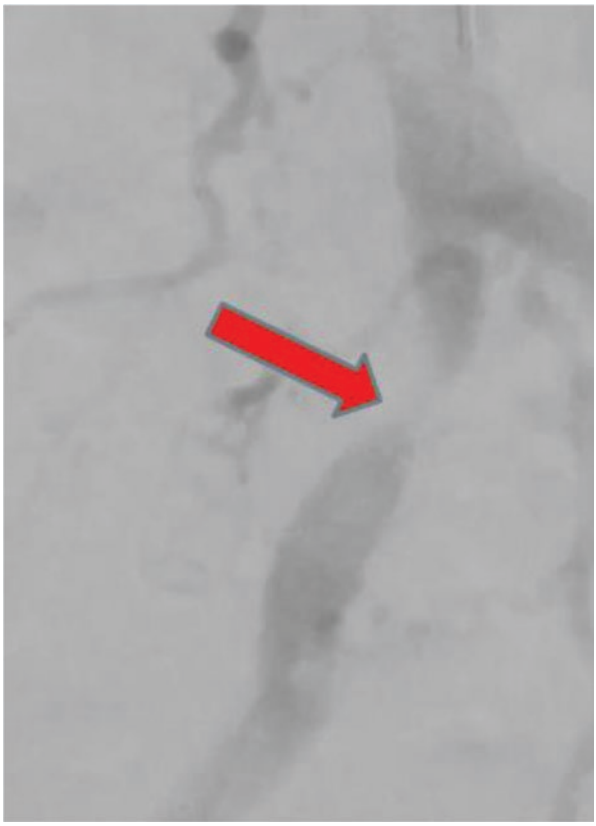

Fig. 9.5 DSA imaging demonstrating short segment area of stenosis of the common iliac artery (arrow)

ultrasound, in addition to CT or MRI, is useful in diagnosis and differentiation from TRAS [18]. Treatment options include angioplasty and/or stent placement versus surgical correction.

Transplant Vascular Thrombosis

Both arterial and venous thromboses are rare complications in renal transplantation with reported prevalence of 0.5–6.2% [19]. It is a major cause of allograft loss especially in the early posttransplant period. The arterial anastomosis may undergo kinking, torsion, or dissection which can lead to thrombosis. Endovascular stenting may prevent thrombosis in those scenarios. There are other nonvascular causes including hypercoagulable states, acute allograft rejection, or external compression by adjacent fluid collections. Specific to venous thrombosis, the presence of deep venous thrombosis (DVT) within the adjacent femoral or iliac veins may propagate into the transplant renal vein. Transplant arterial thrombosis occurs in conjunction with venous thrombosis in 11–15% of

cases [20]. The clinical presentation of transplant arterial thrombosis is relatively nonspecific with a range of symptoms including decreased urine output, anuria, and abdominal pain. In the case of venous thrombosis, an insidious onset of graft dysfunction may be present. Anticoagulation alone has been suggested as treatment for isolated venous thrombosis without extension into the iliac veins [21]. Usage of catheter-directed thrombolysis (CDT) is limited in the early posttransplant period (several weeks following surgery) due to bleeding risks. CDT may decrease periprocedural morbidity in cases of venous thrombosis with associated iliofemoral DVT [22].

Pseudoaneurysms

Pseudoaneurysms of the transplant renal artery may be intrarenal or extrarenal. Intrarenal pseudoaneurysms are most often the complication of renal biopsy (Fig. 9.2). Extrarenal pseudoaneurysms (Fig. 9.6) are a very rare complication in renal transplant patients with a reported rate of occurrence at less than 1% [23]. The possibility for rupture is the most concerning potential outcome. They can be postsurgical or post-infectious and most commonly occur at the arterial anastomosis site. Patients may be asymptomatic or have nonspecific abdominal pain, though the presence of a pulsatile mass in the lower abdomen may be helpful in diagnosis. Extrarenal aneurysms that are located in an inopportune site or reach a critical size can cause compression of the transplant renal artery and effectively present as TRAS with consequences of allograft dysfunction

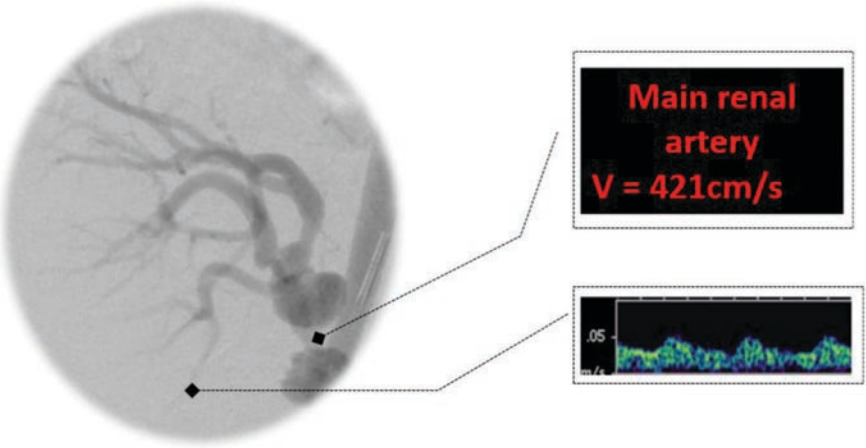

Fig. 9.6 DSA imaging depicting extrarenal pseudoaneurysms. These exert mass effect upon the adjacent renal artery which produces the equivalent of TRAS with elevated velocity and downstream parvus tardus waveform

and hypertension. Surgical repair is required in unstable patients. In the hemodynamically stable patient, endovascular techniques such as coil embolization, ultrasound-guided thrombin injection, and stent exclusion of the pseudoaneurysm are less invasive and proven successful [24]. Endovascular treatment for mycotic pseudoaneurysms has also shown to be effective in the stable patient. These patients should be monitored closely and complete a course of antibiotics prior to intervention [24].

Transplant Renal Vein Stenosis

Venous complications of renal transplants are very rare [25, 26]. Acquired transplant renal vein stenosis may be caused by technical problems with the anastomosis, compression from perigraft collections or a crossing iliac artery, local infection, or perivascular fibrosis (Fig. 9.7). Low-grade renal vein stenosis is usually hemodynamically insignificant and clinically occult, whereas high-grade stenosis may cause renal impairment (oliguria, anuria, azotemia, or delayed graft function) [26]. Similar to venous thrombosis, the diagnosis of venous stenosis can be made on US, CT, or MRI. Treatment has not yet been thoroughly established; only case reports have been published. The usage of balloon angioplasty with or without stent placement may improve renal function while avoiding risks associated with surgical revision [26].

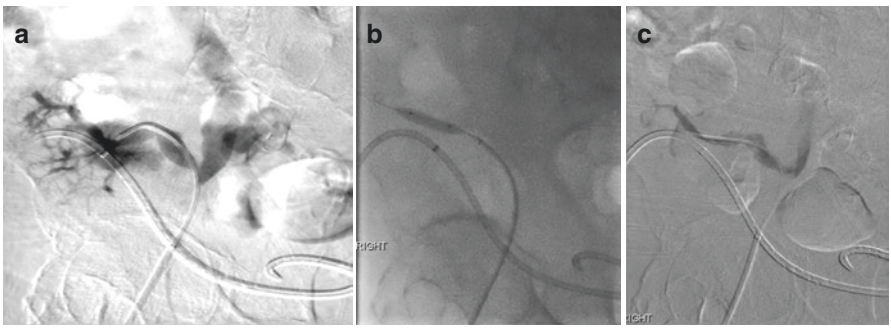

Fig. 9.7 (**a**) Transplant renal venogram demonstrates moderate narrowing of the upper segmental renal vein as it confluences with other segmental renal veins in the renal hilum over a length of 5 mm. Transplant renal vein is patent though tortuous with visible 90-degree angle in its course which does not constitute narrowing. Incidental note of transplant nephroureteral catheter overlying the allograft and bladder. (**b**) Angioplasty was performed using 5 mm × 2 cm and then 6 mm × 2 cm (shown here) balloon angioplasty catheters. (**c**) Repeat transplant renal venogram demonstrates mild residual stenosis which represents an overall improvement. Pressure measurements were obtained pre- and post-angioplasty which demonstrated improved venous pressure gradient

Iliac Vein Stenosis

Iliac vein stenosis is a rare complication of renal transplantation (Fig. 9.8). Additional causes outside of the posttransplant context include indwelling femoral dialysis catheters or chronic compression by an overriding iliac artery (May-Thurner syndrome). The presence of postoperative fluid collections, hematoma, urinoma, or lymphocele can generate localized inflammatory reaction and induce endothelial injury and subsequent venous stenosis [27, 28]. Surgical injury, intimal dissection, and faulty suturing may cause direct venous damage and also lead to venous stenosis [29]. Rare but serious potential complications include thrombosis of the transplant renal vein and/or ipsilateral iliofemoral vein.

Stenosis of the native iliac vein may present with clinical findings and graft dysfunction similar to stenosis of the transplant renal vein. Unilateral (ipsilateral to transplant) lower extremity edema can occur with iliac vein stenosis but would not be expected for transplant vein stenosis. Endovascular treatment strategy starts with angiographic confirmation of the stenosis, followed by catheter-directed thrombolysis, angioplasty, and possible stenting. Intravascular ultrasound should be employed as a diagnostic adjunct to determine residual stenosis after angioplasty and aid in the decision to stent.

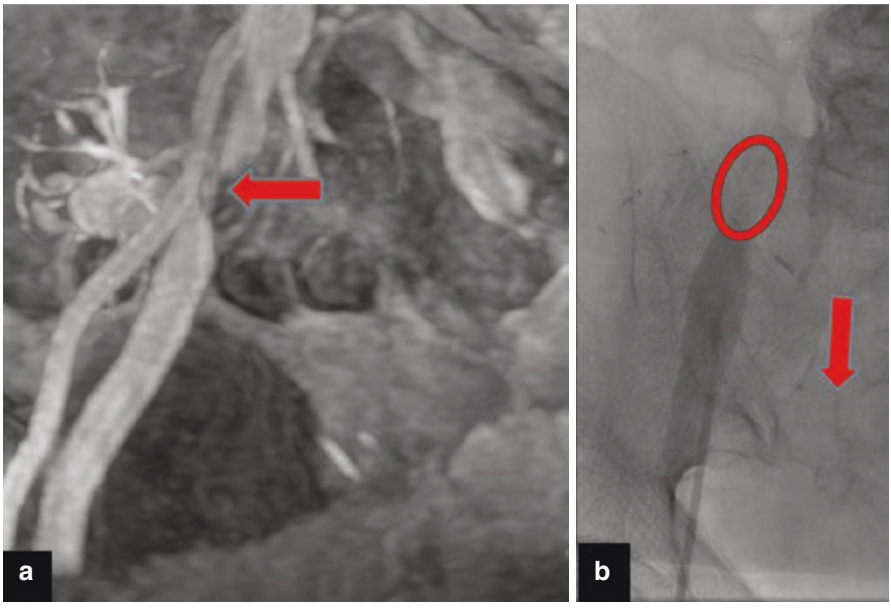

Fig. 9.8 (**a**) MRA with ferumoxytol shows right external iliac vein stenosis (arrow). (**b**) Digital subtraction venogram corroborates stenosis of the external iliac vein (oval) with collateral vessel opacified (arrow)

Ureteral Interventions

Ureteral Obstruction

Ureteral obstruction is the most common urologic complication following renal transplant. Ureteral obstruction of the transplant kidney occurs in 3–8% of patients and most occur within the first 6 months after surgery [30]. It is important for the treating physician to have a basic understanding of urinary tract reconstruction. There are several methods for performing urinary tract reconstruction, and the preferred method varies between transplant centers. The most common method is the creation of a uretero-neocystostomy. There are various techniques for this with the most common being the Politano-Leadbetter technique. In this technique, the ureter is tunneled through the bladder wall, and the ureteral anastomosis is created from inside the bladder. In the Lich-Gregoir technique, the muscle layers of the bladder are wrapped over the distal ureter to create a tunnel and prevent reflux. Other methods include ureteroureterostomy, where the transplant ureter is anastomosed with a native ureter, and ureteropyelostomy, where the transplant renal pelvis is connected to the native ureter [13].

Ureteral obstruction can be divided into early onset and late onset, the latter being defined as occurring after 3 months post transplantation [13, 31, 32]. Early obstruction is most often due to postsurgical factors such as a narrow ureterovesical anastomosis, ureteral kinking, or external compression by hematoma, urinoma, or abscess. Late-onset strictures can be caused by fibrosis due to inadequate vascular supply, and this may be responsible for nearly 90% of ureteral strictures [33].

Once obstruction is diagnosed, it is important to decompress the collecting system to minimize injury to the transplant. Both ureteral stent and nephrostomy tube placement can be considered. If there is concern for infection, decompression with nephrostomy and treatment with antibiotics should be performed initially, with a plan to perform antegrade nephrostogram to diagnose the cause of obstruction after renal function and sepsis has improved. Transplant nephrostomy is usually performed with ultrasound and fluoroscopic guidance, although CT guidance can be used in cases of challenging anatomy. The ideal calyx for renal access is the most superior and lateral to avoid peritoneal reflections and bowel. However, depending on the orientation of the kidney, a mid pole or lower pole calyx may be more appropriate. Careful evaluation with ultrasound is important to avoid bowel injury. The overlying skin and soft tissues are anesthetized with 1% lidocaine. Under real-time ultrasound guidance, the entry needle is directed into the desired calyx. A 21 gauge needle works well for this purpose. Once entry into the calyx is established, a small amount of urine can be aspirated for culture. A 0.018 inch wire is then advanced through the needle and coiled into the collecting system. The tract is dilated to 6 French, and a small amount of iodinated contrast is injected to visualize the renal collecting system using fluoroscopy. It is important to avoid overdistension to minimize the risks of intravasation of possibly infected urine resulting in urosepsis. A

0.038 inch heavy-duty wire is then advanced through the 6 French sheath and coiled in the renal pelvis or advanced down the ureter if possible. Over the wire, the 6 French sheath is exchanged for an 8-French locking pigtail catheter and the pigtail formed in the renal pelvis. Fibrosis can at times make it difficult to advance the catheter, and pre-dilation of the tract to 1 French size larger can facilitate placement of the catheter. The position of the catheter is confirmed, and the catheter is attached to a drainage bag and sutured to the skin.

Following decompression and resolution of sepsis, the cause of obstruction must be fully characterized with antegrade nephrostogram. A stiff 0.035 inch wire can be used to exchange the existing nephrostomy tube for a 6 French vascular sheath to perform antegrade nephrostogram. Multiple obliquities are often required to fully evaluate and lay out the entire transplant ureter. Attempts to cross the obstruction should be made. This can be accomplished with a combination of a hydrophilic wire and 4 French or 5 French angled catheter. Once the obstruction is crossed, the angled catheter is advanced into the bladder, and the hydrophilic wire is exchanged for a steel wire. Repeat nephrostogram can be performed once the wire is across; occasionally, there will be antegrade flow of contrast into the bladder once the ureter is straightened. This can be seen with external compression or kinking of the ureter. If a stricture is identified, this can be treated as described below. In cases of suspected external compression or kink, a nephroureteral stent is placed to facilitate internal drainage. Biliary-type catheters, which have a single distal pigtail but multiple side holes along the body of the catheter (most proximal side hole marked by a radiopaque band), are used for this purpose due to the short distance from the allograft to the bladder (Fig. 9.9). The catheter should initially be connected to bag drainage and in 2–4 days a capping trial can be performed. The patient should be closely monitored with serial serum creatinine levels to ensure internal drainage is successful and that hydronephrosis does not recur. Symptomatic report is unreliable as patients may not have pain when hydronephrosis occurs. Long-term management is challenging. Nephroureteral stents must be exchanged regularly to ensure patency,

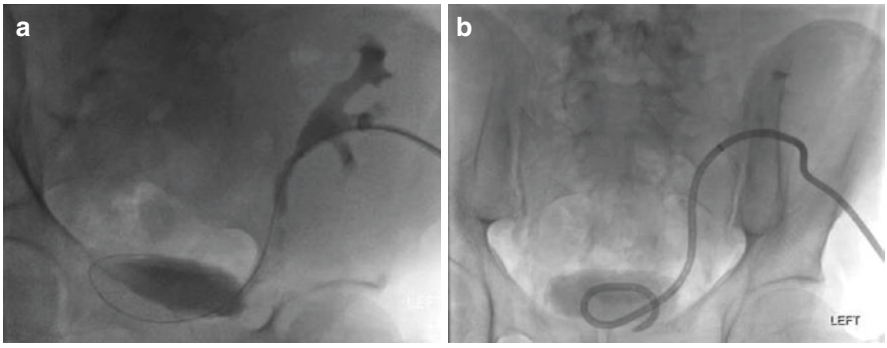

Fig. 9.9 (**a**) Antegrade nephrostogram (RAO projection) through a sheath demonstrates a distal ureteral stricture. (**b**) After ureteroplasty, a nephroureteral stent is placed using a 8.5 French biliary type catheter. The proximal radiopaque marker is in the renal pelvis (AP projection)

every 10–12 weeks. In addition, transplant patients are at high risk for infection and for developing antibiotic-resistant infection. Multidisciplinary care is mandatory to optimize care. Options include internalization of the stent with a double-J catheter with subsequent changes performed through the bladder, continuous percutaneous nephroureteral stent with external changes, or surgical revision.

Ureteral Stricture

Treatment of ureteral strictures can be performed with surgical methods and endoluminal methods. Some authors argue that endoluminal therapy should only be used as a temporary measure until surgical revision can be performed; however, there is no data to show that surgery outperforms endoluminal therapy and vice versa [34]. In a recent study, 51 ureters were surgically reconstructed after renal transplant for a variety of reasons. The 10-year graft outcome (78% graft survival) was not statistically worse than that in a matched control group. The perioperative morbidity (all grades) was 20.1%, and the mortality rate was 1.8% [35]. In another recent study looking at endoluminal treatment, the 10-year graft outcome was not statistically worse than that in a matched control group and the perioperative mortality was zero. In addition, the major complication rate was reported at 5.7% [33]. These data suggest that although outcomes may be similar, an endoluminal approach is safer with less morbidity and mortality.

The success rate of endoluminal ureteroplasty varies in the literature. Several studies have shown a higher success rate with treatment of early stenosis versus late stenosis [36, 37]. However, other studies have shown that the primary patency rate is no different for early stenosis versus late stenosis [34], and another showed a primary success rate of 81% for both early and late stenoses [33]. These later studies suggest that the timing of the obstruction may not affect the outcome.

Several techniques have been described for treating transplant ureteral obstruction. Unfortunately, many studies do not provide details on balloon diameters, inflation pressures, and inflation time making comparison of techniques difficult. Kumar et al. describe a technique using 8 mm high pressure balloons inflated to 30 atm for 5 min; this was then repeated during the same session for a total of three dilations (Fig. 9.10). After performing ureteroplasty an 8.5 French internal double-J stent was placed. The stent was removed cystoscopically in 4–6 weeks. Using this technique they reported an 81% success rate defined as preserved graft function and relief of the obstruction. Two of their patients required pre-dilation with a 6 mm cutting balloon, one was only dilated to 7 mm; however, 95% of their patients were dilated with the 8 mm balloon. There were no major complications after balloon dilation and insertion of the double-J stent [33]. Using larger balloons can increase the risk of ureteral rupture; however, ureteral rupture is rarely reported. When it does occur, it tends to be minor with no clinical consequences, as the ruptured area will be stented by ureteric stent insertion after the procedure [32]. A similar technique for ureteroplasty was described by Aytekin et al. in which they dilated the stenotic seg-

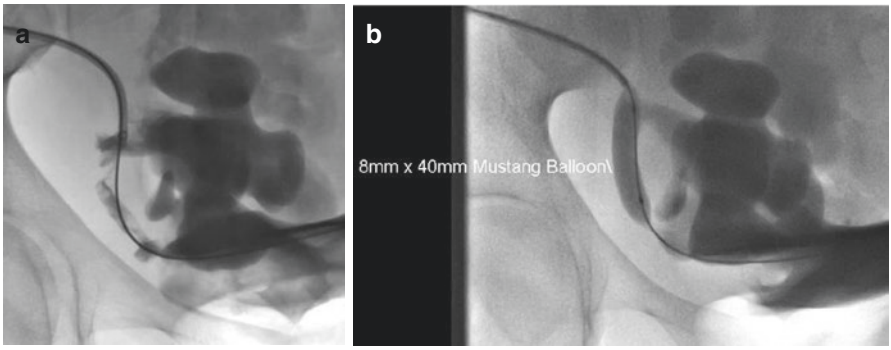

Fig. 9.10 (**a**) Right lower quadrant pediatric en-bloc renal transplant. One moiety suffered renal vein thrombosis and was subsequently removed. The remaining moiety has a proximal ureteral stricture that caused severe hydronephrosis, initially managed with NUS placement. (**b**) A Mustang (Boston Scientific) 8 mm × 40 mm balloon was used to perform serial ureteroplasty using high pressure and prolonged inflation time of 5 min. A total of three dilations were performed

ment with high-pressure balloon catheters ranging from 5 to 8 mm in size. They used lower pressure of 8–15 atm and similar prolonged inflation times of 5–10 min. In patients with resistant stenosis, multiple balloon dilatation sessions at 1 or 2 week intervals were performed. Instead of internalizing the stent, Aytekin opted for external nephroureteral stent placement using biliary catheters to maintain access for repeat interventions. Their success rate, which was for primary assisted patency, was 93.7% [34].

Ureteral Stones

Ureteral stones in transplant kidneys are rare (incidence 0.2–0.5%) [30, 31]. In a series of 1000 renal transplant recipients, only two cases of symptomatic ureteral calculi occurred. Both patients presented at 2 and 5 years after transplantation with atypical abdominal pain. Both were treated by ureteroscopic stone manipulation successfully with no further recurrences [31]. Another series of 1535 renal transplant recipients reported only 9 ureteral stones, only 6 of which caused obstruction [30].

Pyeloureteritis Cystica

Pyeloureteritis cystica or ureteritis cystica is a benign condition of the ureter representing multiple small submucosal cysts (Fig. 9.11). Histologically there are numerous small submucosal epithelial-lined cysts representing cystic degeneration of metaplastic epithelium or submucosal Brunn cell nests [38–40]. The appearance is

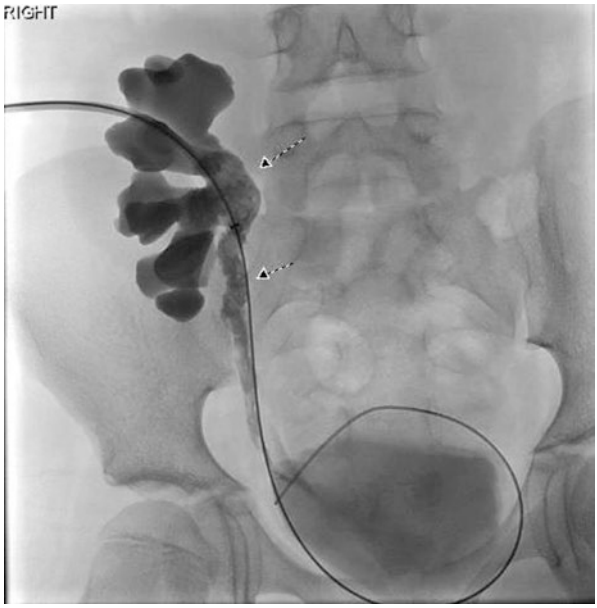

Fig. 9.11 Right lower quadrant renal transplant with history of nephroureterolithiasis, status post removal, and placement of nephroureteral stent. On this follow-up antegrade nephrostogram, pyeloureteritis cystica was noted. This is due to chronic inflammation from a combination of stones and indwelling stent

that of multiple small 2–5 mm smooth-walled, rounded lucent filling defects projecting into the lumen of the ureter. Rarely they can be up to 2–3 cm in size [39]. The etiology of pyeloureteritis cystica is chronic inflammation. This can be due to chronic infection, chronic irritation from indwelling stents, or nephrolithiasis. Treatment is not required for pyeloureteritis cystica if the cause is thought to be due to chronic stent placement, but if underlying chronic infection is suspected, treatment may be warranted.

Perigraft Fluid Collections

Perigraft fluid collections are the most common complications of renal transplantation, occurring in approximately 50% of transplant patients [41]. External fluid collections can be due to urinoma, hematoma, seroma, abscess, or lymphocele. Ultrasound-guided percutaneous drainage is effective in treating perinephric fluid collections. It is important to sample the fluid and test it to determine the etiology and to rule out infection.

Urinomas due to a urine leak is a common early urologic complication following renal transplantation with an incidence ranging from 1.2 to 8.9%. On ultrasound, urinomas are typically anechoic and may have few septations. Urinomas can be diagnosed by demonstrating an elevated creatinine concentration within the collection that is significantly higher than serum creatinine. When urinoma is diagnosed, an antegrade nephrostogram to evaluate the size and location of urine leak is mandatory (Fig. 9.12). Ureteral leak is most often due to devascularization of the distal

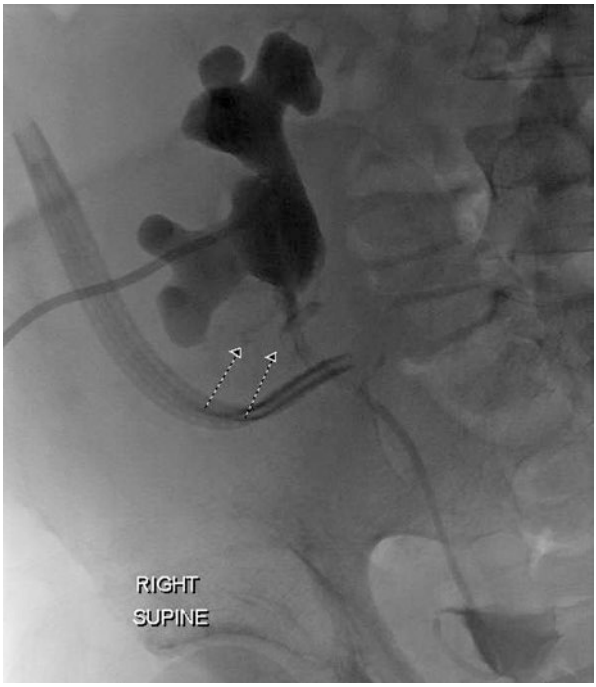

Fig. 9.12 Right lower quadrant renal transplant with history of prior ureteral stricture. Patient underwent a ureteropyelostomy which was complicated by ureteral leak at the anastomosis. This was managed with nephroureteral stent and repeat nephrostogram until resolution

ureter during organ harvest [13, 41]. If the degree of urine leak is mild and in the distal ureter, conservative management can be considered. This requires urinary diversion with nephroureteral stent and bladder catheter. Ureteral stenting should be left in place for 4–6 weeks [41]. Outcomes of percutaneous management vary, and success rates are reported from 36 to 100% [13]. Large ureteral leaks are often managed with surgical intervention.

Postoperative hematomas are common perioperative collections; however, most are small and asymptomatic. Large hematomas can cause symptoms secondary to mass effect on the transplant. The main concern for large hematomas is that they may become secondarily infected. Ultrasound evaluation of perigraft hematomas reveals a complex fluid collection with echogenic debris [13]. Drainage of perigraft hematomas can be challenging due to the viscosity of the fluid. Larger drains are often required (12 to 14 French) and tissue plasminogen activator (tPA) injections may be required to assist in drainage. A technique was described by Beland et al. [41] in 2008 where the alteplase (tPA) dose was standardized to 4–6 mg diluted in 25 mL of 0.9% saline, administered entirely through a single catheter or divided equally through multiple catheters. The catheter was clamped for 30 min after which it was opened to gravity drainage without aspiration. Each cycle lasted 2–3 days with two to six doses administered in each cycle. If required, a second cycle was performed within 14 days of completion of the first lasting for 2–3 days. 89.1% (41 of 46) of collections refractory to simple percutaneous drainage were completely drained following

the instillation of tPA, and there were no systemic or intracavitary hemorrhagic complications identified while the catheters remained in place.

Postoperative lymphoceles occur in 0.6–18% of renal transplants and usually occur weeks to months after transplant. Lymphoceles are caused by lymphatic leakage from the allograft bed or from the transplant itself [13, 42, 43]. Prolonged lymphatic leakage occurs as a result of graft rejection, the use of steroids or diuretics, or re-transplantation. Laboratory evaluation of lymphoceles reveals the same levels of protein, urea nitrogen, creatinine, and electrolytes as serum. This helps to differentiate from urinomas that have elevated creatinine compared to serum. On ultrasound, lymphoceles are typically anechoic and may have septations. Lymphoceles are more difficult to manage than other perigraft fluid collections. Initial aspiration is performed to confirm the diagnosis; however, aspiration alone results in an 80–90% recurrence rate [42]. Percutaneous drainage also results in high recurrence rates. The best results are achieved with a combination of indwelling catheter drainage and sclerotherapy with a reported success rate of 68–100% [42]. The most common complication of sclerotherapy is secondary infection of the lymphocele which is reported to occur in approximately 7–17% of cases. Johnson and Berry [42] described a technique for treating lymphoceles. Their technique involves ultrasound-guided percutaneous drainage with an 8 French locking pigtail drain. Septations can be disrupted with a wire. Next, the lymphocele is aspirated and the volume of fluid measured. Absolute alcohol is then injected into the cavity, the total volume of alcohol used equals 1/3 of the initial aspirated volume. The tube is then capped for 30 min. Sclerotherapy is repeated every 3 days until catheter drainage has decreased to 10–20 mL per day, at which point the catheter is removed. Serial ultrasounds are performed to evaluate for recurrence. This technique is effective but is time consuming and requires multiple follow-up visits. Other sclerotherapy agents have also been described such as povidone-iodine, doxycycline, and bleomycin [13]. If sclerotherapy fails and the lymphocele recurs, surgery may be required.

Any perigraft fluid collection can become infected and become a perinephric abscess. Patients will often present with fever or local pain. Ultrasound and CT findings are nonspecific, but air within the collection is highly suggestive of abscess [13]. Aggressive treatment with image-guided percutaneous drainage and systemic antibiotics is important because of the immunosuppressed state of transplant patients. Percutaneous drainage under ultrasound or CT guidance has a high rate of success (70–96%) and a low complication rate [41].

Pediatric En-Bloc Renal Transplant

Pediatric en-bloc renal transplants involve both kidneys from the donor with two ureters and two ureteral anastomoses. Ureteral complications are managed the same as single transplants; however, often both ureters are affected requiring separate procedures for each ureter and separate nephrostomy tube access into each kidney (Fig. 9.13).

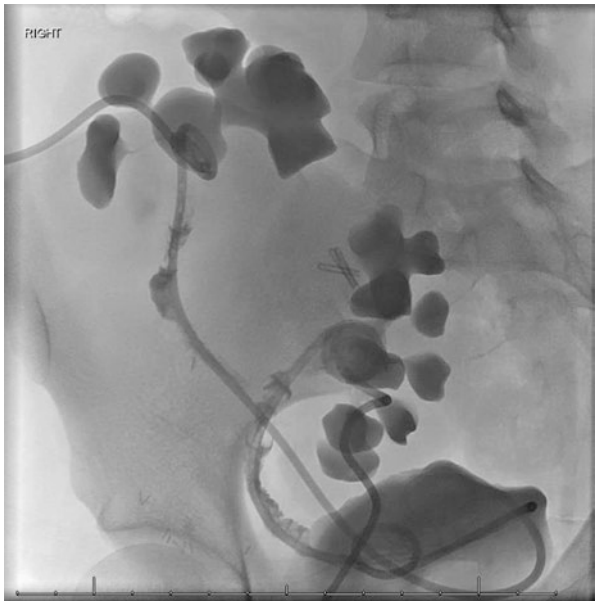

Fig. 9.13 Pediatric en-bloc renal transplant in the right lower quadrant with bilateral ureteral stenoses, managed with serial balloon ureteroplasty and nephroureteral stents in both kidneys

References

1. Kasiske B, Vazquez M, Harmon W, Brown R, Danovitch G, Gaston R. Recommendations for the outpatient surveillance of renal transplant recipients. J Am Soc Nephrol. 2000;11(Suppl 15):S1–86.
2. Racusen LC, Solez K, Colvin RB, et al. The Banff 97 working classification of renal allograft pathology. Kidney Int. 1999;55(2):713–23.
3. Patel MD, Phillips CJ, Young SW, et al. US-guided renal transplant biopsy: efficacy of a cortical tangential approach. Radiology. 2010;256:290–6.
4. LaBerge JM. Interventional management of renal transplant arteriovenous fistula. Semin Interv Radiol. 2004;21(4):239–46.
5. Bach D, Wirth C, Schott G, Hollenbeck M, Grabensee B. Percutaneous renal biopsy: 3 years of experience with the biopsy gun in 761 cases—a survey of results and complications. Int Urol Nephrol. 1999;31:15–22.
6. Copelan A, George D, Kapoor B, et al. Iatrogenic-related transplant injuries: the role of the interventional radiologist. Semin Intervent Radiol. 2015;32:133–55.
7. Martinez T, Palomares M, Bravo JA, et al. Biopsy induced arteriovenous fistula and venous aneurysm in a renal transplant. Nephrol Dial Transplant. 1998;13:2937–9.
8. Ray CE Jr. Renal embolization. Semin Interv Radiol. 2001;18:37–45.
9. Maleux G, Messiaen T, Stockx L, Vanrenterghem Y, Wilms G. Transcatheter embolization of biopsy-related vascular injuries in renal allografts. Long-term technical, clinical and biochemical results. Acta Radiol. 2003;44(1):13–7.
10. Srivastava A, Kumar J, Sharma S, et al. Vascular complication in live related renal transplant: an experience of 1945 cases. Indian J Urol. 2013;29:42–7.
11. Chen W, Kayler LK, Zand MS, et al. Transplant renal artery stenosis: clinical manifestations, diagnosis and therapy. Clin Kidney J. 2015;8:71–8.
12. Pappas P, Zavos G, Kaza S, et al. Angioplasty and stenting of arterial stenosis affecting renal transplant function. Transplant Proc. 2008;40(5):1391–6.

13. Kobayashi K, Censullo ML, Rossman LL, et al. Interventional radiologic management of renal transplant dysfunction: indications, limitations, and technical considerations. Radiographics. 2007;27:1109–30.
14. Rajan DK, Stavropoulos SW, Shlansky-Goldberg RD. Management of transplant renal artery stenosis. Semin Intervent Radiol. 2004;21(4):259–69.
15. Biederman DM, Fischman AM, Titano JJ, et al. Tailoring the endovascular management of transplant renal artery stenosis. Am J Transplant. 2015;15:1039–49.
16. Estrada CC, Musani M, Darras F, et al. 5 years experience with drug eluting and bare metal stents as primary intervention in transplant renal artery stenosis. Transplantation Direct. 2017;3:e128.
17. Hanna RF, Hao F, Kraus G, et al. Renal transplant arterial stenosis treated with bare-metal versus drug-eluting stents: comparison of treatment outcomes. Transplant Proc. 2015;47: 2881–5.
18. Merkus JW, Van Asten WN, Hoitsma AJ, et al. Iliac artery stenosis after kidney transplantation. Acta Chir Belg. 1993;93(5):242–8.
19. Rerolle JP, Antoine C, Raynaud A, et al. Successful endoluminal thrombo-aspiration of renal graft venous thrombosis. Transpl Int. 2000;13:82–6.
20. Bakir N, Sluiter WJ, Ploeg RJ, van Son WJ, Tegzess AM. Primary renal graft thrombosis. Nephrol Dial Transplant. 1996;11(1):140–7.
21. Ortega Herrera R, Medina Benítez A, Hernández Abad MJ. Renal vein partial thrombosis in 3 recipients of kidney transplantation. Arch Esp Urol. 2000;53(1):45–8.
22. Giustacchini P, Pisanti F, Citterio F, De Gaetano AM, Castagneto M, Nanni G. Renal vein thrombosis after renal transplantation: an important cause of graft loss. Transplant Proc. 2002;34(6):2126–7.
23. Donckier V, De Pauw L, Ferreira J, et al. False aneurysm after transplant nephrectomy: report of two cases. Transplantation. 1995;60:303–4.
24. Fananapazir G, Hannsun G, Wright LA, Corwin MT, Troppmann C. Diagnosis and management of transplanted kidney extrarenal pseudoaneurysms: a series of four cases and a review of the literature. Cardiovasc Intervent Radiol. 2016;39:1649–53.
25. Low G, Crockett AM, Leung K, et al. Imaging of vascular complications and their consequences following transplantation in the abdomen. Radiographics. 2013;33:633–52.
26. Obed A, Uihlein DC, Zorger N, et al. Severe renal vein stenosis of a kidney transplant with beneficial clinical course after successful percutaneous stenting. Am J Transplant. 2008;8: 2173–6.
27. Jones G, Tibballs J, Al-Akraa M, et al. Iliac vein stenosis as a reversible cause of renal transplant dysfunction. Nephrol Dial Transplant. 2004;19:2415–6.
28. Kim JH, Bae SM, Park S. Ipsilateral leg swelling after renal transplantation as an alarming sign of iliac vein stenosis. Kidney Res Clin Pract. 2014;33:217–21.
29. Cercueil JP, Chevet D, Mousson C, et al. Acquired vein stenosis of renal allograft—percutaneous treatment with self-expanding metallic stent. Nephrol Dial Transplant. 1997;12:825–6.
30. Streeter EH, Little DM, Cranston DW, Morris PJ. The urological complications of renal transplantation: a series of 1535 patients. BJU Int. 2002;90(7):627–34.
31. Shoskes DA, Hanbury D, Cranston D, Morris PJ. Urological complications in 1,000 consecutive renal transplant recipients. J Urol. 1995;153(1):18–21.
32. Kumar S, Ameli-Renani S, Hakim A, Jeon JH, Shrivastava S, Patel U. Ureteral obstruction following renal transplantation: causes, diagnosis and management. Br J Radiol. 2014;87:20140169.
33. Kumar S, Jeon JH, Hakim A, Shrivastava S, Banerjee D, Patel U. Long-term graft and patient survival after balloon dilation of ureteric stenosis after renal transplant: a 23-year retrospective matched cohort study. Radiology. 2016;281(1):301–10. https://doi.org/10.1148/radiol.2016151629.
34. Aytekin C, Boyvat F, Harman A, Ozyer U, Colak T, Haberal M. Percutaneous therapy of ureteral obstructions and leak after renal transplantation: long-term results. Cardiovasc Intervent Radiol. 2007;30(6):1178–84.

35. Berli JU, Montgomery JR, Segev DL, et al. Surgical management of early and late ureteral complications after renal transplantation: techniques and outcomes. Clin Transplant. 2015;29(1):26–33.
36. Fontaine AB, Nijjar A, Rangaraj R. Update on the use of percutaneous nephrostomy/balloon dilation for the treatment of renal transplant leak/obstruction. J Vasc Interv Radiol. 1997;8(4):649–53.
37. Lojanapiwat B, Mital D, Fallon L, et al. Management of ureteral stenosis after renal transplantation. J Am Coll Surg. 1994;179(1):21–4.
38. Kawashima A, Vrtiska TJ, Leroy AJ, et al. CT urography. Radiographics. 2004;24(Suppl 1):S35–54.
39. Joffre F, Otal P, Soulie M. Radiological imaging of the ureter. Springer; 2003. ISBN: 3540655212.
40. Petersen RO, Sesterhenn IA, Davis CJ. Urologic pathology. Farrar, Straus, and Giroux; 2009. ISBN: 0781753430.
41. Beland MD, Gervais DA, Levis DA, Hahn PF, Arellano RS, Mueller PR. Complex abdominal and pelvic abscesses: efficacy of adjunctive tissue-type plasminogen activator for drainage. Radiology. 2008;247(2):567–73.
42. Johnson SP, Berry RS. Interventional radiological management of the complications of renal transplantation. Semin Interv Radiol. 2001;18:47–58.
43. Akbar SA, Jafri SZ, Amendola MA, Madrazo BL, Salem R, Bis KG. Complications of renal transplantation. RadioGraphics. 2005;25(5):1335–56.

Chapter 10
Posttransplant Lymphoproliferative Disorder

Michael T. Corwin

Introduction

Recipients of solid organ transplants are at increased risk for a wide variety of cancers compared to the general population [1–3]. This is largely due to the effects of immunosuppression as many of the malignancies are related to underlying infections. Aside from skin cancers, posttransplant lymphoproliferative disorder (PTLD) is the most common malignancy to affect solid organ transplant recipients [4]. PTLD represents a range of diseases from lymphoid hyperplasia to malignant lymphoma. It is most commonly a B-lymphocyte proliferation and many are thought to be associated with Epstein-Barr viral infection [5]. However, other forms exist including T-cell- and natural killer cell-derived PTLD. There are four main pathological categories: hyperplastic (early) lesions, polymorphic lesions, monomorphic (lymphomatous) lesions, and Hodgkin's disease. The different forms of PTLD are not reliably distinguished at imaging however.

The prevalence of PTLD depends on the type of organ transplantation. The highest rates are seen with multi-organ transplant recipients (13–33%) and small bowel transplants (up to 20%) and less frequently in heart-lung (4–10%), renal (1–2%), and liver (1–3%) transplants [4, 6–9]. The incidence is also higher in pediatric patients and varies with the immunosuppression regimen. There is a dual peak of PTLD in relation to time from transplantation. The highest incidence occurs within the first year after transplantation and second peak 4–5 years following transplantation [10].

Clinical manifestations are usually absent or nonspecific and depend on the location of disease. When the allograft is involved, graft dysfunction is common, but this is difficult to distinguish from rejection on a clinical basis. Nonspecific symptoms include fever, weight loss, and fatigue which can also be seen with

M. T. Corwin, M.D.
University of California, Davis, Sacramento, CA, USA
e-mail: mtcorwin@ucdavis.edu

G. Fananapazir, R. Lamba (eds.), *Transplantation Imaging*,
https://doi.org/10.1007/978-3-319-75266-2_10

infection [4]. Because of the difficulty in making the diagnosis of PTLD clinically, imaging plays a crucial role.

Imaging Modalities

Ultrasound (US) is generally the first-line imaging modality to evaluate abdominal solid organ transplants. Doppler US allows assessment of transplant vasculature, and US is readily accessible and relatively inexpensive and lacks ionizing radiation or iodinated contrast utilization. Thus, PTLD may be first encountered on US, particularly when it affects the transplanted organ itself. However, US is more limited for detection of gastrointestinal and nodal disease, especially in the retroperitoneum.

Computed tomography (CT) is the most widely used imaging modality for evaluation of PTLD. It provides the most comprehensive assessment of both nodal and extra-nodal sites of disease. Limitations include the use of ionizing radiation and risks of contrast-induced nephropathy (CIN). The latter is of particular concern in renal transplant recipients; however, a recent study found no cases of CIN in 104 renal transplant recipients who underwent contrast-enhanced CT and had an estimated glomerular filtration rate >60 mL/min/1.73 m^2 [11]. Furthermore, no cases of graft loss or emergent dialysis were seen in any of 224 patients who underwent contrast-enhanced CT.

Magnetic resonance imaging (MRI) is reserved as a problem-solving tool when CT is inconclusive or there are particular concerns regarding radiation (pediatric patients) or CIN. Although gadolinium must be used with caution in patients with renal failure due to risks of nephrogenic systemic fibrosis, a noncontrast MRI may provide more information than noncontrast CT, particularly in solid organ disease. PTLD is often low signal intensity on T2-weighted images, which may help distinguish it from other malignancies and infectious processes that are typically hyperintense on T2.

Positron emission tomography/CT (PET/CT) is also useful to detect and characterize both nodal and extra-nodal PTLD. PTLD demonstrates increased fluoro-2-deoxy-d-glucose (FDG) uptake and has shown to be more sensitive and specific for PTLD than CT alone [12–14]. PET/CT is also useful in evaluating the response to therapy longitudinally.

Imaging Features of PTLD

Imaging manifestations of PTLD vary with the type of organ transplantation; however, unlike lymphomas in the general population, PTLD is more commonly extranodal than nodal for all types of organ transplants. As a general rule, the transplanted organ itself is a common location for extra-nodal PTLD. For example, the transplanted kidney is the most common site of PTLD in renal transplant recipients, and

lung and liver PTLD is most common in recipients of those organs [5, 15]. PTLD is also more common intra-abdominally than above the diaphragm with the bowel and liver being the most common sites. The imaging appearance of PTLD can be primarily divided by nodal and extra-nodal patterns and secondarily by the location and pattern of organ involvement.

Extra-Nodal PTLD

Gastrointestinal Tract

The mid and distal small bowel is the most common location of gastrointestinal tract involvement with PTLD. The imaging manifestations of small bowel PTLD largely mimic those of lymphoma in the non-transplant patient where a variety of appearances can manifest. The most common finding at CT is circumferential wall thickening with or without aneurysmal dilation (Fig. 10.1) [16]. The aneurysmal dilation is a classic feature of small bowel lymphoma and is thought to be due to tumor replacement of the muscularis propria and destruction of the myenteric plexus [17]. Other appearances of small bowel PTLD include an eccentric polypoid mass and ulceration. Intussusceptions and skip lesions can also be seen. Notably, bowel obstruction is usually absent, even with very large masses.

Colonic and gastric involvement is less common than small bowel, and wall thickening is the most common appearance. As this finding is nonspecific, attention to the enhancement of the bowel wall is crucial to distinguish PTLD from infectious etiologies. The bowel wall should be high attenuation due to tumor enhancement in PTLD, while inflammatory etiologies may show low-attenuation submucosal edema between enhancing mucosa and serosa.

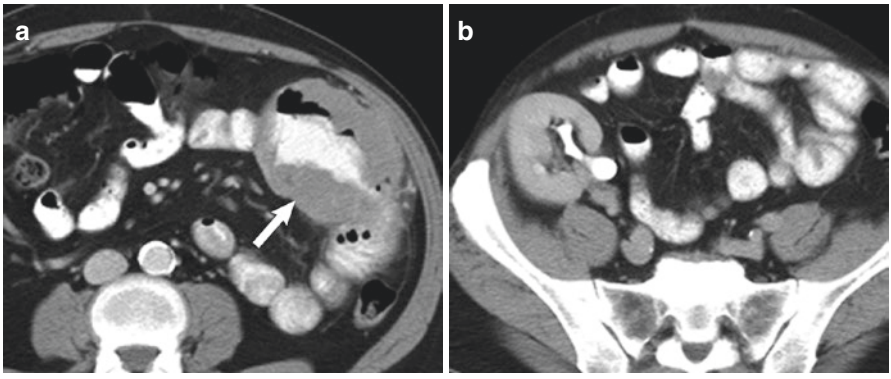

Fig. 10.1 A 60-year-old man status post renal transplant with small bowel PTLD. (**a**) Contrast-enhanced CT shows marked circumferential small bowel wall thickening with aneurysmal dilation (arrow). Note the oral contrast in the lumen and lack of obstruction. (**b**) Right lower quadrant renal transplant

Liver

The liver is the most commonly involved solid organ with PTLD, seen most frequently with liver transplants but also with pancreas, heart, lung, and renal transplants [5, 18]. On CT, the most common appearance is multiple discrete low-attenuation hypo-enhancing nodules. On ultrasound, these nodules are hypoechoic and on MR may demonstrate low signal on T1-weighted images and low to mildly hyper-intense signal on T2-weighted images. The second most common pattern is an infiltrative mass demonstrating a geographic or ill-defined region of low attenuation in the liver (Fig. 10.2). A pattern unique to liver transplant recipients is that of a porta hepatis mass with periportal infiltration that may cause biliary obstruction (Fig. 10.3) [16, 19]. The common presentations of liver PTLD mimic both metastatic diseases from another primary as well as opportunistic infections, and therefore percutaneous biopsy may be needed for definitive diagnosis and subtyping in the case of PTLD.

Spleen

Unlike lymphoma in immunocompetent patients, the spleen is a less common site of disease in PTLD. The most common presentation is splenomegaly, with multiple focal low-attenuation lesions less frequent (Fig. 10.4). The differential diagnosis for multiple low-attenuation lesions in the spleen is similar to that in the liver and includes opportunistic infections such as fungal disease. T2-weighted MR imaging may be helpful as focal PTLD lesions are iso- to hypo-intense, while the focal abscesses in splenic fungal disease are markedly hyper-intense [5, 20].

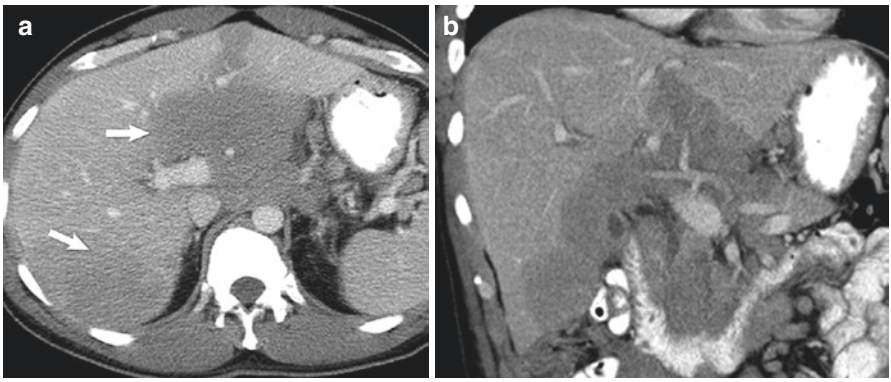

Fig. 10.2 A 50-year-old man status post liver transplant with infiltrative liver PTLD. (**a**) Contrast-enhanced CT shows multifocal geographic areas of low attenuation in the liver (arrows). (**b**) Coronal image shows a portal vein coursing through the tumor without narrowing or occlusion

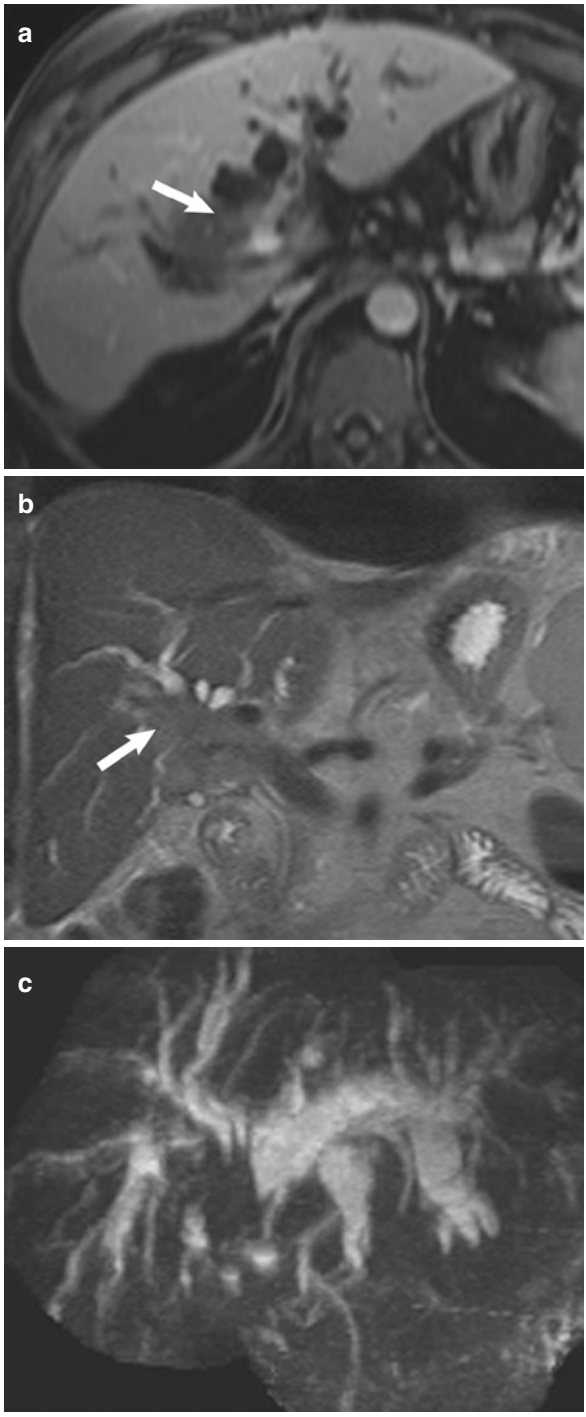

Fig. 10.3 A 54-year-old man status post liver transplant with porta hepatis PTLD. (**a**) Contrast-enhanced T1-weighted image shows hypo-enhancing infiltrative mass within the porta hepatis (arrow). (**b**) Coronal single-shot fast spin echo image reveals intermediate signal mass in the porta hepatis (arrow) causing biliary obstruction. (**c**) Maximum intensity projection image from a 3D MRCP shows the biliary dilation. Images courtesy of Dr. Shawn Hajimomenian

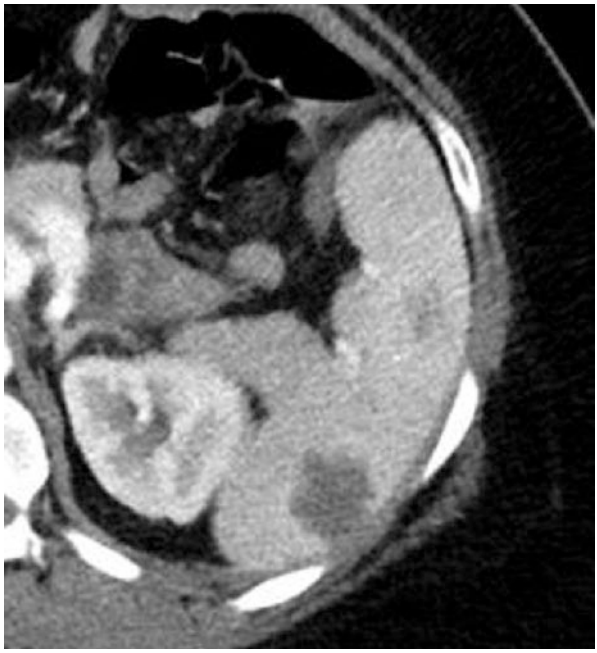

Fig. 10.4 A 48-year-old woman status post renal transplant with splenic PTLD. Contrast-enhanced CT image reveals multiple low-attenuation masses in the spleen. The imaging features are not specific and the differential diagnosis includes infection and metastatic disease

Renal

The renal allograft is a common location of PTLD in kidney transplant recipients although one study found a higher incidence of gastrointestinal and CNS PTLD in these patients [10]. Imaging appearances include solitary (Fig. 10.5) or multiple parenchymal masses or an infiltrating mass that often surrounds the hilar structures. The later form may cause hydronephrosis or vascular compromise. As with PTLD in other locations, masses are hypo-enhancing and hypo-intense on both T1-weighted and T2-weighted MR imaging and hypoechoic at US [21, 22].

PTLD can also affect the native kidneys in patients with renal and nonrenal solid organ transplants. PTLD most often affects a single native kidney, whereas lymphoma in immunocompetent patients is often bilateral. The most frequent pattern of renal involvement is a solitary hypo-enhancing mass with diffuse infiltration and enlargement of the kidney less common [16].

Pancreas

Pancreatic involvement with PTLD is rare and only reported in pancreas or kidney-pancreas transplants. Reported appearances include diffuse pancreatic enlargement which may be indistinguishable from rejection or pancreatitis and less commonly a focal pancreatic mass [23, 24].

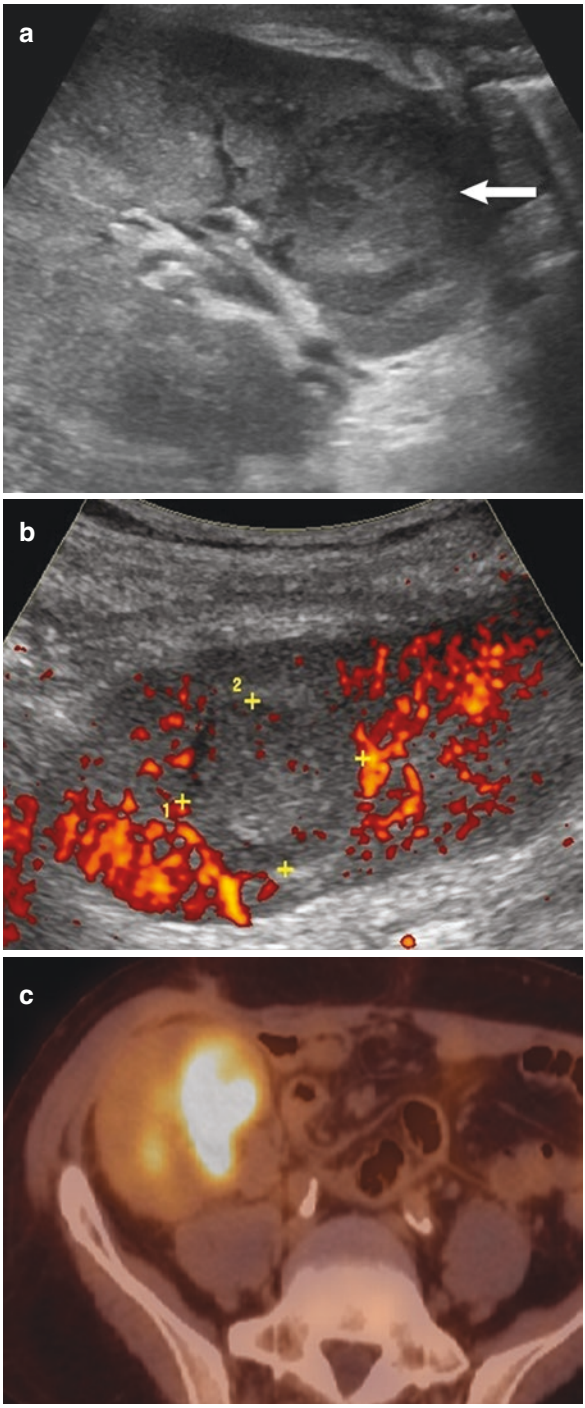

Fig. 10.5 Status post renal transplant. (**a**) Ultrasound image of the renal transplant reveals a mixed iso- to hypoechoic mass (arrow). (**b**) Power Doppler shows the mass to be hypovascular. (**c**) Fused images from PET/CT reveal marked hypermetabolic activity in the mass. Images courtesy of Dr. Tara Morgan

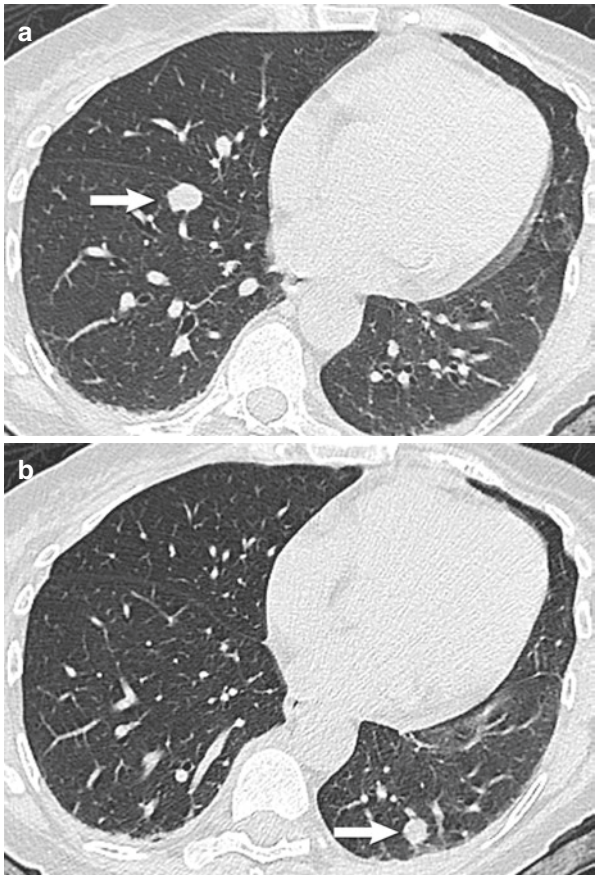

Fig. 10.6 A 64-year-old female status post renal transplant with lung PTLD. (**a**, **b**) Noncontrast chest CT shows multiple well-defined lung nodules (arrows) in a lower lung distribution, the most common appearance of pulmonary PTLD

Lungs

PTLD involvement of the lungs is highest in lung, lung-heart, and heart transplant recipients but can occur with liver and renal transplants. Multiple well-defined pulmonary nodules or masses are the most common pattern of pulmonary PTLD (Fig. 10.6). There is a peripheral and mid to lower lung predominance as well as a peribronchovascular and subpleural distribution [25, 26]. A solitary pulmonary mass is a less common presentation. Although the nodules are typically solid, a ground glass halo and cavitation have been reported, features that mimic fungal infection such as invasive aspergillosis [27]. Pulmonary PTLD can also present as areas of ground glass or consolidation which are nonspecific and can mimic pulmonary infection or rejection. Because of this, biopsy is often needed to confirm the diagnosis.

Head and Neck

The central nervous system is involved with PTLD in 12% of renal, 4% of liver, and 3–4% of heart and heart-lung transplant recipients [10]. Importantly, it is often the sole location of PTLD in a given patient [28]. Within the brain, common sites of disease include periventricular regions and subcortical white matter, while infratentorial structures are less frequently involved [29]. Lesions can be solitary or multifocal [30]. Unlike CNS lymphomas in immunocompetent patients, PTLD often demonstrates hemorrhage and/or necrosis. Focal lesions appear iso- or hyperdense on CT and typically hypodense on T1-weighted and T2-weighted imaging. However, areas of hemorrhage may be hyper-intense on T1-weighted images, and areas of necrosis can be hyper-intense on T2-weighted imaging. Surrounding vasogenic edema is common. Lesions may enhance homogeneously or demonstrate ringlike enhancement due to central necrosis (Fig. 10.7) [29, 30].

In contradistinction to CNS involvement, PTLD in the head and neck is most often seen in the setting of more widespread disease in the chest and abdomen. The most common extra-nodal site of disease is the pharynx due to the prominent lymphoid tissue in this region. PTLD appears as a focal mass in Waldeyer's ring, with or without central necrosis [31]. Other less common sites of disease include the orbits and sinuses.

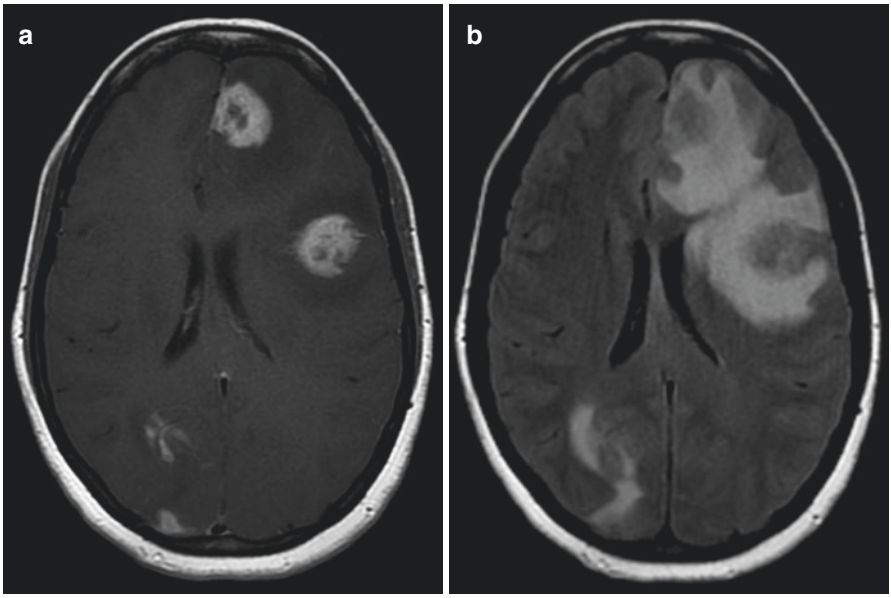

Fig. 10.7 A 40-year-old female status post renal transplant with CNS PTLD. (**a**) Contrast-enhanced T1-weighted image shows multiple enhancing brain masses in the subcortical white matter. Note the central necrosis resulting in ringlike enhancement. (**b**) Fluid attenuation inversion recovery image shows prominent vasogenic edema surrounded the lesions

Nodal PTLD

Abdominal

Extra-nodal PTLD is more common in the abdomen with only approximately 20% of cases demonstrating abdominal lymph node involvement [16]. Furthermore, most of these cases occur in the setting of extra-nodal disease and isolated lymphadenopathy is an uncommon presentation. The retroperitoneum is the most common site of lymphadenopathy in abdominal PTLD. The appearance of nodal PTLD on CT is similar to lymphadenopathy from other malignant causes and includes lymph node enlargement or conglomeration of nodal masses, as well as loss of the normal fatty hilum (Fig. 10.8). Necrosis is rare. PET will usually demonstrate increased FDG uptake in PTLD and can be useful to differentiate PTLD from inflammatory etiologies of lymphadenopathy.

Thoracic

Like lung involvement, thoracic nodal disease is less common than disease below the diaphragm and occurs more frequently with recipients of heart or lung transplants. However, nodal disease is relatively more common in cases of thoracic PTLD compared to abdominal disease with similar prevalence of nodal and extra-nodal disease [32]. Lymphadenopathy can involve the mediastinum, hila, axilla, and supraclavicular regions and is often seen in conjunction with abdominal lymphadenopathy [33]. It can be unilateral or bilateral. Like nodal disease in the abdomen, necrosis is rare and increased FDG uptake is seen in affected lymph nodes.

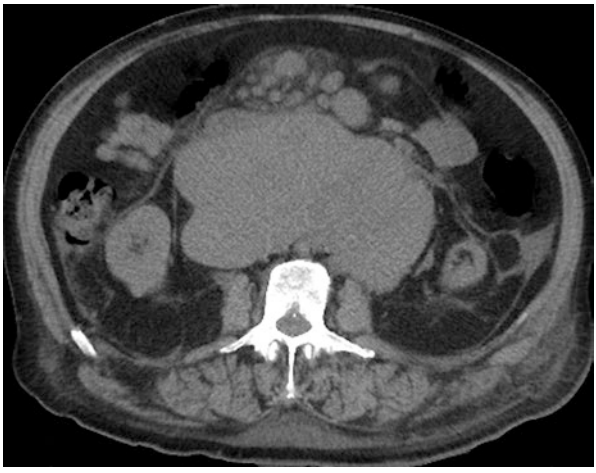

Fig. 10.8 A 77-year-old male status post renal transplant with intra-abdominal nodal PTLD. Noncontrast CT shows a massive nodal conglomerate in the retroperitoneum encasing the aorta and IVC as well as multiple enlarged mesenteric lymph nodes

Summary

PTLD is an important complication following solid organ transplantation, and imaging plays a crucial role in the diagnosis of PTLD as the clinical features are nonspecific. The affected organs are largely dependent on the type of organ transplantation but extra-nodal disease is most common. Knowledge of the various appearances of PTLD will allow the radiologist to identify this disease on multiple different imaging modalities.

References

1. Engels EA, Pfeiffer RM, Fraumeni JF Jr, Kasiske BL, Israni AK, Snyder JJ, et al. Spectrum of cancer risk among US solid organ transplant recipients. JAMA. 2011;306(17):1891–901.
2. Collett D, Mumford L, Banner NR, Neuberger J, Watson C. Comparison of the incidence of malignancy in recipients of different types of organ: a UK Registry audit. Am J Transplant. 2010;10(8):1889–96.
3. Adami J, Gabel H, Lindelof B, Ekstrom K, Rydh B, Glimelius B, et al. Cancer risk following organ transplantation: a nationwide cohort study in Sweden. Br J Cancer. 2003;89(7):1221–7.
4. Taylor AL, Marcus R, Bradley JA. Post-transplant lymphoproliferative disorders (PTLD) after solid organ transplantation. Crit Rev Oncol Hematol. 2005;56(1):155–67.
5. Borhani AA, Hosseinzadeh K, Almusa O, Furlan A, Nalesnik M. Imaging of posttransplantation lymphoproliferative disorder after solid organ transplantation. Radiographics. 2009;29(4):981–1000; discussion-2.
6. Gao SZ, Chaparro SV, Perlroth M, Montoya JG, Miller JL, DiMiceli S, et al. Post-transplantation lymphoproliferative disease in heart and heart-lung transplant recipients: 30-year experience at Stanford University. J Heart Lung Transplant. 2003;22(5):505–14.
7. Libertiny G, Watson CJ, Gray DW, Welsh KI, Morris PJ. Rising incidence of post-transplant lymphoproliferative disease in kidney transplant recipients. Br J Surg. 2001;88(10):1330–4.
8. Paranjothi S, Yusen RD, Kraus MD, Lynch JP, Patterson GA, Trulock EP. Lymphoproliferative disease after lung transplantation: comparison of presentation and outcome of early and late cases. J Heart Lung Transplant. 2001;20(10):1054–63.
9. Dhillon MS, Rai JK, Gunson BK, Olliff S, Olliff J. Post-transplant lymphoproliferative disease in liver transplantation. Br J Radiol. 2007;80(953):337–46.
10. Opelz G, Dohler B. Lymphomas after solid organ transplantation: a collaborative transplant study report. Am J Transplant. 2004;4(2):222–30.
11. Fananapazir G, Troppmann C, Corwin MT, Nikpour AM, Naderi S, Lamba R. Incidences of acute kidney injury, dialysis, and graft loss following intravenous administration of low-osmolality iodinated contrast in patients with kidney transplants. Abdom Radiol. 2016;41(11):2182–6.
12. Bianchi E, Pascual M, Nicod M, Delaloye AB, Duchosal MA. Clinical usefulness of FDG-PET/CT scan imaging in the management of posttransplant lymphoproliferative disease. Transplantation. 2008;85(5):707–12.
13. McCormack L, Hany TI, Hubner M, Petrowsky H, Mullhaupt B, Knuth A, et al. How useful is PET/CT imaging in the management of post-transplant lymphoproliferative disease after liver transplantation? Am J Transplant. 2006;6(7):1731–6.
14. Vali R, Punnett A, Bajno L, Moineddin R, Shammas A. The value of 18F-FDG PET in pediatric patients with post-transplant lymphoproliferative disorder at initial diagnosis. Pediatr Transplant. 2015;19(8):932–9.

15. Miller WT Jr, Siegel SG, Montone KT. Posttransplantation lymphoproliferative disorder: changing manifestations of disease in a renal transplant population. Crit Rev Diagn Imaging. 1997;38(6):569–85.
16. Pickhardt PJ, Siegel MJ. Posttransplantation lymphoproliferative disorder of the abdomen: CT evaluation in 51 patients. Radiology. 1999;213(1):73–8.
17. Ghai S, Pattison J, Ghai S, O'Malley ME, Khalili K, Stephens M. Primary gastrointestinal lymphoma: spectrum of imaging findings with pathologic correlation. Radiographics. 2007;27(5):1371–88.
18. Shin YM. Posttransplantation lymphoproliferative disorder involving liver after renal transplantation. Korean J Hepatol. 2011;17(2):165–9.
19. Wu L, Rappaport DC, Hanbidge A, Merchant N, Shepherd FA, Greig PD. Lymphoproliferative disorders after liver transplantation: imaging features. Abdom Imaging. 2001;26(2):200–6.
20. Semelka RC, Kelekis NL, Sallah S, Worawattanakul S, Ascher SM. Hepatosplenic fungal disease: diagnostic accuracy and spectrum of appearances on MR imaging. AJR Am J Roentgenol. 1997;169(5):1311–6.
21. Lopez-Ben R, Smith JK, Kew CE 2nd, Kenney PJ, Julian BA, Robbin ML. Focal posttransplantation lymphoproliferative disorder at the renal allograft hilum. AJR Am J Roentgenol. 2000;175(5):1417–22.
22. Ali MG, Coakley FV, Hricak H, Bretan PN. Complex posttransplantation abnormalities of renal allografts: evaluation with MR imaging. Radiology. 1999;211(1):95–100.
23. Meador TL, Krebs TL, Cheong JJWY, Daly B, Keay S, Bartlett S. Imaging features of posttransplantation lymphoproliferative disorder in pancreas transplant recipients. Am J Roentgenol. 2000;174(1):121–4.
24. Dyckmans K, Lerut E, Gillard P, Lannoo M, Ectors N, Hoorens A, et al. Post-transplant lymphoma of the pancreatic allograft in a kidney-pancreas transplant recipient: a misleading presentation. Nephrol Dial Transplant. 2006;21(11):3306–10.
25. Hare SS, Souza CA, Bain G, Seely JM, Frcpc, Gomes MM, et al. The radiological spectrum of pulmonary lymphoproliferative disease. Br J Radiol. 2012;85(1015):848–64.
26. Collins J, Muller NL, Leung AN, McGuinness G, Mergo PJ, Flint JD, et al. Epstein-Barr-virus-associated lymphoproliferative disease of the lung: CT and histologic findings. Radiology. 1998;208(3):749–59.
27. Pickhardt PJ, Siegel MJ, Anderson DC, Hayashi R, DeBaun MR. Chest radiography as a predictor of outcome in posttransplantation lymphoproliferative disorder in lung allograft recipients. AJR Am J Roentgenol. 1998;171(2):375–82.
28. Castellano-Sanchez AA, Li S, Qian J, Lagoo A, Weir E, Brat DJ. Primary central nervous system posttransplant lymphoproliferative disorders. Am J Clin Pathol. 2004;121(2):246–53.
29. Pickhardt PJ, Wippold FJ 2nd. Neuroimaging in posttransplantation lymphoproliferative disorder. AJR Am J Roentgenol. 1999;172(4):1117–21.
30. Cavaliere R, Petroni G, Lopes MB, Schiff D, International Primary Central Nervous System Lymphoma Collaborative Group. Primary central nervous system post-transplantation lymphoproliferative disorder: an International Primary Central Nervous System Lymphoma Collaborative Group Report. Cancer. 2010;116(4):863–70.
31. Loevner LA, Karpati RL, Kumar P, Yousem DM, Hsu W, Montone KT. Posttransplantation lymphoproliferative disorder of the head and neck: imaging features in seven adults. Radiology. 2000;216(2):363–9.
32. Halkos ME, Miller JI, Mann KP, Miller DL, Gal AA. Thoracic presentations of posttransplant lymphoproliferative disorders. Chest. 2004;126(6):2013–20.
33. Yoon GY, Kim MY, Huh JR, Jo KW, Shim TS. Posttransplant lymphoproliferative disorder of the thorax: CT and FDG-PET features in a single tertiary Referral Center. Medicine. 2015;94(31):e1274.

Index

G. Fananapazir, R. Lamba (eds.), *Transplantation Imaging*,
https://doi.org/10.1007/978-3-319-75266-2